

10-64
33837
p-124

New Developments in the Method of Space-Time Conservation Element and Solution Element-Applications to Two-Dimensional Time-Marching Problems

Sin-Chung Chang
Lewis Research Center
Cleveland, Ohio

Xiao-Yen Wang and Chuen-Yen Chow
University of Colorado
Boulder, Colorado

(NASA-TM-106758) NEW DEVELOPMENTS
IN THE METHOD OF SPACE-TIME
CONSERVATION ELEMENT AND SOLUTION
ELEMENT-APPLICATIONS TO
TWO-DIMENSIONAL TIME-MARCHING
PROBLEMS (NASA. Lewis Research
Center) 124 p

N95-16885

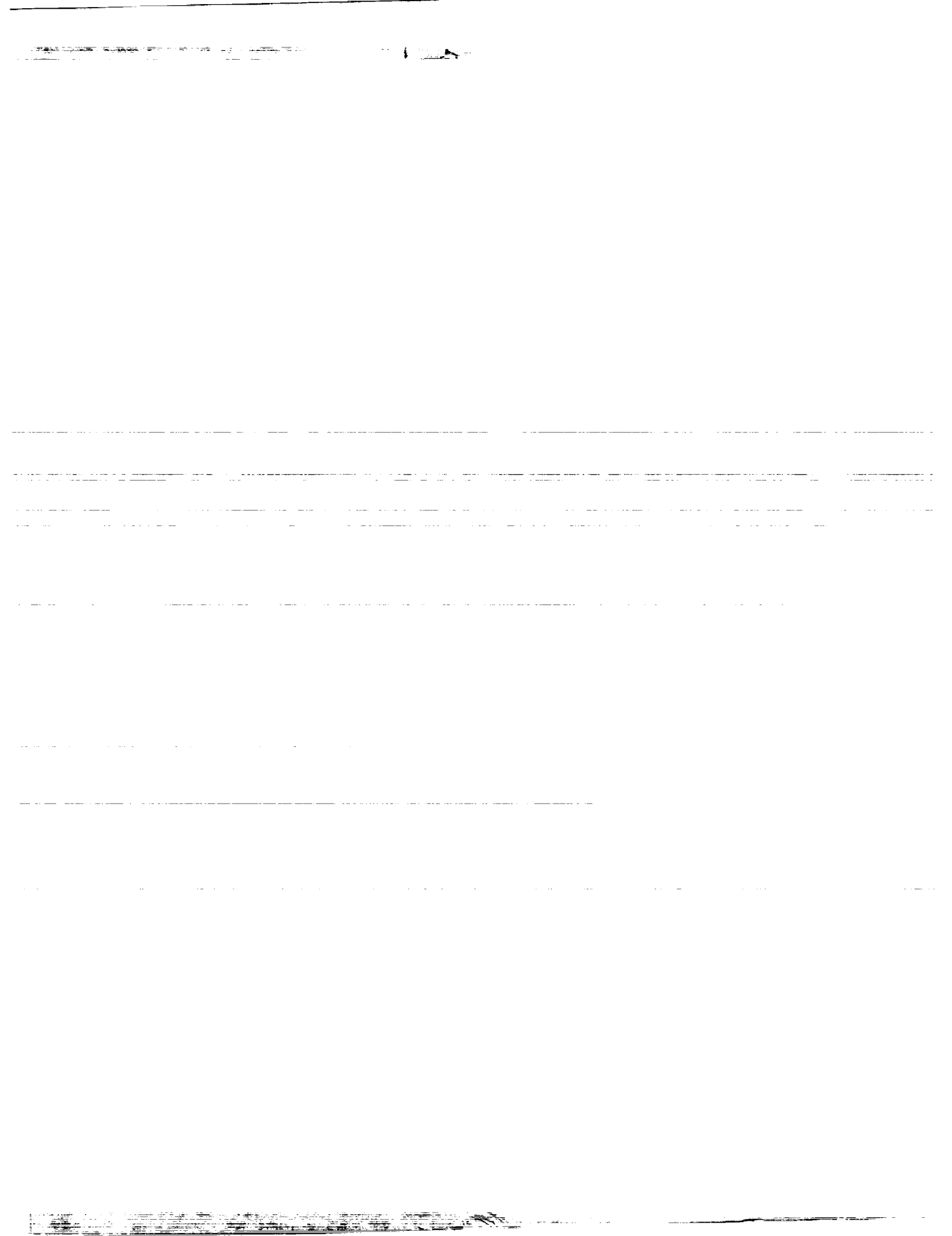
Unclass

63/64 0033837

December 1994



National Aeronautics and
Space Administration



New Developments in the Method of Space-Time Conservation Element and Solution Element—Applications to Two-Dimensional Time-Marching Problems

by

Sin-Chung Chang
National Aeronautics and Space Administration
Lewis Research Center
Cleveland, Ohio 44135

and

Xiao-Yen Wang, Chuen-Yen Chow
University of Colorado at Boulder
Department of Aerospace Engineering Science
Boulder, Colorado 80309-0429

Abstract

A new numerical discretization method for solving conservation laws is being developed. This new approach differs substantially in both concept and methodology from the well-established methods—i.e., finite difference, finite volume, finite element, and spectral methods. It is motivated by several important physical/numerical considerations and designed to avoid several key limitations of the above traditional methods.

As a result of the above considerations, a set of key principles for the design of numerical schemes was put forth in a previous report. These principles were used to construct several numerical schemes that model a 1-D time-dependent convection-diffusion equation. These schemes were then extended to solve the time-dependent Euler and Navier-Stokes equations of a perfect gas. It was shown that the above schemes compared favorably with the traditional schemes in *simplicity, generality, and accuracy*.

In this report, the 2-D versions of the above schemes, except the Navier-Stokes solver, are constructed using the same set of design principles. Their constructions are simplified greatly by the use of a nontraditional space-time mesh. Its use results in the simplest stencil possible, i.e., a tetrahedron in a 3-D space-time with a vertex at the upper time level and other three at the lower time level. Because of the similarity in their design, each of the present 2-D solvers virtually shares with its 1-D counterpart the same fundamental characteristics. Moreover, it will be shown that the present Euler solver is capable of generating highly accurate solutions for a famous 2-D shock reflection problem. Specifically, both the incident and the reflected shocks can be resolved by a single data point without the presence of numerical oscillations near the discontinuity.

1. Introduction

A new numerical discretization method for solving conservation laws is being developed [1-8]. This new approach differs substantially in both concept and methodology from the well-established methods—i.e., finite difference, finite volume, finite element, and spectral methods [9-13]. It is conceptually simple and designed to overcome several key limitations of the above traditional methods.

A two-level explicit scheme for solving a 1-D convection-diffusion equation was constructed in [1] using this new method. Because the convection speed and the viscosity coefficient in the above equation are denoted by a and μ , respectively, the new scheme is referred to as the 1-D a - μ scheme. In [1], this scheme is subjected to a thorough theoretical and numerical analysis on stability, dissipation, dispersion, consistency, truncation error, and accuracy. The 1-D a - μ scheme is a two-way marching scheme [5], i.e., *the forward marching scheme can be inverted to become the backward marching scheme. In other words, the marching variables at a lower time level can also be determined in terms of those at higher time levels.* The special case of the the 1-D a - μ scheme which solves only the convection equation is referred to as the 1-D a scheme. This scheme is the only two-level explicit scheme known to the authors to be neutrally stable, i.e., free from numerical diffusion. Note that the solution of a pure convection problem has three fundamental properties: (i) it does not dissipate with time, (ii) its value at a spatial point at a later time has a finite domain of dependence at an earlier time, and (iii) it is completely determined by the initial data at a given time. Because the a scheme is a *two-level, explicit, and neutrally stable* scheme, the above three properties are also shared by a solution of the a scheme. Contrarily, (i) a solution of a *diffusive* scheme will dissipate with time; (ii) the value of a solution of an *implicit* scheme at any space-time mesh point is dependent on all initial data, and all the boundary data up to the time level of the mesh point under consideration; and (iii) the unique determination of a solution of a *multi-level* scheme requires the specification of the initial data at two or more time levels.

Because the a scheme is free from numerical diffusion and it is a special case of the a - μ scheme with $\mu = 0$, the a - μ scheme has a special property that a classical scheme generally lacks, i.e., as the physical diffusion approaches zero, so does the numerical diffusion. Without this property, *numerical dissipation may overwhelm physical dissipation and cause a complete distortion of solutions for problems with small viscosity.*

The 1-D a - μ scheme was derived again in [5] using a different type of conservation element and solution element. In [5], it also was extended to solve the 1-D time-dependent Navier-Stokes equations of a perfect gas. In spite of the fact that it does not use (i) any techniques related to the high-resolution upwind methods, (ii) any mesh-refinement techniques, (iii) any moving meshes, and (iv) any ad hoc parameter, the new Navier-Stokes solver is capable of generating highly accurate shock tube solutions. Particularly, for high-Reynolds-number flows, shock discontinuities can be resolved almost within one mesh interval.

The 1-D a scheme is neutrally stable and reversible in time. It is well known that such

a scheme generally becomes unstable when it is extended to model the Euler equations. It is also obvious that a scheme that is reversible in time cannot model a physical problem that is irreversible in time, e.g., an inviscid flow problem involving shocks. As a result, the 1-D a scheme was modified in [5]. Stability of this modified scheme, referred to as the 1-D $a-\epsilon$ scheme, is limited by the CFL condition and $0 \leq \epsilon \leq 1$ where ϵ is a special parameter that controls numerical diffusion. The 1-D $a-\epsilon$ scheme is reduced to the 1-D a scheme (which is free of numerical diffusion) when $\epsilon = 0$.

The 1-D $a-\epsilon$ scheme also was extended in [5] to become an Euler solver. The stability conditions of the Euler solver are similar to those of the 1-D $a-\epsilon$ scheme. It was shown in [5] that the Euler solver is capable of generating accurate shock tube solutions within a wide range of CFL number.

In this report, it will be explained how the 2-D versions of the $a-\mu$, the a , and the $a-\epsilon$ schemes can be constructed using the same set of design principles which were used to construct their 1-D counterparts. Because of this similarity in design, each of these 2-D versions virtually shares with its 1-D counterpart the same fundamental characteristics. Moreover, the 2-D $a-\epsilon$ scheme will also be extended to become an Euler solver. This extension is also very similar to its 1-D counterpart. We will not, however, discuss in this report the Navier-Stokes extension of the 2-D $a-\mu$ scheme. Because a Navier-Stokes problem is fundamentally an initial-value/boundary value problem, the above extension (which is explicit and thus can not transmit information from one end of the boundary to another end in one time step) obviously cannot model such a problem unless the contribution of the viscous terms is small compared to that of the convection (inertial) terms. In general, this implies that the Navier-Stokes extension of the 2-D $a-\mu$ scheme is applicable only to high-Reynolds-number flows. In a future report, this extension will be introduced as a special case of a more general Navier-Stokes solver.

The current method emphasizes *simplicity, generality, and accuracy*. It represents a clear break from the traditional methods in the basic concept of discretization. Most of the considerations that motivate its development and the key differences that separate the current method from the traditional methods were discussed in [5]. In the following, we present a more up-to-date version of these discussions:

- (a) A set of physical conservation laws is a collection of statements of *flux conservation in space-time*. Mathematically, these laws are represented by a set of integral equations. The differential form of these laws is obtained from the integral form with the assumption that *the physical solution is smooth*. For a physical solution in a region of rapid change (e.g., a boundary layer), this smoothness assumption is difficult to realize by a numerical approximation that can use only a limited number of discrete variables. This difficulty becomes even worse in the presence of discontinuities (e.g., shocks). Thus, a method designed to obtain numerical solutions to the differential form without enforcing flux conservation is at a fundamental disadvantage in modeling physical phenomena with high-gradient regions. Particularly, it may not be used to solve flow problems involving shocks. Contrarily, a numerical solution obtained from a method that also enforces flux-conservation locally (i.e., down to a computational cell) and

globally (i.e., over the entire computational domain) will always retain the basic physical reality of flux conservation even in a region involving discontinuities. For this reason, the enforcement of *both local and global flux conservation in space and time* is a tenet in the current development. The concept of *space-time conservation element* is introduced to serve this purpose.

Among the traditional methods, finite difference, finite element, and spectral methods are designed to solve the differential form of the conservation laws. Note that the set of integral equations usually solved in a finite-element scheme is equivalent to the differential form of the conservation laws assuming certain smoothness conditions. However, these integral equations generally are different from the integral equations representing the conservation laws. Even if they are cast into a conservative form, the resulting flux-conservation conditions generally do not represent the physical conservation laws.

The finite volume method is the only traditional method designed to enforce flux conservation. A finite-volume scheme may enforce flux conservation in space only, or in both space and time. As a preliminary to this enforcement, a flux must be assigned at any interface separating two neighboring conservation cells. In a typical finite-volume scheme, it is evaluated by extrapolating or interpolating the mesh values at the neighboring cells. This evaluation generally requires an ad hoc choice of a special flux model among many models available [14-16]. Generally numerical results obtained are dependent on which model one chooses. Also this process of interpolation and extrapolation generally is time consuming and may result in numerical smearing.

Contrarily, by using the concept of *space-time solution element*, and considering the spatial derivatives of dynamic variables as independent variables (to be discussed further shortly), in the current method, flux evaluation at an interface is carried out without interpolation or extrapolation. It is an integral part of the solution procedure.

- (b) The numerical variables used in a spectral method, i.e., the expansion coefficients, are global parameters pertaining to the entire computational domain. As a result, a spectral method generally (i) lacks local flexibility and thus may be applied only to problems with simple geometry, and (ii) is hindered by the fact that it must deal with a full matrix that is difficult to invert.

By design, only local parameters will be used in the current method. Moreover, the set of discrete variables in any one of the numerical equations to be solved generally is associated with only two neighboring solution elements. The exception to this general rule occurs only in the situation in which numerical diffusion is to be introduced deliberately (see [5], [6], and Secs. 3 and 4). Even in this special case, only the discrete variables associated with a few *immediately* neighboring solution elements will enter any equation to be solved. Thus, one needs only to deal with a very sparse matrix. Moreover, the maximum number of solution elements involved in a numerical equation of the current discretization framework is independent of the order of accuracy of a particular scheme. Contrarily, the order of accuracy of a classical finite-difference scheme generally can be increased only by using variables at more mesh points in

each of its equations. Usually, a side effect of this practice is an increase in numerical diffusion. Also it may be difficult to implement a high-order finite-difference scheme near a boundary because there are no real mesh points outside the boundary. Note that, in the absence of body force, direct physical interactions occur only among the immediate neighbors. The current design is also consistent with this physical reality.

- (c) Space and time traditionally are treated separately in the time marching schemes. Generally one obtains a system of ordinary differential equations with time being the independent variable after a spatial discretization. As an example, elements in the finite element method usually are used for spatial discretization. These elements are domains in space only.

Because flux conservation is fundamentally a property in *space-time*, space and time are unified and treated on the same footing in the current method. Thus, conservation elements and solution elements used in the time-dependent version of the current method are domains in space-time. The significance of this unified approach cannot be overemphasized. It makes it easier for a numerical analogue to share the same space-time symmetry of the physical laws (see [2], [5], [6] and the following sections).

- (d) In a finite-difference scheme, derivatives at mesh points are expressed in terms of mesh values of dependent variables by using finite-difference approximations. Accuracy of these approximations, especially those of higher-order accuracy, generally is excellent as long as dependent variables vary slowly across a mesh interval. However, it may not be adequate if these variables vary too rapidly. Thus, in a high-gradient region, e.g., a boundary layer, accuracy may demand the use of an extremely fine mesh. In turn, a prohibitively high computing cost may result.

The current method avoids the above pitfall by expressing the numerical solution within a solution element as an expansion in terms of certain base functions. As in a spectral method, the expansion coefficients are considered as *the independent numerical variables to be solved for simultaneously*. For simplicity, Taylor's expansions will be used in the current paper. For this special case, the expansion coefficients are interpreted as the numerical analogues of the derivatives. Note that:

- (i) Because the derivatives are considered as independent variables, their values at the initial/boundary surfaces may be specified as a part of the initial/boundary conditions. *This specification may result in more accurate initial/boundary conditions;*
- (ii) van Leer [17] also has attempted to improve accuracy by introducing two independent numerical variables for each independent physical variable, and (iii) the current solution procedure has no resemblance with those used in compact difference schemes.

- (e) With a few exceptions, numerical diffusion generally appears in a numerical solution of a time-marching problem. In other words, the numerical solution dissipates faster than the corresponding physical solution. For a nearly inviscid problem, e.g., flow with a high Reynolds number, this could be very serious because numerical dissipation may overwhelm physical dissipation and cause a complete distortion of solutions. One may argue that numerical diffusion can be reduced by increasing the order of accuracy of the scheme used. However, because the order of accuracy of a scheme is generally

determined with the aid of Taylor's expansion, and the latter is valid only for a smooth solution, it has meaning only for a smooth solution. Thus the use of a scheme of higher-order accuracy may not reduce numerical diffusion associated with high-frequency Fourier components of a numerical solution. This is the reason that the Leapfrog scheme, which is free from numerical diffusion, can outperform schemes with higher-order accuracy in solving some wave equations [18].

In a study of finite-difference analogues of a simple convection equation [2], it was shown that a numerical analogue will be free from numerical diffusion if it does not violate certain space-time invariant properties of the convection equation. In other words, numerical diffusion may be considered as a result of *symmetry-breaking* by the numerical scheme. Because of its intrinsic nature of space-time unity, the current framework is an excellent vehicle for constructing a numerical analogue that shares the same space-time invariant properties with the physical equation (see [5], [6], and the following sections).

It is recognized that a certain amount of numerical diffusion may be needed to prevent large dispersive errors [19] that are often caused by the presence of high-frequency disturbances (such as round-off errors). Therefore, schemes were constructed such that the numerical diffusion can be controlled by a single adjustable parameter (see [5], [6], and Secs. 3 and 4). The numerical diffusion is shut off when this parameter is set to zero.

- (f) High-resolution upwind methods [13], which we consider to be a branch of the finite volume method, are heavily dependent on characteristics-based techniques. For the 1-D time-dependent case, the characteristics are curves in space-time, and the coefficient matrix associated with the Euler equations [20] also can be diagonalized easily. As a result, these techniques are easy to apply. However, for multidimensional cases, the characteristics are 2-D or 3-D surfaces in space-time [21]. Moreover, the coefficient matrices cannot be diagonalized simultaneously by the same matrix [20]. Because of the above complexities, application of these techniques to multi-dimensional problems is much more difficult. Furthermore, high-resolution methods generally require the use of ad hoc parameters, e.g., flux-limiters and/or slope-limiters, and other ad hoc techniques. These ad hoc techniques may lead to numerical diffusion which varies from one place to another and from one Fourier component to another. In other words, numerical solutions may suffer annihilation of sharply different degrees at different locations and different frequencies [22]. Also, these techniques generally are also difficult to extend to a space of higher dimension.

Because the current framework is developed to solve multidimensional problems (see the following sections), simplicity and generality weigh heavily in its design. Thus, we do not use the characteristics-based techniques, and also try to avoid the use of ad hoc techniques. Moreover, the concept of characteristics generally is not applicable to the Navier-Stokes equations, which are non-hyperbolic in nature. Therefore, the above decision also makes it easier for the current framework to solve the Navier-Stokes equations [5].

This completes the discussion of the motivation for the current development. In summary, the development is guided by the following requirements: (i) To enforce both local and global flux conservation in space and time with flux evaluation at an interface being an integral part of the solution procedure and requiring no interpolation or extrapolation; (ii) To use local discrete variables such that the set of variables in any one of the numerical equations to be solved is associated with a set of immediately neighboring cells; (iii) Space and time are unified and treated on the same footing; (iv) Mesh values of dependent variables and their derivatives are considered as independent variables to be solved for simultaneously; (v) To minimize numerical diffusion, a numerical analogue should be constructed, as much as possible, to be compatible with the space-time invariant properties of the corresponding physical equations; and (vi) *To exclude the use of the characteristics-based techniques, and to avoid the use of ad hoc techniques as much as possible.* It is the purpose of this report to show that *the above requirements can be met with a simple unified numerical framework even for multidimensional problems.*

2. The a - μ Scheme

In this section, we consider a dimensionless form of the 2-D convection–diffusion equation, i.e.,

$$\frac{\partial u}{\partial t} + a_x \frac{\partial u}{\partial x} + a_y \frac{\partial u}{\partial y} - \mu \left(\frac{\partial^2 u}{\partial x^2} + \frac{\partial^2 u}{\partial y^2} \right) = 0 \quad (2.1)$$

where a_x , a_y , and μ (≥ 0) are constants. Let $x_1 = x$, $x_2 = y$, and $x_3 = t$ be the coordinates of a three-dimensional Euclidean space E_3 . By using Gauss' divergence theorem in the space-time E_3 , it can be shown that Eq. (2.1) is the differential form of the integral conservation law

$$\oint_{S(V)} \vec{h} \cdot d\vec{s} = 0. \quad (2.2)$$

Here (i) $S(V)$ is the boundary of an arbitrary space-time region V in E_3 , (ii)

$$\vec{h} \stackrel{\text{def}}{=} (a_x u - \mu \partial u / \partial x, a_y u - \mu \partial u / \partial y, u) \quad (2.3)$$

is a current density vector in E_3 , and (iii) $d\vec{s} = d\sigma \vec{n}$ with $d\sigma$ and \vec{n} , respectively, being the area and the outward unit normal of a surface element on $S(V)$. Note that (i) $\vec{h} \cdot d\vec{s}$ is the space-time flux of \vec{h} leaving the region V through the surface element $d\vec{s}$, and (ii) all mathematical operations can be carried out as though E_3 were an ordinary three-dimensional Euclidean space. As will be shown shortly, E_3 will be divided into nonoverlapping space-time regions referred to as conservation elements (CEs).

Let n denote the time level and

$$t^n \stackrel{\text{def}}{=} n \Delta t, \quad n = 0, \pm 1/2, \pm 1, \pm 3/2, \dots \quad (2.4)$$

Let j and k be spatial mesh indices with $j, k = 0, \pm 1/3, \pm 2/3, \pm 1, \dots$ (see Figs. 1–4). Let Ω_1 denote the set of mesh points (j, k, n) with $j, k = 0, \pm 1, \pm 2, \dots$, and $n = \pm 1/2, \pm 3/2, \pm 5/2, \dots$. These mesh points are marked by solid circles. Let Ω_2 denote the set of mesh points (j, k, n) with $j, k = 1/3, 1/3 \pm 1, 1/3 \pm 2, \dots$, and $n = 0, \pm 1, \pm 2, \dots$. These mesh points are marked by open circles. The union of Ω_1 and Ω_2 will be denoted by Ω .

Each mesh point $(j, k, n+1/2)$ in Ω_1 (by definition, this implies that $n = 0, \pm 1, \pm 2, \dots$) is associated with three CEs, denoted by $\text{CE}_\ell^{(1)}(j, k, n+1/2)$, $\ell = 1, 2, 3$ (see Fig. 5(a)). It is also associated with a solution element (SE), denoted by $\text{SE}^{(1)}(j, k, n+1/2)$ (see Fig. 5(b)). Similarly, each mesh point $(j, k, n+1)$ in Ω_2 is associated with three conservation elements $\text{CE}_\ell^{(2)}(j, k, n+1)$, $\ell = 1, 2, 3$ (see Fig. 6(a)), and a solution element $\text{SE}^{(2)}(j, k, n+1)$ (see Fig. 6(b)). Each CE is a quadrilateral cylinder in space-time while each SE is the union of three vertical planes, a horizontal plane, and their immediate neighborhood. The geometry of the hexagon $ABCDEF$, which appears in both Figs. 5(a) and 6(a), is determined by three positive parameters w , b and h (see Fig. 7(a)). Without any loss of generality, we

assume that the line segment joining points D and A in Fig. 7(a) is parallel to the x -axis. Note that the form of Eq. (2.1) will not change under an orthogonal transformation on the x - y plane. Thus one always can introduce a set of Cartesian coordinates (x, y) such that the above line segment is parallel to the x -axis. However, the values of a_x and a_y may change as a result of such a transformation.

According to Fig. 1, E_3 can be filled with the CEs defined above. Moreover, it is seen from Figs. 5(a), 5(b), 6(a), and 6(b) that the boundary of a CE is formed by the subsets of two neighboring SEs.

Let the space-time mesh be uniform, i.e., the parameters Δt , w , b , and h be constants. Let $x_{j,k}$ and $y_{j,k}$ be the x - and y -coordinates of any mesh points $(j, k, n) \in \Omega$. Let $x_{0,0} = 0$ and $y_{0,0} = 0$. Then information provided by Figs. 7(a) and 7(b) implies that

$$x_{j,k} = (j+k)w + (k-j)b, \quad y_{j,k} = (k-j)h. \quad (2.5)$$

Let $\vec{n}_1, \vec{n}_2, \vec{n}_3, \vec{n}_4, \vec{n}_5$, and \vec{n}_6 be the vectors depicted in Fig. 7(a). They lie on the x - y plane and are the outward unit normals to \overline{AB} , \overline{BC} , \overline{CD} , \overline{DE} , \overline{EF} , and \overline{FA} , respectively. It can be shown that

$$\vec{n}_1 = \frac{(h, -b + w/3, 0)}{\sqrt{h^2 + (b - w/3)^2}}, \quad \vec{n}_4 = -\vec{n}_1, \quad (2.6a)$$

$$\vec{n}_2 = (0, 1, 0), \quad \vec{n}_5 = -\vec{n}_2, \quad (2.6b)$$

and

$$\vec{n}_3 = \frac{(-h, b + w/3, 0)}{\sqrt{h^2 + (b + w/3)^2}}, \quad \vec{n}_6 = -\vec{n}_3, \quad (2.6c)$$

For any $(j, k, n) \in \Omega$, let

$$\text{SE}(j, k, n) \stackrel{\text{def}}{=} \begin{cases} \text{SE}^{(1)}(j, k, n), & \text{if } (j, k, n) \in \Omega_1; \\ \text{SE}^{(2)}(j, k, n), & \text{if } (j, k, n) \in \Omega_2. \end{cases} \quad (2.7)$$

For any $(x, y, t) \in \text{SE}(j, k, n)$, $u(x, y, t)$ and $\vec{h}(x, y, t)$, respectively, are approximated by

$$u^*(x, y, t; j, k, n) \stackrel{\text{def}}{=} u_{j,k}^n + (u_x)_{j,k}^n(x - x_{j,k}) + (u_y)_{j,k}^n(y - y_{j,k}) + (u_t)_{j,k}^n(t - t^n), \quad (2.8)$$

and

$$\vec{h}^*(x, y, t; j, k, n) \stackrel{\text{def}}{=} [a_x u^*(x, y, t; j, k, n) - \mu \partial u^*(x, y, t; j, k, n) / \partial x, \quad (2.9) \\ a_y u^*(x, y, t; j, k, n) - \mu \partial u^*(x, y, t; j, k, n) / \partial y, u^*(x, y, t; j, k, n)],$$

where $u_{j,k}^n$, $(u_x)_{j,k}^n$, $(u_y)_{j,k}^n$, and $(u_t)_{j,k}^n$ are constants within $\text{SE}(j, k, n)$. The last four coefficients, respectively, can be considered as the numerical analogues of the values of u ,

$\partial u/\partial x$, $\partial u/\partial y$, and $\partial u/\partial t$ at (x_j, y_k, t^n) . As a result, the expression on the right side of Eq. (2.8) can be considered as the first-order Taylor's expansion of $u(x, y, t)$ at (x_j, y_k, t^n) . Also note that Eq. (2.9) is the numerical analogue of Eq. (2.3).

We shall require that $u = u^*(x, y, t; j, k, n)$ satisfies Eq. (2.1) within $SE(j, k, n)$. As a result,

$$(u_t)_{j,k}^n = - [a_x(u_x)_{j,k}^n + a_y(u_y)_{j,k}^n]. \quad (2.10)$$

Because Eq. (2.8) is a first-order Taylor's expansion, the diffusion term in Eq. (2.1) has no counterpart in Eq. (2.10). As a result, the diffusion term has no impact on how $u^*(x, y, t; j, k, n)$ varies with time *within* $SE(j, k, n)$. However, as will be shown shortly, through its role in the numerical analogue of Eq. (2.2), it does influence time-dependence of numerical solutions. Note that, for a higher-order scheme, how $u^*(x, y, t; j, k, n)$ varies with time within $SE(j, k, n)$ will be influenced by the presence of the diffusion term. Substituting Eq. (2.10) into Eq. (2.8), one has

$$u^*(x, y, t; j, k, n) = u_{j,k}^n + (u_x)_{j,k}^n [(x - x_{j,k}) - a_x(t - t^n)] \\ + (u_y)_{j,k}^n [(y - y_{j,k}) - a_y(t - t^n)]. \quad (2.11)$$

Thus there are three independent marching variables, i.e., $u_{j,k}^n$, $(u_x)_{j,k}^n$, and $(u_y)_{j,k}^n$ associated with a mesh point $(j, k, n) \in \Omega$. For any $(j, k, n + 1/2) \in \Omega_1$, these variables will be determined in terms of those associated with the mesh points $(j + 1/3, k + 1/3, n)$, $(j - 2/3, k + 1/3, n)$, and $(j + 1/3, k - 2/3, n)$ (see Fig. 8(a)) by using the flux conservation relations:

$$\oint_{S(CE_i^{(1)}(j,k,n+1/2))} \vec{h}^* \cdot d\vec{s} = 0, \quad \ell = 1, 2, 3. \quad (2.12)$$

Similarly, the marching variables at any $(j, k, n + 1) \in \Omega_2$ are determined in terms of those associated with the mesh points $(j - 1/3, k + 2/3, n + 1/2)$, $(j - 1/3, k - 1/3, n + 1/2)$, and $(j + 2/3, k - 1/3, n + 1/2)$ (see Fig. 8(b)) by using the flux conservation relations:

$$\oint_{S(CE_i^{(2)}(j,k,n+1))} \vec{h}^* \cdot d\vec{s} = 0, \quad \ell = 1, 2, 3. \quad (2.13)$$

Obviously, Eqs. (2.12) and (2.13) are the numerical analogues of Eq. (2.2).

As a result of Eqs. (2.12) and (2.13), the total flux leaving the boundary of any CE is zero. Because the flux at any interface separating two neighboring CEs is calculated using the information from a single SE, the flux entering one of these CEs is equal to that leaving another. It follows that the local conservation conditions Eqs. (2.12) and (2.13) will lead to a global conservation condition, i.e., *the total flux leaving the boundary of any space-time region that is the union of any combination of CEs will also vanish.*

In the following, several preliminaries will be given prior to the evaluation of Eqs. (2.12) and (2.13). To proceed, note that a mesh line with j and n being constant or a mesh line with k and n being constant is not aligned with the x -axis or the y -axis. We shall introduce

a new spatial coordinate system (ζ, η) with its axes aligned with the above mesh lines (see Fig. 7(c)).

Let \vec{e}_x and \vec{e}_y be the unit vectors in the x - and the y - directions, respectively. Let \vec{e}_ζ and \vec{e}_η be the unit vectors in the directions of \overrightarrow{DF} and \overrightarrow{DB} (i.e., the j - and the k - directions—see Figs. 7(a)-(c)), respectively. It can be shown that

$$\vec{e}_\zeta = [(w - b)\vec{e}_x - h\vec{e}_y] / \Delta\zeta, \quad (2.14)$$

and

$$\vec{e}_\eta = [(w + b)\vec{e}_x + h\vec{e}_y] / \Delta\eta, \quad (2.15)$$

where

$$\Delta\zeta \stackrel{\text{def}}{=} |\overrightarrow{DF}| = \sqrt{(w - b)^2 + h^2}, \quad (2.16)$$

and

$$\Delta\eta \stackrel{\text{def}}{=} |\overrightarrow{DB}| = \sqrt{(w + b)^2 + h^2}. \quad (2.17)$$

Let the origin of (x, y) also be that of (ζ, η) . Then the spatial coordinates (x, y) and (ζ, η) of any point in E_3 are related by the condition

$$\zeta \vec{e}_\zeta + \eta \vec{e}_\eta = x \vec{e}_x + y \vec{e}_y. \quad (2.18)$$

Substituting Eqs. (2.14) and (2.15) into Eq. (2.18), one has

$$\begin{pmatrix} x \\ y \end{pmatrix} = T \begin{pmatrix} \zeta \\ \eta \end{pmatrix}, \quad (2.19)$$

and

$$\begin{pmatrix} \zeta \\ \eta \end{pmatrix} = T^{-1} \begin{pmatrix} x \\ y \end{pmatrix}. \quad (2.20)$$

Here

$$T \stackrel{\text{def}}{=} \begin{pmatrix} \frac{w - b}{\Delta\zeta} & \frac{w + b}{\Delta\eta} \\ -\frac{h}{\Delta\zeta} & \frac{h}{\Delta\eta} \end{pmatrix}, \quad (2.21)$$

and

$$T^{-1} \stackrel{\text{def}}{=} \begin{pmatrix} \frac{\Delta\zeta}{2w} & -\frac{(w + b)\Delta\zeta}{2wh} \\ \frac{\Delta\eta}{2w} & \frac{(w - b)\Delta\eta}{2wh} \end{pmatrix}. \quad (2.22)$$

Note that the existence of T^{-1} , the inverse of T , is assured if $wh \neq 0$.

With the aid of Eqs. (2.5), (2.20), and (2.22), it can be shown that the coordinates (ζ, η) of any mesh point $(j, k, n) \in \Omega$ are given by

$$\zeta = j \Delta\zeta, \quad \text{and} \quad \eta = k \Delta\eta, \quad (2.23)$$

i.e., $\Delta\zeta$ and $\Delta\eta$ are the mesh intervals in the ζ - and the η - directions, respectively.

Next we shall introduce several coefficients which are tied to the coordinate system (ζ, η) . Let

$$\begin{pmatrix} a_\zeta \\ a_\eta \end{pmatrix} \stackrel{\text{def}}{=} T^{-1} \begin{pmatrix} a_x \\ a_y \end{pmatrix}. \quad (2.24)$$

Also, for any $(j, k, n) \in \Omega$, let

$$\begin{pmatrix} (u_\zeta)_{j,k}^n \\ (u_\eta)_{j,k}^n \end{pmatrix} \stackrel{\text{def}}{=} T^t \begin{pmatrix} (u_x)_{j,k}^n \\ (u_y)_{j,k}^n \end{pmatrix}, \quad (2.25)$$

where T^t is the transpose of T . For those who are familiar with tensor analysis, the following comments will clarify the meaning of the above definitions:

- (a) (a_ζ, a_η) are the *contravariant* components with respect to the coordinates (ζ, η) for the spatial vector whose x - and y - components are a_x and a_y , respectively.
- (b) $((u_\zeta)_{j,k}^n, (u_\eta)_{j,k}^n)$ are the *covariant* components with respect to the coordinates (ζ, η) for the spatial vector whose x - and y - components are $(u_x)_{j,k}^n$ and $(u_y)_{j,k}^n$, respectively.
- (c) Because the contraction of the contravariant components of a vector and the covariant components of another is a scalar, Eq. (2.10) can be rewritten as

$$(u_t)_{j,k}^n = - [a_\zeta (u_\zeta)_{j,k}^n + a_\eta (u_\eta)_{j,k}^n]. \quad (2.26)$$

- (d) Under the *linear* coordinate transformation defined by Eqs. (2.19) and (2.20), $(\zeta - j\Delta\zeta, \eta - k\Delta\eta)$ are the contravariant components with respect to the coordinates (ζ, η) for the spatial vector whose x - and y - components are $x - x_{j,k}$ and $y - y_{j,k}$, respectively. Using the same reason given in (c), Eq. (2.11) implies that

$$u^*(x, y, t; j, k, n) = u^*(\zeta, \eta, t; j, k, n), \quad (2.27)$$

where

$$\begin{aligned} u^*(\zeta, \eta, t; j, k, n) \stackrel{\text{def}}{=} & u_{j,k}^n + (u_\zeta)_{j,k}^n [(\zeta - j\Delta\zeta) - a_\zeta(t - t^n)] \\ & + (u_\eta)_{j,k}^n [(\eta - k\Delta\eta) - a_\eta(t - t^n)]. \end{aligned} \quad (2.28)$$

Note that Eqs. (2.26) and (2.27) can also be verified directly using Eqs. (2.20), (2.22), (2.24), and (2.25).

Next, let (i)

$$a_{\zeta}^+ \stackrel{\text{def}}{=} \frac{6}{\Delta\zeta} a_{\zeta}, \quad \text{and} \quad a_{\eta}^+ \stackrel{\text{def}}{=} \frac{6}{\Delta\eta} a_{\eta}; \quad (2.29)$$

(ii)

$$(u_{\zeta}^+)^n_{j,k} \stackrel{\text{def}}{=} \frac{\Delta\zeta}{6} (u_{\zeta})^n_{j,k}, \quad \text{and} \quad (u_{\eta}^+)^n_{j,k} \stackrel{\text{def}}{=} \frac{\Delta\eta}{6} (u_{\eta})^n_{j,k}; \quad (2.30)$$

(iii)

$$\nu_{\zeta} \stackrel{\text{def}}{=} \frac{\Delta t}{4} a_{\zeta}^+, \quad \text{and} \quad \nu_{\eta} \stackrel{\text{def}}{=} \frac{\Delta t}{4} a_{\eta}^+; \quad (2.31)$$

and (iv)

$$\xi_{\zeta} \stackrel{\text{def}}{=} \frac{9\mu\Delta t}{8w^2h^2} (\Delta\zeta)^2, \quad \xi_{\eta} \stackrel{\text{def}}{=} \frac{9\mu\Delta t}{8w^2h^2} (\Delta\eta)^2, \quad \text{and} \quad \xi_{\tau} \stackrel{\text{def}}{=} \frac{9\mu\Delta t}{8w^2h^2} (\Delta\tau)^2, \quad (2.32)$$

where

$$\Delta\tau \stackrel{\text{def}}{=} 2\sqrt{b^2 + h^2}. \quad (2.33)$$

The coefficients defined in Eqs. (2.29) and (2.30) can be considered as the *normalized* counterparts of those defined in Eqs. (2.24) and (2.25). Also note that $\Delta\zeta$, $\Delta\eta$, and $\Delta\tau$, respectively, are the lengths of the three sides \overline{DF} , \overline{BD} , and \overline{FB} of $\triangle BDF$ depicted in Figs. 7(a)–(c). Moreover, by substituting Eq. (2.29) into Eq. (2.31), one has

$$\frac{a_{\zeta}\Delta t}{\Delta\zeta} = \frac{2}{3}\nu_{\zeta}, \quad \text{and} \quad \frac{a_{\eta}\Delta t}{\Delta\eta} = \frac{2}{3}\nu_{\eta}. \quad (2.34)$$

In other words, $(2/3)\nu_{\zeta}$ and $(2/3)\nu_{\eta}$ are the Courant numbers in the ζ - and η - directions, respectively.

Furthermore, let $\sigma_{11}^{(1)+}$, $\sigma_{11}^{(1)-}$, ..., be defined by

$$\sigma_{11}^{(1)\pm} \stackrel{\text{def}}{=} 1 - \nu_{\zeta} - \nu_{\eta}, \quad (2.35)$$

$$\sigma_{12}^{(1)\pm} \stackrel{\text{def}}{=} \pm(1 - \nu_{\zeta} - \nu_{\eta})(1 + \nu_{\zeta}) + \xi_{\eta} + \xi_{\tau} - \xi_{\zeta}, \quad (2.36)$$

$$\sigma_{13}^{(1)\pm} \stackrel{\text{def}}{=} \pm(1 - \nu_{\zeta} - \nu_{\eta})(1 + \nu_{\eta}) + \xi_{\zeta} + \xi_{\tau} - \xi_{\eta}, \quad (2.37)$$

$$\sigma_{21}^{(1)\pm} \stackrel{\text{def}}{=} 1 + \nu_{\zeta}, \quad (2.38)$$

$$\sigma_{22}^{(1)\pm} \stackrel{\text{def}}{=} \mp(1 + \nu_{\zeta})(2 - \nu_{\zeta}) - 2\xi_{\eta}, \quad (2.39)$$

$$\sigma_{23}^{(1)\pm} \stackrel{\text{def}}{=} \pm(1 + \nu_{\zeta})(1 + \nu_{\eta}) + \xi_{\zeta} + \xi_{\eta} - \xi_{\tau}, \quad (2.40)$$

$$\sigma_{31}^{(1)\pm} \stackrel{\text{def}}{=} 1 + \nu_{\eta}, \quad (2.41)$$

$$\sigma_{32}^{(1)\pm} \stackrel{\text{def}}{=} \pm(1 + \nu_\eta)(1 + \nu_\zeta) + \xi_\zeta + \xi_\eta - \xi_\tau, \quad (2.42)$$

$$\sigma_{33}^{(1)\pm} \stackrel{\text{def}}{=} \mp(1 + \nu_\eta)(2 - \nu_\eta) - 2\xi_\zeta, \quad (2.43)$$

$$\sigma_{11}^{(2)\pm} \stackrel{\text{def}}{=} 1 + \nu_\zeta + \nu_\eta, \quad (2.44)$$

$$\sigma_{12}^{(2)\pm} \stackrel{\text{def}}{=} \mp(1 + \nu_\zeta + \nu_\eta)(1 - \nu_\zeta) - \xi_\eta - \xi_\tau + \xi_\zeta, \quad (2.45)$$

$$\sigma_{13}^{(2)\pm} \stackrel{\text{def}}{=} \mp(1 + \nu_\zeta + \nu_\eta)(1 - \nu_\eta) - \xi_\zeta - \xi_\tau + \xi_\eta, \quad (2.46)$$

$$\sigma_{21}^{(2)\pm} \stackrel{\text{def}}{=} 1 - \nu_\zeta, \quad (2.47)$$

$$\sigma_{22}^{(2)\pm} \stackrel{\text{def}}{=} \pm(1 - \nu_\zeta)(2 + \nu_\zeta) + 2\xi_\eta, \quad (2.48)$$

$$\sigma_{23}^{(2)\pm} \stackrel{\text{def}}{=} \mp(1 - \nu_\zeta)(1 - \nu_\eta) - \xi_\zeta - \xi_\eta + \xi_\tau, \quad (2.49)$$

$$\sigma_{31}^{(2)\pm} \stackrel{\text{def}}{=} 1 - \nu_\eta, \quad (2.50)$$

$$\sigma_{32}^{(2)\pm} \stackrel{\text{def}}{=} \mp(1 - \nu_\eta)(1 - \nu_\zeta) - \xi_\zeta - \xi_\eta + \xi_\tau, \quad (2.51)$$

and

$$\sigma_{33}^{(2)\pm} \stackrel{\text{def}}{=} \pm(1 - \nu_\eta)(2 + \nu_\eta) + 2\xi_\zeta. \quad (2.52)$$

Note that:

- (a) Each of Eqs. (2.35)–(2.52) represents two equations. One corresponds to the upper signs while another, to the lower signs.
- (b) The definitions given in Eqs. (2.35)–(2.43) will be used in the first marching step of the a - μ scheme; while those given in Eqs. (2.44)–(2.52) will be used in the second marching step. It is seen that the expressions on the right sides of the former can be converted to those of the latter, respectively, by reversing the “+” and “-” signs. Moreover, for every pair of m and ℓ , $\sigma_{m\ell}^{(1)-}$ and $\sigma_{m\ell}^{(2)-}$ are converted to $\sigma_{m\ell}^{(2)+}$ and $\sigma_{m\ell}^{(1)+}$, respectively, if ν_ζ , ν_η , ξ_ζ , ξ_η , and ξ_τ are replaced by $-\nu_\zeta$, $-\nu_\eta$, $-\xi_\zeta$, $-\xi_\eta$, and $-\xi_\tau$, respectively.

Equations (2.12) and (2.13) are evaluated in Appendix A. With the aid of the above definitions, the results are summarized as follows:

- (a) Eq. (2.12) with $\ell = 1$:

$$\left[\sigma_{11}^{(1)+} u + \sigma_{12}^{(1)+} u_\zeta^+ + \sigma_{13}^{(1)+} u_\eta^+ \right]_{j,k}^{n+1/2} = \left[\sigma_{11}^{(1)-} u + \sigma_{12}^{(1)-} u_\zeta^+ + \sigma_{13}^{(1)-} u_\eta^+ \right]_{j+1/3, k+1/3}^n. \quad (2.53)$$

- (b) Eq. (2.12) with $\ell = 2$:

$$\left[\sigma_{21}^{(1)+} u + \sigma_{22}^{(1)+} u_\zeta^+ + \sigma_{23}^{(1)+} u_\eta^+ \right]_{j,k}^{n+1/2} = \left[\sigma_{21}^{(1)-} u + \sigma_{22}^{(1)-} u_\zeta^+ + \sigma_{23}^{(1)-} u_\eta^+ \right]_{j-2/3, k+1/3}^n. \quad (2.54)$$

(c) Eq. (2.12) with $\ell = 3$:

$$\left[\sigma_{31}^{(1)+} u + \sigma_{32}^{(1)+} u_{\zeta}^+ + \sigma_{33}^{(1)+} u_{\eta}^+ \right]_{j,k}^{n+1/2} = \left[\sigma_{31}^{(1)-} u + \sigma_{32}^{(1)-} u_{\zeta}^+ + \sigma_{33}^{(1)-} u_{\eta}^+ \right]_{j+1/3, k-2/3}^n. \quad (2.55)$$

(d) Eq. (2.13) with $\ell = 1$:

$$\left[\sigma_{11}^{(2)+} u + \sigma_{12}^{(2)+} u_{\zeta}^+ + \sigma_{13}^{(2)+} u_{\eta}^+ \right]_{j,k}^{n+1} = \left[\sigma_{11}^{(2)-} u + \sigma_{12}^{(2)-} u_{\zeta}^+ + \sigma_{13}^{(2)-} u_{\eta}^+ \right]_{j-1/3, k-1/3}^{n+1/2}. \quad (2.56)$$

(e) Eq. (2.13) with $\ell = 2$:

$$\left[\sigma_{21}^{(2)+} u + \sigma_{22}^{(2)+} u_{\zeta}^+ + \sigma_{23}^{(2)+} u_{\eta}^+ \right]_{j,k}^{n+1} = \left[\sigma_{21}^{(2)-} u + \sigma_{22}^{(2)-} u_{\zeta}^+ + \sigma_{23}^{(2)-} u_{\eta}^+ \right]_{j+2/3, k-1/3}^{n+1/2}. \quad (2.57)$$

(f) Eq. (2.13) with $\ell = 3$:

$$\left[\sigma_{31}^{(2)+} u + \sigma_{32}^{(2)+} u_{\zeta}^+ + \sigma_{33}^{(2)+} u_{\eta}^+ \right]_{j,k}^{n+1} = \left[\sigma_{31}^{(2)-} u + \sigma_{32}^{(2)-} u_{\zeta}^+ + \sigma_{33}^{(2)-} u_{\eta}^+ \right]_{j-1/3, k+2/3}^{n+1/2}. \quad (2.58)$$

Here $(j, k, n+1/2) \in \Omega_1$ is assumed in Eqs. (2.53)–(2.55); while $(j, k, n+1) \in \Omega_2$ is assumed in Eqs. (2.56)–(2.58). Also, to simplify notation, in the above and hereafter we adopt a convention that can be explained using the expression on the left side of Eq. (2.56) as an example, i.e.,

$$\left[\sigma_{11}^{(2)+} u + \sigma_{12}^{(2)+} u_{\zeta}^+ + \sigma_{13}^{(2)+} u_{\eta}^+ \right]_{j,k}^{n+1} \stackrel{\text{def}}{=} \left[\sigma_{11}^{(2)+} u_{j,k}^{n+1} + \sigma_{12}^{(2)+} (u_{\zeta}^+)_{j,k}^{n+1} + \sigma_{13}^{(2)+} (u_{\eta}^+)_{j,k}^{n+1} \right].$$

Consider the special case with $\mu = 0$. It follows from Eq. (2.32) that

$$\xi_{\zeta} = \xi_{\eta} = \xi_r = 0. \quad (\mu = 0) \quad (2.59)$$

Combining Eq. (2.59) with Eqs. (2.35)–(2.37), one concludes that $\sigma_{11}^{(1)\pm}$, $\sigma_{12}^{(1)\pm}$, and $\sigma_{13}^{(1)\pm}$ contain a common factor $(1 - \nu_{\zeta} - \nu_{\eta})$. Similarly, each of three consecutive pairs of coefficients defined in Eqs. (2.38)–(2.52) also contain a common factor. As a result, one concludes that:

(a) Eq. (2.53) is satisfied by either $1 - \nu_{\zeta} - \nu_{\eta} = 0$ or

$$\left[u + (1 + \nu_{\zeta}) u_{\zeta}^+ + (1 + \nu_{\eta}) u_{\eta}^+ \right]_{j,k}^{n+1/2} = \left[u - (1 + \nu_{\zeta}) u_{\zeta}^+ - (1 + \nu_{\eta}) u_{\eta}^+ \right]_{j+1/3, k+1/3}^n. \quad (2.60)$$

(b) Eq. (2.54) is satisfied by either $1 + \nu_{\zeta} = 0$ or

$$\left[u - (2 - \nu_{\zeta}) u_{\zeta}^+ + (1 + \nu_{\eta}) u_{\eta}^+ \right]_{j,k}^{n+1/2} = \left[u + (2 - \nu_{\zeta}) u_{\zeta}^+ - (1 + \nu_{\eta}) u_{\eta}^+ \right]_{j-2/3, k+1/3}^n. \quad (2.61)$$

(c) Eq. (2.55) is satisfied by either $1 + \nu_\eta = 0$ or

$$\left[u + (1 + \nu_\zeta)u_\zeta^+ - (2 - \nu_\eta)u_\eta^+ \right]_{j,k}^{n+1/2} = \left[u - (1 + \nu_\zeta)u_\zeta^+ + (2 - \nu_\eta)u_\eta^+ \right]_{j+1/3, k-2/3}^n. \quad (2.62)$$

(d) Eq. (2.56) is satisfied by either $1 + \nu_\zeta + \nu_\eta = 0$ or

$$\left[u - (1 - \nu_\zeta)u_\zeta^+ - (1 - \nu_\eta)u_\eta^+ \right]_{j,k}^{n+1} = \left[u + (1 - \nu_\zeta)u_\zeta^+ + (1 - \nu_\eta)u_\eta^+ \right]_{j-1/3, k-1/3}^{n+1/2}. \quad (2.63)$$

(e) Eq. (2.57) is satisfied by either $1 - \nu_\zeta = 0$ or

$$\left[u + (2 + \nu_\zeta)u_\zeta^+ - (1 - \nu_\eta)u_\eta^+ \right]_{j,k}^{n+1} = \left[u - (2 + \nu_\zeta)u_\zeta^+ + (1 - \nu_\eta)u_\eta^+ \right]_{j+2/3, k-1/3}^{n+1/2}. \quad (2.64)$$

(f) Eq. (2.58) is satisfied by either $1 - \nu_\eta = 0$ or

$$\left[u - (1 - \nu_\zeta)u_\zeta^+ + (2 + \nu_\eta)u_\eta^+ \right]_{j,k}^{n+1} = \left[u + (1 - \nu_\zeta)u_\zeta^+ - (2 + \nu_\eta)u_\eta^+ \right]_{j-1/3, k+2/3}^{n+1/2}. \quad (2.65)$$

Here $(j, k, n+1/2) \in \Omega_1$ is assumed in Eqs. (2.60)–(2.62); while $(j, k, n+1) \in \Omega_2$ is assumed in Eqs. (2.63)–(2.65). The current “a” scheme, i.e., the scheme that solves Eq. (2.1) with $\mu = 0$, will be constructed using Eqs. (2.60)–(2.65) instead of Eqs. (2.53)–(2.58). Assuming $\mu = 0$, Eqs. (2.60)–(2.65) imply Eqs. (2.53)–(2.58). However, the reverse is false unless one assumes that

$$\left[1 - (\nu_\zeta + \nu_\eta)^2 \right] (1 - \nu_\zeta^2) (1 - \nu_\eta^2) \neq 0. \quad (2.66)$$

Note that the expressions within the brackets in the first three equations in Eqs. (2.60)–(2.65), respectively, can be converted to those in the last three by reversing the “+” and “−” signs.

Let $s_1^{(1)}$, $s_2^{(1)}$, $s_3^{(1)}$, $s_1^{(2)}$, $s_2^{(2)}$, and $s_3^{(2)}$ denote the expressions on the right sides of Eqs. (2.60)–(2.65), respectively. Then it can be shown that Eqs. (2.60)–(2.62) are equivalent to

$$u_{j,k}^{n+1/2} = \frac{1}{3} \left[(1 - \nu_\zeta - \nu_\eta)s_1^{(1)} + (1 + \nu_\zeta)s_2^{(1)} + (1 + \nu_\eta)s_3^{(1)} \right], \quad (2.67)$$

$$(u_\zeta^+)^{n+1/2} = \frac{1}{3} \left(s_1^{(1)} - s_2^{(1)} \right), \quad (2.68)$$

and

$$(u_\eta^+)^{n+1/2} = \frac{1}{3} \left(s_1^{(1)} - s_3^{(1)} \right), \quad (2.69)$$

where $(j, k, n+1/2) \in \Omega_1$. Also Eqs. (2.63)–(2.65) are equivalent to

$$u_{j,k}^{n+1} = \frac{1}{3} \left[(1 + \nu_\zeta + \nu_\eta)s_1^{(2)} + (1 - \nu_\zeta)s_2^{(2)} + (1 - \nu_\eta)s_3^{(2)} \right], \quad (2.70)$$

$$(u_{\zeta}^+)_{j,k}^{n+1} = \frac{1}{3} (s_2^{(2)} - s_1^{(2)}), \quad (2.71)$$

and

$$(u_{\eta}^+)_{j,k}^{n+1} = \frac{1}{3} (s_3^{(2)} - s_1^{(2)}). \quad (2.72)$$

where $(j, k, n+1) \in \Omega_2$.

To proceed, for any $(j, k, n) \in \Omega$, let

$$\vec{q}(j, k, n) \stackrel{\text{def}}{=} \begin{pmatrix} u \\ u_{\zeta}^+ \\ u_{\eta}^+ \end{pmatrix}_{j,k}^n. \quad (2.73)$$

Let the column matrices $\vec{\alpha}_{\ell}^{(k)}$ and $\vec{\beta}_{\ell}^{(k)}$, $k = 1, 2$, and $\ell = 1, 2, 3$, be defined by

$$\vec{\alpha}_1^{(1)} \stackrel{\text{def}}{=} \frac{1}{3} \begin{pmatrix} 1 - \nu_{\zeta} - \nu_{\eta} \\ 1 \\ 1 \end{pmatrix}, \quad \text{and} \quad \vec{\beta}_1^{(1)} \stackrel{\text{def}}{=} \begin{pmatrix} 1 \\ -(1 + \nu_{\zeta}) \\ -(1 + \nu_{\eta}) \end{pmatrix}, \quad (2.74)$$

$$\vec{\alpha}_2^{(1)} \stackrel{\text{def}}{=} \frac{1}{3} \begin{pmatrix} 1 + \nu_{\zeta} \\ -1 \\ 0 \end{pmatrix}, \quad \text{and} \quad \vec{\beta}_2^{(1)} \stackrel{\text{def}}{=} \begin{pmatrix} 1 \\ 2 - \nu_{\zeta} \\ -(1 + \nu_{\eta}) \end{pmatrix}, \quad (2.75)$$

$$\vec{\alpha}_3^{(1)} \stackrel{\text{def}}{=} \frac{1}{3} \begin{pmatrix} 1 + \nu_{\eta} \\ 0 \\ -1 \end{pmatrix}, \quad \text{and} \quad \vec{\beta}_3^{(1)} \stackrel{\text{def}}{=} \begin{pmatrix} 1 \\ -(1 + \nu_{\zeta}) \\ 2 - \nu_{\eta} \end{pmatrix}, \quad (2.76)$$

$$\vec{\alpha}_1^{(2)} \stackrel{\text{def}}{=} \frac{1}{3} \begin{pmatrix} 1 + \nu_{\zeta} + \nu_{\eta} \\ -1 \\ -1 \end{pmatrix}, \quad \text{and} \quad \vec{\beta}_1^{(2)} \stackrel{\text{def}}{=} \begin{pmatrix} 1 \\ 1 - \nu_{\zeta} \\ 1 - \nu_{\eta} \end{pmatrix}, \quad (2.77)$$

$$\vec{\alpha}_2^{(2)} \stackrel{\text{def}}{=} \frac{1}{3} \begin{pmatrix} 1 - \nu_{\zeta} \\ 1 \\ 0 \end{pmatrix}, \quad \text{and} \quad \vec{\beta}_2^{(2)} \stackrel{\text{def}}{=} \begin{pmatrix} 1 \\ -(2 + \nu_{\zeta}) \\ 1 - \nu_{\eta} \end{pmatrix}, \quad (2.78)$$

and

$$\vec{\alpha}_3^{(2)} \stackrel{\text{def}}{=} \frac{1}{3} \begin{pmatrix} 1 - \nu_{\eta} \\ 0 \\ 1 \end{pmatrix}, \quad \text{and} \quad \vec{\beta}_3^{(2)} \stackrel{\text{def}}{=} \begin{pmatrix} 1 \\ 1 - \nu_{\zeta} \\ -(2 + \nu_{\eta}) \end{pmatrix}. \quad (2.79)$$

Let the 3×3 matrices of rank one $Q_\ell^{(k)}$, $k = 1, 2$, and $\ell = 1, 2, 3$, be defined by

$$Q_\ell^{(k)} \stackrel{\text{def}}{=} \alpha_\ell^{(k)} \left(\bar{\beta}_\ell^{(k)} \right)^t, \quad (2.80)$$

where the row matrix $\left(\bar{\beta}_\ell^{(k)} \right)^t$ is the transpose of the column matrix $\bar{\beta}_\ell^{(k)}$. Note that the explicit forms of the matrices $Q_\ell^{(k)}$ defined above, respectively, can be obtained from Eqs. (3.50)–(3.55) by letting $\epsilon = 0$.

By their definitions, each of $s_\ell^{(k)}$, $k = 1, 2$, and $\ell = 1, 2, 3$, can be expressed as the product of one of the row matrices $\left(\bar{\beta}_\ell^{(k)} \right)^t$, $k = 1, 2$ and $\ell = 1, 2, 3$, and one of the column matrices defined in Eq. (2.73). As an example,

$$s_1^{(1)} = \left(\bar{\beta}_1^{(1)} \right)^t \bar{q}(j + 1/3, k + 1/3, n). \quad (2.81)$$

Thus, Eqs. (2.67)–(2.69) can be expressed as

$$\begin{aligned} \bar{q}(j, k, n + 1/2) &= Q_1^{(1)} \bar{q}(j + 1/3, k + 1/3, n) + Q_2^{(1)} \bar{q}(j - 2/3, k + 1/3, n) \\ &+ Q_3^{(1)} \bar{q}(j + 1/3, k - 2/3, n), \quad (j, k, n + 1/2) \in \Omega_1. \end{aligned} \quad (2.82)$$

Similarly, Eqs. (2.70)–(2.72) can be expressed as

$$\begin{aligned} \bar{q}(j, k, n + 1) &= Q_1^{(2)} \bar{q}(j - 1/3, k - 1/3, n + 1/2) + Q_2^{(2)} \bar{q}(j + 2/3, k - 1/3, n + 1/2) \\ &+ Q_3^{(2)} \bar{q}(j - 1/3, k + 2/3, n + 1/2), \quad (j, k, n + 1) \in \Omega_2. \end{aligned} \quad (2.83)$$

The marching procedure in the a scheme is formed by applying the marching steps defined by Eqs. (2.82) and (2.83) successively.

As a preliminary for future development, we apply Eq. (2.82) and then Eq. (2.83). The result is:

$$\begin{aligned} \bar{q}(j, k, n + 1/2) &= Q_1^{(1)} Q_2^{(2)} \bar{q}(j + 1, k, n - 1/2) + Q_1^{(1)} Q_3^{(2)} \bar{q}(j, k + 1, n - 1/2) \\ &+ Q_2^{(1)} Q_1^{(2)} \bar{q}(j - 1, k, n - 1/2) + Q_2^{(1)} Q_3^{(2)} \bar{q}(j - 1, k + 1, n - 1/2) \\ &+ Q_3^{(1)} Q_1^{(2)} \bar{q}(j, k - 1, n - 1/2) + Q_3^{(1)} Q_2^{(2)} \bar{q}(j + 1, k - 1, n - 1/2) \\ &+ (Q_1^{(1)} Q_1^{(2)} + Q_2^{(1)} Q_2^{(2)} + Q_3^{(1)} Q_3^{(2)}) \bar{q}(j, k, n - 1/2), \end{aligned} \quad (2.84)$$

where $(j, k, n + 1/2) \in \Omega_1$. Similarly, by applying Eq. (2.83) and then Eq. (2.82), one concludes that

$$\begin{aligned} \bar{q}(j, k, n + 1) &= Q_1^{(2)} Q_2^{(1)} \bar{q}(j - 1, k, n) + Q_1^{(2)} Q_3^{(1)} \bar{q}(j, k - 1, n) \\ &+ Q_2^{(2)} Q_1^{(1)} \bar{q}(j + 1, k, n) + Q_2^{(2)} Q_3^{(1)} \bar{q}(j + 1, k - 1, n) \\ &+ Q_3^{(2)} Q_1^{(1)} \bar{q}(j, k + 1, n) + Q_3^{(2)} Q_2^{(1)} \bar{q}(j - 1, k + 1, n) \\ &+ (Q_1^{(2)} Q_1^{(1)} + Q_2^{(2)} Q_2^{(1)} + Q_3^{(2)} Q_3^{(1)}) \bar{q}(j, k, n), \end{aligned} \quad (2.85)$$

where $(j, k, n + 1) \in \Omega_2$.

Next we shall consider the flux conservation conditions Eqs. (2.53)–(2.58) assuming $\mu > 0$. Let $\Delta^{(1)}$ and $\Delta^{(2)}$ be the determinants of the matrices formed by $\sigma_{k\ell}^{(1)+}$ and $\sigma_{k\ell}^{(2)+}$, $k, \ell = 1, 2, 3$, respectively. It is shown in Appendix A that, for any μ ,

$$\Delta^{(1)} = 3 \left[3(1 + \nu_\zeta)(1 + \nu_\eta)(1 - \nu_\zeta - \nu_\eta) + 2(1 + \nu_\zeta)(1 - \nu_\zeta - \nu_\eta)\xi_\zeta \right. \\ \left. + 2(1 + \nu_\eta)(1 - \nu_\zeta - \nu_\eta)\xi_\eta + 2(1 + \nu_\zeta)(1 + \nu_\eta)\xi_\tau + \left(\frac{9\mu\Delta t}{2wh} \right)^2 \right], \quad (2.86)$$

and

$$\Delta^{(2)} = 3 \left[3(1 - \nu_\zeta)(1 - \nu_\eta)(1 + \nu_\zeta + \nu_\eta) + 2(1 - \nu_\zeta)(1 + \nu_\zeta + \nu_\eta)\xi_\zeta \right. \\ \left. + 2(1 - \nu_\eta)(1 + \nu_\zeta + \nu_\eta)\xi_\eta + 2(1 - \nu_\zeta)(1 - \nu_\eta)\xi_\tau + \left(\frac{9\mu\Delta t}{2wh} \right)^2 \right]. \quad (2.87)$$

Because $\mu > 0$, $\xi_\zeta > 0$, $\xi_\eta > 0$, and $\xi_\tau > 0$, it follows from Eqs. (2.86) and (2.87) that $\Delta^{(1)} > 0$ and $\Delta^{(2)} > 0$ if

$$|\nu_\zeta| \leq 1, \quad |\nu_\eta| \leq 1, \quad \text{and} \quad |\nu_\zeta + \nu_\eta| \leq 1. \quad (2.88)$$

In the following discussions, we assume $\Delta^{(1)} \neq 0$ and $\Delta^{(2)} \neq 0$.

Let $\acute{s}_1^{(1)}$, $\acute{s}_2^{(1)}$, $\acute{s}_3^{(1)}$, $\acute{s}_1^{(2)}$, $\acute{s}_2^{(2)}$, and $\acute{s}_3^{(2)}$ denote the expressions on the right sides of Eqs. (2.53)–(2.58), respectively. Let

$$\rho_{21}^{(1)} \stackrel{\text{def}}{=} [3(1 + \nu_\zeta)(1 + \nu_\eta) + (3 + 2\nu_\zeta + \nu_\eta)\xi_\zeta + (1 + \nu_\eta)(\xi_\eta - \xi_\tau)] / \Delta^{(1)}, \quad (2.89)$$

$$\rho_{22}^{(1)} \stackrel{\text{def}}{=} [-3(1 + \nu_\eta)(1 - \nu_\zeta - \nu_\eta) - (3 - 2\nu_\zeta - \nu_\eta)\xi_\zeta + (1 + \nu_\eta)(\xi_\eta - \xi_\tau)] / \Delta^{(1)}, \quad (2.90)$$

$$\rho_{23}^{(1)} \stackrel{\text{def}}{=} [(2\nu_\zeta + \nu_\eta)\xi_\zeta + (2 - \nu_\eta)(\xi_\tau - \xi_\eta)] / \Delta^{(1)}, \quad (2.91)$$

$$\rho_{31}^{(1)} \stackrel{\text{def}}{=} [3(1 + \nu_\zeta)(1 + \nu_\eta) + (3 + \nu_\zeta + 2\nu_\eta)\xi_\eta + (1 + \nu_\zeta)(\xi_\zeta - \xi_\tau)] / \Delta^{(1)}, \quad (2.92)$$

$$\rho_{32}^{(1)} \stackrel{\text{def}}{=} [(\nu_\zeta + 2\nu_\eta)\xi_\eta + (2 - \nu_\zeta)(\xi_\tau - \xi_\zeta)] / \Delta^{(1)}, \quad (2.93)$$

$$\rho_{33}^{(1)} \stackrel{\text{def}}{=} [-3(1 + \nu_\zeta)(1 - \nu_\zeta - \nu_\eta) - (3 - \nu_\zeta - 2\nu_\eta)\xi_\eta + (1 + \nu_\zeta)(\xi_\zeta - \xi_\tau)] / \Delta^{(1)}, \quad (2.94)$$

$$\rho_{21}^{(2)} \stackrel{\text{def}}{=} [-3(1 - \nu_\zeta)(1 - \nu_\eta) - (3 - 2\nu_\zeta - \nu_\eta)\xi_\zeta + (1 - \nu_\eta)(\xi_\tau - \xi_\eta)] / \Delta^{(2)}, \quad (2.95)$$

$$\rho_{22}^{(2)} \stackrel{\text{def}}{=} [3(1 - \nu_\eta)(1 + \nu_\zeta + \nu_\eta) + (3 + 2\nu_\zeta + \nu_\eta)\xi_\zeta + (1 - \nu_\eta)(\xi_\tau - \xi_\eta)] / \Delta^{(2)}, \quad (2.96)$$

$$\rho_{23}^{(2)} \stackrel{\text{def}}{=} [(2\nu_\zeta + \nu_\eta)\xi_\zeta + (2 + \nu_\eta)(\xi_\eta - \xi_\tau)] / \Delta^{(2)}, \quad (2.97)$$

$$\rho_{31}^{(2)} \stackrel{\text{def}}{=} [-3(1 - \nu_\zeta)(1 - \nu_\eta) - (3 - \nu_\zeta - 2\nu_\eta)\xi_\eta + (1 - \nu_\zeta)(\xi_\tau - \xi_\zeta)] / \Delta^{(2)}, \quad (2.98)$$

$$\rho_{32}^{(2)} \stackrel{\text{def}}{=} [(\nu_\zeta + 2\nu_\eta)\xi_\eta + (2 + \nu_\zeta)(\xi_\zeta - \xi_\tau)] / \Delta^{(2)}, \quad (2.99)$$

and

$$\rho_{33}^{(2)} \stackrel{\text{def}}{=} [3(1 - \nu_\zeta)(1 + \nu_\zeta + \nu_\eta) + (3 + \nu_\zeta + 2\nu_\eta)\xi_\eta + (1 - \nu_\zeta)(\xi_\tau - \xi_\zeta)] / \Delta^{(2)}. \quad (2.100)$$

Then it can be shown that Eqs. (2.53)–(2.55) are equivalent to

$$u_{j,k}^{n+1/2} = \frac{1}{3} \left(\dot{s}_1^{(1)} + \dot{s}_2^{(1)} + \dot{s}_3^{(1)} \right), \quad (2.101)$$

$$(u_\zeta^+)^{n+1/2}_{j,k} = \rho_{21}^{(1)} \dot{s}_1^{(1)} + \rho_{22}^{(1)} \dot{s}_2^{(1)} + \rho_{23}^{(1)} \dot{s}_3^{(1)}, \quad (2.102)$$

and

$$(u_\eta^+)^{n+1/2}_{j,k} = \rho_{31}^{(1)} \dot{s}_1^{(1)} + \rho_{32}^{(1)} \dot{s}_2^{(1)} + \rho_{33}^{(1)} \dot{s}_3^{(1)}, \quad (2.103)$$

where $(j, k, n + 1/2) \in \Omega_1$. Also Eqs. (2.56)–(2.58) are equivalent to

$$u_{j,k}^{n+1} = \frac{1}{3} \left(\dot{s}_1^{(2)} + \dot{s}_2^{(2)} + \dot{s}_3^{(2)} \right), \quad (2.104)$$

$$(u_\zeta^+)^{n+1}_{j,k} = \rho_{21}^{(2)} \dot{s}_1^{(2)} + \rho_{22}^{(2)} \dot{s}_2^{(2)} + \rho_{23}^{(2)} \dot{s}_3^{(2)}, \quad (2.105)$$

and

$$(u_\eta^+)^{n+1}_{j,k} = \rho_{31}^{(2)} \dot{s}_1^{(2)} + \rho_{32}^{(2)} \dot{s}_2^{(2)} + \rho_{33}^{(2)} \dot{s}_3^{(2)}, \quad (2.106)$$

where $(j, k, n + 1) \in \Omega_2$. Equations (2.101)–(2.103), and Eqs. (2.104)–(2.106), respectively, can be expressed as Eqs. (2.82) and (2.83) if one defines

$$Q_\ell^{(k)} \stackrel{\text{def}}{=} \begin{pmatrix} \frac{1}{3} \\ \rho_{2\ell}^{(k)} \\ \rho_{3\ell}^{(k)} \end{pmatrix} (\sigma_{\ell 1}^{(k)-} \quad \sigma_{\ell 2}^{(k)-} \quad \sigma_{\ell 3}^{(k)-}), \quad k = 1, 2, \text{ and } \ell = 1, 2, 3. \quad (2.107)$$

This follows from the fact that $\dot{s}_\ell^{(k)}$ is the product of the row matrix which appears on the right side of Eq. (2.107) and one of the column matrices defined in Eq. (2.73). With the above definition, the marching procedure in the current a - μ scheme, i.e., the scheme which solves Eq. (2.1) with $\mu > 0$, is formed by applying the marching steps defined by Eqs. (2.82) and (2.83) successively. Obviously, Eqs. (2.84) and (2.85) are also valid for the a - μ scheme.

Note that the a - μ scheme can also be used to solve Eq. (2.1) with $\mu = 0$ as long as $\Delta^{(1)} \neq 0$ and $\Delta^{(2)} \neq 0$. According to Eqs. (2.32), (2.86) and (2.87), the last two conditions are reduced to Eq. (2.66) if $\mu = 0$. The current a scheme, however, is still applicable even if Eq. (2.66) is violated.

The a - μ scheme has several nontraditional features. They are summarized in the following remarks:

- (a) Both the a and the a - μ schemes have the simplest stencil in each of their two marching steps, i.e., a tetrahedron with a vertex at the upper time level and the other three vertices at the lower time level.
- (b) Each of the conservation conditions Eqs. (2.53)–(2.58) represents a relation among the marching variables associated with *only two neighboring SEs*. This is a fundamental difference between the current method and other traditional methods.
- (c) For both the a and the a - μ schemes, we have

$$\vec{q}(j, k, n + 1) \rightarrow \vec{q}(j, k, n) \quad \text{as } \Delta t \rightarrow 0, \quad (j, k, n) \in \Omega, \quad (2.108)$$

if a , μ , and Δx are held constant. The above property usually is not shared by other schemes which uses a mesh that is staggered in time, e.g., the Lax scheme [9, p.97]. The proof of Eq. (2.108) follows from Eqs. (2.84) and (2.85), and the fact that, as $\Delta t \rightarrow 0$,

$$\begin{aligned} Q_1^{(1)} Q_2^{(2)} &\rightarrow 0, & Q_1^{(1)} Q_3^{(2)} &\rightarrow 0, & Q_2^{(1)} Q_1^{(2)} &\rightarrow 0, & Q_2^{(1)} Q_3^{(2)} &\rightarrow 0, \\ Q_3^{(1)} Q_1^{(2)} &\rightarrow 0, & Q_3^{(1)} Q_2^{(2)} &\rightarrow 0, & (Q_1^{(1)} Q_1^{(2)} + Q_2^{(1)} Q_2^{(2)} + Q_3^{(1)} Q_3^{(2)}) &\rightarrow 1, \\ Q_1^{(2)} Q_2^{(1)} &\rightarrow 0, & Q_1^{(2)} Q_3^{(1)} &\rightarrow 0, & Q_2^{(2)} Q_1^{(1)} &\rightarrow 0, & Q_2^{(2)} Q_3^{(1)} &\rightarrow 0, \\ Q_3^{(2)} Q_1^{(1)} &\rightarrow 0, & Q_3^{(2)} Q_2^{(1)} &\rightarrow 0, & (Q_1^{(2)} Q_1^{(1)} + Q_2^{(2)} Q_2^{(1)} + Q_3^{(2)} Q_3^{(1)}) &\rightarrow 1. \end{aligned} \quad (2.109)$$

Alternatively, Eq. (2.108) can be proved using a line of argument involving flux conservation similar to that given in the last paragraph on p.8 of [5].

- (d) Both the a and the a - μ schemes are so called “two-way” marching schemes [5, p.11]. In other words, the same flux conservation relations Eqs. (2.12) and (2.13) can be used to construct the backward time marching versions of the a and a - μ schemes. More discussions on this subject are given in Appendix C.
- (e) It will be shown in Sec. 5 that the a scheme is stable if

$$|\nu_\zeta| < 1.5, \quad |\nu_\eta| < 1.5, \quad \text{and} \quad |\nu_\zeta + \nu_\eta| < 1.5. \quad (2.110)$$

As depicted in Fig. 9, the domain of stability defined by Eq. (2.110) is a hexagonal region in the ν_ζ - ν_η space. Moreover, it will be shown that (i) Eq. (2.110) can be interpreted as the requirement that the physical domain of dependence of Eq. (3.1) should fall within the numerical domain of dependence; and (ii) the a scheme is neutrally stable, i.e., free from numerical diffusion, if it is stable.

Also it will be shown that the $a-\mu$ scheme is unconditionally stable for the pure diffusion case, i.e., when $a = 0$. The stability conditions of the $a-\mu$ scheme with $\mu \neq 0$ and $a \neq 0$ are more complex. They also will be discussed in Sec. 5.

Finally, it should be emphasized that, with the aid of Eqs. (2.19)–(2.22), (2.24), and (2.25), the a and the $a-\mu$ schemes can also be expressed in terms of the marching variables and the coefficients tied to the coordinates (x, y) . In other words, the coordinates (ζ, η) are introduced solely for the purpose of simplifying the current development. *The essence of the a and $a-\mu$ schemes, and the schemes to be introduced in the following sections, is not dependent on the choice of the coordinates in terms of which these schemes are expressed.*

3. The a - ϵ Scheme

The a scheme is neutrally stable and reversible in time. It is well known that a neutrally stable numerical analogue of

$$\frac{\partial u}{\partial t} + a_x \frac{\partial u}{\partial x} + a_y \frac{\partial u}{\partial y} = 0, \quad (3.1)$$

such as the a scheme, generally becomes unstable when it is extended to model the Euler equations. It is also obvious that a scheme that is reversible in time cannot model a physical problem that is irreversible in time, e.g., an inviscid flow problem involving shocks. In this section, we consider Eq. (3.1) and attempt to modify the a scheme such that it can be extended to model the Euler equations.

To proceed, note that the CEs used in Sec. 2 will not be used in this section. As a result, Eqs. (2.12) and (2.13) will no longer be assumed. Instead, the CEs to be used are

$$CE^{(1)}(j, k, n + 1/2) \stackrel{\text{def}}{=} [CE_1^{(1)}(j, k, n + 1/2)] \cup [CE_2^{(1)}(j, k, n + 1/2)] \cup [CE_3^{(1)}(j, k, n + 1/2)], \quad (3.2)$$

where $(j, k, n + 1/2) \in \Omega_1$, and

$$CE^{(2)}(j, k, n + 1) \stackrel{\text{def}}{=} [CE_1^{(2)}(j, k, n + 1)] \cup [CE_2^{(2)}(j, k, n + 1)] \cup [CE_3^{(2)}(j, k, n + 1)], \quad (3.3)$$

where $(j, k, n + 1) \in \Omega_2$. We shall assume that the total flux leaving the boundary of any new CE vanishes, i.e.,

$$\oint_{S(CE^{(1)}(j, k, n + 1/2))} \vec{h}^* \cdot d\vec{s} = 0, \quad (3.4)$$

and

$$\oint_{S(CE^{(2)}(j, k, n + 1))} \vec{h}^* \cdot d\vec{s} = 0. \quad (3.5)$$

Obviously, (i) E_3 can be filled with the new CEs, and (ii) the total flux leaving the boundary of any space-time region that is the union of any new CEs will also vanish.

Moreover, it can be shown that Eqs. (3.4) and (3.5), respectively, are equivalent to Eqs. (2.67) and (2.70).

Proof: By subtracting the expressions on the right sides of Eqs. (2.53)–(2.55), respectively, from those on the left sides, and then multiplying the results by $2wh/3$, we obtain the fluxes leaving $CE_1^{(1)}(j, k, n + 1/2)$, $CE_2^{(1)}(j, k, n + 1/2)$, and $CE_3^{(1)}(j, k, n + 1/2)$, respectively (see Appendix A). Because the flux leaving an interface from the CE on one side is the negative of that leaving the same interface from the CE on the other side, it is easy to see that the flux leaving $CE^{(1)}(j, k, n + 1/2)$ (which is the union of $CE_\ell^{(1)}(j, k, n + 1/2)$, $\ell = 1, 2, 3$)

is the sum of the fluxes leaving $CE_\ell^{(1)}(j, k, n + 1/2)$, $\ell = 1, 2, 3$. Thus, the flux leaving $CE^{(1)}(j, k, n + 1/2)$ can be obtained by subtracting the sum of the expressions on the right sides of Eqs. (2.53)–(2.55) from that on the left side, and then multiplying the result by $2wh/3$. Furthermore, we have

$$\sigma_{11}^{(k)\pm} + \sigma_{21}^{(k)\pm} + \sigma_{31}^{(k)\pm} = 3, \quad k = 1, 2, \quad (3.6)$$

and

$$\sigma_{12}^{(k)\pm} + \sigma_{22}^{(k)\pm} + \sigma_{32}^{(k)\pm} = \sigma_{13}^{(k)\pm} + \sigma_{23}^{(k)\pm} + \sigma_{33}^{(k)\pm} = 0, \quad k = 1, 2. \quad (3.7)$$

With the aid of the above considerations, and the fact that the expressions on the left sides of Eqs. (2.53)–(2.55) are all evaluated at the same mesh point $(j, k, n + 1/2)$, it becomes obvious that Eq. (3.4) is equivalent to the statement that $u_{j,k}^{n+1/2}$ is $1/3$ of the sum on the right sides of Eqs. (2.53)–(2.55). By using Eqs. (2.35)–(2.43) and the assumption $\mu = 0$, we arrive at the conclusion that Eq. (3.4) is equivalent to Eq. (2.67). By invoking a similar argument involving Eqs. (2.56)–(2.58), and (2.44)–(2.52), we also conclude that Eq. (3.5) is equivalent to Eq. (2.70). QED.

As a result, Eqs. (2.67) and (2.70) are shared by the a scheme and the current modified scheme. In this section we shall describe how the other equations in the a scheme i.e., Eqs. (2.68), (2.69), (2.71), and (2.72), can be modified such that the numerical diffusion of the resulting new scheme can be controlled by an adjustable parameter ϵ .

To proceed, for any $(j, k, n + 1/2) \in \Omega_1$, let

$$u'_{j+1/3, k+1/3}{}^{n+1/2} \stackrel{\text{def}}{=} \left(u + \frac{\Delta t}{2} u_t \right)_{j+1/3, k+1/3}^n, \quad (3.8)$$

$$u'_{j-2/3, k+1/3}{}^{n+1/2} \stackrel{\text{def}}{=} \left(u + \frac{\Delta t}{2} u_t \right)_{j-2/3, k+1/3}^n, \quad (3.9)$$

and

$$u'_{j+1/3, k-2/3}{}^{n+1/2} \stackrel{\text{def}}{=} \left(u + \frac{\Delta t}{2} u_t \right)_{j+1/3, k-2/3}^n. \quad (3.10)$$

By their definitions, $u'_{j+1/3, k+1/3}{}^{n+1/2}$, $u'_{j-2/3, k+1/3}{}^{n+1/2}$, and $u'_{j+1/3, k-2/3}{}^{n+1/2}$ can be considered as the finite-difference approximations of u at $(j + 1/3, k + 1/3, n + 1/2)$, $(j - 2/3, k + 1/3, n + 1/2)$, and $(j + 1/3, k - 2/3, n + 1/2)$, respectively. With the aid of Eqs. (2.10), (A.10) and (2.31), Eqs. (3.8)–(3.10) imply that

$$u'_{j+1/3, k+1/3}{}^{n+1/2} = \left[u - 2 \left(\nu_\zeta u_\zeta^+ + \nu_\eta u_\eta^+ \right) \right]_{j+1/3, k+1/3}^n, \quad (3.11)$$

$$u'_{j-2/3, k+1/3}{}^{n+1/2} = \left[u - 2 \left(\nu_\zeta u_\zeta^+ + \nu_\eta u_\eta^+ \right) \right]_{j-2/3, k+1/3}^n, \quad (3.12)$$

and

$$u'_{j+1/3,k-2/3}{}^{n+1/2} = \left[u - 2 \left(\nu_\zeta u_\zeta^+ + \nu_\eta u_\eta^+ \right) \right]_{j+1/3,k-2/3}^n \quad (3.13)$$

In Fig. 10(a), P , Q , and R are three points in the ζ - η - u space. Using the coordinates given in the same figure, it can be shown that these points are on a plane represented by

$$u = (u'_\zeta)_{j,k}{}^{n+1/2}(\zeta - j\Delta\zeta) + (u'_\eta)_{j,k}{}^{n+1/2}(\eta - k\Delta\eta) + u'_{j,k}{}^{n+1/2}, \quad (3.14)$$

where

$$u'_{j,k}{}^{n+1/2} \stackrel{\text{def}}{=} \frac{1}{3} \left(u'_{j+1/3,k+1/3}{}^{n+1/2} + u'_{j-2/3,k+1/3}{}^{n+1/2} + u'_{j+1/3,k-2/3}{}^{n+1/2} \right), \quad (3.15)$$

$$(u'_\zeta)_{j,k}{}^{n+1/2} \stackrel{\text{def}}{=} \left(u'_{j+1/3,k+1/3}{}^{n+1/2} - u'_{j-2/3,k+1/3}{}^{n+1/2} \right) / \Delta\zeta, \quad (3.16)$$

and

$$(u'_\eta)_{j,k}{}^{n+1/2} \stackrel{\text{def}}{=} \left(u'_{j+1/3,k+1/3}{}^{n+1/2} - u'_{j+1/3,k-2/3}{}^{n+1/2} \right) / \Delta\eta. \quad (3.17)$$

Equation (3.14) implies that point O depicted in Fig. 10(a) is also a point on the plane spanned by P , Q , and R (i.e., the plane that contains P , Q , R). Moreover, for every point on the plane represented by Eq. (3.14), including point O , we have

$$\left(\frac{\partial u}{\partial \zeta} \right)_\eta = (u'_\zeta)_{j,k}{}^{n+1/2}, \quad \text{and} \quad \left(\frac{\partial u}{\partial \eta} \right)_\zeta = (u'_\eta)_{j,k}{}^{n+1/2}. \quad (3.18)$$

As a result of the above considerations, $u'_{j,k}{}^{n+1/2}$, $(u'_\zeta)_{j,k}{}^{n+1/2}$, and $(u'_\eta)_{j,k}{}^{n+1/2}$ can be considered as the finite-difference approximations of u , $\partial u / \partial \zeta$, and $\partial u / \partial \eta$ at the mesh point $(j, k, n + 1/2)$, respectively. Note that $u'_{j,k}{}^{n+1/2}$ generally is different from $u_{j,k}{}^{n+1/2}$ which is defined by Eq. (2.67). Furthermore, the former has no role in the future development. Let

$$(u_\zeta^+)_{j,k}{}^{n+1/2} \stackrel{\text{def}}{=} \frac{\Delta\zeta}{6} (u'_\zeta)_{j,k}{}^{n+1/2}, \quad \text{and} \quad (u_\eta^+)_{j,k}{}^{n+1/2} \stackrel{\text{def}}{=} \frac{\Delta\eta}{6} (u'_\eta)_{j,k}{}^{n+1/2}, \quad (3.19)$$

and

$$(u_\zeta^{o+})_{j,k}{}^{n+1/2} \stackrel{\text{def}}{=} \frac{1}{3} \left(s_1^{(1)} - s_2^{(1)} \right), \quad \text{and} \quad (u_\eta^{o+})_{j,k}{}^{n+1/2} \stackrel{\text{def}}{=} \frac{1}{3} \left(s_1^{(1)} - s_3^{(1)} \right). \quad (3.20)$$

where $s_1^{(1)}$, $s_2^{(1)}$, and $s_3^{(1)}$ are the expressions on the right sides of Eqs. (2.60)–(2.62), respectively. Because these expressions are functions of the marching variables at the n th time level, so are $(u_\zeta^{o+})_{j,k}{}^{n+1/2}$ and $(u_\eta^{o+})_{j,k}{}^{n+1/2}$. Moreover, Eqs. (2.68), (2.69) and (3.20) imply that the counterparts of $(u_\zeta^+)_{j,k}{}^{n+1/2}$ and $(u_\eta^+)_{j,k}{}^{n+1/2}$ in the a scheme are $(u_\zeta^{o+})_{j,k}{}^{n+1/2}$ and $(u_\eta^{o+})_{j,k}{}^{n+1/2}$, respectively.

Let

$$(du_{\zeta}^+)_{j,k}^{n+1/2} \stackrel{\text{def}}{=} 2 \left[(u_{\zeta}^+)_{j,k}^{n+1/2} - (u_{\zeta}^o)_{j,k}^{n+1/2} \right], \quad (j, k, n + 1/2) \in \Omega_1, \quad (3.21)$$

and

$$(du_{\eta}^+)_{j,k}^{n+1/2} \stackrel{\text{def}}{=} 2 \left[(u_{\eta}^+)_{j,k}^{n+1/2} - (u_{\eta}^o)_{j,k}^{n+1/2} \right], \quad (j, k, n + 1/2) \in \Omega_1. \quad (3.22)$$

Then, with the aid of Eqs. (3.11)–(3.13), (3.16), (3.17), (3.19), and (3.20), one has

$$(du_{\zeta}^+)_{j,k}^{n+1/2} = \frac{1}{3} \left[\left(u + 4u_{\zeta}^+ - 2u_{\eta}^+ \right)_{j-2/3, k+1/3}^n - \left(u - 2u_{\zeta}^+ - 2u_{\eta}^+ \right)_{j+1/3, k+1/3}^n \right], \quad (3.23)$$

and

$$(du_{\eta}^+)_{j,k}^{n+1/2} = \frac{1}{3} \left[\left(u - 2u_{\zeta}^+ + 4u_{\eta}^+ \right)_{j+1/3, k-2/3}^n - \left(u - 2u_{\zeta}^+ - 2u_{\eta}^+ \right)_{j+1/3, k+1/3}^n \right]. \quad (3.24)$$

Thus both $(du_{\zeta}^+)_{j,k}^{n+1/2}$ and $(du_{\eta}^+)_{j,k}^{n+1/2}$ are functions of the marching variables at the n th time level. As will be shown shortly, they play a key role in the first marching step of the modified scheme.

Next we consider Fig. 10(b). For any $(j, k, n + 1) \in \Omega_2$, let

$$u'_{j-1/3, k-1/3}{}^{n+1} \stackrel{\text{def}}{=} \left(u + \frac{\Delta t}{2} u_t \right)_{j-1/3, k-1/3}^{n+1/2}, \quad (3.25)$$

$$u'_{j+2/3, k-1/3}{}^{n+1} \stackrel{\text{def}}{=} \left(u + \frac{\Delta t}{2} u_t \right)_{j+2/3, k-1/3}^{n+1/2}, \quad (3.26)$$

and

$$u'_{j-1/3, k+2/3}{}^{n+1} \stackrel{\text{def}}{=} \left(u + \frac{\Delta t}{2} u_t \right)_{j-1/3, k+2/3}^{n+1/2}. \quad (3.27)$$

By their definitions, $u'_{j-1/3, k-1/3}{}^{n+1}$, $u'_{j+2/3, k-1/3}{}^{n+1}$, and $u'_{j-1/3, k+2/3}{}^{n+1}$ can be considered as the finite-difference approximations of u at $(j - 1/3, k - 1/3, n + 1)$, $(j + 2/3, k - 1/3, n + 1)$, and $(j - 1/3, k + 2/3, n + 1)$, respectively. With the aid of Eqs. (2.10), (A.10) and (2.31), Eqs. (3.25)–(3.27) imply that

$$u'_{j-1/3, k-1/3}{}^{n+1} = \left[u - 2 \left(\nu_{\zeta} u_{\zeta}^+ + \nu_{\eta} u_{\eta}^+ \right) \right]_{j-1/3, k-1/3}^{n+1/2}, \quad (3.28)$$

$$u'_{j+2/3, k-1/3}{}^{n+1} = \left[u - 2 \left(\nu_{\zeta} u_{\zeta}^+ + \nu_{\eta} u_{\eta}^+ \right) \right]_{j+2/3, k-1/3}^{n+1/2}, \quad (3.29)$$

and

$$u'_{j-1/3, k+2/3}{}^{n+1} = \left[u - 2 \left(\nu_\zeta u_\zeta^+ + \nu_\eta u_\eta^+ \right) \right]_{j-1/3, k+2/3}^{n+1/2}. \quad (3.30)$$

In Fig. 10(b), the points P , Q , and R are on a plane represented by

$$u = (u'_\zeta)_{j,k}{}^{n+1}(\zeta - j\Delta\zeta) + (u'_\eta)_{j,k}{}^{n+1}(\eta - k\Delta\eta) + u'_{j,k}{}^{n+1}, \quad (3.31)$$

where

$$u'_{j,k}{}^{n+1} \stackrel{\text{def}}{=} \frac{1}{3} \left(u'_{j-1/3, k-1/3}{}^{n+1} + u'_{j+2/3, k-1/3}{}^{n+1} + u'_{j-1/3, k+2/3}{}^{n+1} \right), \quad (3.32)$$

$$(u'_\zeta)_{j,k}{}^{n+1} \stackrel{\text{def}}{=} \left(u'_{j+2/3, k-1/3}{}^{n+1} - u'_{j-1/3, k-1/3}{}^{n+1} \right) / \Delta\zeta, \quad (3.33)$$

and

$$(u'_\eta)_{j,k}{}^{n+1} \stackrel{\text{def}}{=} \left(u'_{j-1/3, k+2/3}{}^{n+1} - u'_{j-1/3, k-1/3}{}^{n+1} \right) / \Delta\eta. \quad (3.34)$$

Moreover, we introduce the current counterparts to Eqs. (3.19) and (3.20), i.e.,

$$(u_\zeta^+)_{j,k}{}^{n+1} \stackrel{\text{def}}{=} \frac{\Delta\zeta}{6} (u'_\zeta)_{j,k}{}^{n+1}, \quad \text{and} \quad (u_\eta^+)_{j,k}{}^{n+1} \stackrel{\text{def}}{=} \frac{\Delta\eta}{6} (u'_\eta)_{j,k}{}^{n+1}, \quad (3.35)$$

and

$$(u_\zeta^{\circ+})_{j,k}{}^{n+1} \stackrel{\text{def}}{=} \frac{1}{3} \left(s_2^{(2)} - s_1^{(2)} \right), \quad \text{and} \quad (u_\eta^{\circ+})_{j,k}{}^{n+1} \stackrel{\text{def}}{=} \frac{1}{3} \left(s_3^{(2)} - s_1^{(2)} \right). \quad (3.36)$$

where $s_1^{(2)}$, $s_2^{(2)}$, and $s_3^{(2)}$ are the expressions on the right sides of Eqs. (2.63)–(2.65), respectively. Because these expressions are functions of the marching variables at the $(n+1/2)$ th time level, so are $(u_\zeta^{\circ+})_{j,k}{}^{n+1}$ and $(u_\eta^{\circ+})_{j,k}{}^{n+1}$. Moreover, Eqs. (2.71), (2.72) and (3.36) imply that the counterparts of $(u'_\zeta)_{j,k}{}^{n+1}$ and $(u'_\eta)_{j,k}{}^{n+1}$ in the a scheme are $(u_\zeta^{\circ+})_{j,k}{}^{n+1}$ and $(u_\eta^{\circ+})_{j,k}{}^{n+1}$, respectively.

With the above preparations, the current counterparts to Eqs. (3.21) and (3.22) are

$$(du_\zeta^+)_{j,k}{}^{n+1} \stackrel{\text{def}}{=} 2 \left[(u_\zeta^+)_{j,k}{}^{n+1} - (u_\zeta^{\circ+})_{j,k}{}^{n+1} \right], \quad (j, k, n+1) \in \Omega_2, \quad (3.37)$$

and

$$(du_\eta^+)_{j,k}{}^{n+1} \stackrel{\text{def}}{=} 2 \left[(u_\eta^+)_{j,k}{}^{n+1} - (u_\eta^{\circ+})_{j,k}{}^{n+1} \right], \quad (j, k, n+1) \in \Omega_2, \quad (3.38)$$

respectively. With the aid of Eqs. (3.28)–(3.30) and (3.33)–(3.36), Eqs. (3.37) and (3.38) imply that

$$(du_\zeta^+)_{j,k}{}^{n+1} = \frac{1}{3} \left[\left(u + 2u_\zeta^+ + 2u_\eta^+ \right)_{j-1/3, k-1/3}^{n+1/2} - \left(u - 4u_\zeta^+ + 2u_\eta^+ \right)_{j+2/3, k-1/3}^{n+1/2} \right], \quad (3.39)$$

and

$$(du_{\eta}^+)^{n+1}_{j,k} = \frac{1}{3} \left[\left(u + 2u_{\zeta}^+ + 2u_{\eta}^+ \right)_{j-1/3, k-1/3}^{n+1/2} - \left(u + 2u_{\zeta}^+ - 4u_{\eta}^+ \right)_{j-1/3, k+2/3}^{n+1/2} \right]. \quad (3.40)$$

Thus both $(du_{\zeta}^+)^{n+1}_{j,k}$ and $(du_{\eta}^+)^{n+1}_{j,k}$ are functions of the marching variables at the $(n+1/2)$ th time level.

The modified scheme can now be stated using the above definitions. It consists of two marching steps. The first is formed by Eq. (2.67),

$$(u_{\zeta}^+)^{n+1/2}_{j,k} = (u_{\zeta}^{o+})^{n+1/2}_{j,k} + \epsilon (du_{\zeta}^+)^{n+1/2}_{j,k}, \quad (3.41)$$

and

$$(u_{\eta}^+)^{n+1/2}_{j,k} = (u_{\eta}^{o+})^{n+1/2}_{j,k} + \epsilon (du_{\eta}^+)^{n+1/2}_{j,k}, \quad (3.42)$$

where $(j, k, n + 1/2) \in \Omega_1$, and ϵ is an adjustable parameter. It was explained earlier that the expressions on the right sides of Eqs. (3.41) and (3.42) are functions of the marching variables at the n th time level. Moreover, according to Eqs. (3.21) and (3.22), Eqs. (3.41) and (3.42) can also be expressed as

$$(u_{\zeta}^+)^{n+1/2}_{j,k} = (u_{\zeta}^{\prime+})^{n+1/2}_{j,k} + (\epsilon - 1/2)(du_{\zeta}^+)^{n+1/2}_{j,k}, \quad (3.43)$$

and

$$(u_{\eta}^+)^{n+1/2}_{j,k} = (u_{\eta}^{\prime+})^{n+1/2}_{j,k} + (\epsilon - 1/2)(du_{\eta}^+)^{n+1/2}_{j,k}, \quad (3.44)$$

respectively.

The second marching step is formed by Eq. (2.70),

$$(u_{\zeta}^+)^{n+1}_{j,k} = (u_{\zeta}^{o+})^{n+1}_{j,k} + \epsilon (du_{\zeta}^+)^{n+1}_{j,k}, \quad (3.45)$$

and

$$(u_{\eta}^+)^{n+1}_{j,k} = (u_{\eta}^{o+})^{n+1}_{j,k} + \epsilon (du_{\eta}^+)^{n+1}_{j,k}, \quad (3.46)$$

where $(j, k, n + 1) \in \Omega_2$. It was explained earlier that the expressions on the right sides of Eqs. (3.45) and (3.46) are functions of the marching variables at the $(n + 1/2)$ th time level. Furthermore, according to Eqs. (3.37) and (3.38), Eqs. (3.45) and (3.46) can also be expressed as

$$(u_{\zeta}^+)^{n+1}_{j,k} = (u_{\zeta}^{\prime+})^{n+1}_{j,k} + (\epsilon - 1/2)(du_{\zeta}^+)^{n+1}_{j,k}, \quad (3.47)$$

and

$$(u_{\eta}^+)^{n+1}_{j,k} = (u_{\eta}^{\prime+})^{n+1}_{j,k} + (\epsilon - 1/2)(du_{\eta}^+)^{n+1}_{j,k}, \quad (3.48)$$

respectively.

Because the modified scheme is characterized by two parameters a and ϵ , hereafter it is referred to as the a - ϵ scheme.

At this juncture, note that:

- (a) With the aid of Eqs. (3.20) and (3.36), it is seen that Eqs. (3.41), (3.42), (3.45), and (3.46), respectively, are reduced to Eqs. (2.68), (2.69), (2.71), and (2.72) when $\epsilon = 0$. As a result, the a - ϵ scheme becomes the a scheme when $\epsilon = 0$.
- (b) For the special case with $\epsilon = 1/2$, Eqs. (3.43), (3.44), (3.47), and (3.48) are reduced to the forms that represent the finite-difference approximations defined in Eqs. (3.16), (3.17), (3.19), (3.33), (3.34) and (3.35). However, Eqs. (2.67) and (2.70), which are independent of ϵ and therefore always part of the a - ϵ scheme, are the results of the flux conservation conditions Eqs. (3.4) and (3.5).
- (c) With the aid of Eqs. (2.30) and (3.23), Eq. (3.41) can be rewritten as

$$(u_\zeta)_{j,k}^{n+1/2} = \frac{6}{\Delta\zeta} (u_\zeta^+)_{j,k}^{n+1/2} + \frac{\epsilon}{3} \left[\left(\frac{6u}{\Delta\zeta} + 4u_\zeta - \frac{2\Delta\eta}{\Delta\zeta} u_\eta \right)_{j-2/3,k+1/3}^n - \left(\frac{6u}{\Delta\zeta} - 2u_\zeta - \frac{2\Delta\eta}{\Delta\zeta} u_\eta \right)_{j+1/3,k+1/3}^n \right]. \quad (3.49)$$

Let (i) $u_{j-2/3,k+1/3}^n$, $(u_\zeta)_{j-2/3,k+1/3}^n$ and $(u_\eta)_{j-2/3,k+1/3}^n$ be identified with the values of u , $\partial u/\partial\zeta$ and $\partial u/\partial\eta$ at the mesh point $(j-2/3, k+1/3, n)$, respectively; and (ii) $u_{j+1/3,k+1/3}^n$, $(u_\zeta)_{j+1/3,k+1/3}^n$ and $(u_\eta)_{j+1/3,k+1/3}^n$ be identified with the values of u , $\partial u/\partial\zeta$ and $\partial u/\partial\eta$ at the mesh point $(j+1/3, k+1/3, n)$, respectively. Then it can be shown that the expression within the brackets on the right side of Eq. (3.49) is $O(\Delta\zeta, \Delta\eta)$. Furthermore, because Eq. (2.28) is applicable within $SE(j, k, n)$ only, the expression that is enclosed within the first bracket on the right side of Eq. (2.28) is $O(\Delta\zeta, \Delta t)$. From the above considerations, one concludes that the addition of the extra term involving ϵ on the right side of Eq. (3.49) may result in errors that are second order in $\Delta\zeta$, $\Delta\eta$, and Δt . In other words, the addition of the term involving ϵ does not result in a scheme of lower order of accuracy. A similar conclusion is also applicable to Eqs. (3.42), (3.45), and (3.46).

- (d) Equations (3.16), (3.18) and (3.19) imply that $(u_\zeta^+)_{j,k}^{n+1/2}$ is proportional to the directional derivative along the ζ -direction on the plane spanned by points P , Q , and R depicted in Fig. 10(a). According to Eq. (3.21), $(du_\zeta^+)_{j,k}^{n+1/2}$ is twice the difference between $(u_\zeta^+)_{j,k}^{n+1/2}$ and its counterpart in the a scheme. Note that the variable $(du_x)_j^n$, that appears in Eqs. (3.2) and (3.10) of [5], plays a role in the 1-D a - ϵ scheme [5] similar to that of $(du_\zeta^+)_{j,k}^{n+1/2}$ in the present 2-D a - ϵ scheme. It can be shown that $(du_x)_j^n$ is equal to the difference between two slopes. The first is the slope of a line spanned by $u'_{j+1/2}^n$ and $u'_{j-1/2}^n$, which are defined in Eq. (3.11) in [5]. The second is the counterpart of the first in the 1-D a scheme. Thus the 2-D a - ϵ scheme is a natural extension of the 1-D a - ϵ scheme.

The a - ϵ scheme will take the form of Eqs. (2.82) and (2.83) if

$$Q_1^{(1)} \stackrel{\text{def}}{=} \frac{1}{3} \begin{pmatrix} 1 - \nu_\zeta - \nu_\eta & -(1 - \nu_\zeta - \nu_\eta)(1 + \nu_\zeta) & -(1 - \nu_\zeta - \nu_\eta)(1 + \nu_\eta) \\ 1 - \epsilon & -(1 + \nu_\zeta - 2\epsilon) & -(1 + \nu_\eta - 2\epsilon) \\ 1 - \epsilon & -(1 + \nu_\zeta - 2\epsilon) & -(1 + \nu_\eta - 2\epsilon) \end{pmatrix}, \quad (3.50)$$

$$Q_2^{(1)} \stackrel{\text{def}}{=} \frac{1}{3} \begin{pmatrix} 1 + \nu_\zeta & (1 + \nu_\zeta)(2 - \nu_\zeta) & -(1 + \nu_\zeta)(1 + \nu_\eta) \\ -(1 - \epsilon) & -(2 - \nu_\zeta - 4\epsilon) & 1 + \nu_\eta - 2\epsilon \\ 0 & 0 & 0 \end{pmatrix}, \quad (3.51)$$

$$Q_3^{(1)} \stackrel{\text{def}}{=} \frac{1}{3} \begin{pmatrix} 1 + \nu_\eta & -(1 + \nu_\eta)(1 + \nu_\zeta) & (1 + \nu_\eta)(2 - \nu_\eta) \\ 0 & 0 & 0 \\ -(1 - \epsilon) & 1 + \nu_\zeta - 2\epsilon & -(2 - \nu_\eta - 4\epsilon) \end{pmatrix}, \quad (3.52)$$

$$Q_1^{(2)} \stackrel{\text{def}}{=} \frac{1}{3} \begin{pmatrix} 1 + \nu_\zeta + \nu_\eta & (1 + \nu_\zeta + \nu_\eta)(1 - \nu_\zeta) & (1 + \nu_\zeta + \nu_\eta)(1 - \nu_\eta) \\ -(1 - \epsilon) & -(1 - \nu_\zeta - 2\epsilon) & -(1 - \nu_\eta - 2\epsilon) \\ -(1 - \epsilon) & -(1 - \nu_\zeta - 2\epsilon) & -(1 - \nu_\eta - 2\epsilon) \end{pmatrix}, \quad (3.53)$$

$$Q_2^{(2)} \stackrel{\text{def}}{=} \frac{1}{3} \begin{pmatrix} 1 - \nu_\zeta & -(1 - \nu_\zeta)(2 + \nu_\zeta) & (1 - \nu_\zeta)(1 - \nu_\eta) \\ 1 - \epsilon & -(2 + \nu_\zeta - 4\epsilon) & 1 - \nu_\eta - 2\epsilon \\ 0 & 0 & 0 \end{pmatrix}, \quad (3.54)$$

and

$$Q_3^{(2)} \stackrel{\text{def}}{=} \frac{1}{3} \begin{pmatrix} 1 - \nu_\eta & (1 - \nu_\eta)(1 - \nu_\zeta) & -(1 - \nu_\eta)(2 + \nu_\eta) \\ 0 & 0 & 0 \\ 1 - \epsilon & 1 - \nu_\zeta - 2\epsilon & -(2 + \nu_\eta - 4\epsilon) \end{pmatrix}. \quad (3.55)$$

Note that:

- (a) The matrices $Q_i^{(k)}$ defined above are reduced to those defined in Eq. (2.80) when $\epsilon = 0$.
- (b) With the above definitions, Eqs. (2.84) and (2.85) are also valid for the a - ϵ scheme.

In Sec. 5, it will be shown that (i) the a - ϵ scheme is unstable if $\epsilon < 0$ or $\epsilon > 1$, and (ii) numerical diffusion increases as ϵ increases, at least in the range of $0 \leq \epsilon \leq 0.65$. In order to suppress numerical oscillations near a discontinuity, one may be forced to choose a large ϵ . However, with such a choice, the smooth part of a solution may become highly diffusive. To solve this dilemma, in the following, we shall construct a generalization of the a - ϵ scheme.

To proceed, let $(j, k, n + 1/2) \in \Omega_1$ and consider Fig. 11(a). This figure is essentially identical to Fig. 10(a) except that point O in the latter is replaced by point O^* in the former. The coordinates of point O^* are $(j\Delta\zeta, k\Delta\eta, u_{j,k}^{n+1/2})$ where $u_{j,k}^{n+1/2}$ is that defined in Eq. (2.67). Thus point O^* generally is not on the plane spanned by points P , Q , and R . Let planes #1, #2, and #3, respectively, be the planes spanned by the following trios of points: (i) points O^* , Q , and R ; (ii) points O^* , R , and P ; and (iii) points O^* , P , and Q . Then in general these planes differ from each other and from the plane spanned by points P , Q , and R . In the following, first we shall study the former three planes.

As a preliminary, let

$$x_1 \stackrel{\text{def}}{=} u_{j+1/3, k+1/3}^{n+1/2} - u_{j,k}^{n+1/2}, \quad (3.56)$$

$$x_2 \stackrel{\text{def}}{=} u_{j-2/3, k+1/3}^{n+1/2} - u_{j,k}^{n+1/2}, \quad (3.57)$$

$$x_3 \stackrel{\text{def}}{=} u_{j+1/3, k-2/3}^{n+1/2} - u_{j,k}^{n+1/2}, \quad (3.58)$$

$$(u_{\zeta}^{(1)})_{j,k}^{n+1/2} \stackrel{\text{def}}{=} -(2x_2 + x_3)/\Delta\zeta, \quad (3.59)$$

$$(u_{\eta}^{(1)})_{j,k}^{n+1/2} \stackrel{\text{def}}{=} -(x_2 + 2x_3)/\Delta\eta, \quad (3.60)$$

$$(u_{\zeta}^{(2)})_{j,k}^{n+1/2} \stackrel{\text{def}}{=} (2x_1 + x_3)/\Delta\zeta, \quad (3.61)$$

$$(u_{\eta}^{(2)})_{j,k}^{n+1/2} \stackrel{\text{def}}{=} (x_1 - x_3)/\Delta\eta, \quad (3.62)$$

$$(u_{\zeta}^{(3)})_{j,k}^{n+1/2} \stackrel{\text{def}}{=} (x_1 - x_2)/\Delta\zeta, \quad (3.63)$$

and

$$(u_{\eta}^{(3)})_{j,k}^{n+1/2} \stackrel{\text{def}}{=} (2x_1 + x_2)/\Delta\eta. \quad (3.64)$$

Moreover, let

$$(u_x^{(\ell)})_{j,k}^{n+1/2} \stackrel{\text{def}}{=} (u_{\zeta}^{(\ell)})_{j,k}^{n+1/2} \frac{\partial\zeta}{\partial x} + (u_{\eta}^{(\ell)})_{j,k}^{n+1/2} \frac{\partial\eta}{\partial x}, \quad \ell = 1, 2, 3, \quad (3.65)$$

and

$$(u_y^{(\ell)})_{j,k}^{n+1/2} \stackrel{\text{def}}{=} (u_\zeta^{(\ell)})_{j,k}^{n+1/2} \frac{\partial \zeta}{\partial y} + (u_\eta^{(\ell)})_{j,k}^{n+1/2} \frac{\partial \eta}{\partial y}, \quad \ell = 1, 2, 3. \quad (3.66)$$

With the aid of Eqs. (2.20) and (2.22), we have

$$(u_x^{(\ell)})_{j,k}^{n+1/2} = \frac{\Delta \zeta}{2w} (u_\zeta^{(\ell)})_{j,k}^{n+1/2} + \frac{\Delta \eta}{2w} (u_\eta^{(\ell)})_{j,k}^{n+1/2}, \quad \ell = 1, 2, 3, \quad (3.67)$$

and

$$(u_y^{(\ell)})_{j,k}^{n+1/2} = -\frac{(w+b)\Delta \zeta}{2wh} (u_\zeta^{(\ell)})_{j,k}^{n+1/2} + \frac{(w-b)\Delta \eta}{2wh} (u_\eta^{(\ell)})_{j,k}^{n+1/2}, \quad \ell = 1, 2, 3. \quad (3.68)$$

Combining Eqs. (3.59)–(3.64) with Eqs. (3.67) and (3.68), one has

$$(u_x^{(1)})_{j,k}^{n+1/2} = -\frac{3}{2w}(x_2 + x_3), \quad (3.69)$$

$$(u_y^{(1)})_{j,k}^{n+1/2} = \frac{(3b+w)x_2 + (3b-w)x_3}{2wh}, \quad (3.70)$$

$$(u_x^{(2)})_{j,k}^{n+1/2} = \frac{3x_1}{2w}, \quad (3.71)$$

$$(u_y^{(2)})_{j,k}^{n+1/2} = -\frac{(3b+w)x_1 + 2wx_3}{2wh}, \quad (3.72)$$

$$(u_x^{(3)})_{j,k}^{n+1/2} = \frac{3x_1}{2w}, \quad (3.73)$$

and

$$(u_y^{(3)})_{j,k}^{n+1/2} = \frac{(w-3b)x_1 + 2wx_2}{2wh}. \quad (3.74)$$

With the above preparations, it can be shown that planes # ℓ , $\ell = 1, 2, 3$, are represented by

$$u = (u_\zeta^{(\ell)})_{j,k}^{n+1/2} (\zeta - j\Delta \zeta) + (u_\eta^{(\ell)})_{j,k}^{n+1/2} (\eta - k\Delta \eta) + u_{j,k}^{n+1/2}, \quad \ell = 1, 2, 3, \quad (3.75)$$

respectively, if the coordinates (ζ, η) are used. Alternatively, they can be represented by

$$u = (u_x^{(\ell)})_{j,k}^{n+1/2} (x - x_{j,k}) + (u_y^{(\ell)})_{j,k}^{n+1/2} (y - y_{j,k}) + u_{j,k}^{n+1/2}, \quad \ell = 1, 2, 3, \quad (3.76)$$

respectively, if the coordinates (x, y) are used. Using Eqs. (3.75) and (3.76), one concludes that, at any point on plane # ℓ , $\ell = 1, 2, 3$, we have

$$\left(\frac{\partial u}{\partial \zeta}\right)_\eta = (u_\zeta^{(\ell)})_{j,k}^{n+1/2}, \quad \text{and} \quad \left(\frac{\partial u}{\partial \eta}\right)_\zeta = (u_\eta^{(\ell)})_{j,k}^{n+1/2}, \quad (3.77)$$

and

$$\left(\frac{\partial u}{\partial x}\right)_y = (u_x^{(\ell)})_{j,k}^{n+1/2}, \quad \text{and} \quad \left(\frac{\partial u}{\partial y}\right)_x = (u_y^{(\ell)})_{j,k}^{n+1/2}. \quad (3.78)$$

Note that Eq. (3.77) is the current counterpart to Eq. (3.18) which is applicable to any point on the plane spanned by points P , Q , and R . Let ∇u be the gradient of u . Then Eq. (3.78) implies that, at any point on plane # ℓ , $\ell = 1, 2, 3$, we have

$$|\nabla u| = (\theta_\ell)_{j,k}^{n+1/2} \stackrel{\text{def}}{=} \left[\sqrt{(u_x^{(\ell)})^2 + (u_y^{(\ell)})^2} \right]_{j,k}^{n+1/2}. \quad (3.79)$$

To proceed further, we introduce the current counterpart to Eq. (3.19), i.e.,

$$(u_\zeta^{(\ell)+})_{j,k}^{n+1/2} \stackrel{\text{def}}{=} \frac{\Delta \zeta}{6} (u_\zeta^{(\ell)})_{j,k}^{n+1/2}, \quad \text{and} \quad (u_\eta^{(\ell)+})_{j,k}^{n+1/2} \stackrel{\text{def}}{=} \frac{\Delta \eta}{6} (u_\eta^{(\ell)})_{j,k}^{n+1/2}. \quad (3.80)$$

Then Eqs. (3.16), (3.17), (3.19), and (3.56)–(3.64) imply that

$$(u_\zeta^{'+})_{j,k}^{n+1/2} = \frac{1}{3} \left[u_\zeta^{(1)+} + u_\zeta^{(2)+} + u_\zeta^{(3)+} \right]_{j,k}^{n+1/2}, \quad (3.81)$$

and

$$(u_\eta^{'+})_{j,k}^{n+1/2} = \frac{1}{3} \left[u_\eta^{(1)+} + u_\eta^{(2)+} + u_\eta^{(3)+} \right]_{j,k}^{n+1/2}, \quad (3.82)$$

i.e., (i) $(u_\zeta^{'+})_{j,k}^{n+1/2}$ is the simple average of

$$(u_\zeta^{(1)+})_{j,k}^{n+1/2}, \quad (u_\zeta^{(2)+})_{j,k}^{n+1/2}, \quad \text{and} \quad (u_\zeta^{(3)+})_{j,k}^{n+1/2}, \quad (3.83)$$

and (ii) $(u_\eta^{'+})_{j,k}^{n+1/2}$ is the simple average of

$$(u_\eta^{(1)+})_{j,k}^{n+1/2}, \quad (u_\eta^{(2)+})_{j,k}^{n+1/2}, \quad \text{and} \quad (u_\eta^{(3)+})_{j,k}^{n+1/2}. \quad (3.84)$$

The first marching step of the generalized a - ϵ scheme will be formed using Eqs. (2.67), (3.43), and (3.44) except that (i) $(u_\zeta^{'+})_{j,k}^{n+1/2}$ in Eq. (3.43) is replaced by the weighted average of those given in Eq. (3.83); and (ii) $(u_\eta^{'+})_{j,k}^{n+1/2}$ in Eq. (3.44) is replaced by the weighted average of those given in Eq. (3.84). The design of these weighted averages will

be guided by the requirement that the weight assigned to a quantity associated with plane # ℓ is bigger if $(\theta_\ell)_{j,k}^{n+1/2}$ is smaller. This requirement is similar to that put forward on p.28 of [5].

For any $\alpha \geq 0$, the weighted-average counterparts to $(u'_\zeta)_{j,k}^{n+1/2}$ and $(u'_\eta)_{j,k}^{n+1/2}$ are

$$u_\zeta^{w+} \stackrel{\text{def}}{=} \begin{cases} 0, & \text{if } \theta_1 = \theta_2 = \theta_3 = 0; \\ \frac{(\theta_2\theta_3)^\alpha u_\zeta^{(1)+} + (\theta_3\theta_1)^\alpha u_\zeta^{(2)+} + (\theta_1\theta_2)^\alpha u_\zeta^{(3)+}}{(\theta_1\theta_2)^\alpha + (\theta_2\theta_3)^\alpha + (\theta_3\theta_1)^\alpha}, & \text{otherwise,} \end{cases} \quad (3.85)$$

and

$$u_\eta^{w+} \stackrel{\text{def}}{=} \begin{cases} 0, & \text{if } \theta_1 = \theta_2 = \theta_3 = 0; \\ \frac{(\theta_2\theta_3)^\alpha u_\eta^{(1)+} + (\theta_3\theta_1)^\alpha u_\eta^{(2)+} + (\theta_1\theta_2)^\alpha u_\eta^{(3)+}}{(\theta_1\theta_2)^\alpha + (\theta_2\theta_3)^\alpha + (\theta_3\theta_1)^\alpha}, & \text{otherwise,} \end{cases} \quad (3.86)$$

respectively. Here, for simplicity, we suppress the indices j , k , and $n + 1/2$ which are associated with all symbols in Eqs. (3.85) and (3.86). Because the denominators of the fractions on the right sides of Eqs. (3.85) and (3.86) vanish if $\alpha > 0$, and any two of θ_1 , θ_2 , and θ_3 vanish, consistency of the above definitions requires the proof of the proposition: $\theta_1 = \theta_2 = \theta_3 = 0$, if any two of θ_1 , θ_2 , and θ_3 vanish.

Proof: As an example, let $\theta_1 = \theta_2 = 0$. Then Eq. (3.79) implies that $u_x^{(\ell)} = u_y^{(\ell)} = 0$, $\ell = 1, 2$. In turn, Eqs. (3.69)–(3.72) imply that $x_1 = x_2 = x_3 = 0$. $\theta_3 = 0$ now follows from Eqs. (3.73), (3.74), and (3.79). QED.

Next we consider several special cases of Eq. (3.85). We have

$$u_\zeta^{w+} = \begin{cases} u_\zeta^{(1)+}, & \text{if } \theta_1 = 0, \theta_2 > 0, \text{ and } \theta_3 > 0; \\ u_\zeta^{(2)+}, & \text{if } \theta_2 = 0, \theta_1 > 0, \text{ and } \theta_3 > 0; \\ u_\zeta^{(3)+}, & \text{if } \theta_3 = 0, \theta_1 > 0, \text{ and } \theta_2 > 0. \end{cases} \quad (3.87)$$

Assuming $\theta_\ell > 0$, $\ell = 1, 2, 3$, we have

$$u_\zeta^{w+} = \frac{(1/\theta_1)^\alpha u_\zeta^{(1)+} + (1/\theta_2)^\alpha u_\zeta^{(2)+} + (1/\theta_3)^\alpha u_\zeta^{(3)+}}{(1/\theta_1)^\alpha + (1/\theta_2)^\alpha + (1/\theta_3)^\alpha}. \quad (3.88)$$

Thus the weight assigned to $u_\zeta^{(\ell)+}$ is proportional to $(1/\theta_\ell)^\alpha$. By using Eqs. (3.81), (3.85), and (3.88), one arrives at the conclusion that

$$u_\zeta^{w+} = u_\zeta'^+, \quad \text{if } \theta_1 = \theta_2 = \theta_3. \quad (3.89)$$

Obviously Eqs. (3.87)–(3.89) are still valid if each symbol ζ in them is replaced by the symbol η .

On the smooth part of a solution, θ_1 , θ_2 , and θ_3 are nearly equal. Thus the weighted averages u_ζ^{w+} and u_η^{w+} are nearly equal to the simple averages $u_\zeta^{'+}$, and $u_\eta^{'+}$, respectively (see Eqs. (3.81) and (3.82)). In other words, *the effect of weighted-averaging generally is not discernible on the smooth part of a solution.*

Next let $(j, k, n+1) \in \Omega_2$ and consider Fig. 11(b). The third coordinate $u_{j,k}^{n+1}$ of point O^* is that defined in Eq. (2.70). Let planes #1, #2, and #3, respectively, be the planes spanned by the following trios of points: (i) points O^* , Q , and R ; (ii) points O^* , R , and P ; and (iii) points O^* , P , and Q . In the following, we shall study these planes.

As a preliminary, let

$$y_1 \stackrel{\text{def}}{=} u_{j-1/3, k-1/3}^{n+1} - u_{j,k}^{n+1}, \quad (3.90)$$

$$y_2 \stackrel{\text{def}}{=} u_{j+2/3, k-1/3}^{n+1} - u_{j,k}^{n+1}, \quad (3.91)$$

$$y_3 \stackrel{\text{def}}{=} u_{j-1/3, k+2/3}^{n+1} - u_{j,k}^{n+1}, \quad (3.92)$$

$$(u_\zeta^{(1)})_{j,k}^{n+1} \stackrel{\text{def}}{=} (2y_2 + y_3)/\Delta\zeta, \quad (3.93)$$

$$(u_\eta^{(1)})_{j,k}^{n+1} \stackrel{\text{def}}{=} (y_2 + 2y_3)/\Delta\eta, \quad (3.94)$$

$$(u_\zeta^{(2)})_{j,k}^{n+1} \stackrel{\text{def}}{=} -(2y_1 + y_3)/\Delta\zeta, \quad (3.95)$$

$$(u_\eta^{(2)})_{j,k}^{n+1} \stackrel{\text{def}}{=} (y_3 - y_1)/\Delta\eta, \quad (3.96)$$

$$(u_\zeta^{(3)})_{j,k}^{n+1} \stackrel{\text{def}}{=} (y_2 - y_1)/\Delta\zeta, \quad (3.97)$$

and

$$(u_\eta^{(3)})_{j,k}^{n+1} \stackrel{\text{def}}{=} -(2y_1 + y_2)/\Delta\eta. \quad (3.98)$$

Moreover, let

$$(u_x^{(\ell)})_{j,k}^{n+1} \stackrel{\text{def}}{=} (u_\zeta^{(\ell)})_{j,k}^{n+1} \frac{\partial\zeta}{\partial x} + (u_\eta^{(\ell)})_{j,k}^{n+1} \frac{\partial\eta}{\partial x}, \quad \ell = 1, 2, 3, \quad (3.99)$$

and

$$(u_y^{(\ell)})_{j,k}^{n+1} \stackrel{\text{def}}{=} (u_\zeta^{(\ell)})_{j,k}^{n+1} \frac{\partial\zeta}{\partial y} + (u_\eta^{(\ell)})_{j,k}^{n+1} \frac{\partial\eta}{\partial y}, \quad \ell = 1, 2, 3. \quad (3.100)$$

With the above definitions, Eqs. (3.67) and (3.68) remain valid if each upper index $n + 1/2$ is replaced by $n + 1$. As a result, Eqs. (3.93)–(3.98) imply that

$$(u_x^{(1)})_{j,k}^{n+1} = \frac{3}{2w}(y_2 + y_3), \quad (3.101)$$

$$(u_y^{(1)})_{j,k}^{n+1} = -\frac{(3b+w)y_2 + (3b-w)y_3}{2wh}, \quad (3.102)$$

$$(u_x^{(2)})_{j,k}^{n+1} = -\frac{3y_1}{2w}, \quad (3.103)$$

$$(u_y^{(2)})_{j,k}^{n+1} = \frac{(3b+w)y_1 + 2wy_3}{2wh}, \quad (3.104)$$

$$(u_x^{(3)})_{j,k}^{n+1} = -\frac{3y_1}{2w}, \quad (3.105)$$

and

$$(u_y^{(3)})_{j,k}^{n+1} = -\frac{(w-3b)y_1 + 2wy_2}{2wh}. \quad (3.106)$$

With the above preparations, the earlier developments that involve Eqs. (3.75)–(3.89) can be repeated for the current case with the only change being the replacement of each upper index $n + 1/2$ by $n + 1$. Particularly, $(u_\zeta^{w+})_{j,k}^{n+1}$ and $(u_\eta^{w+})_{j,k}^{n+1}$ can be defined using Eqs. (3.85) and (3.86) with the understanding that each symbol in these equations is associated with the mesh point $(j, k, n + 1)$.

The generalized a - ϵ scheme, referred to as the weighted-average a - ϵ scheme, can now be stated. It consists of two marching steps. The first is formed by Eq. (2.67),

$$(u_\zeta^+)^{n+1/2}_{j,k} = (u_\zeta^{w+})^{n+1/2}_{j,k} + (\epsilon - 1/2)(du_\zeta^+)^{n+1/2}_{j,k}, \quad (3.107)$$

and

$$(u_\eta^+)^{n+1/2}_{j,k} = (u_\eta^{w+})^{n+1/2}_{j,k} + (\epsilon - 1/2)(du_\eta^+)^{n+1/2}_{j,k}, \quad (3.108)$$

where $(j, k, n + 1/2) \in \Omega_1$. The second is formed by Eq. (2.70),

$$(u_\zeta^+)^{n+1}_{j,k} = (u_\zeta^{w+})^{n+1}_{j,k} + (\epsilon - 1/2)(du_\zeta^+)^{n+1}_{j,k}, \quad (3.109)$$

and

$$(u_\eta^+)^{n+1}_{j,k} = (u_\eta^{w+})^{n+1}_{j,k} + (\epsilon - 1/2)(du_\eta^+)^{n+1}_{j,k}, \quad (3.110)$$

where $(j, k, n + 1) \in \Omega_2$.

Note that, according to Eq. (3.79), the evaluation of $(\theta_\ell)^\alpha$ does not involve a fractional power if α is an even integer. Because a fractional power is costly to evaluate, the use of the generalized a - ϵ scheme is less costly when α is an even integer.

4. The Euler Solver

We consider a dimensionless form of the 2-D unsteady Euler equations of a perfect gas. Let ρ , u , v , p , and γ be the mass density, x -velocity component, y -velocity component, static pressure, and constant specific heat ratio, respectively. Let

$$u_1 = \rho, \quad u_2 = \rho u, \quad u_3 = \rho v, \quad u_4 = p/(\gamma - 1) + \rho(u^2 + v^2)/2, \quad (4.1)$$

$$f_1^x = u_2, \quad (4.2)$$

$$f_2^x = (\gamma - 1)u_4 + (3 - \gamma)(u_2)^2/(2u_1) - (\gamma - 1)(u_3)^2/(2u_1), \quad (4.3)$$

$$f_3^x = u_2 u_3/u_1, \quad (4.4)$$

$$f_4^x = \gamma u_2 u_4/u_1 - (1/2)(\gamma - 1)u_2 [(u_2)^2 + (u_3)^2]/(u_1)^2, \quad (4.5)$$

$$f_1^y = u_3, \quad (4.6)$$

$$f_2^y = u_2 u_3/u_1, \quad (4.7)$$

$$f_3^y = (\gamma - 1)u_4 + (3 - \gamma)(u_3)^2/(2u_1) - (\gamma - 1)(u_2)^2/(2u_1), \quad (4.8)$$

and

$$f_4^y = \gamma u_3 u_4/u_1 - (1/2)(\gamma - 1)u_3 [(u_2)^2 + (u_3)^2]/(u_1)^2. \quad (4.9)$$

Then the Euler equations can be expressed as

$$\frac{\partial u_m}{\partial t} + \frac{\partial f_m^x}{\partial x} + \frac{\partial f_m^y}{\partial y} = 0, \quad m = 1, 2, 3, 4. \quad (4.10)$$

The integral form of Eq. (4.10) in space-time E_3 is

$$\oint_{S(V)} \vec{h}_m \cdot d\vec{s} = 0, \quad m = 1, 2, 3, 4, \quad (4.11)$$

where

$$\vec{h}_m = (f_m^x, f_m^y, u_m), \quad m = 1, 2, 3, 4, \quad (4.12)$$

are the space-time mass, x -momentum component, y -momentum component, and energy current density vectors, respectively.

As a preliminary, let

$$f_{m,\ell}^x \stackrel{\text{def}}{=} \partial f_m^x / \partial u_\ell, \quad \text{and} \quad f_{m,\ell}^y \stackrel{\text{def}}{=} \partial f_m^y / \partial u_\ell, \quad m, \ell = 1, 2, 3, 4, \quad (4.13)$$

$$\hat{u}_\ell \stackrel{\text{def}}{=} u_\ell / u_1, \quad \ell = 2, 3, 4, \quad (4.14)$$

and

$$\hat{u}^2 \stackrel{\text{def}}{=} (\hat{u}_2)^2 + (\hat{u}_3)^2. \quad (4.15)$$

Let F^x and F^y denote the matrices formed by $f_{m,\ell}^x$ and $f_{m,\ell}^y$, $m, \ell = 1, 2, 3, 4$, respectively. Then

$$F^x = \begin{pmatrix} 0 & 1 & 0 & 0 \\ \frac{\gamma-1}{2}\hat{u}^2 - (\hat{u}_2)^2 & (3-\gamma)\hat{u}_2 & (1-\gamma)\hat{u}_3 & \gamma-1 \\ -\hat{u}_2\hat{u}_3 & \hat{u}_3 & \hat{u}_2 & 0 \\ (\gamma-1)\hat{u}_2\hat{u}^2 - \gamma\hat{u}_2\hat{u}_4 & \gamma\hat{u}_4 - \frac{\gamma-1}{2}[2(\hat{u}_2)^2 + \hat{u}^2] & (1-\gamma)\hat{u}_2\hat{u}_3 & \gamma\hat{u}_2 \end{pmatrix}, \quad (4.16)$$

and

$$F^y = \begin{pmatrix} 0 & 0 & 1 & 0 \\ -\hat{u}_2\hat{u}_3 & \hat{u}_3 & \hat{u}_2 & 0 \\ \frac{\gamma-1}{2}\hat{u}^2 - (\hat{u}_3)^2 & (1-\gamma)\hat{u}_2 & (3-\gamma)\hat{u}_3 & \gamma-1 \\ (\gamma-1)\hat{u}_3\hat{u}^2 - \gamma\hat{u}_3\hat{u}_4 & (1-\gamma)\hat{u}_2\hat{u}_3 & \gamma\hat{u}_4 - \frac{\gamma-1}{2}[2(\hat{u}_3)^2 + \hat{u}^2] & \gamma\hat{u}_3 \end{pmatrix}. \quad (4.17)$$

Because f_m^x and f_m^y , $m = 1, 2, 3, 4$, are homogeneous functions of degree 1 [23] in u_1 , u_2 , u_3 , and u_4 , we have

$$f_m^x = \sum_{\ell=1}^4 f_{m,\ell}^x u_\ell, \quad \text{and} \quad f_m^y = \sum_{\ell=1}^4 f_{m,\ell}^y u_\ell. \quad (4.18)$$

For any $(x, y, t) \in \text{SE}(j, k, n)$, $u_m(x, y, t)$, $f_m^x(x, y, t)$, $f_m^y(x, y, t)$, and $\vec{h}_m(x, y, t)$, respectively, are approximated by $u_m^*(x, y, t; j, k, n)$, $f_m^{x*}(x, y, t; j, k, n)$, $f_m^{y*}(x, y, t; j, k, n)$, and $\vec{h}_m^*(x, y, t; j, k, n)$. They will be defined shortly. Let

$$u_m^*(x, y, t; j, k, n) \stackrel{\text{def}}{=} (u_m)_{j,k}^n + (u_{mx})_{j,k}^n(x - x_{j,k}) + (u_{my})_{j,k}^n(y - y_{j,k}) + (u_{mt})_{j,k}^n(t - t^n), \quad m = 1, 2, 3, 4, \quad (4.19)$$

where $(u_m)_{j,k}^n$, $(u_{mx})_{j,k}^n$, $(u_{my})_{j,k}^n$, and $(u_{mt})_{j,k}^n$ are constants in $\text{SE}(j, k, n)$. Obviously, they can be considered as the numerical analogues of the values of u_m , $\partial u_m / \partial x$, $\partial u_m / \partial y$, and $\partial u_m / \partial t$ at (x_j, y_k, t^n) , respectively.

Let $(f_m^x)_{j,k}^n$, $(f_m^y)_{j,k}^n$, $(f_{m,\ell}^x)_{j,k}^n$, and $(f_{m,\ell}^y)_{j,k}^n$ denote the values of f_m^x , f_m^y , $f_{m,\ell}^x$, and $f_{m,\ell}^y$, respectively, when u_m , $m = 1, 2, 3, 4$, respectively, assume the values of $(u_m)_{j,k}^n$, $m = 1, 2, 3, 4$. Let

$$(f_{mx}^x)_{j,k}^n \stackrel{\text{def}}{=} \sum_{\ell=1}^4 (f_{m,\ell}^x)_{j,k}^n (u_{\ell x})_{j,k}^n, \quad m = 1, 2, 3, 4, \quad (4.20)$$

$$(f_{my}^x)_{j,k}^n \stackrel{\text{def}}{=} \sum_{\ell=1}^4 (f_{m,\ell}^x)_{j,k}^n (u_{\ell y})_{j,k}^n, \quad m = 1, 2, 3, 4, \quad (4.21)$$

$$(f_{mt}^x)_{j,k}^n \stackrel{\text{def}}{=} \sum_{\ell=1}^4 (f_{m,\ell}^x)_{j,k}^n (u_{\ell t})_{j,k}^n, \quad m = 1, 2, 3, 4, \quad (4.22)$$

$$(f_{mx}^y)_{j,k}^n \stackrel{\text{def}}{=} \sum_{\ell=1}^4 (f_{m,\ell}^y)_{j,k}^n (u_{\ell x})_{j,k}^n, \quad m = 1, 2, 3, 4, \quad (4.23)$$

$$(f_{my}^y)_{j,k}^n \stackrel{\text{def}}{=} \sum_{\ell=1}^4 (f_{m,\ell}^y)_{j,k}^n (u_{\ell y})_{j,k}^n, \quad m = 1, 2, 3, 4, \quad (4.24)$$

and

$$(f_{mt}^y)_{j,k}^n \stackrel{\text{def}}{=} \sum_{\ell=1}^4 (f_{m,\ell}^y)_{j,k}^n (u_{\ell t})_{j,k}^n, \quad m = 1, 2, 3, 4. \quad (4.25)$$

Because (i)

$$\frac{\partial f_m^x}{\partial x} = \sum_{\ell=1}^4 f_{m,\ell}^x \frac{\partial u_{\ell}}{\partial x}, \quad m = 1, 2, 3, 4; \quad (4.26)$$

and (ii) the expression on the right side of Eq. (4.20) is the numerical analogue of that on the right side of Eq. (4.26) at (x_j, y_k, t^n) , $(f_{mx}^x)_{j,k}^n$ can be considered as the numerical analogue of the value of $\partial f_m^x / \partial x$ at (x_j, y_k, t^n) . Similarly, $(f_{my}^x)_{j,k}^n$, $(f_{mt}^x)_{j,k}^n$, $(f_{mx}^y)_{j,k}^n$, $(f_{my}^y)_{j,k}^n$, and $(f_{mt}^y)_{j,k}^n$ can be considered as the numerical analogues of the values of $\partial f_m^x / \partial y$, $\partial f_m^x / \partial t$, $\partial f_m^y / \partial x$, $\partial f_m^y / \partial y$, and $\partial f_m^y / \partial t$ at (x_j, y_k, t^n) , respectively. As a result, we assume that

$$f_m^{x*}(x, y, t; j, k, n) \stackrel{\text{def}}{=} (f_m^x)_{j,k}^n + (f_{mx}^x)_{j,k}^n (x - x_{j,k}) + (f_{my}^x)_{j,k}^n (y - y_{j,k}) + (f_{mt}^x)_{j,k}^n (t - t^n), \quad m = 1, 2, 3, 4, \quad (4.27)$$

and

$$f_m^{y*}(x, y, t; j, k, n) \stackrel{\text{def}}{=} (f_m^y)_{j,k}^n + (f_{mx}^y)_{j,k}^n (x - x_{j,k}) + (f_{my}^y)_{j,k}^n (y - y_{j,k}) + (f_{mt}^y)_{j,k}^n (t - t^n), \quad m = 1, 2, 3, 4, \quad (4.28)$$

Also, as an analogue to Eq. (4.12), we assume that

$$\vec{h}_m^*(x, y, t; j, k, n) \stackrel{\text{def}}{=} \left(f_m^{x*}(x, y, t; j, k, n), f_m^{y*}(x, y, t; j, k, n), u_m^*(x, y, t; j, k, n) \right), \quad m = 1, 2, 3, 4. \quad (4.29)$$

Note that, by their definitions: (i) $f_m^x, f_m^y, f_{m,\ell}^x$, and $f_{m,\ell}^y$, $m, \ell = 1, 2, 3, 4$, are functions of $(u_m)_{j,k}^n$, $m = 1, 2, 3, 4$; (ii) $(f_{mx}^x)_{j,k}^n$ and $(f_{mx}^y)_{j,k}^n$, $m = 1, 2, 3, 4$, are functions of $(u_m)_{j,k}^n$ and $(u_{mx})_{j,k}^n$, $m = 1, 2, 3, 4$; (iii) $(f_{my}^x)_{j,k}^n$ and $(f_{my}^y)_{j,k}^n$, $m = 1, 2, 3, 4$, are functions of $(u_m)_{j,k}^n$ and $(u_{my})_{j,k}^n$, $m = 1, 2, 3, 4$; and (iv) $(f_{mt}^x)_{j,k}^n$ and $(f_{mt}^y)_{j,k}^n$ are functions of $(u_m)_{j,k}^n$ and $(u_{mt})_{j,k}^n$, $m = 1, 2, 3, 4$.

Moreover, we assume that, for any $(x, y, t) \in \text{SE}(j, k, n)$, and $m = 1, 2, 3, 4$,

$$\frac{\partial u_m^*(x, y, t; j, k, n)}{\partial t} + \frac{\partial f_m^{x*}(x, y, t; j, k, n)}{\partial x} + \frac{\partial f_m^{y*}(x, y, t; j, k, n)}{\partial y} = 0. \quad (4.30)$$

Note that Eq. (4.30) is the numerical analogue of Eq. (4.10). With the aid of Eqs. (4.19), (4.27), (4.28), (4.20), and (4.24), Eq. (4.30) implies that, for $m = 1, 2, 3, 4$,

$$(u_{mt})_{j,k}^n = -(f_{mx}^x)_{j,k}^n - (f_{my}^y)_{j,k}^n = - \sum_{\ell=1}^4 \left[f_{m,\ell}^x u_{\ell x} + f_{m,\ell}^y u_{\ell y} \right]_{j,k}^n. \quad (4.31)$$

Thus $(u_{mt})_{j,k}^n$ are functions of $(u_m)_{j,k}^n$, $(u_{mx})_{j,k}^n$, and $(u_{my})_{j,k}^n$. From this result and the facts stated following Eq. (4.29), one concludes that *the only independent discrete variables needed to be solved in the current marching scheme are $(u_m)_{j,k}^n$, $(u_{mx})_{j,k}^n$, and $(u_{my})_{j,k}^n$.*

Consider the conservation elements depicted in Figs. 5(a) and 6(a). The Euler counterparts to Eqs. (2.12) and (2.13), respectively, are (i)

$$\oint_{S(CE_i^{(1)}(j,k,n+1/2))} \vec{h}_m^* \cdot d\vec{s} = 0, \quad \ell = 1, 2, 3, \quad m = 1, 2, 3, 4, \quad (4.32)$$

where $(j, k, n + 1/2) \in \Omega_1$; and (ii)

$$\oint_{S(CE_i^{(2)}(j,k,n+1))} \vec{h}_m^* \cdot d\vec{s} = 0, \quad \ell = 1, 2, 3, \quad m = 1, 2, 3, 4, \quad (4.33)$$

where $(j, k, n + 1) \in \Omega_2$.

Next we shall introduce the Euler counterparts of Eqs. (2.24), (2.25), (2.30), and (2.31). For any $(j, k, n) \in \Omega$, let

$$\begin{pmatrix} (f_{m,\ell}^x)_{j,k}^n \\ (f_{m,\ell}^y)_{j,k}^n \end{pmatrix} \stackrel{\text{def}}{=} T^{-1} \begin{pmatrix} (f_{m,\ell}^x)_{j,k}^n \\ (f_{m,\ell}^y)_{j,k}^n \end{pmatrix}, \quad m, \ell = 1, 2, 3, 4, \quad (4.34)$$

and

$$\begin{pmatrix} (u_{m\zeta})_{j,k}^n \\ (u_{m\eta})_{j,k}^n \end{pmatrix} \stackrel{\text{def}}{=} T^t \begin{pmatrix} (u_{mz})_{j,k}^n \\ (u_{my})_{j,k}^n \end{pmatrix}, \quad m, \ell = 1, 2, 3, 4, \quad (4.35)$$

The normalized counterparts of those parameters defined in Eqs. (4.34) and (4.35) are

$$(f_{m,\ell}^{\zeta+})_{j,k}^n \stackrel{\text{def}}{=} \frac{3\Delta t}{2\Delta\zeta} (f_{m,\ell}^{\zeta})_{j,k}^n, \quad \text{and} \quad (f_{m,\ell}^{\eta+})_{j,k}^n \stackrel{\text{def}}{=} \frac{3\Delta t}{2\Delta\eta} (f_{m,\ell}^{\eta})_{j,k}^n, \quad (4.36)$$

and

$$(u_{m\zeta}^+)_{j,k}^n \stackrel{\text{def}}{=} \frac{\Delta\zeta}{6} (u_{m\zeta})_{j,k}^n, \quad \text{and} \quad (u_{m\eta}^+)_{j,k}^n \stackrel{\text{def}}{=} \frac{\Delta\eta}{6} (u_{m\eta})_{j,k}^n. \quad (4.37)$$

In the following development, for simplicity, we may strip from every variable in an equation its indices j, k , and n if all variables are associated with the same mesh point $(j, k, n) \in \Omega$. Let $F^{\zeta+}$ and $F^{\eta+}$, respectively, denote the matrices formed by $f_{m,\ell}^{\zeta+}$ and $f_{m,\ell}^{\eta+}$, $m, \ell = 1, 2, 3, 4$. Let I be the 4×4 identity matrix. Then the current counterparts to Eqs. (2.35)–(2.52) are

$$\Sigma_{11}^{(1)\pm} \stackrel{\text{def}}{=} I - F^{\zeta+} - F^{\eta+}, \quad (4.38)$$

$$\Sigma_{12}^{(1)\pm} \stackrel{\text{def}}{=} \pm(I - F^{\zeta+} - F^{\eta+})(I + F^{\zeta+}), \quad (4.39)$$

$$\Sigma_{13}^{(1)\pm} \stackrel{\text{def}}{=} \pm(I - F^{\zeta+} - F^{\eta+})(I + F^{\eta+}), \quad (4.40)$$

$$\Sigma_{21}^{(1)\pm} \stackrel{\text{def}}{=} I + F^{\zeta+}, \quad (4.41)$$

$$\Sigma_{22}^{(1)\pm} \stackrel{\text{def}}{=} \mp(I + F^{\zeta+})(2I - F^{\zeta+}), \quad (4.42)$$

$$\Sigma_{23}^{(1)\pm} \stackrel{\text{def}}{=} \pm(I + F^{\zeta+})(I + F^{\eta+}), \quad (4.43)$$

$$\Sigma_{31}^{(1)\pm} \stackrel{\text{def}}{=} I + F^{\eta+}, \quad (4.44)$$

$$\Sigma_{32}^{(1)\pm} \stackrel{\text{def}}{=} \pm(I + F^{\eta+})(I + F^{\zeta+}), \quad (4.45)$$

$$\Sigma_{33}^{(1)\pm} \stackrel{\text{def}}{=} \mp(I + F^{\eta+})(2I - F^{\eta+}), \quad (4.46)$$

$$\Sigma_{11}^{(2)\pm} \stackrel{\text{def}}{=} I + F^{\zeta+} + F^{\eta+}, \quad (4.47)$$

$$\Sigma_{12}^{(2)\pm} \stackrel{\text{def}}{=} \mp(I + F^{\zeta+} + F^{\eta+})(I - F^{\zeta+}), \quad (4.48)$$

$$\Sigma_{13}^{(2)\pm} \stackrel{\text{def}}{=} \mp(I + F^{\zeta+} + F^{\eta+})(I - F^{\eta+}), \quad (4.49)$$

$$\Sigma_{21}^{(2)\pm} \stackrel{\text{def}}{=} I - F^{\zeta+}, \quad (4.50)$$

$$\Sigma_{22}^{(2)\pm} \stackrel{\text{def}}{=} \pm(I - F^{\zeta+})(2I + F^{\zeta+}), \quad (4.51)$$

$$\Sigma_{23}^{(2)\pm} \stackrel{\text{def}}{=} \mp(I - F^{\zeta+})(I - F^{\eta+}), \quad (4.52)$$

$$\Sigma_{31}^{(2)\pm} \stackrel{\text{def}}{=} I - F^{\eta+}, \quad (4.53)$$

$$\Sigma_{32}^{(2)\pm} \stackrel{\text{def}}{=} \mp(I - F^{\eta+})(I - F^{\zeta+}), \quad (4.54)$$

and

$$\Sigma_{33}^{(2)\pm} \stackrel{\text{def}}{=} \pm(I - F^{\eta+})(2I + F^{\eta+}). \quad (4.55)$$

Note that, for the case $\mu = 0$, Eqs. (2.35)–(2.52) become Eqs. (4.38)–(4.55), respectively, if (i) 1, ν_ζ , and ν_η , are replaced by I , $F^{\zeta+}$, and $F^{\eta+}$, respectively, and (ii) $\sigma_{m\ell}^{(1)\pm}$ and $\sigma_{m\ell}^{(2)\pm}$ are replaced by $\Sigma_{m\ell}^{(1)\pm}$ and $\Sigma_{m\ell}^{(2)\pm}$, $m, \ell = 1, 2, 3$, respectively.

Equations (4.32) and (4.33) are evaluated in Appendix B. Let \vec{u} , \vec{u}_ζ^+ , and \vec{u}_η^+ , respectively, be the 4×1 column matrices formed by u_m , $u_{m\zeta}^+$, and $u_{m\eta}^+$, $m = 1, 2, 3, 4$. Then the results can be expressed as:

(a) Eq. (4.32) with $\ell = 1$:

$$\left[\Sigma_{11}^{(1)+} \vec{u} + \Sigma_{12}^{(1)+} \vec{u}_\zeta^+ + \Sigma_{13}^{(1)+} \vec{u}_\eta^+ \right]_{j,k}^{n+1/2} = \left[\Sigma_{11}^{(1)-} \vec{u} + \Sigma_{12}^{(1)-} \vec{u}_\zeta^+ + \Sigma_{13}^{(1)-} \vec{u}_\eta^+ \right]_{j+1/3, k+1/3}^n. \quad (4.56)$$

(b) Eq. (4.32) with $\ell = 2$:

$$\left[\Sigma_{21}^{(1)+} \vec{u} + \Sigma_{22}^{(1)+} \vec{u}_\zeta^+ + \Sigma_{23}^{(1)+} \vec{u}_\eta^+ \right]_{j,k}^{n+1/2} = \left[\Sigma_{21}^{(1)-} \vec{u} + \Sigma_{22}^{(1)-} \vec{u}_\zeta^+ + \Sigma_{23}^{(1)-} \vec{u}_\eta^+ \right]_{j-2/3, k+1/3}^n. \quad (4.57)$$

(c) Eq. (4.32) with $\ell = 3$:

$$\left[\Sigma_{31}^{(1)+} \vec{u} + \Sigma_{32}^{(1)+} \vec{u}_\zeta^+ + \Sigma_{33}^{(1)+} \vec{u}_\eta^+ \right]_{j,k}^{n+1/2} = \left[\Sigma_{31}^{(1)-} \vec{u} + \Sigma_{32}^{(1)-} \vec{u}_\zeta^+ + \Sigma_{33}^{(1)-} \vec{u}_\eta^+ \right]_{j+1/3, k-2/3}^n. \quad (4.58)$$

(d) Eq. (4.33) with $\ell = 1$:

$$\left[\Sigma_{11}^{(2)+} \vec{u} + \Sigma_{12}^{(2)+} \vec{u}_\zeta^+ + \Sigma_{13}^{(2)+} \vec{u}_\eta^+ \right]_{j,k}^{n+1} = \left[\Sigma_{11}^{(2)-} \vec{u} + \Sigma_{12}^{(2)-} \vec{u}_\zeta^+ + \Sigma_{13}^{(2)-} \vec{u}_\eta^+ \right]_{j-1/3, k-1/3}^{n+1/2}. \quad (4.59)$$

(e) Eq. (4.33) with $\ell = 2$:

$$\left[\Sigma_{21}^{(2)+} \vec{u} + \Sigma_{22}^{(2)+} \vec{u}_\zeta^+ + \Sigma_{23}^{(2)+} \vec{u}_\eta^+ \right]_{j,k}^{n+1} = \left[\Sigma_{21}^{(2)-} \vec{u} + \Sigma_{22}^{(2)-} \vec{u}_\zeta^+ + \Sigma_{23}^{(2)-} \vec{u}_\eta^+ \right]_{j+2/3, k-1/3}^{n+1/2}. \quad (4.60)$$

(f) Eq. (4.33) with $\ell = 3$:

$$\left[\Sigma_{31}^{(2)+} \vec{u} + \Sigma_{32}^{(2)+} \vec{u}_\zeta^+ + \Sigma_{33}^{(2)+} \vec{u}_\eta^+ \right]_{j,k}^{n+1} = \left[\Sigma_{31}^{(2)-} \vec{u} + \Sigma_{32}^{(2)-} \vec{u}_\zeta^+ + \Sigma_{33}^{(2)-} \vec{u}_\eta^+ \right]_{j-1/3, k+2/3}^{n+1/2}. \quad (4.61)$$

Here $(j, k, n+1/2) \in \Omega_1$ is assumed in Eqs. (4.56)–(4.58) while $(j, k, n+1) \in \Omega_2$ is assumed in Eqs. (4.59)–(4.61). Note that the forms of Eqs. (4.56)–(4.61) are very similar to those of Eqs. (2.53)–(2.58).

As a result of Eqs. (4.38)–(4.55), we have

$$\Sigma_{11}^{(k)\pm} + \Sigma_{21}^{(k)\pm} + \Sigma_{31}^{(k)\pm} = 3I, \quad k = 1, 2, \quad (4.62)$$

and

$$\Sigma_{12}^{(k)\pm} + \Sigma_{22}^{(k)\pm} + \Sigma_{32}^{(k)\pm} = \Sigma_{13}^{(k)\pm} + \Sigma_{23}^{(k)\pm} + \Sigma_{33}^{(k)\pm} = 0, \quad k = 1, 2. \quad (4.63)$$

Equations (4.62) and (4.63) are the Euler counterparts of Eqs. (3.6) and (3.7), respectively. By summing over Eqs. (4.56)–(4.58), and using Eqs. (4.62) and (4.63) with $k = 1$, one concludes that, for any $(j, k, n+1/2) \in \Omega_1$,

$$\begin{aligned} \bar{u}_{j,k}^{n+1/2} = \frac{1}{3} & \left\{ \left[\Sigma_{11}^{(1)-} \bar{u} + \Sigma_{12}^{(1)-} \bar{u}_\zeta^+ + \Sigma_{13}^{(1)-} \bar{u}_\eta^+ \right]_{j+1/3, k+1/3}^n \right. \\ & + \left[\Sigma_{21}^{(1)-} \bar{u} + \Sigma_{22}^{(1)-} \bar{u}_\zeta^+ + \Sigma_{23}^{(1)-} \bar{u}_\eta^+ \right]_{j-2/3, k+1/3}^n \\ & \left. + \left[\Sigma_{31}^{(1)-} \bar{u} + \Sigma_{32}^{(1)-} \bar{u}_\zeta^+ + \Sigma_{33}^{(1)-} \bar{u}_\eta^+ \right]_{j+1/3, k-2/3}^n \right\}. \end{aligned} \quad (4.64)$$

As a result, $\bar{u}_{j,k}^{n+1/2}$ can be evaluated in terms of the marching variables at the n th time level. Similarly, by summing over Eqs. (4.59)–(4.61), and using Eqs. (4.62) and (4.63) with $k = 2$, one concludes that, for any $(j, k, n+1) \in \Omega_2$,

$$\begin{aligned} \bar{u}_{j,k}^{n+1} = \frac{1}{3} & \left\{ \left[\Sigma_{11}^{(2)-} \bar{u} + \Sigma_{12}^{(2)-} \bar{u}_\zeta^+ + \Sigma_{13}^{(2)-} \bar{u}_\eta^+ \right]_{j-1/3, k-1/3}^{n+1/2} \right. \\ & + \left[\Sigma_{21}^{(2)-} \bar{u} + \Sigma_{22}^{(2)-} \bar{u}_\zeta^+ + \Sigma_{23}^{(2)-} \bar{u}_\eta^+ \right]_{j+2/3, k-1/3}^{n+1/2} \\ & \left. + \left[\Sigma_{31}^{(2)-} \bar{u} + \Sigma_{32}^{(2)-} \bar{u}_\zeta^+ + \Sigma_{33}^{(2)-} \bar{u}_\eta^+ \right]_{j-1/3, k+2/3}^{n+1/2} \right\}. \end{aligned} \quad (4.65)$$

As a result, $\bar{u}_{j,k}^{n+1}$ can be evaluated in terms of the marching variables at the $(n+1/2)$ th time level.

For any $(j, k, n+1/2) \in \Omega_1$, the matrices $(\Sigma_{m\ell}^{(1)+})_{j,k}^{n+1/2}$, $m, \ell = 1, 2, 3$, are functions of $\bar{u}_{j,k}^{n+1/2}$. Thus they are also functions of the marching variables at the n th time level. Assuming the existence of the inverse of each of the matrices $(\Sigma_{m1}^{(1)+})_{j,k}^{n+1/2}$, $m = 1, 2, 3$, one can define

$$\bar{S}_1^{(1)} \stackrel{\text{def}}{=} \left[(\Sigma_{11}^{(1)+})_{j,k}^{n+1/2} \right]^{-1} \left[\Sigma_{11}^{(1)-} \bar{u} + \Sigma_{12}^{(1)-} \bar{u}_\zeta^+ + \Sigma_{13}^{(1)-} \bar{u}_\eta^+ \right]_{j+1/3, k+1/3}^n, \quad (4.66)$$

$$\vec{S}_2^{(1)} \stackrel{\text{def}}{=} \left[\left(\Sigma_{21}^{(1)+} \right)_{j,k}^{n+1/2} \right]^{-1} \left[\Sigma_{21}^{(1)-} \vec{u} + \Sigma_{22}^{(1)-} \vec{u}_\zeta^+ + \Sigma_{23}^{(1)-} \vec{u}_\eta^+ \right]_{j-2/3, k+1/3}^n, \quad (4.67)$$

and

$$\vec{S}_3^{(1)} \stackrel{\text{def}}{=} \left[\left(\Sigma_{31}^{(1)+} \right)_{j,k}^{n+1/2} \right]^{-1} \left[\Sigma_{31}^{(1)-} \vec{u} + \Sigma_{32}^{(1)-} \vec{u}_\zeta^+ + \Sigma_{33}^{(1)-} \vec{u}_\eta^+ \right]_{j+1/3, k-2/3}^n, \quad (4.68)$$

where the inverse of a matrix A is denoted by $[A]^{-1}$. As a result of their definitions, $\vec{S}_\ell^{(1)}$, $\ell = 1, 2, 3$, can be evaluated using the marching variables at the n th time level.

For any $(j, k, n+1) \in \Omega_2$, the matrices $(\Sigma_{m\ell}^{(2)+})_{j,k}^{n+1}$, $m, \ell = 1, 2, 3$, are functions of $\vec{u}_{j,k}^{n+1}$. Thus they are also functions of the marching variables at the $(n+1/2)$ th time level. Assuming the existence of the inverse of each of the matrices $(\Sigma_{m1}^{(2)+})_{j,k}^{n+1}$, $m = 1, 2, 3$, one can define

$$\vec{S}_1^{(2)} \stackrel{\text{def}}{=} \left[\left(\Sigma_{11}^{(2)+} \right)_{j,k}^{n+1} \right]^{-1} \left[\Sigma_{11}^{(2)-} \vec{u} + \Sigma_{12}^{(2)-} \vec{u}_\zeta^+ + \Sigma_{13}^{(2)-} \vec{u}_\eta^+ \right]_{j-1/3, k-1/3}^{n+1/2}, \quad (4.69)$$

$$\vec{S}_2^{(2)} \stackrel{\text{def}}{=} \left[\left(\Sigma_{21}^{(2)+} \right)_{j,k}^{n+1} \right]^{-1} \left[\Sigma_{21}^{(2)-} \vec{u} + \Sigma_{22}^{(2)-} \vec{u}_\zeta^+ + \Sigma_{23}^{(2)-} \vec{u}_\eta^+ \right]_{j+2/3, k-1/3}^{n+1/2}, \quad (4.70)$$

and

$$\vec{S}_3^{(2)} \stackrel{\text{def}}{=} \left[\left(\Sigma_{31}^{(2)+} \right)_{j,k}^{n+1} \right]^{-1} \left[\Sigma_{31}^{(2)-} \vec{u} + \Sigma_{32}^{(2)-} \vec{u}_\zeta^+ + \Sigma_{33}^{(2)-} \vec{u}_\eta^+ \right]_{j-1/3, k+2/3}^{n+1/2}. \quad (4.71)$$

As a result of their definitions, $\vec{S}_\ell^{(2)}$, $\ell = 1, 2, 3$, can be evaluated using the marching variables at the $(n+1/2)$ th time level.

Using Eqs. (4.38), (4.41), (4.44), (4.47), (4.50), (4.53), and (4.66)–(4.71), Eqs. (4.64) and (4.65) can be recast as

$$\vec{u}_{j,k}^{n+1/2} = \frac{1}{3} \left[(I - F^{\zeta+} - F^{\eta+})_{j,k}^{n+1/2} \vec{S}_1^{(1)} + (I + F^{\zeta+})_{j,k}^{n+1/2} \vec{S}_2^{(1)} + (I + F^{\eta+})_{j,k}^{n+1/2} \vec{S}_3^{(1)} \right], \quad (4.72)$$

and

$$\vec{u}_{j,k}^{n+1} = \frac{1}{3} \left[(I + F^{\zeta+} + F^{\eta+})_{j,k}^{n+1} \vec{S}_1^{(2)} + (I - F^{\zeta+})_{j,k}^{n+1} \vec{S}_2^{(2)} + (I - F^{\eta+})_{j,k}^{n+1} \vec{S}_3^{(2)} \right], \quad (4.73)$$

respectively. Equations (4.72) and (4.73) are the Euler counterparts of Eqs. (2.67) and (2.70), respectively.

Furthermore, Eqs. (4.38)–(4.55) imply that:

(a) At any $(j, k, n + 1/2) \in \Omega_1$, we have

$$\left[\Sigma_{11}^{(1)+} \right]^{-1} \Sigma_{12}^{(1)\pm} = \pm (I + F^{\zeta+}), \quad (4.74)$$

$$\left[\Sigma_{11}^{(1)+} \right]^{-1} \Sigma_{13}^{(1)\pm} = \pm (I + F^{\eta+}), \quad (4.75)$$

$$\left[\Sigma_{21}^{(1)+} \right]^{-1} \Sigma_{22}^{(1)\pm} = \mp (2I - F^{\zeta+}), \quad (4.76)$$

$$\left[\Sigma_{21}^{(1)+} \right]^{-1} \Sigma_{23}^{(1)\pm} = \pm (I + F^{\eta+}), \quad (4.77)$$

$$\left[\Sigma_{31}^{(1)+} \right]^{-1} \Sigma_{32}^{(1)\pm} = \pm (I + F^{\zeta+}), \quad (4.78)$$

and

$$\left[\Sigma_{31}^{(1)+} \right]^{-1} \Sigma_{33}^{(1)\pm} = \mp (2I - F^{\eta+}). \quad (4.79)$$

(b) At any $(j, k, n + 1) \in \Omega_2$, we have

$$\left[\Sigma_{11}^{(2)+} \right]^{-1} \Sigma_{12}^{(2)\pm} = \mp (I - F^{\zeta+}), \quad (4.80)$$

$$\left[\Sigma_{11}^{(2)+} \right]^{-1} \Sigma_{13}^{(2)\pm} = \mp (I - F^{\eta+}), \quad (4.81)$$

$$\left[\Sigma_{21}^{(2)+} \right]^{-1} \Sigma_{22}^{(2)\pm} = \pm (2I + F^{\zeta+}), \quad (4.82)$$

$$\left[\Sigma_{21}^{(2)+} \right]^{-1} \Sigma_{23}^{(2)\pm} = \mp (I - F^{\eta+}), \quad (4.83)$$

$$\left[\Sigma_{31}^{(2)+} \right]^{-1} \Sigma_{32}^{(2)\pm} = \mp (I - F^{\zeta+}), \quad (4.84)$$

and

$$\left[\Sigma_{31}^{(2)+} \right]^{-1} \Sigma_{33}^{(2)\pm} = \pm (2I + F^{\eta+}). \quad (4.85)$$

By using Eqs. (4.74)–(4.85), Eqs. (4.56)–(4.61) imply that

$$\left[\vec{u} + (I + F^{\zeta+}) \vec{u}_{\zeta}^+ + (I + F^{\eta+}) \vec{u}_{\eta}^+ \right]_{j,k}^{n+1/2} = \vec{S}_1^{(1)}, \quad (4.86)$$

$$\left[\vec{u} - (2I - F^{\zeta+}) \vec{u}_{\zeta}^+ + (I + F^{\eta+}) \vec{u}_{\eta}^+ \right]_{j,k}^{n+1/2} = \vec{S}_2^{(1)}, \quad (4.87)$$

$$\left[\vec{u} + (I + F^{\zeta+}) \vec{u}_{\zeta}^+ - (2I - F^{\eta+}) \vec{u}_{\eta}^+ \right]_{j,k}^{n+1/2} = \vec{S}_3^{(1)}, \quad (4.88)$$

$$\left[\vec{u} - (I - F^{\zeta+}) \vec{u}_{\zeta}^+ - (I - F^{\eta+}) \vec{u}_{\eta}^+ \right]_{j,k}^{n+1} = \vec{S}_1^{(2)}, \quad (4.89)$$

$$\left[\vec{u} + (2I + F^{\zeta+}) \vec{u}_{\zeta}^+ - (I - F^{\eta+}) \vec{u}_{\eta}^+ \right]_{j,k}^{n+1} = \vec{S}_2^{(2)}, \quad (4.90)$$

$$\left[\vec{u} - (I - F^{\zeta+}) \vec{u}_{\zeta}^+ + (2I + F^{\eta+}) \vec{u}_{\eta}^+ \right]_{j,k}^{n+1} = \vec{S}_3^{(2)}, \quad (4.91)$$

where $(j, k, n + 1/2) \in \Omega_1$ is assumed in Eqs. (4.86)–(4.88), while $(j, k, n + 1) \in \Omega_2$ is assumed in Eqs. (4.89)–(4.91). Because $s_1^{(1)}$, $s_2^{(1)}$, $s_3^{(1)}$, $s_1^{(2)}$, $s_2^{(2)}$, and $s_3^{(2)}$, denote the expressions on the right sides of Eqs. (2.60)–(2.65), respectively, a comparison between these equations and Eqs. (4.86)–(4.91) reveals that the latter are the Euler counterparts of the former, respectively.

Note that, by multiplying Eqs. (4.86)–(4.88) from left with $(I - F^{\zeta+} - F^{\eta+})_{j,k}^{n+1/2}$, $(I + F^{\zeta+})_{j,k}^{n+1/2}$, and $(I + F^{\eta+})_{j,k}^{n+1/2}$, respectively, and summing over the resulting equations, one can obtain Eq. (4.72). Similarly, one can obtain Eq. (4.73) from Eqs. (4.89)–(4.91). Moreover, (i) Eqs. (4.86)–(4.88) also imply that

$$\left(\vec{u}_{\zeta}^+ \right)_{j,k}^{n+1/2} = \frac{1}{3} \left(\vec{S}_1^{(1)} - \vec{S}_2^{(1)} \right), \quad \text{and} \quad \left(\vec{u}_{\eta}^+ \right)_{j,k}^{n+1/2} = \frac{1}{3} \left(\vec{S}_1^{(1)} - \vec{S}_3^{(1)} \right), \quad (4.92)$$

where $(j, k, n + 1/2) \in \Omega_1$; and (ii) Eqs. (4.89)–(4.91) also imply that

$$\left(\vec{u}_{\zeta}^+ \right)_{j,k}^{n+1} = \frac{1}{3} \left(\vec{S}_2^{(2)} - \vec{S}_1^{(2)} \right), \quad \text{and} \quad \left(\vec{u}_{\eta}^+ \right)_{j,k}^{n+1} = \frac{1}{3} \left(\vec{S}_3^{(2)} - \vec{S}_1^{(2)} \right), \quad (4.93)$$

where $(j, k, n + 1) \in \Omega_2$. By using the above results, and directly substituting Eqs. (4.72), (4.73), (4.92), and (4.93) into Eqs. (4.86)–(4.91), one concludes that: (i) Eqs. (4.72) and (4.92) are equivalent to Eqs. (4.86)–(4.88); and (ii) Eqs. (4.73) and (4.93) are equivalent to Eqs. (4.89)–(4.91).

With the above preparations, an Euler solver can now be defined. It consists of two marching steps. The first is formed by Eqs. (4.64) and (4.92), while the second is formed by Eqs. (4.65) and (4.93). As explained earlier, $\vec{S}_{\ell}^{(k)}$, $k = 1, 2$, and $\ell = 1, 2, 3$, become

known after $\bar{u}_{j,k}^{n+1/2}$ and $\bar{u}_{j,k}^{n+1}$ are evaluated using Eqs. (4.64) and (4.65), respectively. This Euler solver has a two-way marching nature similar to that of the a scheme. As a result, it must be neutrally stable, (i.e., no numerical diffusion) if it is stable. Because it is reversible in time, this solver cannot model a physical problem that is irreversible in time, e.g., an inviscid flow problem involving shocks. Hereafter, this new Euler solver will be referred to as the Euler a scheme.

At this juncture, note that the Euler a scheme is greatly simplified by the fact that $\bar{u}_{j,k}^{n+1/2}$ and $\bar{u}_{j,k}^{n+1}$, respectively, can be directly evaluated in terms of the marching variables at the n th and $(n + 1/2)$ th time levels (see Eqs. (4.64) and (4.65)). As a result, the matrices $(\Sigma_{ml}^{(1+)})_{j,k}^{n+1/2}$ and $(\Sigma_{ml}^{(2+)})_{j,k}^{n+1}$, which are nonlinear functions of $\bar{u}_{j,k}^{n+1/2}$ and $\bar{u}_{j,k}^{n+1}$, respectively, can be evaluated easily. In other words, nonlinearity of the above matrix functions does not cause a particular problem for the Euler a scheme.

To explain how Eqs. (4.64) and (4.65) arise, note that

$$\oint_{S(CE^{(1)}(j,k,n+1/2))} \vec{h}_m^* \cdot d\vec{s} = 0, \quad (j, k, n + 1/2) \in \Omega_1, \quad (4.94)$$

and

$$\oint_{S(CE^{(2)}(j,k,n+1))} \vec{h}_m^* \cdot d\vec{s} = 0. \quad (j, k, n + 1) \in \Omega_2, \quad (4.95)$$

respectively, are the direct results of Eqs. (4.32) and (4.33), the basic assumptions of the Euler a scheme. According to Eq. (3.2), $CE^{(1)}(j, k, n + 1/2)$ is the hexagonal cylinder $A'B'C'D'E'F'ABCDEF$ depicted in Fig. 5(a). Except for the top face $A'B'C'D'E'F'$, the other boundaries of this cylinder are the subsets of three solution elements at the n th time level. Thus, for any $m = 1, 2, 3, 4$, the flux of \vec{h}_m^* leaving $CE^{(1)}(j, k, n + 1/2)$ through all the boundaries except the top face can be evaluated in terms of the marching variables at the n th time level. On the other hand, because the top face is a subset of $SE(j, k, n + 1/2)$, the flux leaving there is a function of the marching variables associated with $SE(j, k, n + 1/2)$. Furthermore, because the outward normal to the top face has no spatial component, Eq. (4.29) implies that the total flux of \vec{h}_m^* leaving $CE^{(1)}(j, k, n + 1/2)$ through the top face is the surface integration of u_m^* over the top face. Because the center of $SE(j, k, n + 1/2)$ coincides with the center of the top face, it is easy to see that the first-order terms in Eqs. (4.19) do not contribute to the total flux leaving the top face. It follows that the total flux leaving the top face is a function of $(u_m)_{j,k}^{n+1/2}$ only. As a result of the above considerations, $\bar{u}_{j,k}^{n+1/2}$ can be determined in terms of the marching variables at the n th time level by using Eq. (4.94) only. Similarly, $\bar{u}_{j,k}^{n+1}$ can be determined in terms of the marching variables at the $(n + 1/2)$ th time level by using Eq. (4.95) only. Eqs. (4.64) and (4.65) are the direct results of Eqs. (4.94) and (4.95), respectively.

In an extension currently under development, the mesh used is not uniform in space. As a result, point G' depicted in Fig. 5(a) generally is not the center of the top face referred

to earlier. To simplify the development, we have moved the center of $SE(j, k, n + 1/2)$ to the center of the top face, i.e., away from point G' .

Next we shall construct the Euler a - ϵ scheme, i.e., the Euler version of the a - ϵ scheme. For this scheme, we shall use the CEs defined in Eqs. (3.2) and (3.3), i.e., Eqs. (4.94) and (4.95) will be assumed. Thus Eqs. (4.64) and (4.65) will also be part of the Euler a - ϵ scheme. In the following, we shall describe the rest of the Euler a - ϵ scheme.

As a result of their definitions, evaluation of $\vec{S}_\ell^{(k)}$ involves the inversion of the 4×4 matrices $\left(\Sigma_{m1}^{(1)+}\right)_{j,k}^{n+1/2}$, and $\left(\Sigma_{m1}^{(2)+}\right)_{j,k}^{n+1}$, $m = 1, 2, 3$. To simplify computation, we shall assume that

$$\left(\Sigma_{11}^{(1)+}\right)_{j,k}^{n+1/2} = \left(\Sigma_{11}^{(1)+}\right)_{j+1/3, k+1/3}^n, \quad (j, k, n + 1/2) \in \Omega_1, \quad (4.96)$$

$$\left(\Sigma_{21}^{(1)+}\right)_{j,k}^{n+1/2} = \left(\Sigma_{21}^{(1)+}\right)_{j-2/3, k+1/3}^n, \quad (j, k, n + 1/2) \in \Omega_1, \quad (4.97)$$

$$\left(\Sigma_{31}^{(1)+}\right)_{j,k}^{n+1/2} = \left(\Sigma_{31}^{(1)+}\right)_{j+1/3, k-2/3}^n, \quad (j, k, n + 1/2) \in \Omega_1, \quad (4.98)$$

$$\left(\Sigma_{11}^{(2)+}\right)_{j,k}^{n+1} = \left(\Sigma_{11}^{(2)+}\right)_{j-1/3, k-1/3}^{n+1/2}, \quad (j, k, n + 1) \in \Omega_2, \quad (4.99)$$

$$\left(\Sigma_{21}^{(2)+}\right)_{j,k}^{n+1} = \left(\Sigma_{21}^{(2)+}\right)_{j+2/3, k-1/3}^{n+1/2}, \quad (j, k, n + 1) \in \Omega_2, \quad (4.100)$$

and

$$\left(\Sigma_{31}^{(2)+}\right)_{j,k}^{n+1} = \left(\Sigma_{31}^{(2)+}\right)_{j-1/3, k+2/3}^{n+1/2}, \quad (j, k, n + 1) \in \Omega_2. \quad (4.101)$$

By using Eqs. (4.38), (4.41), (4.44), (4.47), (4.50), (4.53), (4.74)–(4.85), and (4.96)–(4.101), Eqs. (4.66)–(4.71) imply that (i)

$$\vec{S}_1^{(1)} = \vec{s}_1^{(1)} \stackrel{\text{def}}{=} \left[\vec{u} - (I + F^{\zeta+}) \vec{u}_\zeta^+ - (I + F^{\eta+}) \vec{u}_\eta^+ \right]_{j+1/3, k+1/3}^n, \quad (4.102)$$

$$\vec{S}_2^{(1)} = \vec{s}_2^{(1)} \stackrel{\text{def}}{=} \left[\vec{u} + (2I - F^{\zeta+}) \vec{u}_\zeta^+ - (I + F^{\eta+}) \vec{u}_\eta^+ \right]_{j-2/3, k+1/3}^n, \quad (4.103)$$

and

$$\vec{S}_3^{(1)} = \vec{s}_3^{(1)} \stackrel{\text{def}}{=} \left[\vec{u} - (I + F^{\zeta+}) \vec{u}_\zeta^+ + (2I - F^{\eta+}) \vec{u}_\eta^+ \right]_{j+1/3, k-2/3}^n, \quad (4.104)$$

where $(j, k, n + 1/2) \in \Omega_1$; and (ii)

$$\vec{S}_1^{(2)} = \vec{s}_1^{(2)} \stackrel{\text{def}}{=} \left[\vec{u} + (I - F^{\zeta+}) \vec{u}_\zeta^+ + (I - F^{\eta+}) \vec{u}_\eta^+ \right]_{j-1/3, k-1/3}^{n+1/2}, \quad (4.105)$$

$$\vec{S}_2^{(2)} = \vec{s}_2^{(2)} \stackrel{\text{def}}{=} \left[\vec{u} - (2I + F^{\zeta+}) \vec{u}_\zeta^+ + (I - F^{\eta+}) \vec{u}_\eta^+ \right]_{j+2/3, k-1/3}^{n+1/2}, \quad (4.106)$$

and

$$\vec{S}_3^{(2)} = \vec{s}_3^{(2)} \stackrel{\text{def}}{=} \left[\vec{u} + (I - F^{\zeta+}) \vec{u}_\zeta^+ - (2I + F^{\eta+}) \vec{u}_\eta^+ \right]_{j-1/3, k+2/3}^{n+1/2}, \quad (4.107)$$

where $(j, k, n + 1) \in \Omega_2$. Note that $\vec{s}_\ell^{(k)}$, $k = 1, 2$, and $\ell = 1, 2, 3$, respectively, are structurally similar to $s_\ell^{(k)}$, $k = 1, 2$, and $\ell = 1, 2, 3$, which were defined in Sec. 2.

Equation (4.92) coupled with Eqs. (4.102)–(4.104) implies that

$$\left(\vec{u}_\zeta^+ \right)_{j,k}^{n+1/2} = \left(\vec{u}_\zeta^{o+} \right)_{j,k}^{n+1/2}, \quad \text{and} \quad \left(\vec{u}_\eta^+ \right)_{j,k}^{n+1/2} = \left(\vec{u}_\eta^{o+} \right)_{j,k}^{n+1/2}, \quad (4.108)$$

where $(j, k, n + 1/2) \in \Omega_1$, and

$$\left(\vec{u}_\zeta^{o+} \right)_{j,k}^{n+1/2} \stackrel{\text{def}}{=} \frac{1}{3} \left(\vec{s}_1^{(1)} - \vec{s}_2^{(1)} \right), \quad \text{and} \quad \left(\vec{u}_\eta^{o+} \right)_{j,k}^{n+1/2} \stackrel{\text{def}}{=} \frac{1}{3} \left(\vec{s}_1^{(1)} - \vec{s}_3^{(1)} \right). \quad (4.109)$$

Note that: (i) As a result of Eqs. (4.102)–(4.104) and (4.109), $\left(\vec{u}_\zeta^{o+} \right)_{j,k}^{n+1/2}$ and $\left(\vec{u}_\eta^{o+} \right)_{j,k}^{n+1/2}$ can be evaluated in terms of the marching variables at the n th time level; and (ii) Eq. (4.109) is the Euler version of Eq. (3.20).

Similarly, Eq. (4.93) coupled with Eqs. (4.105)–(4.107) implies that

$$\left(\vec{u}_\zeta^+ \right)_{j,k}^{n+1} = \left(\vec{u}_\zeta^{o+} \right)_{j,k}^{n+1}, \quad \text{and} \quad \left(\vec{u}_\eta^+ \right)_{j,k}^{n+1} = \left(\vec{u}_\eta^{o+} \right)_{j,k}^{n+1}, \quad (4.110)$$

where $(j, k, n + 1) \in \Omega_2$, and

$$\left(\vec{u}_\zeta^{o+} \right)_{j,k}^{n+1} \stackrel{\text{def}}{=} \frac{1}{3} \left(\vec{s}_2^{(2)} - \vec{s}_1^{(2)} \right), \quad \text{and} \quad \left(\vec{u}_\eta^{o+} \right)_{j,k}^{n+1} \stackrel{\text{def}}{=} \frac{1}{3} \left(\vec{s}_3^{(2)} - \vec{s}_1^{(2)} \right). \quad (4.111)$$

Note that: (i) As a result of Eqs. (4.105)–(4.107) and (4.111), $\left(\vec{u}_\zeta^{o+} \right)_{j,k}^{n+1}$ and $\left(\vec{u}_\eta^{o+} \right)_{j,k}^{n+1}$ can be evaluated in terms of the marching variables at the $(n + 1/2)$ th time level; and (ii) Eq. (4.111) is the Euler version of Eq. (3.36).

Furthermore, for any $(j, k, n) \in \Omega$, let $(\vec{u}_t)_{j,k}^n$ denote the column matrix formed by $(u_{mt})_{j,k}^n$, $m = 1, 2, 3, 4$. Then Eq. (4.31) coupled with Eq. (B.5) implies that

$$\vec{u}_t = -\frac{4}{\Delta t} \left(F^{\zeta+} \vec{u}_\zeta^+ + F^{\eta+} \vec{u}_\eta^+ \right). \quad (4.112)$$

With the aid of Eq. (4.112), we shall carry out a development parallel to an earlier one that involves Eqs. (3.8)–(3.48). As will be shown, equations obtained in the new development are essentially the “images” of Eqs. (3.8)–(3.48) under the following mapping:

$$\begin{aligned}
u &\rightarrow \bar{u}, & u' &\rightarrow \bar{u}', & u_t &\rightarrow \bar{u}_t, & \nu_\zeta &\rightarrow F^{\zeta+}, & \nu_\eta &\rightarrow F^{\eta+}, \\
u'_\zeta &\rightarrow \bar{u}'_\zeta, & u'_\eta &\rightarrow \bar{u}'_\eta, & u_\zeta^+ &\rightarrow \bar{u}_\zeta^+, & u_\eta^+ &\rightarrow \bar{u}_\eta^+, \\
u_\zeta^{\circ+} &\rightarrow \bar{u}_\zeta^{\circ+}, & u_\eta^{\circ+} &\rightarrow \bar{u}_\eta^{\circ+}, & u_\zeta'^+ &\rightarrow \bar{u}_\zeta'^+, & \text{and} & u_\eta'^+ &\rightarrow \bar{u}_\eta'^+.
\end{aligned} \tag{4.113}$$

To proceed, for any $(j, k, n + 1/2) \in \Omega_1$, let

$$\bar{u}'_{j+1/3, k+1/3}{}^{n+1/2} \stackrel{\text{def}}{=} \left(\bar{u} + \frac{\Delta t}{2} \bar{u}_t \right)_{j+1/3, k+1/3}^n, \tag{4.114}$$

$$\bar{u}'_{j-2/3, k+1/3}{}^{n+1/2} \stackrel{\text{def}}{=} \left(\bar{u} + \frac{\Delta t}{2} \bar{u}_t \right)_{j-2/3, k+1/3}^n, \tag{4.115}$$

and

$$\bar{u}'_{j+1/3, k-2/3}{}^{n+1/2} \stackrel{\text{def}}{=} \left(\bar{u} + \frac{\Delta t}{2} \bar{u}_t \right)_{j+1/3, k-2/3}^n. \tag{4.116}$$

With the aid of Eq. (4.112), Eqs. (4.114)–(4.116) imply that

$$\bar{u}'_{j+1/3, k+1/3}{}^{n+1/2} = \left[\bar{u} - 2 \left(F^{\zeta+} \bar{u}_\zeta^+ + F^{\eta+} \bar{u}_\eta^+ \right) \right]_{j+1/3, k+1/3}^n, \tag{4.117}$$

$$\bar{u}'_{j-2/3, k+1/3}{}^{n+1/2} = \left[\bar{u} - 2 \left(F^{\zeta+} \bar{u}_\zeta^+ + F^{\eta+} \bar{u}_\eta^+ \right) \right]_{j-2/3, k+1/3}^n, \tag{4.118}$$

and

$$\bar{u}'_{j+1/3, k-2/3}{}^{n+1/2} = \left[\bar{u} - 2 \left(F^{\zeta+} \bar{u}_\zeta^+ + F^{\eta+} \bar{u}_\eta^+ \right) \right]_{j+1/3, k-2/3}^n. \tag{4.119}$$

For each $m = 1, 2, 3, 4$, the earlier geometric argument involving Fig. 10(a) can be repeated here with $u'_{j+1/3, k+1/3}{}^{n+1/2}$, $u'_{j-2/3, k+1/3}{}^{n+1/2}$, and $u'_{j+1/3, k-2/3}{}^{n+1/2}$, in Fig. 10(a) being replaced by the m -th components of $\bar{u}'_{j+1/3, k+1/3}{}^{n+1/2}$, $\bar{u}'_{j-2/3, k+1/3}{}^{n+1/2}$ and $\bar{u}'_{j+1/3, k-2/3}{}^{n+1/2}$, respectively. This new argument leads to the definitions:

$$(\bar{u}'_\zeta)_{j, k}{}^{n+1/2} \stackrel{\text{def}}{=} \left(\bar{u}'_{j+1/3, k+1/3}{}^{n+1/2} - \bar{u}'_{j-2/3, k+1/3}{}^{n+1/2} \right) / \Delta \zeta, \tag{4.120}$$

$$(\bar{u}'_\eta)_{j, k}{}^{n+1/2} \stackrel{\text{def}}{=} \left(\bar{u}'_{j+1/3, k+1/3}{}^{n+1/2} - \bar{u}'_{j+1/3, k-2/3}{}^{n+1/2} \right) / \Delta \eta, \tag{4.121}$$

and

$$(\bar{u}'_{\zeta})_{j,k}^{n+1/2} \stackrel{\text{def}}{=} \frac{\Delta\zeta}{6} (\bar{u}'_{\zeta})_{j,k}^{n+1/2}, \quad \text{and} \quad (\bar{u}'_{\eta})_{j,k}^{n+1/2} \stackrel{\text{def}}{=} \frac{\Delta\eta}{6} (\bar{u}'_{\eta})_{j,k}^{n+1/2}. \quad (4.122)$$

Equations (4.120)–(4.122) are the Euler versions of Eqs. (3.16), (3.17) and (3.19), respectively.

Next we introduce the Euler versions of Eqs. (3.21) and (3.22), i.e.,

$$(d\bar{u}'_{\zeta})_{j,k}^{n+1/2} \stackrel{\text{def}}{=} 2 \left[(\bar{u}'_{\zeta})_{j,k}^{n+1/2} - (\bar{u}'_{\zeta})_{j,k}^{o+} \right], \quad (j, k, n + 1/2) \in \Omega_1, \quad (4.123)$$

and

$$(d\bar{u}'_{\eta})_{j,k}^{n+1/2} \stackrel{\text{def}}{=} 2 \left[(\bar{u}'_{\eta})_{j,k}^{n+1/2} - (\bar{u}'_{\eta})_{j,k}^{o+} \right], \quad (j, k, n + 1/2) \in \Omega_1. \quad (4.124)$$

Then, with the aid of Eqs. (4.102)–(4.104), (4.109) and (4.117)–(4.122), one has

$$(d\bar{u}'_{\zeta})_{j,k}^{n+1/2} = \frac{1}{3} \left[(\bar{u} + 4\bar{u}'_{\zeta} - 2\bar{u}'_{\eta})_{j-2/3, k+1/3}^n - (\bar{u} - 2\bar{u}'_{\zeta} - 2\bar{u}'_{\eta})_{j+1/3, k+1/3}^n \right], \quad (4.125)$$

and

$$(d\bar{u}'_{\eta})_{j,k}^{n+1/2} = \frac{1}{3} \left[(\bar{u} - 2\bar{u}'_{\zeta} + 4\bar{u}'_{\eta})_{j+1/3, k-2/3}^n - (\bar{u} - 2\bar{u}'_{\zeta} - 2\bar{u}'_{\eta})_{j+1/3, k+1/3}^n \right]. \quad (4.126)$$

Thus both $(d\bar{u}'_{\zeta})_{j,k}^{n+1/2}$ and $(d\bar{u}'_{\eta})_{j,k}^{n+1/2}$ are functions of the marching variables at the n th time level.

Similarly, for any $(j, k, n + 1) \in \Omega_2$, let

$$\bar{u}'_{j-1/3, k-1/3}^{n+1} \stackrel{\text{def}}{=} \left(\bar{u} + \frac{\Delta t}{2} \bar{u}_t \right)_{j-1/3, k-1/3}^{n+1/2}, \quad (4.127)$$

$$\bar{u}'_{j+2/3, k-1/3}^{n+1} \stackrel{\text{def}}{=} \left(\bar{u} + \frac{\Delta t}{2} \bar{u}_t \right)_{j+2/3, k-1/3}^{n+1/2}, \quad (4.128)$$

and

$$\bar{u}'_{j-1/3, k+2/3}^{n+1} \stackrel{\text{def}}{=} \left(\bar{u} + \frac{\Delta t}{2} \bar{u}_t \right)_{j-1/3, k+2/3}^{n+1/2}. \quad (4.129)$$

With the aid of Eq. (4.112), Eqs. (4.127)–(4.128) imply that

$$\bar{u}'_{j-1/3, k-1/3}^{n+1} = \left[\bar{u} - 2 \left(F^{\zeta+} \bar{u}'_{\zeta} + F^{\eta+} \bar{u}'_{\eta} \right) \right]_{j-1/3, k-1/3}^{n+1/2}, \quad (4.130)$$

$$\bar{u}'_{j+2/3,k-1/3}{}^{n+1} = \left[\bar{u} - 2 \left(F^{\zeta+} \bar{u}'_{\zeta}{}^+ + F^{\eta+} \bar{u}'_{\eta}{}^+ \right) \right]_{j+2/3,k-1/3}^{n+1/2}, \quad (4.131)$$

and

$$\bar{u}'_{j-1/3,k+2/3}{}^{n+1} = \left[\bar{u} - 2 \left(F^{\zeta+} \bar{u}'_{\zeta}{}^+ + F^{\eta+} \bar{u}'_{\eta}{}^+ \right) \right]_{j-1/3,k+2/3}^{n+1/2}, \quad (4.132)$$

The Euler versions of Eqs. (3.33)–(3.35), (3.37), and (3.38) are

$$(\bar{u}'_{\zeta})_{j,k}{}^{n+1} \stackrel{\text{def}}{=} \left(\bar{u}'_{j+2/3,k-1/3}{}^{n+1} - \bar{u}'_{j-1/3,k-1/3}{}^{n+1} \right) / \Delta \zeta, \quad (4.133)$$

$$(\bar{u}'_{\eta})_{j,k}{}^{n+1} \stackrel{\text{def}}{=} \left(\bar{u}'_{j-1/3,k+2/3}{}^{n+1} - \bar{u}'_{j-1/3,k-1/3}{}^{n+1} \right) / \Delta \eta, \quad (4.134)$$

$$(\bar{u}'_{\zeta}{}^+)_{j,k}{}^{n+1} \stackrel{\text{def}}{=} \frac{\Delta \zeta}{6} (\bar{u}'_{\zeta})_{j,k}{}^{n+1}, \quad \text{and} \quad (\bar{u}'_{\eta}{}^+)_{j,k}{}^{n+1} \stackrel{\text{def}}{=} \frac{\Delta \eta}{6} (\bar{u}'_{\eta})_{j,k}{}^{n+1}, \quad (4.135)$$

$$(d\bar{u}'_{\zeta}{}^+)_{j,k}{}^{n+1} \stackrel{\text{def}}{=} 2 \left[(\bar{u}'_{\zeta}{}^+)_{j,k}{}^{n+1} - (\bar{u}'_{\zeta}{}^{o+})_{j,k}{}^{n+1} \right], \quad (j, k, n+1) \in \Omega_2, \quad (4.136)$$

and

$$(d\bar{u}'_{\eta}{}^+)_{j,k}{}^{n+1} \stackrel{\text{def}}{=} 2 \left[(\bar{u}'_{\eta}{}^+)_{j,k}{}^{n+1} - (\bar{u}'_{\eta}{}^{o+})_{j,k}{}^{n+1} \right], \quad (j, k, n+1) \in \Omega_2. \quad (4.137)$$

Combining Eqs. (4.105)–(4.107), and (4.130)–(4.137), one has

$$(d\bar{u}'_{\zeta}{}^+)_{j,k}{}^{n+1} = \frac{1}{3} \left[\left(\bar{u} + 2\bar{u}'_{\zeta}{}^+ + 2\bar{u}'_{\eta}{}^+ \right)_{j-1/3,k-1/3}^{n+1/2} - \left(\bar{u} - 4\bar{u}'_{\zeta}{}^+ + 2\bar{u}'_{\eta}{}^+ \right)_{j+2/3,k-1/3}^{n+1/2} \right], \quad (4.138)$$

and

$$(d\bar{u}'_{\eta}{}^+)_{j,k}{}^{n+1} = \frac{1}{3} \left[\left(\bar{u} + 2\bar{u}'_{\zeta}{}^+ + 2\bar{u}'_{\eta}{}^+ \right)_{j-1/3,k-1/3}^{n+1/2} - \left(\bar{u} + 2\bar{u}'_{\zeta}{}^+ - 4\bar{u}'_{\eta}{}^+ \right)_{j-1/3,k+2/3}^{n+1/2} \right]. \quad (4.139)$$

Thus both $(d\bar{u}'_{\zeta}{}^+)_{j,k}{}^{n+1}$ and $(d\bar{u}'_{\eta}{}^+)_{j,k}{}^{n+1}$ are functions of the marching variables at the $(n+1/2)$ th time level.

The Euler a - ϵ scheme can now be stated using the above definitions. It consists of two marching steps. The first is formed by Eq. (4.64),

$$\left(\bar{u}'_{\zeta}{}^+ \right)_{j,k}{}^{n+1/2} = \left(\bar{u}'_{\zeta}{}^{o+} \right)_{j,k}{}^{n+1/2} + \epsilon (d\bar{u}'_{\zeta}{}^+)_{j,k}{}^{n+1/2}, \quad (4.140)$$

and

$$\left(\bar{u}'_{\eta}{}^+ \right)_{j,k}{}^{n+1/2} = \left(\bar{u}'_{\eta}{}^{o+} \right)_{j,k}{}^{n+1/2} + \epsilon (d\bar{u}'_{\eta}{}^+)_{j,k}{}^{n+1/2}, \quad (4.141)$$

where $(j, k, n + 1/2) \in \Omega_1$, and ϵ is an adjustable parameter. It was explained earlier that the expressions on the right sides of Eqs. (4.140) and (4.141) are functions of the marching variables at the n th time level. Moreover, according to Eqs. (4.123) and (4.124), Eqs. (4.140) and (4.141) can also be expressed as

$$\left(\bar{u}_\zeta^+\right)_{j,k}^{n+1/2} = \left(\bar{u}_\zeta'^+\right)_{j,k}^{n+1/2} + (\epsilon - 1/2)(d\bar{u}_\zeta^+)_{j,k}^{n+1/2}, \quad (4.142)$$

and

$$\left(\bar{u}_\eta^+\right)_{j,k}^{n+1/2} = \left(\bar{u}_\eta'^+\right)_{j,k}^{n+1/2} + (\epsilon - 1/2)(d\bar{u}_\eta^+)_{j,k}^{n+1/2}, \quad (4.143)$$

respectively.

The second marching step is formed by Eq. (4.65),

$$\left(\bar{u}_\zeta^+\right)_{j,k}^{n+1} = \left(\bar{u}_\zeta^{o+}\right)_{j,k}^{n+1} + \epsilon(d\bar{u}_\zeta^+)_{j,k}^{n+1}, \quad (4.144)$$

and

$$\left(\bar{u}_\eta^+\right)_{j,k}^{n+1} = \left(\bar{u}_\eta^{o+}\right)_{j,k}^{n+1} + \epsilon(d\bar{u}_\eta^+)_{j,k}^{n+1}, \quad (4.145)$$

where $(j, k, n + 1) \in \Omega_2$. It was explained earlier that the expressions on the right sides of Eqs. (4.144) and (4.145) are functions of the marching variables at the $(n + 1/2)$ th time level. Furthermore, according to Eqs. (4.136) and (4.137), Eqs. (4.144) and (4.145) can also be expressed as

$$\left(\bar{u}_\zeta^+\right)_{j,k}^{n+1} = \left(\bar{u}_\zeta'^+\right)_{j,k}^{n+1} + (\epsilon - 1/2)(d\bar{u}_\zeta^+)_{j,k}^{n+1}, \quad (4.146)$$

and

$$\left(\bar{u}_\eta^+\right)_{j,k}^{n+1} = \left(\bar{u}_\eta'^+\right)_{j,k}^{n+1} + (\epsilon - 1/2)(d\bar{u}_\eta^+)_{j,k}^{n+1}, \quad (4.147)$$

respectively.

Note that, because of the assumptions made in Eqs. (4.96)–(4.101), the Euler a scheme is not the special case of the Euler a - ϵ scheme with $\epsilon = 0$.

Finally we shall construct the weighted-average Euler a - ϵ scheme, i.e., the Euler version of the weighted-average a - ϵ scheme. The development follows a line of argument similar to that used in the construction of the weighted-average a - ϵ scheme. Thus only the key definitions will be given.

For any $(j, k, n + 1/2) \in \Omega_1$, the Euler versions of Eqs. (3.56)–(3.66), (3.69)–(3.74), and (3.80) are

$$\bar{x}_1 \stackrel{\text{def}}{=} \bar{u}_{j+1/3, k+1/3}^{n+1/2} - \bar{u}_{j,k}^{n+1/2}, \quad (4.148)$$

$$\bar{x}_2 \stackrel{\text{def}}{=} \bar{u}_{j-2/3, k+1/3}^{n+1/2} - \bar{u}_{j,k}^{n+1/2}, \quad (4.149)$$

$$\vec{x}_3 \stackrel{\text{def}}{=} \vec{u}_{j+1/3, k-2/3}^{n+1/2} - \vec{u}_{j, k}^{n+1/2}, \quad (4.150)$$

$$(\vec{u}_\zeta^{(1)})_{j, k}^{n+1/2} \stackrel{\text{def}}{=} -(2\vec{x}_2 + \vec{x}_3)/\Delta\zeta, \quad (4.151)$$

$$(\vec{u}_\eta^{(1)})_{j, k}^{n+1/2} \stackrel{\text{def}}{=} -(\vec{x}_2 + 2\vec{x}_3)/\Delta\eta, \quad (4.152)$$

$$(\vec{u}_\zeta^{(2)})_{j, k}^{n+1/2} \stackrel{\text{def}}{=} (2\vec{x}_1 + \vec{x}_3)/\Delta\zeta, \quad (4.153)$$

$$(\vec{u}_\eta^{(2)})_{j, k}^{n+1/2} \stackrel{\text{def}}{=} (\vec{x}_1 - \vec{x}_3)/\Delta\eta, \quad (4.154)$$

$$(\vec{u}_\zeta^{(3)})_{j, k}^{n+1/2} \stackrel{\text{def}}{=} (\vec{x}_1 - \vec{x}_2)/\Delta\zeta, \quad (4.155)$$

$$(\vec{u}_\eta^{(3)})_{j, k}^{n+1/2} \stackrel{\text{def}}{=} (2\vec{x}_1 + \vec{x}_2)/\Delta\eta. \quad (4.156)$$

$$(\vec{u}_x^{(\ell)})_{j, k}^{n+1/2} \stackrel{\text{def}}{=} (\vec{u}_\zeta^{(\ell)})_{j, k}^{n+1/2} \frac{\partial\zeta}{\partial x} + (\vec{u}_\eta^{(\ell)})_{j, k}^{n+1/2} \frac{\partial\eta}{\partial x}, \quad \ell = 1, 2, 3, \quad (4.157)$$

$$(\vec{u}_y^{(\ell)})_{j, k}^{n+1/2} \stackrel{\text{def}}{=} (\vec{u}_\zeta^{(\ell)})_{j, k}^{n+1/2} \frac{\partial\zeta}{\partial y} + (\vec{u}_\eta^{(\ell)})_{j, k}^{n+1/2} \frac{\partial\eta}{\partial y}, \quad \ell = 1, 2, 3, \quad (4.158)$$

$$(\vec{u}_x^{(1)})_{j, k}^{n+1/2} = -\frac{3}{2w}(\vec{x}_2 + \vec{x}_3), \quad (4.159)$$

$$(\vec{u}_y^{(1)})_{j, k}^{n+1/2} = \frac{(3b+w)\vec{x}_2 + (3b-w)\vec{x}_3}{2wh}, \quad (4.160)$$

$$(\vec{u}_x^{(2)})_{j, k}^{n+1/2} = \frac{3\vec{x}_1}{2w}, \quad (4.161)$$

$$(\vec{u}_y^{(2)})_{j, k}^{n+1/2} = -\frac{(3b+w)\vec{x}_1 + 2w\vec{x}_3}{2wh}, \quad (4.162)$$

$$(\vec{u}_x^{(3)})_{j, k}^{n+1/2} = \frac{3\vec{x}_1}{2w}, \quad (4.163)$$

$$(\vec{u}_y^{(3)})_{j, k}^{n+1/2} = \frac{(w-3b)\vec{x}_1 + 2w\vec{x}_2}{2wh}, \quad (4.164)$$

and

$$(\vec{u}_\zeta^{(\ell)+})_{j,k}^{n+1/2} \stackrel{\text{def}}{=} \frac{\Delta\zeta}{6} (\vec{u}_\zeta^{(\ell)})_{j,k}^{n+1/2}, \quad \text{and} \quad (\vec{u}_\eta^{(\ell)+})_{j,k}^{n+1/2} \stackrel{\text{def}}{=} \frac{\Delta\eta}{6} (\vec{u}_\eta^{(\ell)})_{j,k}^{n+1/2}, \quad (4.165)$$

respectively.

Let the m th components of the 4×1 column matrices $(\vec{u}_\zeta^{(\ell)+})_{j,k}^{n+1/2}$, $(\vec{u}_\eta^{(\ell)+})_{j,k}^{n+1/2}$, $(\vec{u}_x^{(\ell)})_{j,k}^{n+1/2}$, and $(\vec{u}_y^{(\ell)})_{j,k}^{n+1/2}$, be denoted by $(u_{m\zeta}^{(\ell)+})_{j,k}^{n+1/2}$, $(u_{m\eta}^{(\ell)+})_{j,k}^{n+1/2}$, $(u_{mx}^{(\ell)})_{j,k}^{n+1/2}$, and $(u_{my}^{(\ell)})_{j,k}^{n+1/2}$, respectively. Then, for $m = 1, 2, 3, 4$, and $\ell = 1, 2, 3$, the Euler versions of Eqs. (3.79), (3.85), and (3.86) are

$$\theta_{m\ell} \stackrel{\text{def}}{=} \sqrt{(u_{mx}^{(\ell)})^2 + (u_{my}^{(\ell)})^2}, \quad (4.166)$$

$$u_{m\zeta}^{w+} \stackrel{\text{def}}{=} \begin{cases} 0, & \text{if } \theta_{m1} = \theta_{m2} = \theta_{m3} = 0; \\ \frac{(\theta_{m2}\theta_{m3})^\alpha u_{m\zeta}^{(1)+} + (\theta_{m3}\theta_{m1})^\alpha u_{m\zeta}^{(2)+} + (\theta_{m1}\theta_{m2})^\alpha u_{m\zeta}^{(3)+}}{(\theta_{m1}\theta_{m2})^\alpha + (\theta_{m2}\theta_{m3})^\alpha + (\theta_{m3}\theta_{m1})^\alpha}, & \text{otherwise,} \end{cases} \quad (4.167)$$

and

$$u_{m\eta}^{w+} \stackrel{\text{def}}{=} \begin{cases} 0, & \text{if } \theta_{m1} = \theta_{m2} = \theta_{m3} = 0; \\ \frac{(\theta_{m2}\theta_{m3})^\alpha u_{m\eta}^{(1)+} + (\theta_{m3}\theta_{m1})^\alpha u_{m\eta}^{(2)+} + (\theta_{m1}\theta_{m2})^\alpha u_{m\eta}^{(3)+}}{(\theta_{m1}\theta_{m2})^\alpha + (\theta_{m2}\theta_{m3})^\alpha + (\theta_{m3}\theta_{m1})^\alpha}, & \text{otherwise,} \end{cases} \quad (4.168)$$

respectively. Here (i) $\alpha \geq 0$, and (ii) each symbol in the last two equations is associated with the mesh point $(j, k, n + 1/2)$.

Next we consider the case with $(j, k, n + 1) \in \Omega_2$. The Euler versions of Eqs. (3.90)–(3.106) are

$$\vec{y}_1 \stackrel{\text{def}}{=} \vec{u}_{j-1/3, k-1/3}^{n+1} - \vec{u}_{j,k}^{n+1}, \quad (4.169)$$

$$\vec{y}_2 \stackrel{\text{def}}{=} \vec{u}_{j+2/3, k-1/3}^{n+1} - \vec{u}_{j,k}^{n+1}, \quad (4.170)$$

$$\vec{y}_3 \stackrel{\text{def}}{=} \vec{u}_{j-1/3, k+2/3}^{n+1} - \vec{u}_{j,k}^{n+1}, \quad (4.171)$$

$$(\vec{u}_\zeta^{(1)})_{j,k}^{n+1} \stackrel{\text{def}}{=} (2\vec{y}_2 + \vec{y}_3)/\Delta\zeta, \quad (4.172)$$

$$(\vec{u}_\eta^{(1)})_{j,k}^{n+1} \stackrel{\text{def}}{=} (\vec{y}_2 + 2\vec{y}_3)/\Delta\eta, \quad (4.173)$$

$$(\vec{u}_\zeta^{(2)})_{j,k}^{n+1} \stackrel{\text{def}}{=} -(2\vec{y}_1 + \vec{y}_3)/\Delta\zeta, \quad (4.174)$$

$$(\vec{u}_\eta^{(2)})_{j,k}^{n+1} \stackrel{\text{def}}{=} (\vec{y}_3 - \vec{y}_1)/\Delta\eta, \quad (4.175)$$

$$(\vec{u}_\zeta^{(3)})_{j,k}^{n+1} \stackrel{\text{def}}{=} (\vec{y}_2 - \vec{y}_1)/\Delta\zeta, \quad (4.176)$$

and

$$(\vec{u}_\eta^{(3)})_{j,k}^{n+1} \stackrel{\text{def}}{=} -(2\vec{y}_1 + \vec{y}_2)/\Delta\eta, \quad (4.177)$$

$$(\vec{u}_x^{(\ell)})_{j,k}^{n+1} \stackrel{\text{def}}{=} (\vec{u}_\zeta^{(\ell)})_{j,k}^{n+1} \frac{\partial\zeta}{\partial x} + (\vec{u}_\eta^{(\ell)})_{j,k}^{n+1} \frac{\partial\eta}{\partial x}, \quad \ell = 1, 2, 3, \quad (4.178)$$

$$(\vec{u}_y^{(\ell)})_{j,k}^{n+1} \stackrel{\text{def}}{=} (\vec{u}_\zeta^{(\ell)})_{j,k}^{n+1} \frac{\partial\zeta}{\partial y} + (\vec{u}_\eta^{(\ell)})_{j,k}^{n+1} \frac{\partial\eta}{\partial y}, \quad \ell = 1, 2, 3, \quad (4.179)$$

$$(\vec{u}_x^{(1)})_{j,k}^{n+1} = \frac{3}{2w}(\vec{y}_2 + \vec{y}_3), \quad (4.180)$$

$$(\vec{u}_y^{(1)})_{j,k}^{n+1} = -\frac{(3b+w)\vec{y}_2 + (3b-w)\vec{y}_3}{2wh}, \quad (4.181)$$

$$(\vec{u}_x^{(2)})_{j,k}^{n+1} = -\frac{3\vec{y}_1}{2w}, \quad (4.182)$$

$$(\vec{u}_y^{(2)})_{j,k}^{n+1} = \frac{(3b+w)\vec{y}_1 + 2w\vec{y}_3}{2wh}, \quad (4.183)$$

$$(\vec{u}_x^{(3)})_{j,k}^{n+1} = -\frac{3\vec{y}_1}{2w}, \quad (4.184)$$

and

$$(\vec{u}_y^{(3)})_{j,k}^{n+1} = -\frac{(w-3b)\vec{y}_1 + 2w\vec{y}_2}{2wh}, \quad (4.185)$$

respectively. Moreover, with the understanding that all symbols are associated with the mesh point $(j, k, n+1) \in \Omega_2$, Eqs. (4.165)–(4.168) remain valid for the current case.

The weighted-average Euler a - ϵ scheme can now be stated. It consists of two marching steps. The first is formed by Eq. (4.64),

$$\left(\bar{u}_\zeta^+\right)_{j,k}^{n+1/2} = \left(\bar{u}_\zeta^{w+}\right)_{j,k}^{n+1/2} + (\epsilon - 1/2)(d\bar{u}_\zeta^+)_{j,k}^{n+1/2}, \quad (4.186)$$

and

$$\left(\bar{u}_\eta^+\right)_{j,k}^{n+1/2} = \left(\bar{u}_\eta^{w+}\right)_{j,k}^{n+1/2} + (\epsilon - 1/2)(d\bar{u}_\eta^+)_{j,k}^{n+1/2}, \quad (4.187)$$

where $(j, k, n + 1/2) \in \Omega_1$. The second is formed by Eq. (4.65),

$$\left(\bar{u}_\zeta^+\right)_{j,k}^{n+1} = \left(\bar{u}_\zeta^{w+}\right)_{j,k}^{n+1} + (\epsilon - 1/2)(d\bar{u}_\zeta^+)_{j,k}^{n+1}, \quad (4.188)$$

and

$$\left(\bar{u}_\eta^+\right)_{j,k}^{n+1} = \left(\bar{u}_\eta^{w+}\right)_{j,k}^{n+1} + (\epsilon - 1/2)(d\bar{u}_\eta^+)_{j,k}^{n+1}, \quad (4.189)$$

where $(j, k, n + 1) \in \Omega_2$.

Because (i) a fractional power is costly to evaluate, and (ii) evaluation of $(\theta_{m\ell})^\alpha$ does not involve a fractional power if α is an even integer, the weighted-average Euler a - ϵ scheme is more computationally efficient if α is an even integer.

5. Stability Analysis

The stability of the a , the $a-\mu$, and the $a-\epsilon$ schemes will be studied using the von Neumann analysis. For all $(j, k, n) \in \Omega$, let

$$\bar{q}(j, k, n) = \bar{q}^*(n, \theta_\zeta, \theta_\eta) e^{i(j\theta_\zeta + k\theta_\eta)}, \quad (i \stackrel{\text{def}}{=} \sqrt{-1}, \quad -\pi < \theta_\zeta, \theta_\eta \leq \pi). \quad (5.1)$$

where $\bar{q}^*(n, \theta_\zeta, \theta_\eta)$ is a 3×1 column matrix. Substituting Eq. (5.1) into Eqs. (2.84) and (2.85), one obtains

$$\bar{q}^*(n + m - 1/2, \theta_\zeta, \theta_\eta) = \left[M^{(1)}(\theta_\zeta, \theta_\eta) M^{(2)}(\theta_\zeta, \theta_\eta) \right]^m \bar{q}^*(n - 1/2, \theta_\zeta, \theta_\eta), \quad (5.2)$$

and

$$\bar{q}^*(n + m, \theta_\zeta, \theta_\eta) = \left[M^{(2)}(\theta_\zeta, \theta_\eta) M^{(1)}(\theta_\zeta, \theta_\eta) \right]^m \bar{q}^*(n, \theta_\zeta, \theta_\eta), \quad (5.3)$$

respectively. Here (i) $n = 0, \pm 1, \pm 2, \dots$; (ii) $m = 0, 1, 2, \dots$; and (iii)

$$M^{(1)}(\theta_\zeta, \theta_\eta) \stackrel{\text{def}}{=} Q_1^{(1)} e^{(i/3)(\theta_\zeta + \theta_\eta)} + Q_2^{(1)} e^{(i/3)(-2\theta_\zeta + \theta_\eta)} + Q_3^{(1)} e^{(i/3)(\theta_\zeta - 2\theta_\eta)}, \quad (5.4)$$

and

$$M^{(2)}(\theta_\zeta, \theta_\eta) \stackrel{\text{def}}{=} Q_1^{(2)} e^{-(i/3)(\theta_\zeta + \theta_\eta)} + Q_2^{(2)} e^{-(i/3)(-2\theta_\zeta + \theta_\eta)} + Q_3^{(2)} e^{-(i/3)(\theta_\zeta - 2\theta_\eta)}. \quad (5.5)$$

Note that Eqs. (2.84) and (2.85) are valid for the above three schemes if $Q_\ell^{(k)}$, $k = 1, 2$, and $\ell = 1, 2, 3$, are defined using (i) Eq. (2.80) for the a scheme, (ii) Eq. (2.107) for the $a-\mu$ scheme, and (iii) Eqs. (3.50)–(3.55) for the $a-\epsilon$ scheme. Equation (5.2) implies that the amplification matrix among the half-integer time levels is $M^{(1)}(\theta_\zeta, \theta_\eta) M^{(2)}(\theta_\zeta, \theta_\eta)$; while Eq. (5.3) implies that the amplification matrix among the whole-integer time levels is $M^{(2)}(\theta_\zeta, \theta_\eta) M^{(1)}(\theta_\zeta, \theta_\eta)$.

According to a theorem given in Appendix C, the above two amplification matrices have the same eigenvalues. These eigenvalues may be referred to as the amplification factors. The amplification factors are functions of phase angles θ_ζ and θ_η . In addition, they are functions of a set of coefficients which are dependent on the physical properties and the mesh parameters. These coefficients are (i) ν_ζ and ν_η for the a scheme; (ii) ν_ζ , ν_η , and ϵ for the $a-\epsilon$ scheme; and (iii) ν_ζ , ν_η , ξ_ζ , ξ_η , and ξ_r for the $a-\mu$ scheme. Let λ_1 , λ_2 , and λ_3 denote the amplification factors. In the present paper, a scheme is said to be stable in a domain of the above coefficients if, for all coefficients belonging to this domain, and all θ_ζ and θ_η with $-\pi < \theta_\zeta, \theta_\eta \leq \pi$,

$$|\lambda_1| \leq 1, \quad |\lambda_2| \leq 1, \quad \text{and} \quad |\lambda_3| \leq 1. \quad (5.6)$$

Consider the a scheme. By using its two-way marching nature (see Fig. 12), it is shown in Appendix C that, for any given ν_ζ , ν_η , θ_ζ , and θ_η ,

$$|\lambda_1 \lambda_2 \lambda_3| = 1. \quad (5.7)$$

It follows from Eqs. (5.6) and (5.7) that the a scheme must be neutrally stable, i.e.,

$$|\lambda_1| = |\lambda_2| = |\lambda_3| = 1, \quad -\pi < \theta_\zeta, \theta_\eta \leq \pi, \quad (5.8)$$

if it is stable. In other words, the a scheme is free of numerical diffusion [5, p.18] if it is stable. Moreover, a systematic numerical evaluation of λ_1 , λ_2 , and λ_3 , for different values of ν_ζ , ν_η , θ_ζ , and θ_η , has confirmed that the a scheme is indeed neutrally stable in the stability domain defined by Eq. (2.110). In the following, we shall discuss the meaning of this stability domain.

Let $(j, k, n + 1/2) \in \Omega_1$. According to Eq. (2.84), the marching variables at $(j, k, n + 1/2)$ are completely determined by those of seven mesh points at the $(n - 1/2)$ th time level. According to Fig. 13(a), one of them, i.e., the mesh point $(j, k, n - 1/2)$, is located directly "below" the mesh point $(j, k, n + 1/2)$. The other six are the vertices of a hexagon. As a result, in this paper, the interior and boundary of the hexagon shall be considered as the numerical domain of dependence of $(j, k, n + 1/2)$ at the $(n - 1/2)$ th time level. Note that the dashed lines depicted in Figs. 13(a) and 13(b) are the spatial projections of the boundaries of CEs.

The a scheme is designed to solve Eq. (3.1). For Eq. (3.1), the value of u is a constant along a characteristic line. The characteristic line passing through the mesh point $(j, k, n + 1/2)$ will intersect a point on the plane $t = t^{n-1/2}$. The latter, referred to as the backward characteristic projection of the former at the $(n - 1/2)$ th time level, is the "domain" of dependence of the former at the $(n - 1/2)$ th time level. It is shown in Appendix C that the backward characteristic projection is in the interior of the numerical domain of dependence if and only if Eq. (2.110) is satisfied.

Let $(j, k, n + 1) \in \Omega_2$ and consider Fig. 13(b). Using a line of argument similar to that presented above, it can be shown that the backward characteristic projection of the mesh point $(j, k, n + 1)$ at the n th time level is in the interior of the numerical domain of dependence at the n th time level if and only if Eq. (2.110) is satisfied.

At this juncture, note that the concept of characteristics was never used in the design of the a scheme. Nevertheless, its stability condition is completely consistent with the general requirement that an explicit scheme for Eq. (3.1) is stable when the domain of dependence of Eq. (3.1) is a subset of the numerical domain of dependence.

Next we consider the stability of the a - ϵ scheme. Recall that the 1-D a - ϵ scheme [5] is not stable for any Courant number ν if $\epsilon < 0$, or $\epsilon > 1$. Similarly, the results of numerical experiments indicate that the current a - ϵ scheme, except for some possible isolated points, is not stable in any domain on the ν_ζ - ν_η plane if $\epsilon < 0$ or $\epsilon > 1$. For any ϵ with $0 \leq \epsilon \leq 1$, the a - ϵ scheme has a stability domain on the ν_ζ - ν_η plane. The stability domains for several values of ϵ were obtained numerically. As shown in Figs. 14(a)-(c), these domains (shaded areas) vary only slightly in shape and size from that depicted in Fig. 9. They become smaller in size as ϵ increases.

Let λ_1 , λ_2 , and λ_3 be defined such that

$$|\lambda_3| \leq |\lambda_2| \leq |\lambda_1|. \quad (5.9)$$

Then λ_1 can be referred to as the principal amplification factor; while λ_2 and λ_3 referred to as the spurious amplification factors [1]. In general, the principal amplification factor is the deciding factor in determining the accuracy of computation [1]. Particularly, numerical solutions may suffer annihilations of sharply different degrees at different locations and different frequencies if numerical diffusion associated with λ_1 varies greatly with respect to θ_ζ , θ_η , ν_ζ , and ν_η [5, p.20]. Assuming Eq. (5.6), then $(1 - |\lambda_\ell|)$ is a measure of the numerical diffusion associated with λ_ℓ , $\ell = 1, 2, 3$ [5, p.18]. For a given ϵ , let $D(\epsilon)$ denote the stability domain of the a - ϵ scheme on the ν_ζ - ν_η plane. Let

$$\chi_\ell(\epsilon) \stackrel{\text{def}}{=} \max_{-\pi < \theta_\zeta, \theta_\eta \leq \pi; (\nu_\zeta, \nu_\eta) \in D(\epsilon)} (1 - |\lambda_\ell|), \quad \ell = 1, 2, 3; \quad 0 \leq \epsilon \leq 1. \quad (5.10)$$

Then, for a given ϵ and each ℓ , $(1 - |\lambda_\ell|)$ is bounded *uniformly* from above by $\chi_\ell(\epsilon)$. The numerically estimated values of $\chi_\ell(\epsilon)$ are plotted in Fig. 15. From this figure, one concludes that the numerical diffusion, particularly that associated with λ_1 , can be bounded *uniformly* from above by an arbitrary small number by choosing an ϵ small enough. Note that this property is also shared by the 1-D a - ϵ scheme (see Eq. (3.19) in [5]). Moreover, the results shown in Fig. 15 indicate that $\chi_2(\epsilon)$ and $\chi_3(\epsilon)$ are much larger than $\chi_1(\epsilon)$ in the range of $0 \leq \epsilon \leq 0.5$. Thus, in this range, the spurious part of a numerical solution is annihilated much faster than the principal part. Also it is seen that the numerical diffusion associated with the principal solution, measured by $\chi_1(\epsilon)$, increases with ϵ in the range of $0 \leq \epsilon \leq 0.7$.

Finally we discuss the stability of the a - μ scheme. Note that this scheme is not defined if $\Delta^{(1)} = 0$ or $\Delta^{(2)} = 0$. One form of $\Delta^{(1)}$ and $\Delta^{(2)}$ is given in Eqs. (2.86) and (2.87). Another form is given in Eqs. (A.15) and (A.16). Let $\mu = 0$. Then $\Delta^{(1)} = 0$ or $\Delta^{(2)} = 0$ occurs only on the six straight lines on the ν_ζ - ν_η plane which are depicted in Fig. 16. The shaded area depicted in the same figure is the region that satisfies Eq. (2.88). It was explained in Sec. 2 that the curves of singularity on which $\Delta^{(1)} = 0$ or $\Delta^{(2)} = 0$ cannot enter the shaded region if $\mu > 0$. In general, for a given set of $\xi_\zeta > 0$, $\xi_\eta > 0$ and $\xi_\tau > 0$, the ν_ζ - ν_η plane can be divided into two regions by the curves of singularity. The “inside” region R_1 is the maximal connected open set on the ν_ζ - ν_η plane that contains (i) the shaded area depicted in Fig. 16, and (ii) no point at which $\Delta^{(1)} = 0$, or $\Delta^{(2)} = 0$. The “outside” region R_2 is the rest of the ν_ζ - ν_η plane.

For the a - μ scheme, λ_ℓ , $\ell = 1, 2, 3$, are functions of the phase angles θ_ζ and θ_η , and the coefficients ν_ζ , ν_η , ξ_ζ , ξ_η , and ξ_τ . For a given set of ξ_ζ , ξ_η , and ξ_τ , the stability domain on the ν_ζ - ν_η plane generally covers part of R_1 and part of R_2 . In the following discussion, only the stability domains in R_1 are considered.

For the special case with $\Delta\zeta = \Delta\eta = \Delta\tau$, ξ_ζ , ξ_η , and ξ_τ share a common value, say ξ . The stability domains (shaded areas) for $\xi = 10^{-5}$, $\xi = 10^{-3}$, and $\xi = 0.1$ are plotted in Figs. 17(a)-(c), respectively.

Next we assume that $\Delta\zeta = \Delta\eta$. Then $\xi_\zeta = \xi_\eta$. Let α be the angle formed by the sides \overline{DB} and \overline{DF} which are depicted in Figs. 7(a)-(c). Then Eq. (2.32) implies that

$$\xi_\tau = 2(1 - \cos \alpha)\xi, \quad (5.11)$$

where ξ is the common value of ξ_ζ and ξ_η . The stability domains for two pairs of (ξ, α) are depicted in Figs. 18(a) and (b).

From the results shown in Figs. 17 and 18, and the results of other numerical experiments, it appears that the a - μ scheme is unconditionally stable when $\nu_\zeta = \nu_\eta = 0$. The last condition is equivalent to $a_\zeta = a_\eta = 0$ or $a_x = a_y = 0$.

6. Numerical Results

In [8], several numerical solutions of Eqs. (2.1) and (3.1) generated using the $a-\mu$ and the $a-\epsilon$ schemes are compared with the exact solutions or the numerical solutions generated using traditional methods. These comparisons show that the $a-\epsilon$ scheme, which includes the a scheme as a special case with $\epsilon = 0$, is an accurate solver for Eq. (3.1). They also show that the $a-\mu$ scheme can obtain highly accurate solutions of Eq. (2.1) as long as the viscosity coefficient μ is not too large. Note that a convection-diffusion problem is fundamentally an initial-value/boundary-value problem. The current *explicit* $a-\mu$ scheme obviously cannot model such a problem unless the contribution of the diffusion term is small compared to that of the convection term.

The $a-\epsilon$ scheme was also generalized in [8] to solve the 2-D inviscid Burgers' equation. In spite of its simplicity, particularly the fact that it does not use (i) any mesh refinement technique, and (ii) any moving meshes, this new solver is capable of generating highly accurate shock solutions. The shock discontinuities are almost resolved within one mesh intervals.

In this section, accuracy of the weighted-average Euler $a-\epsilon$ scheme defined in Sec. 4 will be evaluated using a steady-state shock reflection problem [24]. The computation domain and the shock locations (\overline{AE} and \overline{EF}) are depicted in Fig. 19. The lower boundary is a solid wall. Assuming $\gamma = 1.4$, the exact Euler solution to this problem is:

(a) In the region ABE ,

$$u = 2.9, \quad v = 0., \quad \rho = 1.0, \quad p = 1.0/1.4. \quad (6.1)$$

(b) In the region $AEFD$,

$$u = 2.6193, \quad v = -0.50632, \quad \rho = 1.7000, \quad p = 1.5282. \quad (6.2)$$

(c) In the region ECF ,

$$u = 2.4015, \quad v = 0., \quad \rho = 2.6872, \quad p = 2.9340. \quad (6.3)$$

Note that the Mach number is equal to (i) 2.9 in the region ABE ; (ii) 2.3781 in the region $AEFD$; and (iii) 1.9424 in the region ECF .

The mesh used in the current numerical calculations is depicted in Fig. 20. Again a mesh point $\in \Omega_1$ is marked by a solid circle; while a mesh point $\in \Omega_2$ is marked by an open circle. The mesh is a special case of that depicted in Figs. 1-4 with $b = 0$. Note that (i) only the mesh points $\in \Omega_2$ are present at the inflow boundary, and (ii) the mesh parameter w is so chosen that only the mesh points $\in \Omega_2$ are present at the outflow boundary. Moreover, for simplicity, a mesh point and the corresponding marching variable will be identified by the time-level number n , and two new mesh indices r and s which are given in Fig. 20 as a pair of integers enclosed in a parenthesis. Note that, for the mesh

points $\in \Omega_1$, $r = 1, 2, 3, \dots, R, R + 1$, and $s = 1, 2, 3, \dots, S$. On the other hand, for the mesh points $\in \Omega_2$, $r = 1, 2, 3, \dots, R, R + 1$, and $s = 1, 2, 3, \dots, S, S + 1$. Obviously two different mesh points at the same time level always have different pairs of r and s .

In the current numerical calculation, at the time level $n = 0$, u_m , $m = 1, 2, 3, 4$, at all mesh points are calculated using Eq. (6.1). Also we assume that

$$u_{m\zeta}^+ = u_{m\eta}^+ = 0, \quad m = 1, 2, 3, 4. \quad (6.4)$$

The above initial conditions are also assumed at the inflow boundary for all $n = 1, 2, 3, \dots$. At the upper boundary, for all $n = 1/2, 1, 3/2, 2, \dots$, Eq. (6.4) is also assumed. Moreover, u_m , $m = 1, 2, 3, 4$, are calculated using Eq. (6.2).

To impose the proper boundary conditions at the lower boundary, note that the solid wall boundary conditions at \overline{BC} (see Fig. 19) are equivalent to the condition that the flow field below \overline{BC} is the mirror image of that above. By using Eq. (4.1) and the fact that $y = 0$ at any point on \overline{BC} , it can be shown that the last condition implies that

$$u_m(x, -y) = u_m(x, y), \quad m = 1, 2, 4, \quad \text{and} \quad u_3(x, -y) = -u_3(x, y). \quad (6.5)$$

$$\frac{\partial u_m(x, -y)}{\partial x} = \frac{\partial u_m(x, y)}{\partial x}, \quad \text{and} \quad \frac{\partial u_m(x, -y)}{\partial y} = -\frac{\partial u_m(x, y)}{\partial y}, \quad m = 1, 2, 4, \quad (6.6)$$

and

$$\frac{\partial u_3(x, -y)}{\partial x} = -\frac{\partial u_3(x, y)}{\partial x}, \quad \text{and} \quad \frac{\partial u_3(x, -y)}{\partial y} = \frac{\partial u_3(x, y)}{\partial y}. \quad (6.7)$$

Consider the mesh depicted in Fig. 20. Then it becomes clear that the numerical analogues of Eqs. (6.5)–(6.7) are

$$(u_m)_{R+1,s}^n = (u_m)_{R,s}^n, \quad m = 1, 2, 4, \quad \text{and} \quad (u_3)_{R+1,s}^n = -(u_3)_{R,s}^n, \quad (6.8)$$

$$(u_{mx})_{R+1,s}^n = (u_{mx})_{R,s}^n, \quad \text{and} \quad (u_{my})_{R+1,s}^n = -(u_{my})_{R,s}^n, \quad m = 1, 2, 4, \quad (6.9)$$

and

$$(u_{3x})_{R+1,s}^n = -(u_{3x})_{R,s}^n, \quad \text{and} \quad (u_{3y})_{R+1,s}^n = (u_{3y})_{R,s}^n, \quad (6.10)$$

respectively. According to Fig. 20, the range of s in Eqs. (6.8)–(6.10) is dependent on the time level n . Let (i) $S^+ \stackrel{\text{def}}{=} S + 1$, and $S^- \stackrel{\text{def}}{=} S$ if S is even; and (ii) $S^+ \stackrel{\text{def}}{=} S$, and $S^- \stackrel{\text{def}}{=} S - 1$ if S is odd. Then (i) $s = 2, 4, 6, \dots, S^-$ if $n = 1/2, 3/2, \dots$, and (ii) $s = 1, 3, 5, \dots, S^+$ if $n = 1, 2, \dots$. Furthermore, by using Eq. (B.4) with $b = 0$, it can be shown that Eqs. (6.9) and (6.10) are equivalent to

$$(u_{m\zeta}^+)^n_{R+1,s} = (u_{m\eta}^+)^n_{R,s}, \quad \text{and} \quad (u_{m\eta}^+)^n_{R+1,s} = (u_{m\zeta}^+)^n_{R,s}, \quad m = 1, 2, 4, \quad (6.11)$$

and

$$\left(u_{3\zeta}^+\right)_{R+1,s}^n = -\left(u_{3\eta}^+\right)_{R,s}^n, \quad \text{and} \quad \left(u_{3\eta}^+\right)_{R+1,s}^n = -\left(u_{3\zeta}^+\right)_{R,s}^n, \quad (6.12)$$

respectively. Equations (6.8), (6.11) and (6.12) are the boundary conditions at the lower wall (a solid wall) in the current numerical calculations. In other words, the marching variables associated with the mesh points below the solid wall will be determined using Eqs. (6.8), (6.11), and (6.12).

Next we discuss the outflow boundary conditions. For any $n = 1, 2, 3, \dots$, and $r = 1, 2, 3, \dots, R$, we assume that

$$\left(u_m\right)_{r,S+1}^n = \left(u_m\right)_{r,S}^{n-1/2}, \quad m = 1, 2, 3, 4, \quad (6.13)$$

$$\left(u_{mx}\right)_{r,S+1}^n = 0, \quad m = 1, 2, 3, 4, \quad (6.14)$$

and

$$\left(u_{my}\right)_{r,S+1}^n = \left(u_{my}\right)_{r,S}^{n-1/2}, \quad m = 1, 2, 3, 4. \quad (6.15)$$

When the time-marching solution reaches its steady-state limit, the above conditions can be considered as a result of the requirement that the partial derivatives of the flow variables with respect to x are zero at the outflow boundary. By using Eq. (B.4) with $b = 0$, it can be shown that Eqs. (6.14) and (6.15) are equivalent to

$$\left(u_{m\zeta}^+\right)_{r,S+1}^n = \frac{1}{2} \left(u_{m\zeta}^+ - u_{m\eta}^+\right)_{r,S}^{n-1/2}, \quad m = 1, 2, 3, 4, \quad (6.16)$$

and

$$\left(u_{m\eta}^+\right)_{r,S+1}^n = \frac{1}{2} \left(u_{m\eta}^+ - u_{m\zeta}^+\right)_{r,S}^{n-1/2}, \quad m = 1, 2, 3, 4, \quad (6.17)$$

where $n = 1, 2, 3, \dots$, and $r = 1, 2, 3, \dots, R$. Equations (6.13), (6.16), and (6.17) are the outflow boundary conditions in the current numerical calculations. As a result, the marching variables at the outflow boundary will be determined using these equations.

With the aid of the above initial and boundary conditions, the marching variables at all time levels can be determined using the weighted-averaged Euler a - ϵ scheme. As an example, at any $n = 1/2, 3/2, \dots$, the marching variables associated with the mesh point (2, 1) (marked by a solid circle in Fig. 20) can be determined in terms of those associated with the mesh points (1, 1), (2, 1), and (2, 2) at the $(n - 1/2)$ th time level (marked by open circles). As another example, at any $n = 1, 2, 3, \dots$, the marching variables associated with the mesh point (1, 3) (marked by an open circle) can be determined in terms of those associated with the mesh points (1, 2), (2, 3), and (1, 3) at the $(n - 1/2)$ th time level (marked by solid circles).

According to Fig. 19, the distance between the inflow and the outflow boundaries is 4., while the distance between the upper and the lower boundaries is 1.. On the other hand, according to Fig. 20, the above two distances are $w \cdot S$ and $2h \cdot R$, respectively. Thus

$$w = \frac{4}{S}, \quad \text{and} \quad h = \frac{1}{2R}. \quad (6.18)$$

Because $b = 0$, the geometric parameters w , h , and b are determined if R and S are given. In addition to the initial conditions, the boundary conditions, and the integers R and S , the other input parameters for the current numerical calculations are ϵ , α , Δt , and a positive integer n_t . Here we assume that the time marching ends at the n_t th time level, i.e., at $t = T \stackrel{\text{def}}{=} n_t \cdot \Delta t$.

It is shown in Appendix D that, for any Euler solver constructed in Sec. 4, a local *CFL* number ν_e associated with any mesh point $(j, k, n) \in \Omega$ can be defined in terms of u , v , c , w , h and Δt . Here u , v , and c are the x -velocity, the y -velocity, and the sonic speed at the mesh point, respectively. Two global *CFL* numbers are considered in the current calculations. The first, denoted by ν_{ems} , is the maximum of ν_e with respect to the steady-state solution given in Eqs. (6.1)–(6.3). The second, denoted by ν_{em} , is the largest value of ν_e ever reached at any mesh point $(j, k, n) \in \Omega$, where $n = 0, 1/2, 2, 3/2, 2, \dots, n_t$. Excluding the initial and the boundary conditions, ν_{ems} is dependent on R , S , and Δt only. On the other hand, ν_{em} is a function of R , S , Δt , n_t , ϵ , and α . According to a series of numerical experiments, the value of α plays only a minor role on the stability of the weighted-average Euler α - ϵ scheme. Generally the scheme is stable if

$$0 \leq \epsilon \leq 1 \quad \text{and} \quad \nu_{em} \leq 1. \quad (6.19)$$

To measure the convergence of a time-marching solution to the corresponding steady-state solution (note: this steady-state solution generally differs from the exact solution given in Eqs. (6.1)–(6.3)), for any $n = 1, 2, 3, \dots, n_t$, and $m = 1, 2, 3, 4$, let

$$E_m(n) \stackrel{\text{def}}{=} -\log_{10} \left\{ \frac{1}{RSc_m} \left[\sum_{s=2}^{S+1} \sum_{r=r(s)}^{r(s)+R-1} |(u_m)_{r,s}^n - (u_m)_{r,s}^{n-1}| \right] \right\}. \quad (6.20)$$

Here, for any $m = 1, 2, 3, 4$, c_m is the maximal value of $|u_m|$ within the exact steady-state solution defined by Eqs. (6.1)–(6.3). It can be shown that $c_1 = 2.6872$, $c_2 = 6.4534$, $c_3 = 0.86073$, and $c_4 = 15.084$. Moreover,

$$r(s) \stackrel{\text{def}}{=} \begin{cases} 1, & \text{if } s \text{ is odd;} \\ 2, & \text{otherwise.} \end{cases} \quad (6.21)$$

According to Fig. 20, the summation which takes place in Eq. (6.20) involves all the mesh points at the n th time level excluding those located (i) at the inflow boundary, (ii) at the upper boundary, and (iii) below the lower boundary. Because $n = 1, 2, 3, \dots, n_t$, the mesh points involved in summation are all marked by open circles in Fig. 20. The values of u_m at the inflow and the upper boundaries do not change with time, while those at the mesh points in (iii) are dependent on the values of u_m at other interior mesh points. Note that the values of u_m at the outflow boundary change with time and are dependent on those at a lower time level. Because the summation involves a total of $R \times S$ mesh

points, the result of this summation divided by $R \times S$ is the average value of the change of u_m at the same spatial mesh point (measured by the absolute value of this change) from the $(n - 1)$ th time level to the n th time level per mesh point. This average value is further normalized using the constant c_m . If we further assume that the time-marching solution converges to a steady-state solution which is similar to the exact steady-state solution (such that the normalization by c_m makes sense), then $E_m(n)$ more or less can be interpreted as the average number of correct significant figures in u_m at the n th time level as compared with the converged value of u_m (which, of course, is not identical to that given in Eqs. (6.1)–(6.3)).

Because the time marching solution can not reach a steady-state solution before the boundary conditions are fully felt at all interior points, rapid convergence generally can not occur before the time has elapsed which allows a fluid particle to travel the full length of the computation domain. It can be shown that, for the solution given in Eqs. (6.1)–(6.3), the average value of u over the computational domain is 2.6261. Thus an average fluid particle requires $4.0/2.6261 = 1.5232$ time units to travel from the inflow boundary to the outflow boundary. The number of time steps corresponding to the above number of time units is

$$n_c \stackrel{\text{def}}{=} \frac{1.5232}{\Delta t}, \quad (6.22)$$

i.e., rapid convergence can not occur before $n > n_c$.

With the above preliminaries, the numerical results generated using the weighted-average Euler a - ϵ scheme can now be presented. Six test problems, with different combinations of ϵ , α , R , S , Δt , and n_t , are defined in Table 1. For each problem, the values of T , ν_{ems} , ν_{em} , and n_c are also given in the same table. In Figs. 22–27, the numerical results (triangular symbols) of the pressure coefficient c_p at $n = n_t$ for Problems #1–#6 are compared with the exact solution (solid lines). Here

$$c_p \stackrel{\text{def}}{=} \frac{2}{\gamma M_\infty^2} \left(\frac{p}{p_\infty} - 1 \right), \quad (6.23)$$

with $M_\infty = 2.9$ and $p_\infty = 1.0/1.4$ being the inflow Mach number and pressure, respectively. Note that: (i) at the mid-section of the computation domain ($y = 0.5$ in Fig. 19), two neighboring mesh points at the same time level are separated by a distance = $2w$, and (ii) the mesh points at the n_t th time level are marked by open circles in Fig. 20 because n_t is a whole number. In Figs. 22–27, the values of $E_m(n)$, $m = 1, 2, 3, 4$, are also plotted against n for all six test problems. In Fig. 28, twenty-six pressure contour levels between the values of 0.6 and 3.1 with uniform increment 0.1 were used for the contour plots of Problem #3. Finally, for Problem #3, a 3-D pressure-distribution plot is shown in Fig. 29.

The significance of the results shown in Figs. 22–29 is discussed in the following remarks:

- (a) From Table 1 and the results shown in Figs. 22–24, it appears that the convergence to steady-state is much faster with a smaller value of ν_{em} (or ν_{ems}). As a matter of fact,

convergence to steady-state can reach a plateau representing some number of correct significant figures if ν_{em} is too close to 1. From Table 1 and a comparison among Figs. 22, 25, and 26, one also concludes that slower convergence generally occurs with a value of ϵ much smaller than 0.5. A comparison between Figs. 22 and 27 reveals that a change of the value of α from 2 to 1 also cause a slight decrease in convergence rate. Because numerical diffusion generally increases with (i) a smaller value of ν_{em} , (ii) a larger value of ϵ , and (iii) a larger value of α , one may conclude that faster convergence generally occurs with larger numerical diffusion. This trend is consistent with the fact that shocks cannot be formed without physical or numerical diffusion.

- (b) The effectiveness of the weighted-averaging as a tool to suppress numerical oscillations near discontinuities is clearly demonstrated by the results shown in Figs. 22-29. Moreover, the present weighted-averaging does not cause the smearing of shock discontinuities and has no discernible effect on the smooth part of the solution. From table 1 and a comparison between Fig. 22 and 27, one also concludes that the increase of the value of α from 1 to 2 has a marginal impact on the numerical results.
- (c) Comparing the numerical results shown in Figs. 22-27 with the exact solution, one concludes that the weighted-average Euler a - ϵ scheme is capable of generating highly accurate solutions for the steady-state shock reflection problem under consideration. Also a comparison of the results shown in Figs. 22, 23, and 25-27 reveals that accuracy of the numerical results generally is not sensitive to the change of the values of ν_{em} , ϵ , and α . An exception is that numerical results may become more diffusive and thus shock resolution becomes less sharp if the value of ϵ is too large, e.g., $\epsilon = 0.8$ in Problem #5. Finally, a comparison of the results shown in Fig. 24 (Problem #3) with the results of other test problems reveals that accuracy increases sharply with the decrease of the mesh size. It is seen that both the primary and the reflected shocks are resolved by a single data point in Fig. 24.

7. Conclusions and Discussions

A new numerical method is being developed for solving one-dimensional and multidimensional flow problems. This new method represents a clear break from the traditional methods in the basic concept of *numerical discretization*. It emphasizes *simplicity, generality, and accuracy*. The history of this new method and the considerations that motivates its development are clearly described in Sec. 1.

In this report, we explain how the same set of design principles which was used to construct several solvers for 1-D time-marching problems [5] can be used to construct their 2-D counterparts. Because of the similarity in their design, each of the present 2-D solvers virtually shares with its 1-D counterpart the same fundamental characteristics. Furthermore, it has been shown that the 2-D solvers, as in the case of the 1-D solvers, generally are more accurate than the traditional solvers in spite of the advantage the present solvers have over the latter in *simplicity and generality*. Accuracy of the present 2-D Euler solver is most vividly demonstrated by the pressure-contour plot (Fig. 28) and the 3-D pressure-distribution plot (Fig. 29) it generates for a famous shock reflection problem [24]. Both the primary and the reflected shocks are resolved by a single data point without the presence of numerical oscillations near the discontinuity.

The construction of the 1-D solvers referred to above is simplified by the use of a mesh which is staggered in time [5]. Its use results in the simplest stencil possible, i.e., a triangle in a 2-D space-time with a vertex at the upper time level and other two at the lower time level. Similarly, the construction of the present 2-D solvers is simplified by the use of a nontraditional space-time mesh which is also staggered in time (Figs. 1-4). Its use results in the simplest stencil possible, i.e., a tetrahedron (Fig. 8) in a 3-D space-time with a vertex at the upper time level and other three at the lower time levels.

The meshes used by the 1-D and the 2-D solvers consist of whole-integer and half-integer time levels with a half-integer time level being sandwiched between two whole-integer time levels and vice versa. The spatial positions of the mesh points at a whole-integer (half-integer) time level coincide with those at another whole-integer (half-integer) time level. However, the spatial positions of the mesh points at a whole-integer time level shift from those at a half-integer time level. For the mesh used by the 1-D solvers, the spatial projection of a mesh point at a whole-integer time level is right at the center of those of two neighboring mesh points at a half-integer time level and vice versa [5]. It follows that the stencil of the 1-D solvers is always an isosceles triangle, i.e., one cannot distinguish a stencil with its upper vertex at a whole-integer time level from another with its upper vertex at a half-integer time level. As a result, each of the 1-D solvers constructed in [5] is formed by two identical marching steps. Contrarily, for the present 2-D solvers, a stencil (a tetrahedron) with its vertex at a whole-integer time level is different from another with its vertex at a half-integer time level (Fig. 8). Thus each of the present 2-D solvers is formed by two distinctly different marching steps. In spite of their structural differences, the last two marching steps *compensate* each other and its combination results in several important symmetric properties which were discussed in Sec. 5 and Appendix C.

The Euler a scheme constructed in Sec. 4 is free from numerical diffusion when it is stable. This scheme is a limiting case of a Navier-Stokes solver currently under development, i.e., the former is a special case of the latter when the viscosity vanishes. As a result, the new Navier-Stokes solver will have a special property that a classical solver lacks, i.e., as the physical diffusion (viscosity) approaches zero, so does the numerical diffusion. Without this property, *numerical dissipation may overwhelm physical dissipation and cause a complete distortion of solutions for problems with small viscosity.* Because a Navier-Stokes problem fundamentally is an initial-value/boundary-value problem, i.e., information from any spatial point can be felt instantly by other spatial points, the new Navier-Stokes solver is implicit when the viscosity is present. However, it is reduced to the Euler a - ϵ scheme, i.e., an explicit scheme, when the viscosity is absent.

Finally, an alternate space-time mesh is depicted in Fig. 30. The intrinsic geometry of this mesh is determined by four parameters h , r , w , and θ with $0 \leq r \leq 1$. The use of this mesh also results in a stencil with the shape of a tetrahedron in a 3-D space-time. In this Figure, mesh points marked with solid circles are centers of the SEs at the half-integer time levels; while those marked with open circles are centers of the SEs at the whole-integer time levels. Also spatial projections of the interfaces which divide CEs are marked with dash lines. It is easy to see that each SE is associated with three CEs. According to a discussion given in Sec. 4 (p.46), there is an advantage that the center of each SE be located at the geometric center of the top face of the union of the three CEs which are associated with this SE. It can be shown that the mesh has the above property if $x = \sqrt{19} - 4 \approx 0.3589$.

Appendix A

The proofs for several results presented in Sec. 2 are given here.

To prove Eqs. (2.53)–(2.58), first we shall evaluate the flux leaving each of six quadrilaterals that form the boundary of a CE (see Figs. 5(a) and 6(a)). As a preliminary, note that, in Fig. 5(a),

$$\text{area of } ABGF = \text{area of } CDGB = \text{area of } EFGD = \frac{2wh}{3}. \quad (\text{A.1})$$

In Fig. 6(a), we have

$$\text{area of } BCGA = \text{area of } DEGC = \text{area of } FAGE = \frac{2wh}{3}. \quad (\text{A.2})$$

Equations (A.1) and (A.2) can be proved easily using the information provided in Fig. 7(a). Moreover, because $u^*(x, y, t; j, k, n)$ is linear in x , y , and t (see Eq. (2.11)), its average value over any quadrilateral is equal to its value at the geometric center of the quadrilateral. With the above preparations, flux evaluation can be carried out easily using Eqs. (2.6a)–(2.6c), (2.9), (2.11), (A.1), and (A.2).

For each quadrilateral, the result of flux evaluation is a formula involving a_x , a_y , $u_{j,k}^n$, $(u_x)_{j,k}^n$, and $(u_y)_{j,k}^n$. It can be converted to another formula involving a_ζ^+ , a_η^+ , $u_{j,k}^n$, $(u_\zeta^+)_{j,k}^n$, and $(u_\eta^+)_{j,k}^n$. To carry out the above conversion, note that Eqs. (2.24), (2.25), (2.29), and (2.30) imply that

$$\begin{pmatrix} a_x \\ a_y \end{pmatrix} = \frac{1}{6} \begin{pmatrix} w-b & w+b \\ -h & h \end{pmatrix} \begin{pmatrix} a_\zeta^+ \\ a_\eta^+ \end{pmatrix}, \quad (\text{A.3})$$

and, for any $(j, k, n) \in \Omega$,

$$\begin{pmatrix} (u_x)_{j,k}^n \\ (u_y)_{j,k}^n \end{pmatrix} = \frac{3}{w} \begin{pmatrix} 1 & 1 \\ -\frac{w+b}{h} & \frac{w-b}{h} \end{pmatrix} \begin{pmatrix} (u_\zeta^+)_{j,k}^n \\ (u_\eta^+)_{j,k}^n \end{pmatrix}. \quad (\text{A.4})$$

Let $(u_x)_{j,k}^n$, $(u_y)_{j,k}^n$, \dots , be abbreviated as u_x , u_y , \dots , respectively. Then Eqs. (A.3) and (A.4) imply that

$$a_y = \frac{h}{6} (a_\eta^+ - a_\zeta^+), \quad (\text{A.5})$$

$$ha_x + \left(\frac{w}{3} - b\right) a_y = \frac{wh}{9} (a_\zeta^+ + 2a_\eta^+), \quad (\text{A.6})$$

$$ha_x - \left(\frac{w}{3} + b\right) a_y = \frac{wh}{9} (2a_\zeta^+ + a_\eta^+), \quad (\text{A.7})$$

$$u_x = \frac{3}{w} (u_\zeta^+ + u_\eta^+), \quad (\text{A.8})$$

$$u_y = \frac{3}{wh} [(w-b)u_\eta^+ - (w+b)u_\zeta^+], \quad (\text{A.9})$$

$$a_x u_x + a_y u_y = a_\zeta^+ u_\zeta^+ + a_\eta^+ u_\eta^+, \quad (\text{A.10})$$

$$\left(\frac{b}{2} + \frac{w}{6}\right) u_x + \frac{h}{2} u_y = 2u_\eta^+ - u_\zeta^+, \quad (\text{A.11})$$

$$\left(\frac{b}{2} - \frac{w}{6}\right) u_x + \frac{h}{2} u_y = u_\eta^+ - 2u_\zeta^+, \quad (\text{A.12})$$

$$hu_x + \left(\frac{w}{3} - b\right) u_y = \frac{3}{wh} \left[\left(h^2 + b^2 - \frac{w^2}{3} + \frac{2wb}{3}\right) u_\zeta^+ + \left(h^2 + b^2 + \frac{w^2}{3} - \frac{4wb}{3}\right) u_\eta^+ \right], \quad (\text{A.13})$$

and

$$hu_x - \left(\frac{w}{3} + b\right) u_y = \frac{3}{wh} \left[\left(h^2 + b^2 + \frac{w^2}{3} + \frac{4wb}{3}\right) u_\zeta^+ + \left(h^2 + b^2 - \frac{w^2}{3} - \frac{2wb}{3}\right) u_\eta^+ \right]. \quad (\text{A.14})$$

The conversion referred to above can be carried out using Eqs. (A.5)–(A.14).

Consider Fig. 5(a). The results of flux evaluation involving the quadrilaterals that form the boundaries of $CE_\ell^{(1)}(j, k, n + 1/2)$, $\ell = 1, 2, 3$, and $(j, k, n + 1/2) \in \Omega_1$, are:

(1) The flux leaving $CE_1^{(1)}(j, k, n + 1/2)$ through $G'F'A'B'$ is

$$\frac{2wh}{3} (u + u_\zeta^+ + u_\eta^+)_{j,k}^{n+1/2}.$$

(2) The flux leaving $CE_1^{(1)}(j, k, n + 1/2)$ through $G'GFF'$ is

$$\begin{aligned} & -\frac{\Delta t}{2} \left\{ \frac{wh}{9} (a_\zeta^+ + 2a_\eta^+) \left[u + 2u_\zeta^+ - u_\eta^+ + \frac{\Delta t}{4} (a_\zeta^+ u_\zeta^+ + a_\eta^+ u_\eta^+) \right] \right. \\ & \left. - \frac{3\mu}{wh} \left[\left(h^2 + b^2 - \frac{w^2}{3} + \frac{2wb}{3}\right) u_\zeta^+ + \left(h^2 + b^2 + \frac{w^2}{3} - \frac{4wb}{3}\right) u_\eta^+ \right] \right\}_{j,k}^{n+1/2}. \end{aligned}$$

(3) The flux leaving $CE_1^{(1)}(j, k, n + 1/2)$ through $G'B'BG$ is

$$\frac{\Delta t}{2} \left\{ -\frac{wh}{9} (2a_\zeta^+ + a_\eta^+) \left[u - u_\zeta^+ + 2u_\eta^+ + \frac{\Delta t}{4} (a_\zeta^+ u_\zeta^+ + a_\eta^+ u_\eta^+) \right] \right. \\ \left. + \frac{3\mu}{wh} \left[\left(h^2 + b^2 + \frac{w^2}{3} + \frac{4wb}{3} \right) u_\zeta^+ + \left(h^2 + b^2 - \frac{w^2}{3} - \frac{2wb}{3} \right) u_\eta^+ \right] \right\}_{j,k}^{n+1/2}.$$

(4) The flux leaving $CE_1^{(1)}(j, k, n + 1/2)$ through $AFGB$ is

$$-\frac{2wh}{3} (u - u_\zeta^+ - u_\eta^+)_{j+1/3, k+1/3}^n.$$

(5) The flux leaving $CE_1^{(1)}(j, k, n + 1/2)$ through $ABB'A'$ is

$$\frac{\Delta t}{2} \left\{ \frac{wh}{9} (a_\zeta^+ + 2a_\eta^+) \left[u - 2u_\zeta^+ + u_\eta^+ - \frac{\Delta t}{4} (a_\zeta^+ u_\zeta^+ + a_\eta^+ u_\eta^+) \right] \right. \\ \left. - \frac{3\mu}{wh} \left[\left(h^2 + b^2 - \frac{w^2}{3} + \frac{2wb}{3} \right) u_\zeta^+ + \left(h^2 + b^2 + \frac{w^2}{3} - \frac{4wb}{3} \right) u_\eta^+ \right] \right\}_{j+1/3, k+1/3}^n.$$

(6) The flux leaving $CE_1^{(1)}(j, k, n + 1/2)$ through $AA'F'F$ is

$$-\frac{\Delta t}{2} \left\{ -\frac{wh}{9} (2a_\zeta^+ + a_\eta^+) \left[u + u_\zeta^+ - 2u_\eta^+ - \frac{\Delta t}{4} (a_\zeta^+ u_\zeta^+ + a_\eta^+ u_\eta^+) \right] \right. \\ \left. + \frac{3\mu}{wh} \left[\left(h^2 + b^2 + \frac{w^2}{3} + \frac{4wb}{3} \right) u_\zeta^+ + \left(h^2 + b^2 - \frac{w^2}{3} - \frac{2wb}{3} \right) u_\eta^+ \right] \right\}_{j+1/3, k+1/3}^n.$$

(7) The flux leaving $CE_2^{(1)}(j, k, n + 1/2)$ through $G'B'C'D'$ is

$$\frac{2wh}{3} (u - 2u_\zeta^+ + u_\eta^+)_{j,k}^{n+1/2}.$$

(8) The flux leaving $CE_2^{(1)}(j, k, n + 1/2)$ through $G'GBB'$ is

$$-\frac{\Delta t}{2} \left\{ -\frac{wh}{9} (2a_\zeta^+ + a_\eta^+) \left[u - u_\zeta^+ + 2u_\eta^+ + \frac{\Delta t}{4} (a_\zeta^+ u_\zeta^+ + a_\eta^+ u_\eta^+) \right] \right. \\ \left. + \frac{3\mu}{wh} \left[\left(h^2 + b^2 + \frac{w^2}{3} + \frac{4wb}{3} \right) u_\zeta^+ + \left(h^2 + b^2 - \frac{w^2}{3} - \frac{2wb}{3} \right) u_\eta^+ \right] \right\}_{j,k}^{n+1/2}.$$

(9) The flux leaving $CE_2^{(1)}(j, k, n + 1/2)$ through $G'D'DG$ is

$$-\frac{w\Delta t}{3} \left\{ -\frac{h}{6} (a_\zeta^+ - a_\eta^+) \left[u - u_\zeta^+ - u_\eta^+ + \frac{\Delta t}{4} (a_\zeta^+ u_\zeta^+ + a_\eta^+ u_\eta^+) \right] \right. \\ \left. + \frac{3\mu}{wh} \left[(w+b)u_\zeta^+ - (w-b)u_\eta^+ \right] \right\}_{j,k}^{n+1/2}$$

(10) The flux leaving $CE_2^{(1)}(j, k, n + 1/2)$ through $CBGD$ is

$$-\frac{2wh}{3} (u + 2u_\zeta^+ - u_\eta^+)_{j-2/3, k+1/3}^n$$

(11) The flux leaving $CE_2^{(1)}(j, k, n + 1/2)$ through $CDD'C'$ is

$$\frac{\Delta t}{2} \left\{ -\frac{wh}{9} (2a_\zeta^+ + a_\eta^+) \left[u + u_\zeta^+ - 2u_\eta^+ - \frac{\Delta t}{4} (a_\zeta^+ u_\zeta^+ + a_\eta^+ u_\eta^+) \right] \right. \\ \left. + \frac{3\mu}{wh} \left[(h^2 + b^2 + \frac{w^2}{3} + \frac{4wb}{3}) u_\zeta^+ + (h^2 + b^2 - \frac{w^2}{3} - \frac{2wb}{3}) u_\eta^+ \right] \right\}_{j-2/3, k+1/3}^n$$

(12) The flux leaving $CE_2^{(1)}(j, k, n + 1/2)$ through $CC'B'B$ is

$$\frac{w\Delta t}{3} \left\{ -\frac{h}{6} (a_\zeta^+ - a_\eta^+) \left[u + u_\zeta^+ + u_\eta^+ - \frac{\Delta t}{4} (a_\zeta^+ u_\zeta^+ + a_\eta^+ u_\eta^+) \right] \right. \\ \left. + \frac{3\mu}{wh} \left[(w+b)u_\zeta^+ - (w-b)u_\eta^+ \right] \right\}_{j-2/3, k+1/3}^n$$

(13) The flux leaving $CE_3^{(1)}(j, k, n + 1/2)$ through $G'D'E'F'$ is

$$\frac{2wh}{3} (u + u_\zeta^+ - 2u_\eta^+)_{j,k}^{n+1/2}$$

(14) The flux leaving $CE_3^{(1)}(j, k, n + 1/2)$ through $G'GDD'$ is

$$\frac{w\Delta t}{3} \left\{ -\frac{h}{6} (a_\zeta^+ - a_\eta^+) \left[u - u_\zeta^+ - u_\eta^+ + \frac{\Delta t}{4} (a_\zeta^+ u_\zeta^+ + a_\eta^+ u_\eta^+) \right] \right. \\ \left. + \frac{3\mu}{wh} \left[(w+b)u_\zeta^+ - (w-b)u_\eta^+ \right] \right\}_{j,k}^{n+1/2}$$

(15) The flux leaving $CE_3^{(1)}(j, k, n + 1/2)$ through $G'F'FG$ is

$$\frac{\Delta t}{2} \left\{ \frac{wh}{9} (a_\zeta^+ + 2a_\eta^+) \left[u + 2u_\zeta^+ - u_\eta^+ + \frac{\Delta t}{4} (a_\zeta^+ u_\zeta^+ + a_\eta^+ u_\eta^+) \right] \right. \\ \left. - \frac{3\mu}{wh} \left[\left(h^2 + b^2 - \frac{w^2}{3} + \frac{2wb}{3} \right) u_\zeta^+ + \left(h^2 + b^2 + \frac{w^2}{3} - \frac{4wb}{3} \right) u_\eta^+ \right] \right\}_{j,k}^{n+1/2}.$$

(16) The flux leaving $CE_3^{(1)}(j, k, n + 1/2)$ through $EDGF$ is

$$-\frac{2wh}{3} (u - u_\zeta^+ + 2u_\eta^+)_{j+1/3, k-2/3}^n.$$

(17) The flux leaving $CE_3^{(1)}(j, k, n + 1/2)$ through $EFF'E'$ is

$$-\frac{w\Delta t}{3} \left\{ -\frac{h}{6} (a_\zeta^+ - a_\eta^+) \left[u + u_\zeta^+ + u_\eta^+ - \frac{\Delta t}{4} (a_\zeta^+ u_\zeta^+ + a_\eta^+ u_\eta^+) \right] \right. \\ \left. + \frac{3\mu}{wh} \left[(w + b)u_\zeta^+ - (w - b)u_\eta^+ \right] \right\}_{j+1/3, k-2/3}^n.$$

(18) The flux leaving $CE_3^{(1)}(j, k, n + 1/2)$ through $EE'D'D$ is

$$-\frac{\Delta t}{2} \left\{ \frac{wh}{9} (a_\zeta^+ + 2a_\eta^+) \left[u - 2u_\zeta^+ + u_\eta^+ - \frac{\Delta t}{4} (a_\zeta^+ u_\zeta^+ + a_\eta^+ u_\eta^+) \right] \right. \\ \left. - \frac{3\mu}{wh} \left[\left(h^2 + b^2 - \frac{w^2}{3} + \frac{2wb}{3} \right) u_\zeta^+ + \left(h^2 + b^2 + \frac{w^2}{3} - \frac{4wb}{3} \right) u_\eta^+ \right] \right\}_{j+1/3, k-2/3}^n.$$

Consider Fig. 6(a). The results of flux evaluation involving the quadrilaterals that form the boundaries of $CE_\ell^{(2)}(j, k, n + 1)$, $\ell = 1, 2, 3$, and $(j, k, n + 1) \in \Omega_2$, are:

(19) The flux leaving $CE_1^{(2)}(j, k, n + 1)$ through $G'C'D'E'$ is

$$\frac{2wh}{3} (u - u_\zeta^+ - u_\eta^+)_{j,k}^{n+1}.$$

(20) The flux leaving $CE_1^{(2)}(j, k, n + 1)$ through $G'GCC'$ is

$$\frac{\Delta t}{2} \left\{ \frac{wh}{9} (a_\zeta^+ + 2a_\eta^+) \left[u - 2u_\zeta^+ + u_\eta^+ + \frac{\Delta t}{4} (a_\zeta^+ u_\zeta^+ + a_\eta^+ u_\eta^+) \right] \right. \\ \left. - \frac{3\mu}{wh} \left[\left(h^2 + b^2 - \frac{w^2}{3} + \frac{2wb}{3} \right) u_\zeta^+ + \left(h^2 + b^2 + \frac{w^2}{3} - \frac{4wb}{3} \right) u_\eta^+ \right] \right\}_{j,k}^{n+1}.$$

(21) The flux leaving $CE_1^{(2)}(j, k, n + 1)$ through $G'E'EG$ is

$$-\frac{\Delta t}{2} \left\{ -\frac{wh}{9} (2a_\zeta^+ + a_\eta^+) \left[u + u_\zeta^+ - 2u_\eta^+ + \frac{\Delta t}{4} (a_\zeta^+ u_\zeta^+ + a_\eta^+ u_\eta^+) \right] \right. \\ \left. + \frac{3\mu}{wh} \left[\left(h^2 + b^2 + \frac{w^2}{3} + \frac{4wb}{3} \right) u_\zeta^+ + \left(h^2 + b^2 - \frac{w^2}{3} - \frac{2wb}{3} \right) u_\eta^+ \right] \right\}_{j,k}^{n+1}.$$

(22) The flux leaving $CE_1^{(2)}(j, k, n + 1)$ through $DCGE$ is

$$-\frac{2wh}{3} (u + u_\zeta^+ + u_\eta^+)_{j-1/3, k-1/3}^{n+1/2}.$$

(23) The flux leaving $CE_1^{(2)}(j, k, n + 1)$ through $DEE'D'$ is

$$-\frac{\Delta t}{2} \left\{ \frac{wh}{9} (a_\zeta^+ + 2a_\eta^+) \left[u + 2u_\zeta^+ - u_\eta^+ - \frac{\Delta t}{4} (a_\zeta^+ u_\zeta^+ + a_\eta^+ u_\eta^+) \right] \right. \\ \left. - \frac{3\mu}{wh} \left[\left(h^2 + b^2 - \frac{w^2}{3} + \frac{2wb}{3} \right) u_\zeta^+ + \left(h^2 + b^2 + \frac{w^2}{3} - \frac{4wb}{3} \right) u_\eta^+ \right] \right\}_{j-1/3, k-1/3}^{n+1/2}.$$

(24) The flux leaving $CE_1^{(2)}(j, k, n + 1)$ through $DD'C'C$ is

$$\frac{\Delta t}{2} \left\{ -\frac{wh}{9} (2a_\zeta^+ + a_\eta^+) \left[u - u_\zeta^+ + 2u_\eta^+ - \frac{\Delta t}{4} (a_\zeta^+ u_\zeta^+ + a_\eta^+ u_\eta^+) \right] \right. \\ \left. + \frac{3\mu}{wh} \left[\left(h^2 + b^2 + \frac{w^2}{3} + \frac{4wb}{3} \right) u_\zeta^+ + \left(h^2 + b^2 - \frac{w^2}{3} - \frac{2wb}{3} \right) u_\eta^+ \right] \right\}_{j-1/3, k-1/3}^{n+1/2}.$$

(25) The flux leaving $CE_2^{(2)}(j, k, n + 1)$ through $G'E'F'A'$ is

$$\frac{2wh}{3} (u + 2u_\zeta^+ - u_\eta^+)_{j,k}^{n+1}.$$

(26) The flux leaving $CE_2^{(2)}(j, k, n + 1)$ through $G'GEE'$ is

$$\frac{\Delta t}{2} \left\{ -\frac{wh}{9} (2a_\zeta^+ + a_\eta^+) \left[u + u_\zeta^+ - 2u_\eta^+ + \frac{\Delta t}{4} (a_\zeta^+ u_\zeta^+ + a_\eta^+ u_\eta^+) \right] \right. \\ \left. + \frac{3\mu}{wh} \left[\left(h^2 + b^2 + \frac{w^2}{3} + \frac{4wb}{3} \right) u_\zeta^+ + \left(h^2 + b^2 - \frac{w^2}{3} - \frac{2wb}{3} \right) u_\eta^+ \right] \right\}_{j,k}^{n+1}.$$

(27) The flux leaving $CE_2^{(2)}(j, k, n + 1)$ through $G'A'AG$ is

$$\frac{w\Delta t}{3} \left\{ \frac{h}{6} (a_\eta^+ - a_\zeta^+) \left[u + u_\zeta^+ + u_\eta^+ + \frac{\Delta t}{4} (a_\zeta^+ u_\zeta^+ + a_\eta^+ u_\eta^+) \right] \right. \\ \left. + \frac{3\mu}{wh} [(w + b)u_\zeta^+ - (w - b)u_\eta^+] \right\}_{j,k}^{n+1}.$$

(28) The flux leaving $CE_2^{(2)}(j, k, n + 1)$ through $FEGA$ is

$$-\frac{2wh}{3} (u - 2u_\zeta^+ + u_\eta^+)_{j+2/3, k-1/3}^{n+1/2}.$$

(29) The flux leaving $CE_2^{(2)}(j, k, n + 1)$ through $FAA'F'$ is

$$-\frac{\Delta t}{2} \left\{ -\frac{wh}{9} (2a_\zeta^+ + a_\eta^+) \left[u - u_\zeta^+ + 2u_\eta^+ - \frac{\Delta t}{4} (a_\zeta^+ u_\zeta^+ + a_\eta^+ u_\eta^+) \right] \right. \\ \left. + \frac{3\mu}{wh} \left[\left(h^2 + b^2 + \frac{w^2}{3} + \frac{4wb}{3} \right) u_\zeta^+ + \left(h^2 + b^2 - \frac{w^2}{3} - \frac{2wb}{3} \right) u_\eta^+ \right] \right\}_{j+2/3, k-1/3}^{n+1/2}.$$

(30) The flux leaving $CE_2^{(2)}(j, k, n + 1)$ through $FF'E'E$ is

$$-\frac{w\Delta t}{3} \left\{ \frac{h}{6} (a_\eta^+ - a_\zeta^+) \left[u - u_\zeta^+ - u_\eta^+ - \frac{\Delta t}{4} (a_\zeta^+ u_\zeta^+ + a_\eta^+ u_\eta^+) \right] \right. \\ \left. + \frac{3\mu}{wh} [(w + b)u_\zeta^+ - (w - b)u_\eta^+] \right\}_{j+2/3, k-1/3}^{n+1/2}.$$

(31) The flux leaving $CE_3^{(2)}(j, k, n + 1)$ through $G'A'B'C'$ is

$$\frac{2wh}{3} (u - u_\zeta^+ + 2u_\eta^+)_{j,k}^{n+1}.$$

(32) The flux leaving $CE_3^{(2)}(j, k, n + 1)$ through $G'GAA'$ is

$$-\frac{w\Delta t}{3} \left\{ \frac{h}{6} (a_\eta^+ - a_\zeta^+) \left[u + u_\zeta^+ + u_\eta^+ + \frac{\Delta t}{4} (a_\zeta^+ u_\zeta^+ + a_\eta^+ u_\eta^+) \right] \right. \\ \left. + \frac{3\mu}{wh} [(w + b)u_\zeta^+ - (w - b)u_\eta^+] \right\}_{j,k}^{n+1}.$$

(33) The flux leaving $CE_3^{(2)}(j, k, n + 1)$ through $G'C'CG$ is

$$-\frac{\Delta t}{2} \left\{ \frac{wh}{9} (a_\zeta^+ + 2a_\eta^+) \left[u - 2u_\zeta^+ + u_\eta^+ + \frac{\Delta t}{4} (a_\zeta^+ u_\zeta^+ + a_\eta^+ u_\eta^+) \right] \right. \\ \left. - \frac{3\mu}{wh} \left[\left(h^2 + b^2 - \frac{w^2}{3} + \frac{2wb}{3} \right) u_\zeta^+ + \left(h^2 + b^2 + \frac{w^2}{3} - \frac{4wb}{3} \right) u_\eta^+ \right] \right\}_{j,k}^{n+1}.$$

(34) The flux leaving $CE_3^{(2)}(j, k, n + 1)$ through $BAGC$ is

$$-\frac{2wh}{3} (u + u_\zeta^+ - 2u_\eta^+)_{j-1/3, k+2/3}^{n+1/2}.$$

(35) The flux leaving $CE_3^{(2)}(j, k, n + 1)$ through $BCC'B'$ is

$$\frac{w\Delta t}{3} \left\{ \frac{h}{6} (a_\eta^+ - a_\zeta^+) \left[u - u_\zeta^+ - u_\eta^+ - \frac{\Delta t}{4} (a_\zeta^+ u_\zeta^+ + a_\eta^+ u_\eta^+) \right] \right. \\ \left. + \frac{3\mu}{wh} [(w + b)u_\zeta^+ - (w - b)u_\eta^+] \right\}_{j-1/3, k+2/3}^{n+1/2}.$$

(36) The flux leaving $CE_3^{(2)}(j, k, n + 1)$ through $BB'A'A$ is

$$\frac{\Delta t}{2} \left\{ \frac{wh}{9} (a_\zeta^+ + 2a_\eta^+) \left[u + 2u_\zeta^+ - u_\eta^+ - \frac{\Delta t}{4} (a_\zeta^+ u_\zeta^+ + a_\eta^+ u_\eta^+) \right] \right. \\ \left. - \frac{3\mu}{wh} \left[\left(h^2 + b^2 - \frac{w^2}{3} + \frac{2wb}{3} \right) u_\zeta^+ + \left(h^2 + b^2 + \frac{w^2}{3} - \frac{4wb}{3} \right) u_\eta^+ \right] \right\}_{j-1/3, k+2/3}^{n+1/2}.$$

With the aid of Eqs. (2.31), (2.32) and (2.35)–(2.52), Eqs. (2.53)–(2.58) are the results of (1)–(36) and Eqs. (2.12) and (2.13). QED.

To prove Eqs. (2.86) and (2.87), we evaluate $\Delta^{(1)}$ and $\Delta^{(2)}$ using Eqs. (2.35)–(2.52). After simplifications, the results are

$$\Delta^{(1)} = 3 \left[3(1 + \nu_\zeta)(1 + \nu_\eta)(1 - \nu_\zeta - \nu_\eta) + 2(1 + \nu_\zeta)(1 - \nu_\zeta - \nu_\eta)\xi_\zeta \right. \\ \left. + 2(1 + \nu_\eta)(1 - \nu_\zeta - \nu_\eta)\xi_\eta + 2(1 + \nu_\zeta)(1 + \nu_\eta)\xi_\tau \right. \\ \left. - (\xi_\zeta)^2 - (\xi_\eta)^2 - (\xi_\tau)^2 + 2\xi_\zeta\xi_\eta + 2\xi_\zeta\xi_\tau + 2\xi_\eta\xi_\tau \right], \quad (A.15)$$

and

$$\begin{aligned} \Delta^{(2)} = & 3 \left[3(1 - \nu_\zeta)(1 - \nu_\eta)(1 + \nu_\zeta + \nu_\eta) + 2(1 - \nu_\zeta)(1 + \nu_\zeta + \nu_\eta)\xi_\zeta \right. \\ & + 2(1 - \nu_\eta)(1 + \nu_\zeta + \nu_\eta)\xi_\eta + 2(1 - \nu_\zeta)(1 - \nu_\eta)\xi_\tau \\ & \left. - (\xi_\zeta)^2 - (\xi_\eta)^2 - (\xi_\tau)^2 + 2\xi_\zeta\xi_\eta + 2\xi_\zeta\xi_\tau + 2\xi_\eta\xi_\tau \right]. \end{aligned} \quad (\text{A.16})$$

By comparing Eqs. (2.86) and (2.87) with Eqs. (A.15) and (A.16), it is seen that the proof of the former is completed if one can prove

$$-(\xi_\zeta)^2 - (\xi_\eta)^2 - (\xi_\tau)^2 + 2\xi_\zeta\xi_\eta + 2\xi_\zeta\xi_\tau + 2\xi_\eta\xi_\tau = \left(\frac{9\mu\Delta t}{2wh} \right)^2. \quad (\text{A.17})$$

Proof of Eq. (A.17): The area of the hexagon $ABCDEF$ depicted in Fig. 7(a) is $2wh$. The area of $\triangle BDF$ depicted in the same figure is half of that. Thus

$$\text{the area of } \triangle BDF = wh. \quad (\text{A.18})$$

Moreover, because $\Delta\zeta$, $\Delta\eta$, and $\Delta\tau$ are the lengths of the three sides of $\triangle BDF$,

$$\begin{aligned} & \text{the area of } \triangle BDF \\ & = \sqrt{\frac{1}{16}(\Delta\zeta + \Delta\eta + \Delta\tau)(\Delta\zeta + \Delta\eta - \Delta\tau)(\Delta\zeta + \Delta\tau - \Delta\eta)(\Delta\eta + \Delta\tau - \Delta\zeta)}. \end{aligned} \quad (\text{A.19})$$

Combining Eqs. (A.18)–(A.19), one has

$$(\Delta\zeta + \Delta\eta + \Delta\tau)(\Delta\zeta + \Delta\eta - \Delta\tau)(\Delta\zeta + \Delta\tau - \Delta\eta)(\Delta\eta + \Delta\tau - \Delta\zeta) = 16w^2h^2. \quad (\text{A.20})$$

A direct result of Eq. (2.32) is

$$\begin{aligned} -(\xi_\zeta)^2 - (\xi_\eta)^2 - (\xi_\tau)^2 + 2\xi_\zeta\xi_\eta + 2\xi_\zeta\xi_\tau + 2\xi_\eta\xi_\tau = & \frac{81\mu^2(\Delta t)^2}{64w^4h^4} \times \\ & [-(\Delta\zeta)^4 - (\Delta\eta)^4 - (\Delta\tau)^4 + 2(\Delta\zeta)^2(\Delta\eta)^2 + 2(\Delta\zeta)^2(\Delta\tau)^2 + 2(\Delta\eta)^2(\Delta\tau)^2]. \end{aligned} \quad (\text{A.21})$$

Because

$$\begin{aligned} & -(\Delta\zeta)^4 - (\Delta\eta)^4 - (\Delta\tau)^4 + 2(\Delta\zeta)^2(\Delta\eta)^2 + 2(\Delta\zeta)^2(\Delta\tau)^2 + 2(\Delta\eta)^2(\Delta\tau)^2 \\ & \equiv (\Delta\zeta + \Delta\eta + \Delta\tau)(\Delta\zeta + \Delta\eta - \Delta\tau)(\Delta\zeta + \Delta\tau - \Delta\eta)(\Delta\eta + \Delta\tau - \Delta\zeta). \end{aligned} \quad (\text{A.22})$$

Equation (A.17) is a direct result of Eqs. (A.20) and (A.21). QED.

Appendix B

The proof for Eqs. (4.56)–(4.61) is given here.

As a preliminary, note that Eqs. (4.22), (4.25), and (4.31) can be used to obtain

$$f_{mt}^x = - \sum_{\ell,q=1}^4 f_{m,\ell}^x \left(f_{\ell,q}^x u_{qx} + f_{\ell,q}^y u_{qy} \right), \quad (B.1)$$

and

$$f_{mt}^y = - \sum_{\ell,q=1}^4 f_{m,\ell}^y \left(f_{\ell,q}^x u_{qx} + f_{\ell,q}^y u_{qy} \right). \quad (B.2)$$

In this appendix, we adopt the same convention stated following Eq. (4.37). It follows from Eqs. (4.34)–(4.37) that

$$\begin{pmatrix} f_{m,\ell}^x \\ f_{m,\ell}^y \end{pmatrix} = \frac{2}{3\Delta t} \begin{pmatrix} w-b & w+b \\ -h & h \end{pmatrix} \begin{pmatrix} f_{m,\ell}^{\zeta+} \\ f_{m,\ell}^{\eta+} \end{pmatrix}, \quad m = 1, 2, 3, 4, \quad (B.3)$$

and

$$\begin{pmatrix} u_{mx} \\ u_{my} \end{pmatrix} = \frac{3}{w} \begin{pmatrix} 1 & 1 \\ -\frac{w+b}{h} & \frac{w-b}{h} \end{pmatrix} \begin{pmatrix} u_{m\zeta}^+ \\ u_{m\eta}^+ \end{pmatrix}, \quad m = 1, 2, 3, 4. \quad (B.4)$$

An immediate result of Eqs. (B.3) and (B.4) is

$$\sum_{\ell=1}^4 \left(f_{m,\ell}^x u_{\ell x} + f_{m,\ell}^y u_{\ell y} \right) = \frac{4}{\Delta t} \sum_{\ell=1}^4 \left(f_{m,\ell}^{\zeta+} u_{\ell\zeta}^+ + f_{m,\ell}^{\eta+} u_{\ell\eta}^+ \right), \quad m = 1, 2, 3, 4. \quad (B.5)$$

By using Eqs. (4.18), (4.20)–(4.25), and (B.1)–(B.5), it can be shown that

$$u_{mx} = \frac{3}{w} (u_{m\zeta}^+ + u_{m\eta}^+), \quad (B.6)$$

$$\left(\frac{b}{2} + \frac{w}{6} \right) u_{mx} + \frac{h}{2} u_{my} = 2u_{m\eta}^+ - u_{m\zeta}^+, \quad (B.7)$$

$$\left(\frac{b}{2} - \frac{w}{6} \right) u_{mx} + \frac{h}{2} u_{my} = u_{m\eta}^+ - 2u_{m\zeta}^+, \quad (B.8)$$

$$hf_m^x + \left(\frac{w}{3} - b\right) f_m^y = \frac{4wh}{9\Delta t} \sum_{\ell=1}^4 \left(f_{m,\ell}^{\zeta+} + 2f_{m,\ell}^{\eta+}\right) u_\ell, \quad (B.9)$$

$$hf_m^x - \left(\frac{w}{3} + b\right) f_m^y = \frac{4wh}{9\Delta t} \sum_{\ell=1}^4 \left(2f_{m,\ell}^{\zeta+} + f_{m,\ell}^{\eta+}\right) u_\ell, \quad (B.10)$$

$$\begin{aligned} & h \left[\left(\frac{b}{2} + \frac{w}{6}\right) f_{m,x}^x + \frac{h}{2} f_{m,y}^x \right] - \left(\frac{w}{3} + b\right) \left[\left(\frac{b}{2} + \frac{w}{6}\right) f_{m,x}^y + \frac{h}{2} f_{m,y}^y \right] \\ &= \frac{4wh}{9\Delta t} \sum_{\ell=1}^4 \left(2f_{m,\ell}^{\zeta+} + f_{m,\ell}^{\eta+}\right) \left(2u_{\ell\eta}^+ - u_{\ell\zeta}^+\right), \end{aligned} \quad (B.11)$$

$$\begin{aligned} & h \left[\left(\frac{b}{2} - \frac{w}{6}\right) f_{m,x}^x + \frac{h}{2} f_{m,y}^x \right] + \left(\frac{w}{3} - b\right) \left[\left(\frac{b}{2} - \frac{w}{6}\right) f_{m,x}^y + \frac{h}{2} f_{m,y}^y \right] \\ &= \frac{4wh}{9\Delta t} \sum_{\ell=1}^4 \left(f_{m,\ell}^{\zeta+} + 2f_{m,\ell}^{\eta+}\right) \left(u_{\ell\eta}^+ - 2u_{\ell\zeta}^+\right), \end{aligned} \quad (B.12)$$

$$hf_{m,t}^x + \left(\frac{w}{3} - b\right) f_{m,t}^y = -\frac{16wh}{9(\Delta t)^2} \sum_{\ell,q=1}^4 \left(f_{m,\ell}^{\zeta+} + 2f_{m,\ell}^{\eta+}\right) \left(f_{\ell,q}^{\zeta+} u_{q\zeta}^+ + f_{\ell,q}^{\eta+} u_{q\eta}^+\right), \quad (B.13)$$

$$-hf_{m,t}^x + \left(\frac{w}{3} + b\right) f_{m,t}^y = \frac{16wh}{9(\Delta t)^2} \sum_{\ell,q=1}^4 \left(2f_{m,\ell}^{\zeta+} + f_{m,\ell}^{\eta+}\right) \left(f_{\ell,q}^{\zeta+} u_{q\zeta}^+ + f_{\ell,q}^{\eta+} u_{q\eta}^+\right), \quad (B.14)$$

$$\begin{aligned} & f_m^y \pm \frac{w}{3} f_{m,x}^y \pm \frac{\Delta t}{4} f_{m,t}^y \\ &= \frac{2h}{3\Delta t} \sum_{\ell=1}^4 \left(f_{m,\ell}^{\eta+} - f_{m,\ell}^{\zeta+}\right) \left[u_\ell \pm u_{\ell\zeta}^+ \pm u_{\ell\eta}^+ \mp \sum_{q=1}^4 \left(f_{\ell,q}^{\zeta+} u_{q\zeta}^+ + f_{\ell,q}^{\eta+} u_{q\eta}^+\right) \right], \end{aligned} \quad (B.15)$$

and

$$\begin{aligned} & f_m^y \pm \frac{w}{3} f_{m,x}^y \mp \frac{\Delta t}{4} f_{m,t}^y \\ &= \frac{2h}{3\Delta t} \sum_{\ell=1}^4 \left(f_{m,\ell}^{\eta+} - f_{m,\ell}^{\zeta+}\right) \left[u_\ell \pm u_{\ell\zeta}^+ \pm u_{\ell\eta}^+ \pm \sum_{q=1}^4 \left(f_{\ell,q}^{\zeta+} u_{q\zeta}^+ + f_{\ell,q}^{\eta+} u_{q\eta}^+\right) \right]. \end{aligned} \quad (B.16)$$

Note that each of Eqs. (B.15) and (B.16) represents two equations. One corresponds to the upper signs; while the other, to the lower signs.

Next we shall evaluate the flux of \vec{h}_m^* leaving each of the six quadrilaterals that form the boundary of a CE (see Figs. 5(a) and 6(a)). The evaluation procedure is similar to that described in Appendix A. For the current case, the key equations used are Eqs. (2.6a)–(2.6c), (4.19), (4.27)–(4.29), and (B.6)–(B.16).

Consider Fig. 5(a). The results of flux evaluation involving the quadrilaterals that form the boundaries of $CE_\ell^{(1)}(j, k, n + 1/2)$, $\ell = 1, 2, 3$, and $(j, k, n + 1/2) \in \Omega_1$, are:

- (1) The flux of \vec{h}_m^* leaving $CE_1^{(1)}(j, k, n + 1/2)$ through $G'F'A'B'$ is

$$\frac{2wh}{3} \left(u_m + u_{m\zeta}^+ + u_{m\eta}^+ \right)_{j,k}^{n+1/2}$$

- (2) The flux of \vec{h}_m^* leaving $CE_1^{(1)}(j, k, n + 1/2)$ through $G'GFF'$ is

$$-\frac{2wh}{9} \left\{ \sum_{\ell=1}^4 \left(f_{m,\ell}^{\zeta+} + 2f_{m,\ell}^{\eta+} \right) \left[u_\ell + 2u_{\ell\zeta}^+ - u_{\ell\eta}^+ + \sum_{q=1}^4 \left(f_{\ell,q}^{\zeta+} u_{q\zeta}^+ + f_{\ell,q}^{\eta+} u_{q\eta}^+ \right) \right] \right\}_{j,k}^{n+1/2}$$

- (3) The flux of \vec{h}_m^* leaving $CE_1^{(1)}(j, k, n + 1/2)$ through $G'B'BG$ is

$$-\frac{2wh}{9} \left\{ \sum_{\ell=1}^4 \left(2f_{m,\ell}^{\zeta+} + f_{m,\ell}^{\eta+} \right) \left[u_\ell - u_{\ell\zeta}^+ + 2u_{\ell\eta}^+ + \sum_{q=1}^4 \left(f_{\ell,q}^{\zeta+} u_{q\zeta}^+ + f_{\ell,q}^{\eta+} u_{q\eta}^+ \right) \right] \right\}_{j,k}^{n+1/2}$$

- (4) The flux of \vec{h}_m^* leaving $CE_1^{(1)}(j, k, n + 1/2)$ through $AFGB$ is

$$-\frac{2wh}{3} \left(u_m - u_{m\zeta}^+ - u_{m\eta}^+ \right)_{j+1/3, k+1/3}^n$$

- (5) The flux of \vec{h}_m^* leaving $CE_1^{(1)}(j, k, n + 1/2)$ through $ABB'A'$ is

$$\frac{2wh}{9} \left\{ \sum_{\ell=1}^4 \left(f_{m,\ell}^{\zeta+} + 2f_{m,\ell}^{\eta+} \right) \left[u_\ell - 2u_{\ell\zeta}^+ + u_{\ell\eta}^+ - \sum_{q=1}^4 \left(f_{\ell,q}^{\zeta+} u_{q\zeta}^+ + f_{\ell,q}^{\eta+} u_{q\eta}^+ \right) \right] \right\}_{j+1/3, k+1/3}^n$$

- (6) The flux of \vec{h}_m^* leaving $CE_1^{(1)}(j, k, n + 1/2)$ through $AA'F'F$ is

$$\frac{2wh}{9} \left\{ \sum_{\ell=1}^4 \left(2f_{m,\ell}^{\zeta+} + f_{m,\ell}^{\eta+} \right) \left[u_\ell + u_{\ell\zeta}^+ - 2u_{\ell\eta}^+ - \sum_{q=1}^4 \left(f_{\ell,q}^{\zeta+} u_{q\zeta}^+ + f_{\ell,q}^{\eta+} u_{q\eta}^+ \right) \right] \right\}_{j+1/3, k+1/3}^n$$

(7) The flux of \vec{h}_m^* leaving $CE_2^{(1)}(j, k, n + 1/2)$ through $G'B'C'D'$ is

$$\frac{2wh}{3} \left(u_m - 2u_{m\zeta}^+ + u_{m\eta}^+ \right)_{j,k}^{n+1/2}.$$

(8) The flux of \vec{h}_m^* leaving $CE_2^{(1)}(j, k, n + 1/2)$ through $G'GBB'$ is

$$\frac{2wh}{9} \left\{ \sum_{\ell=1}^4 \left(2f_{m,\ell}^{\zeta+} + f_{m,\ell}^{\eta+} \right) \left[u_\ell - u_{\ell\zeta}^+ + 2u_{\ell\eta}^+ + \sum_{q=1}^4 \left(f_{\ell,q}^{\zeta+} u_{q\zeta}^+ + f_{\ell,q}^{\eta+} u_{q\eta}^+ \right) \right] \right\}_{j,k}^{n+1/2}.$$

(9) The flux of \vec{h}_m^* leaving $CE_2^{(1)}(j, k, n + 1/2)$ through $G'D'DG$ is

$$\frac{2wh}{9} \left\{ \sum_{\ell=1}^4 \left(f_{m,\ell}^{\zeta+} - f_{m,\ell}^{\eta+} \right) \left[u_\ell - u_{\ell\zeta}^+ - u_{\ell\eta}^+ + \sum_{q=1}^4 \left(f_{\ell,q}^{\zeta+} u_{q\zeta}^+ + f_{\ell,q}^{\eta+} u_{q\eta}^+ \right) \right] \right\}_{j,k}^{n+1/2}.$$

(10) The flux of \vec{h}_m^* leaving $CE_2^{(1)}(j, k, n + 1/2)$ through $CBGD$ is

$$-\frac{2wh}{3} \left(u_m + 2u_{m\zeta}^+ - u_{m\eta}^+ \right)_{j-2/3, k+1/3}^n.$$

(11) The flux of \vec{h}_m^* leaving $CE_2^{(1)}(j, k, n + 1/2)$ through $CDD'C'$ is

$$-\frac{2wh}{9} \left\{ \sum_{\ell=1}^4 \left(2f_{m,\ell}^{\zeta+} + f_{m,\ell}^{\eta+} \right) \left[u_\ell + u_{\ell\zeta}^+ - 2u_{\ell\eta}^+ - \sum_{q=1}^4 \left(f_{\ell,q}^{\zeta+} u_{q\zeta}^+ + f_{\ell,q}^{\eta+} u_{q\eta}^+ \right) \right] \right\}_{j-2/3, k+1/3}^n.$$

(12) The flux of \vec{h}_m^* leaving $CE_2^{(1)}(j, k, n + 1/2)$ through $CC'B'B$ is

$$\frac{2wh}{9} \left\{ \sum_{\ell=1}^4 \left(f_{m,\ell}^{\eta+} - f_{m,\ell}^{\zeta+} \right) \left[u_\ell + u_{\ell\zeta}^+ + u_{\ell\eta}^+ - \sum_{q=1}^4 \left(f_{\ell,q}^{\zeta+} u_{q\zeta}^+ + f_{\ell,q}^{\eta+} u_{q\eta}^+ \right) \right] \right\}_{j-2/3, k+1/3}^n.$$

(13) The flux of \vec{h}_m^* leaving $CE_3^{(1)}(j, k, n + 1/2)$ through $G'D'E'F'$ is

$$\frac{2wh}{3} \left(u_m + u_{m\zeta}^+ - 2u_{m\eta}^+ \right)_{j,k}^{n+1/2}.$$

(14) The flux of \vec{h}_m^* leaving $CE_3^{(1)}(j, k, n + 1/2)$ through $G'GDD'$ is

$$-\frac{2wh}{9} \left\{ \sum_{\ell=1}^4 \left(f_{m,\ell}^{\zeta+} - f_{m,\ell}^{\eta+} \right) \left[u_\ell - u_{\ell\zeta}^+ - u_{\ell\eta}^+ + \sum_{q=1}^4 \left(f_{\ell,q}^{\zeta+} u_{q\zeta}^+ + f_{\ell,q}^{\eta+} u_{q\eta}^+ \right) \right] \right\}_{j,k}^{n+1/2}.$$

(15) The flux of \vec{h}_m^* leaving $CE_3^{(1)}(j, k, n + 1/2)$ through $G'F'FG$ is

$$\frac{2wh}{9} \left\{ \sum_{\ell=1}^4 (f_{m,\ell}^{\zeta+} + 2f_{m,\ell}^{\eta+}) \left[u_{\ell} + 2u_{\ell\zeta}^+ - u_{\ell\eta}^+ + \sum_{q=1}^4 (f_{\ell,q}^{\zeta+} u_{q\zeta}^+ + f_{\ell,q}^{\eta+} u_{q\eta}^+) \right] \right\}_{j,k}^{n+1/2}$$

(16) The flux of \vec{h}_m^* leaving $CE_3^{(1)}(j, k, n + 1/2)$ through $EDGF$ is

$$-\frac{2wh}{3} (u_m - u_{m\zeta}^+ + 2u_{m\eta}^+)_{j+1/3, k-2/3}^n$$

(17) The flux of \vec{h}_m^* leaving $CE_3^{(1)}(j, k, n + 1/2)$ through $EFF'E'$ is

$$\frac{2wh}{9} \left\{ \sum_{\ell=1}^4 (f_{m,\ell}^{\zeta+} - f_{m,\ell}^{\eta+}) \left[u_{\ell} + u_{\ell\zeta}^+ + u_{\ell\eta}^+ - \sum_{q=1}^4 (f_{\ell,q}^{\zeta+} u_{q\zeta}^+ + f_{\ell,q}^{\eta+} u_{q\eta}^+) \right] \right\}_{j+1/3, k-2/3}^n$$

(18) The flux of \vec{h}_m^* leaving $CE_3^{(1)}(j, k, n + 1/2)$ through $EE'D'D$ is

$$-\frac{2wh}{9} \left\{ \sum_{\ell=1}^4 (f_{m,\ell}^{\zeta+} + 2f_{m,\ell}^{\eta+}) \left[u_{\ell} - 2u_{\ell\zeta}^+ + u_{\ell\eta}^+ - \sum_{q=1}^4 (f_{\ell,q}^{\zeta+} u_{q\zeta}^+ + f_{\ell,q}^{\eta+} u_{q\eta}^+) \right] \right\}_{j+1/3, k-2/3}^n$$

Consider Fig. 6(a). The results of flux evaluation involving the quadrilaterals that form the boundaries of $CE_{\ell}^{(2)}(j, k, n + 1)$, $\ell = 1, 2, 3$, and $(j, k, n + 1) \in \Omega_2$, are:

(19) The flux of \vec{h}_m^* leaving $CE_1^{(2)}(j, k, n + 1)$ through $G'C'D'E'$ is

$$\frac{2wh}{3} (u_m - u_{m\zeta}^+ - u_{m\eta}^+)_{j,k}^{n+1}$$

(20) The flux of \vec{h}_m^* leaving $CE_1^{(2)}(j, k, n + 1)$ through $G'GCC'$ is

$$\frac{2wh}{9} \left\{ \sum_{\ell=1}^4 (f_{m,\ell}^{\zeta+} + 2f_{m,\ell}^{\eta+}) \left[u_{\ell} - 2u_{\ell\zeta}^+ + u_{\ell\eta}^+ + \sum_{q=1}^4 (f_{\ell,q}^{\zeta+} u_{q\zeta}^+ + f_{\ell,q}^{\eta+} u_{q\eta}^+) \right] \right\}_{j,k}^{n+1}$$

(21) The flux of \vec{h}_m^* leaving $CE_1^{(2)}(j, k, n + 1)$ through $G'E'EG$ is

$$\frac{2wh}{9} \left\{ \sum_{\ell=1}^4 (2f_{m,\ell}^{\zeta+} + f_{m,\ell}^{\eta+}) \left[u_{\ell} + u_{\ell\zeta}^+ - 2u_{\ell\eta}^+ + \sum_{q=1}^4 (f_{\ell,q}^{\zeta+} u_{q\zeta}^+ + f_{\ell,q}^{\eta+} u_{q\eta}^+) \right] \right\}_{j,k}^{n+1}$$

(22) The flux of \vec{h}_m^* leaving $CE_1^{(2)}(j, k, n + 1)$ through $DCGE$ is

$$-\frac{2wh}{3} \left(u_m + u_{m\zeta}^+ + u_{m\eta}^+ \right)_{j-1/3, k-1/3}^{n+1/2}.$$

(23) The flux of \vec{h}_m^* leaving $CE_1^{(2)}(j, k, n + 1)$ through $DEE'D'$ is

$$-\frac{2wh}{9} \left\{ \sum_{\ell=1}^4 \left(f_{m,\ell}^{\zeta+} + 2f_{m,\ell}^{\eta+} \right) \left[u_\ell + 2u_{\ell\zeta}^+ - u_{\ell\eta}^+ - \sum_{q=1}^4 \left(f_{\ell,q}^{\zeta+} u_{q\zeta}^+ + f_{\ell,q}^{\eta+} u_{q\eta}^+ \right) \right] \right\}_{j-1/3, k-1/3}^{n+1/2}.$$

(24) The flux of \vec{h}_m^* leaving $CE_1^{(2)}(j, k, n + 1)$ through $DD'C'C$ is

$$-\frac{2wh}{9} \left\{ \sum_{\ell=1}^4 \left(2f_{m,\ell}^{\zeta+} + f_{m,\ell}^{\eta+} \right) \left[u_\ell - u_{\ell\zeta}^+ + 2u_{\ell\eta}^+ - \sum_{q=1}^4 \left(f_{\ell,q}^{\zeta+} u_{q\zeta}^+ + f_{\ell,q}^{\eta+} u_{q\eta}^+ \right) \right] \right\}_{j-1/3, k-1/3}^{n+1/2}.$$

(25) The flux of \vec{h}_m^* leaving $CE_2^{(2)}(j, k, n + 1)$ through $G'E'F'A'$ is

$$\frac{2wh}{3} \left(u_m + 2u_{m\zeta}^+ - u_{m\eta}^+ \right)_{j,k}^{n+1}.$$

(26) The flux of \vec{h}_m^* leaving $CE_2^{(2)}(j, k, n + 1)$ through $G'GEE'$ is

$$-\frac{2wh}{9} \left\{ \sum_{\ell=1}^4 \left(2f_{m,\ell}^{\zeta+} + f_{m,\ell}^{\eta+} \right) \left[u_\ell + u_{\ell\zeta}^+ - 2u_{\ell\eta}^+ + \sum_{q=1}^4 \left(f_{\ell,q}^{\zeta+} u_{q\zeta}^+ + f_{\ell,q}^{\eta+} u_{q\eta}^+ \right) \right] \right\}_{j,k}^{n+1}.$$

(27) The flux of \vec{h}_m^* leaving $CE_2^{(2)}(j, k, n + 1)$ through $G'A'AG$ is

$$\frac{2wh}{9} \left\{ \sum_{\ell=1}^4 \left(f_{m,\ell}^{\eta+} - f_{m,\ell}^{\zeta+} \right) \left[u_\ell + u_{\ell\zeta}^+ + u_{\ell\eta}^+ + \sum_{q=1}^4 \left(f_{\ell,q}^{\zeta+} u_{q\zeta}^+ + f_{\ell,q}^{\eta+} u_{q\eta}^+ \right) \right] \right\}_{j,k}^{n+1}.$$

(28) The flux of \vec{h}_m^* leaving $CE_2^{(2)}(j, k, n + 1)$ through $FEGA$ is

$$-\frac{2wh}{3} \left(u_m - 2u_{m\zeta}^+ + u_{m\eta}^+ \right)_{j+2/3, k-1/3}^{n+1/2}.$$

(29) The flux of \vec{h}_m^* leaving $CE_2^{(2)}(j, k, n + 1)$ through $FAA'F'$ is

$$\frac{2wh}{9} \left\{ \sum_{\ell=1}^4 \left(2f_{m,\ell}^{\zeta+} + f_{m,\ell}^{\eta+} \right) \left[u_\ell - u_{\ell\zeta}^+ + 2u_{\ell\eta}^+ - \sum_{q=1}^4 \left(f_{\ell,q}^{\zeta+} u_{q\zeta}^+ + f_{\ell,q}^{\eta+} u_{q\eta}^+ \right) \right] \right\}_{j+2/3, k-1/3}^{n+1/2}.$$

(30) The flux of \vec{h}_m^* leaving $CE_2^{(2)}(j, k, n+1)$ through $FF'E'E$ is

$$\frac{2wh}{9} \left\{ \sum_{\ell=1}^4 (f_{m,\ell}^{\zeta+} - f_{m,\ell}^{\eta+}) \left[u_{\ell} - u_{\ell\zeta}^+ - u_{\ell\eta}^+ - \sum_{q=1}^4 (f_{\ell,q}^{\zeta+} u_{q\zeta}^+ + f_{\ell,q}^{\eta+} u_{q\eta}^+) \right] \right\}_{j+2/3, k-1/3}^{n+1/2}$$

(31) The flux of \vec{h}_m^* leaving $CE_3^{(2)}(j, k, n+1)$ through $G'A'B'C'$ is

$$\frac{2wh}{3} (u_m - u_{m\zeta}^+ + 2u_{m\eta}^+)_{j,k}^{n+1}$$

(32) The flux of \vec{h}_m^* leaving $CE_3^{(2)}(j, k, n+1)$ through $G'GAA'$ is

$$\frac{2wh}{9} \left\{ \sum_{\ell=1}^4 (f_{m,\ell}^{\zeta+} - f_{m,\ell}^{\eta+}) \left[u_{\ell} + u_{\ell\zeta}^+ + u_{\ell\eta}^+ + \sum_{q=1}^4 (f_{\ell,q}^{\zeta+} u_{q\zeta}^+ + f_{\ell,q}^{\eta+} u_{q\eta}^+) \right] \right\}_{j,k}^{n+1}$$

(33) The flux of \vec{h}_m^* leaving $CE_3^{(2)}(j, k, n+1)$ through $G'C'CG$ is

$$-\frac{2wh}{9} \left\{ \sum_{\ell=1}^4 (f_{m,\ell}^{\zeta+} + 2f_{m,\ell}^{\eta+}) \left[u_{\ell} - 2u_{\ell\zeta}^+ + u_{\ell\eta}^+ + \sum_{q=1}^4 (f_{\ell,q}^{\zeta+} u_{q\zeta}^+ + f_{\ell,q}^{\eta+} u_{q\eta}^+) \right] \right\}_{j,k}^{n+1/2}$$

(34) The flux of \vec{h}_m^* leaving $CE_3^{(2)}(j, k, n+1)$ through $BAGC$ is

$$-\frac{2wh}{3} (u_m + u_{m\zeta}^+ - 2u_{m\eta}^+)_{j-1/3, k+2/3}^{n+1/2}$$

(35) The flux of \vec{h}_m^* leaving $CE_3^{(2)}(j, k, n+1)$ through $BCC'B'$ is

$$\frac{2wh}{9} \left\{ \sum_{\ell=1}^4 (f_{m,\ell}^{\eta+} - f_{m,\ell}^{\zeta+}) \left[u_{\ell} - u_{\ell\zeta}^+ - u_{\ell\eta}^+ - \sum_{q=1}^4 (f_{\ell,q}^{\zeta+} u_{q\zeta}^+ + f_{\ell,q}^{\eta+} u_{q\eta}^+) \right] \right\}_{j-1/3, k+2/3}^{n+1/2}$$

(36) The flux of \vec{h}_m^* leaving $CE_3^{(2)}(j, k, n+1)$ through $BB'A'A$ is

$$\frac{2wh}{9} \left\{ \sum_{\ell=1}^4 (f_{m,\ell}^{\zeta+} + 2f_{m,\ell}^{\eta+}) \left[u_{\ell} + 2u_{\ell\zeta}^+ - u_{\ell\eta}^+ - \sum_{q=1}^4 (f_{\ell,q}^{\zeta+} u_{q\zeta}^+ + f_{\ell,q}^{\eta+} u_{q\eta}^+) \right] \right\}_{j-1/3, k+2/3}^{n+1/2}$$

With the aid of Eqs. (4.38)–(4.55), Eqs. (4.56)–(4.61) are the results of (1)–(36) and Eqs. (4.32) and (4.33). QED.

Appendix C

In this appendix, first we shall prove the following theorem.

Theorem. Let A and B be two arbitrary $n \times n$ matrices. Then AB and BA have the same eigenvalues.

Proof. We have (i)

$$AB = A(BA)A^{-1} \quad \text{if } A^{-1} \text{ exists;} \quad (C.1)$$

and (ii)

$$AB = B^{-1}(BA)B \quad \text{if } B^{-1} \text{ exists.} \quad (C.2)$$

Thus $AB \sim BA$, i.e., AB is similar to BA , if either A , or B , is nonsingular. Because two similar matrices have the same eigenvalues [25, p.45], the proof is complete if either A , or B is nonsingular.

Let both A and B be singular. Because the determinant of AB (or BA) is the product of the determinant of A and the determinant of B , both AB and BA are singular. Thus 0 is an eigenvalue for both AB and BA . We shall prove that a nonzero eigenvalue of AB must also be an eigenvalue of BA , and vice versa.

Let $\vec{\phi}$ be an eigenvector of AB with the eigenvalue $\lambda \neq 0$. Then

$$AB\vec{\phi} = \lambda\vec{\phi}. \quad (C.3)$$

Because $\lambda \neq 0$ and, by definition, $\vec{\phi}$ is not a null vector, Eq. (C.3) implies that $B\vec{\phi}$ is not a null vector too. The last result coupled with another result of Eq. (C.3), i.e.,

$$BA(B\vec{\phi}) = \lambda(B\vec{\phi}), \quad (C.4)$$

implies that λ is also an eigenvalue of BA . Conversely, it can be shown that an eigenvalue $\lambda \neq 0$ of BA is also an eigenvalue of AB . QED.

An immediate result of the above theorem is that the amplification matrices that appear on the right sides of Eqs. (5.2) and (5.3) have the same eigenvalues. Next, as a part of stability study, we shall investigate the two-way marching nature of the a scheme.

According to Figs. 5(a) and 6(a), there are three CEs located immediately below any mesh point $G' \in \Omega$. By definition, the mesh indices of these CEs are those of the mesh point G' . As shown in Figs. 12(a) and 12(b), there are also three CEs located immediately above any mesh point $G \in \Omega$. However, the mesh indices of these CEs differ from those of the mesh point G .

In Fig. 12(a), $B' \in \Omega_1$, $D' \in \Omega_1$, $F' \in \Omega_1$, and $G \in \Omega_2$. The three CEs located immediately above point G have their mesh indices tied to points B' , D' , and F' , respectively. In Fig. 12(b), $A' \in \Omega_2$, $C' \in \Omega_2$, $E' \in \Omega_2$, and $G \in \Omega_1$. The three CEs located immediately above point G have their mesh indices tied to points A' , C' , and E' , respectively.

From Figs. 5(a), 6(a), 12(a), and 12(b), one concludes that each CE is in contact with (i) one and only one mesh point $\in \Omega_1$, and (ii) one and only one mesh point $\in \Omega_2$. Each CE is located immediately below one of these two mesh points and above the other. As an example, let $(j, k, n + 1/2) \in \Omega_1$. Then $(j + 1/3, k + 1/3, n) \in \Omega_2$. According to Fig. 5(a), $CE_1^{(1)}(j, k, n + 1/2)$ is located immediately below the mesh point $(j, k, n + 1/2)$ and above the mesh point $(j + 1/3, k + 1/3, n)$. Note that Eq. (2.60) represents a relation among the marching variables associated with the above two mesh points. A similar interpretation can be given to each of Eqs. (2.61)–(2.65). In Sec. 2, it is shown that Eqs. (2.60)–(2.65) are equivalent to the defining equations of the a scheme, i.e., Eqs. (2.67)–(2.72). In the following, it will be shown that the former also are equivalent to the defining equations of the backward-marching version of the a scheme.

Let $(j, k, n) \in \Omega_2$ and consider Fig. 12(a). Then $(j - 1/3, k - 1/3, n + 1/2) \in \Omega_1$, $(j + 2/3, k - 1/3, n + 1/2) \in \Omega_1$, and $(j - 1/3, k + 2/3, n + 1/2) \in \Omega_1$. By making some substitutions in mesh indices and exchanging expressions on the left and the right sides, Eqs. (2.60)–(2.62) imply that

$$\left[u - (1 + \nu_\zeta)u_\zeta^+ - (1 + \nu_\eta)u_\eta^+ \right]_{j,k}^n = \left[u + (1 + \nu_\zeta)u_\zeta^+ + (1 + \nu_\eta)u_\eta^+ \right]_{j-1/3, k-1/3}^{n+1/2}, \quad (C.5)$$

$$\left[u + (2 - \nu_\zeta)u_\zeta^+ - (1 + \nu_\eta)u_\eta^+ \right]_{j,k}^n = \left[u - (2 - \nu_\zeta)u_\zeta^+ + (1 + \nu_\eta)u_\eta^+ \right]_{j+2/3, k-1/3}^{n+1/2}, \quad (C.6)$$

and

$$\left[u - (1 + \nu_\zeta)u_\zeta^+ + (2 - \nu_\eta)u_\eta^+ \right]_{j,k}^n = \left[u + (1 + \nu_\zeta)u_\zeta^+ - (2 - \nu_\eta)u_\eta^+ \right]_{j-1/3, k+2/3}^{n+1/2}, \quad (C.7)$$

respectively. Let $\hat{s}_1^{(1)}$, $\hat{s}_2^{(1)}$, and $\hat{s}_3^{(1)}$ denote the expressions on the right sides of Eqs. (C.5), (C.6), and (C.7), respectively. Then these equations are equivalent to

$$u_{j,k}^n = \frac{1}{3} \left[(1 - \nu_\zeta - \nu_\eta)\hat{s}_1^{(1)} + (1 + \nu_\zeta)\hat{s}_2^{(1)} + (1 + \nu_\eta)\hat{s}_3^{(1)} \right], \quad (C.8)$$

$$(u_\zeta^+)_{j,k}^n = \frac{1}{3} \left(\hat{s}_2^{(1)} - \hat{s}_1^{(1)} \right), \quad (C.9)$$

and

$$(u_\eta^+)_{j,k}^n = \frac{1}{3} \left(\hat{s}_3^{(1)} - \hat{s}_1^{(1)} \right). \quad (C.10)$$

In other words, the marching variables associated with point G can be expressed in terms of those associated with points B' , D' , and F' .

Let $(j, k, n + 1/2) \in \Omega_1$ and consider Fig. 12(b). Then $(j + 1/3, k + 1/3, n + 1) \in \Omega_2$, $(j - 2/3, k + 1/3, n + 1) \in \Omega_2$, and $(j + 1/3, k - 2/3, n + 1) \in \Omega_2$. By making some

substitutions in mesh indices and exchanging expressions on the left and the right sides, Eqs. (2.63)–(2.65) imply that

$$\left[u + (1 - \nu_\zeta)u_\zeta^+ + (1 - \nu_\eta)u_\eta^+ \right]_{j,k}^{n+1/2} = \left[u - (1 - \nu_\zeta)u_\zeta^+ - (1 - \nu_\eta)u_\eta^+ \right]_{j+1/3, k+1/3}^{n+1}, \quad (C.11)$$

$$\left[u - (2 + \nu_\zeta)u_\zeta^+ + (1 - \nu_\eta)u_\eta^+ \right]_{j,k}^{n+1/2} = \left[u + (2 + \nu_\zeta)u_\zeta^+ - (1 - \nu_\eta)u_\eta^+ \right]_{j-2/3, k+1/3}^{n+1}, \quad (C.12)$$

and

$$\left[u + (1 - \nu_\zeta)u_\zeta^+ - (2 + \nu_\eta)u_\eta^+ \right]_{j,k}^{n+1/2} = \left[u - (1 - \nu_\zeta)u_\zeta^+ + (2 + \nu_\eta)u_\eta^+ \right]_{j+1/3, k-2/3}^{n+1}, \quad (C.13)$$

respectively. Let $\hat{s}_1^{(2)}$, $\hat{s}_2^{(2)}$, and $\hat{s}_3^{(2)}$ denote the expressions on the right sides of Eqs. (C.11), (C.12), and (C.13), respectively. Then these equations are equivalent to

$$u_{j,k}^{n+1/2} = \frac{1}{3} \left[(1 + \nu_\zeta + \nu_\eta)\hat{s}_1^{(2)} + (1 - \nu_\zeta)\hat{s}_2^{(2)} + (1 - \nu_\eta)\hat{s}_3^{(2)} \right], \quad (C.14)$$

$$(u_\zeta^+)_{j,k}^{n+1/2} = \frac{1}{3} \left(\hat{s}_1^{(2)} - \hat{s}_2^{(2)} \right), \quad (C.15)$$

and

$$(u_\eta^+)_{j,k}^{n+1/2} = \frac{1}{3} \left(\hat{s}_1^{(2)} - \hat{s}_3^{(2)} \right). \quad (C.16)$$

In other words, the marching variables associated with point G can be expressed in terms of those associated with points A' , C' , and E' .

The backward marching version of the a scheme consists of two marching steps. The first is formed by Eqs. (C.14)–(C.16); while the second is formed by Eqs. (C.8)–(C.10). To express these steps in the forms of Eqs. (2.82) and (2.83), let the column matrices $\hat{\alpha}_\ell^{(k)}$ and $\hat{\beta}_\ell^{(k)}$, $k = 1, 2$, and $\ell = 1, 2, 3$, be defined by

$$\hat{\alpha}_1^{(1)} \stackrel{\text{def}}{=} \frac{1}{3} \begin{pmatrix} 1 - \nu_\zeta - \nu_\eta \\ -1 \\ -1 \end{pmatrix}, \quad \text{and} \quad \hat{\beta}_1^{(1)} \stackrel{\text{def}}{=} \begin{pmatrix} 1 \\ 1 + \nu_\zeta \\ 1 + \nu_\eta \end{pmatrix}, \quad (C.17)$$

$$\hat{\alpha}_2^{(1)} \stackrel{\text{def}}{=} \frac{1}{3} \begin{pmatrix} 1 + \nu_\zeta \\ 1 \\ 0 \end{pmatrix}, \quad \text{and} \quad \hat{\beta}_2^{(1)} \stackrel{\text{def}}{=} \begin{pmatrix} 1 \\ -(2 - \nu_\zeta) \\ 1 + \nu_\eta \end{pmatrix}, \quad (C.18)$$

$$\hat{\alpha}_3^{(1)} \stackrel{\text{def}}{=} \frac{1}{3} \begin{pmatrix} 1 + \nu_\eta \\ 0 \\ 1 \end{pmatrix}, \quad \text{and} \quad \hat{\beta}_3^{(1)} \stackrel{\text{def}}{=} \begin{pmatrix} 1 \\ 1 + \nu_\zeta \\ -(2 - \nu_\eta) \end{pmatrix}, \quad (\text{C.19})$$

$$\hat{\alpha}_1^{(2)} \stackrel{\text{def}}{=} \frac{1}{3} \begin{pmatrix} 1 + \nu_\zeta + \nu_\eta \\ 1 \\ 1 \end{pmatrix}, \quad \text{and} \quad \hat{\beta}_1^{(2)} \stackrel{\text{def}}{=} \begin{pmatrix} 1 \\ -(1 - \nu_\zeta) \\ -(1 - \nu_\eta) \end{pmatrix}, \quad (\text{C.20})$$

$$\hat{\alpha}_2^{(2)} \stackrel{\text{def}}{=} \frac{1}{3} \begin{pmatrix} 1 - \nu_\zeta \\ -1 \\ 0 \end{pmatrix}, \quad \text{and} \quad \hat{\beta}_2^{(2)} \stackrel{\text{def}}{=} \begin{pmatrix} 1 \\ 2 + \nu_\zeta \\ -(1 - \nu_\eta) \end{pmatrix}, \quad (\text{C.21})$$

and

$$\hat{\alpha}_3^{(2)} \stackrel{\text{def}}{=} \frac{1}{3} \begin{pmatrix} 1 - \nu_\eta \\ 0 \\ -1 \end{pmatrix}, \quad \text{and} \quad \hat{\beta}_3^{(2)} \stackrel{\text{def}}{=} \begin{pmatrix} 1 \\ -(1 - \nu_\zeta) \\ 2 + \nu_\eta \end{pmatrix}. \quad (\text{C.22})$$

Let the 3×3 matrices of rank one $\hat{Q}_\ell^{(k)}$, $k = 1, 2$, and $\ell = 1, 2, 3$, be defined by

$$\hat{Q}_\ell^{(k)} \stackrel{\text{def}}{=} \hat{\alpha}_\ell^{(k)} \left(\hat{\beta}_\ell^{(k)} \right)^t, \quad (\text{C.23})$$

where the row matrix $\left(\hat{\beta}_\ell^{(k)} \right)^t$ is the transpose of the column matrix $\hat{\beta}_\ell^{(k)}$. Then Eqs. (C.8)–(C.10) can be expressed as

$$\begin{aligned} \vec{q}(j, k, n) = & \hat{Q}_1^{(1)} \vec{q}(j - 1/3, k - 1/3, n + 1/2) + \hat{Q}_2^{(1)} \vec{q}(j + 2/3, k - 1/3, n + 1/2) \\ & + \hat{Q}_3^{(1)} \vec{q}(j - 1/3, k + 2/3, n + 1/2), \quad (j, k, n) \in \Omega_2. \end{aligned} \quad (\text{C.24})$$

Similarly, Eqs. (C.14)–(C.16) can be expressed as

$$\begin{aligned} \vec{q}(j, k, n + 1/2) = & \hat{Q}_1^{(2)} \vec{q}(j + 1/3, k + 1/3, n + 1) + \hat{Q}_2^{(2)} \vec{q}(j - 2/3, k + 1/3, n + 1) \\ & + \hat{Q}_3^{(2)} \vec{q}(j + 1/3, k - 2/3, n + 1), \quad (j, k, n + 1/2) \in \Omega_1. \end{aligned} \quad (\text{C.25})$$

Next we shall establish several mathematical relations involving the column matrices $\hat{\alpha}_\ell^{(k)}$, $\hat{\beta}_\ell^{(k)}$, $\hat{\alpha}_\ell^{(k)}$, and $\hat{\beta}_\ell^{(k)}$. To proceed, let

$$M_L^{(1)} \stackrel{\text{def}}{=} \begin{pmatrix} 1 & 1 + \nu_\zeta & 1 + \nu_\eta \\ 1 & -(2 - \nu_\zeta) & 1 + \nu_\eta \\ 1 & 1 + \nu_\zeta & -(2 - \nu_\eta) \end{pmatrix}, \quad (\text{C.26})$$

$$M_R^{(1)} \stackrel{\text{def}}{=} \begin{pmatrix} 1 & -(1 + \nu_\zeta) & -(1 + \nu_\eta) \\ 1 & 2 - \nu_\zeta & -(1 + \nu_\eta) \\ 1 & -(1 + \nu_\zeta) & 2 - \nu_\eta \end{pmatrix}, \quad (\text{C.27})$$

$$M_L^{(2)} \stackrel{\text{def}}{=} \begin{pmatrix} 1 & -(1 - \nu_\zeta) & -(1 - \nu_\eta) \\ 1 & 2 + \nu_\zeta & -(1 - \nu_\eta) \\ 1 & -(1 - \nu_\zeta) & 2 + \nu_\eta \end{pmatrix}, \quad (\text{C.28})$$

and

$$M_R^{(2)} \stackrel{\text{def}}{=} \begin{pmatrix} 1 & 1 - \nu_\zeta & 1 - \nu_\eta \\ 1 & -(2 + \nu_\zeta) & 1 - \nu_\eta \\ 1 & 1 - \nu_\zeta & -(2 + \nu_\eta) \end{pmatrix}. \quad (\text{C.29})$$

Note that: (i) $M_L^{(1)}$ is the coefficient matrix of the expressions on the left sides of Eqs. (2.60)–(2.62). It is also that of the expressions on the right side of Eqs. (C.5)–(C.7); (ii) $M_R^{(1)}$ is the coefficient matrix of the expressions on the right sides of Eqs. (2.60)–(2.62). It is also that of the expressions on the left side of Eqs. (C.5)–(C.7); (iii) $M_L^{(2)}$ is the coefficient matrix of the expressions on the left sides of Eqs. (2.63)–(2.65). It is also that of the expressions on the right side of Eqs. (C.11)–(C.13); and (iv) $M_R^{(2)}$ is the coefficient matrix of the expressions on the right sides of Eqs. (2.63)–(2.65). It is also that of the expressions on the left side of Eqs. (C.11)–(C.13).

Moreover, for each $k = 1, 2$, let (i) $A^{(k)}$ be the 3×3 matrix formed by the column matrices $\vec{\alpha}_\ell^{(k)}$, $\ell = 1, 2, 3$; (ii) $B^{(k)}$ be the 3×3 matrix formed by the column matrices $\vec{\beta}_\ell^{(k)}$, $\ell = 1, 2, 3$; (iii) $\hat{A}^{(k)}$ be the 3×3 matrix formed by the column matrices $\vec{\alpha}_\ell^{(k)}$, $\ell = 1, 2, 3$; and (iv) $\hat{B}^{(k)}$ be the 3×3 matrix formed by the column matrices $\vec{\beta}_\ell^{(k)}$, $\ell = 1, 2, 3$.

With the above preliminaries, it is easy to shown that

$$M_L^{(k)} = [A^{(k)}]^{-1} = [\hat{B}^{(k)}]^t, \quad k = 1, 2, \quad (\text{C.30})$$

and

$$M_R^{(k)} = [\hat{A}^{(k)}]^{-1} = [B^{(k)}]^t, \quad k = 1, 2. \quad (\text{C.31})$$

Here $[A]^{-1}$ and $[A]^t$ denote the inverse and the transpose of any matrix A . It follows from Eqs. (C.30) and (C.31) that

$$[\hat{B}^{(k)}]^t A^{(k)} = I, \quad \text{and} \quad A^{(k)} [\hat{B}^{(k)}]^t = I, \quad k = 1, 2, \quad (\text{C.32})$$

and

$$\left[B^{(k)} \right]^t \hat{A}^{(k)} = I, \quad \text{and} \quad \hat{A}^{(k)} \left[B^{(k)} \right]^t = I, \quad k = 1, 2, \quad (C.33)$$

where I is the 3×3 identity matrix.

Recall the definitions of the matrices $A^{(k)}$, $B^{(k)}$, $\hat{A}^{(k)}$, and $\hat{B}^{(k)}$, $k = 1, 2$. Then the first parts of Eqs. (C.32) and (C.33) can be expressed as

$$\left(\hat{\beta}_\ell^{(k)} \right)^t \hat{\alpha}_{\ell'}^{(k)} = \delta_{\ell\ell'}, \quad k = 1, 2, \quad \text{and} \quad \ell, \ell' = 1, 2, 3, \quad (C.34)$$

and

$$\left(\tilde{\beta}_\ell^{(k)} \right)^t \tilde{\alpha}_{\ell'}^{(k)} = \delta_{\ell\ell'}, \quad k = 1, 2, \quad \text{and} \quad \ell, \ell' = 1, 2, 3, \quad (C.35)$$

respectively. Here $\delta_{\ell\ell'}$ is the Kronecker delta symbol. Also, the second parts of Eqs. (C.32) and (C.33) can be expressed as

$$\sum_\ell^3 \tilde{\alpha}_\ell^{(k)} \left(\hat{\beta}_\ell^{(k)} \right)^t = I, \quad k = 1, 2, \quad (C.36)$$

and

$$\sum_\ell^3 \hat{\alpha}_\ell^{(k)} \left(\tilde{\beta}_\ell^{(k)} \right)^t = I, \quad k = 1, 2, \quad (C.37)$$

respectively.

To proceed further, let

$$P \stackrel{\text{def}}{=} \begin{pmatrix} 1 & 0 & 0 \\ 0 & -1 & 0 \\ 0 & 0 & -1 \end{pmatrix}. \quad (C.38)$$

We have

$$P^{-1} = P, \quad \text{and} \quad P^t = P, \quad (C.39)$$

and

$$M_L^{(k)} = M_R^{(k)} P, \quad k = 1, 2. \quad (C.40)$$

By taking the transpose of the expression on each side of Eq. (C.40), and using Eqs. (C.30), (C.31), and (C.39), one concludes that

$$\hat{\beta}_\ell^{(k)} = P \tilde{\beta}_\ell^{(k)}, \quad k = 1, 2, \quad \text{and} \quad \ell = 1, 2, 3. \quad (C.41)$$

By taking the inverse of the expression on each side of Eq. (C.40), and using Eqs. (C.30), (C.31), and (C.39), one concludes that

$$\hat{\tilde{\alpha}}_\ell^{(k)} = P \tilde{\alpha}_\ell^{(k)}, \quad k = 1, 2, \quad \text{and} \quad \ell = 1, 2, 3. \quad (\text{C.42})$$

Equations (C.34)–(C.37), (C.41), and (C.42) will be used in the following development.

By using Eqs. (2.80), (C.23), (C.34), and (C.35), one has

$$Q_\ell^{(k)} \hat{Q}_{\ell'}^{(k)} = \delta_{\ell\ell'} \tilde{\alpha}_\ell^{(k)} \left(\tilde{\beta}_{\ell'}^{(k)} \right)^t, \quad k = 1, 2, \quad \text{and} \quad \ell, \ell' = 1, 2, 3, \quad (\text{C.43})$$

and

$$\hat{Q}_\ell^{(k)} Q_{\ell'}^{(k)} = \delta_{\ell\ell'} \hat{\tilde{\alpha}}_\ell^{(k)} \left(\tilde{\beta}_{\ell'}^{(k)} \right)^t, \quad k = 1, 2, \quad \text{and} \quad \ell, \ell' = 1, 2, 3. \quad (\text{C.44})$$

It follows from Eqs. (C.43) and (C.44) that,

$$Q_\ell^{(k)} \hat{Q}_{\ell'}^{(k)} = \hat{Q}_\ell^{(k)} Q_{\ell'}^{(k)} = 0, \quad \text{if} \quad \ell \neq \ell'. \quad (k = 1, 2, \text{ and } \ell, \ell' = 1, 2, 3.) \quad (\text{C.45})$$

With the aid of Eqs. (C.36), and (C.37), Eqs. (C.43) and (C.44) also imply that

$$\sum_{\ell=1}^3 Q_\ell^{(k)} \hat{Q}_\ell^{(k)} = \sum_{\ell=1}^3 \hat{Q}_\ell^{(k)} Q_\ell^{(k)} = I, \quad k = 1, 2. \quad (\text{C.46})$$

Furthermore, by using Eqs. (2.80), (C.23), (C.41), and (C.42), one has

$$Q_\ell^{(k)} = P \hat{Q}_\ell^{(k)} P, \quad \text{and} \quad \hat{Q}_\ell^{(k)} = P Q_\ell^{(k)} P. \quad (k = 1, 2, \text{ and } \ell, \ell' = 1, 2, 3.) \quad (\text{C.47})$$

Equations (C.45) and (C.46) can be obtained from a more direct but less revealing approach. To proceed, we substitute Eq. (C.24) into the expression on the right side of (2.82). The result is

$$\begin{aligned} \vec{q}(j, k, n + 1/2) = & Q_1^{(1)} \hat{Q}_2^{(1)} \vec{q}(j + 1, k, n + 1/2) + Q_1^{(1)} \hat{Q}_3^{(1)} \vec{q}(j, k + 1, n + 1/2) \\ & + Q_2^{(1)} \hat{Q}_1^{(1)} \vec{q}(j - 1, k, n + 1/2) + Q_2^{(1)} \hat{Q}_3^{(1)} \vec{q}(j - 1, k + 1, n + 1/2) \\ & + Q_3^{(1)} \hat{Q}_1^{(1)} \vec{q}(j, k - 1, n + 1/2) + Q_3^{(1)} \hat{Q}_2^{(1)} \vec{q}(j + 1, k - 1, n + 1/2) \\ & + (Q_1^{(1)} \hat{Q}_1^{(1)} + Q_2^{(1)} \hat{Q}_2^{(1)} + Q_3^{(1)} \hat{Q}_3^{(1)}) \vec{q}(j, k, n + 1/2), \end{aligned} \quad (\text{C.48})$$

where $(j, k, n + 1/2) \in \Omega_1$. By substituting Eq. (2.82) into the expression on the right side of Eq. (C.24), one has

$$\begin{aligned} \vec{q}(j, k, n) = & \hat{Q}_1^{(1)} Q_2^{(1)} \vec{q}(j - 1, k, n) + \hat{Q}_1^{(1)} Q_3^{(1)} \vec{q}(j, k - 1, n) \\ & + \hat{Q}_2^{(1)} Q_1^{(1)} \vec{q}(j + 1, k, n) + \hat{Q}_2^{(1)} Q_3^{(1)} \vec{q}(j + 1, k - 1, n) \\ & + \hat{Q}_3^{(1)} Q_1^{(1)} \vec{q}(j, k + 1, n) + \hat{Q}_3^{(1)} Q_2^{(1)} \vec{q}(j - 1, k + 1, n) \\ & + (\hat{Q}_1^{(1)} Q_1^{(1)} + \hat{Q}_2^{(1)} Q_2^{(1)} + \hat{Q}_3^{(1)} Q_3^{(1)}) \vec{q}(j, k, n), \end{aligned} \quad (C.49)$$

where $(j, k, n) \in \Omega_2$. Similarly, Eqs. (C.25) and (2.83) imply that

$$\begin{aligned} \vec{q}(j, k, n + 1) = & Q_1^{(2)} \hat{Q}_2^{(2)} \vec{q}(j - 1, k, n + 1) + Q_1^{(2)} \hat{Q}_3^{(2)} \vec{q}(j, k - 1, n + 1) \\ & + Q_2^{(2)} \hat{Q}_1^{(2)} \vec{q}(j + 1, k, n + 1) + Q_2^{(2)} \hat{Q}_3^{(2)} \vec{q}(j + 1, k - 1, n + 1) \\ & + Q_3^{(2)} \hat{Q}_1^{(2)} \vec{q}(j, k + 1, n + 1) + Q_3^{(2)} \hat{Q}_2^{(2)} \vec{q}(j - 1, k + 1, n + 1) \\ & + (Q_1^{(2)} \hat{Q}_1^{(2)} + Q_2^{(2)} \hat{Q}_2^{(2)} + Q_3^{(2)} \hat{Q}_3^{(2)}) \vec{q}(j, k, n + 1), \end{aligned} \quad (C.50)$$

where $(j, k, n + 1) \in \Omega_2$; and

$$\begin{aligned} \vec{q}(j, k, n + 1/2) = & \hat{Q}_1^{(2)} Q_2^{(2)} \vec{q}(j + 1, k, n + 1/2) + \hat{Q}_1^{(2)} Q_3^{(2)} \vec{q}(j, k + 1, n + 1/2) \\ & + \hat{Q}_2^{(2)} Q_1^{(2)} \vec{q}(j - 1, k, n + 1/2) + \hat{Q}_2^{(2)} Q_3^{(2)} \vec{q}(j - 1, k + 1, n + 1/2) \\ & + \hat{Q}_3^{(2)} Q_1^{(2)} \vec{q}(j, k - 1, n + 1/2) + \hat{Q}_3^{(2)} Q_2^{(2)} \vec{q}(j + 1, k - 1, n + 1/2) \\ & + (\hat{Q}_1^{(2)} Q_1^{(2)} + \hat{Q}_2^{(2)} Q_2^{(2)} + \hat{Q}_3^{(2)} Q_3^{(2)}) \vec{q}(j, k, n + 1/2), \end{aligned} \quad (C.51)$$

where $(j, k, n + 1/2) \in \Omega_1$. Because (i) and time level n_0 can be considered as the initial time level, i.e., one can assign arbitrary values to the members of the set $\{\vec{q}(j, k, n_0) \mid (j, k, n_0) \in \Omega\}$; (ii) the column matrices in each of Eqs. (C.48)–(C.51) are associated with the same time level; and (iii) Eqs. (C.48)–(C.51) are valid no matter what values are assigned to the elements of the column matrices in these equations, a comparison of the expressions on the left and the right sides of each of these equations reveals that, in each of Eqs. (C.48)–(C.51), the first six coefficient matrices on the right side (each of them is the product of two matrices) must vanish; while the last coefficient matrix (the sum of three matrix products) must be equal to the identity matrix. As a result, Eqs. (C.45) and (C.46) follow from Eqs. (C.48)–(C.51). QED.

Next Eqs. (C.45)–(C.47) will be used in a study of the amplification matrices of the a scheme. To proceed, let

$$\hat{M}^{(1)}(\theta_\zeta, \theta_\eta) \stackrel{\text{def}}{=} \hat{Q}_1^{(1)} e^{-(i/3)(\theta_\zeta + \theta_\eta)} + \hat{Q}_2^{(1)} e^{-(i/3)(-2\theta_\zeta + \theta_\eta)} + \hat{Q}_3^{(1)} e^{-(i/3)(\theta_\zeta - 2\theta_\eta)}, \quad (C.52)$$

and

$$\hat{M}^{(2)}(\theta_\zeta, \theta_\eta) \stackrel{\text{def}}{=} \hat{Q}_1^{(2)} e^{(i/3)(\theta_\zeta + \theta_\eta)} + \hat{Q}_2^{(2)} e^{(i/3)(-2\theta_\zeta + \theta_\eta)} + \hat{Q}_3^{(2)} e^{(i/3)(\theta_\zeta - 2\theta_\eta)}, \quad (C.53)$$

where $i \equiv \sqrt{-1}$, and $-\pi < \theta_\zeta, \theta_\eta \leq \pi$. Equations (5.4), (5.5), (C.52), and (C.53) coupled with Eqs. (C.45) and (C.46) imply that

$$M^{(k)}(\theta_\zeta, \theta_\eta) \hat{M}^{(k)}(\theta_\zeta, \theta_\eta) = \hat{M}^{(k)}(\theta_\zeta, \theta_\eta) M^{(k)}(\theta_\zeta, \theta_\eta) = I, \quad k = 1, 2. \quad (C.54)$$

In other words, $\hat{M}^{(k)}(\theta_\zeta, \theta_\eta)$ is the inverse of $M^{(k)}(\theta_\zeta, \theta_\eta)$ and vice versa. As a result, both are nonsingular. Equation (C.54) can be used to show that

$$\begin{aligned} & \left[M^{(2)}(\theta_\zeta, \theta_\eta) M^{(1)}(\theta_\zeta, \theta_\eta) \right] \left[\hat{M}^{(1)}(\theta_\zeta, \theta_\eta) \hat{M}^{(2)}(\theta_\zeta, \theta_\eta) \right] \\ &= \left[\hat{M}^{(1)}(\theta_\zeta, \theta_\eta) \hat{M}^{(2)}(\theta_\zeta, \theta_\eta) \right] \left[M^{(2)}(\theta_\zeta, \theta_\eta) M^{(1)}(\theta_\zeta, \theta_\eta) \right] = I. \end{aligned} \quad (C.55)$$

Let $[M^{(k)}(\theta_\zeta, \theta_\eta)]^*$ and $[\hat{M}^{(k)}(\theta_\zeta, \theta_\eta)]^*$, denote the component-wise complex conjugates of $M^{(k)}(\theta_\zeta, \theta_\eta)$ and $\hat{M}^{(k)}(\theta_\zeta, \theta_\eta)$, respectively. Then Eqs. (5.4), (5.5), (C.52), (C.53) coupled with Eq. (C.47) imply that

$$\left[M^{(k)}(\theta_\zeta, \theta_\eta) \right] = P \left[\hat{M}^{(k)}(\theta_\zeta, \theta_\eta) \right]^* P, \quad k = 1, 2. \quad (C.56)$$

Combining Eqs. (C.39), (C.54), and (C.56), one arrives at

$$\begin{aligned} & M^{(2)}(\theta_\zeta, \theta_\eta) M^{(1)}(\theta_\zeta, \theta_\eta) \\ &= \left\{ P \left[\hat{M}^{(2)}(\theta_\zeta, \theta_\eta) \right]^* \right\} \left[\hat{M}^{(1)}(\theta_\zeta, \theta_\eta) \hat{M}^{(2)}(\theta_\zeta, \theta_\eta) \right]^* \left\{ P \left[\hat{M}^{(2)}(\theta_\zeta, \theta_\eta) \right]^* \right\}^{-1}. \end{aligned} \quad (C.57)$$

Thus

$$M^{(2)}(\theta_\zeta, \theta_\eta) M^{(1)}(\theta_\zeta, \theta_\eta) \sim \left[\hat{M}^{(1)}(\theta_\zeta, \theta_\eta) \hat{M}^{(2)}(\theta_\zeta, \theta_\eta) \right]^*. \quad (C.58)$$

Let λ_1, λ_2 , and λ_3 be the eigenvalues of the matrix on the left side of Eq. (C.58). According to Eq. (5.3), the last matrix is the amplification matrix for any two consecutive whole-integer time levels. Equation (C.58) implies that λ_1, λ_2 , and λ_3 are also the eigenvalues of the matrix on the right side of this equation [25, p.45]. Because the eigenvalues of the matrix A^* , the component-wise complex conjugate of a matrix A , are the complex conjugates of the eigenvalues of the matrix A , λ_1^*, λ_2^* , and λ_3^* , the complex conjugates of λ_1, λ_2 , and λ_3 , are the eigenvalues of the matrix enclosed within the brackets on the right side of Eq. (C.58). According to Eq. (C.55), the last matrix is the inverse of the matrix on the left side of Eq. (C.58). Because the eigenvalues of the matrix A^{-1} , the inverse of a matrix A , are the reciprocals of the eigenvalues of A , one concludes that the set of λ_ℓ^* , $\ell = 1, 2, 3$, is identical to the set of $1/\lambda_\ell$, $\ell = 1, 2, 3$. It does not implies that $\lambda_\ell^* = 1/\lambda_\ell$, $\ell = 1, 2, 3$. However, it does implies that the product of λ_ℓ^* , $\ell = 1, 2, 3$, is equal to the product of $1/\lambda_\ell$, $\ell = 1, 2, 3$. As a result, we arrive at Eq. (5.7).

Next we shall prove that the backward characteristic projection of the mesh point $(j, k, n + 1/2) \in \Omega_1$ at the $(n - 1/2)$ th time level is in the interior of the numerical domain of dependence of $(j, k, n + 1/2)$ at the same time level if and only if Eq. (2.110) is satisfied. In Fig. 13(c), the mesh point $(j, k, n + 1/2)$ is represented by point O ; while its backward characteristic projection at the $(n - 1/2)$ th time level is represented by point P . Without any loss of generality, we will assume that $j = k = 0$. Thus

$$\zeta = \eta = 0, \quad \text{and} \quad t = (n + 1/2)\Delta t, \quad (\text{C.59})$$

for point O . Note that only the coordinates (ζ, η) are given in Fig. 13(a).

To simplify the discussion, Eq. (3.1) is converted to an equivalent form in which ζ , η , and t are the independent variables, i.e.,

$$\frac{\partial u}{\partial t} + a_\zeta \frac{\partial u}{\partial \zeta} + a_\eta \frac{\partial u}{\partial \eta} = 0. \quad (\text{C.60})$$

The characteristics of Eq. (C.60) is the family of straight lines defined by

$$\zeta = a_\zeta t + c_1, \quad \text{and} \quad \eta = a_\eta t + c_2, \quad (\text{C.61})$$

where c_1 and c_2 are constant along a characteristic, and vary from one characteristic to another. Because points O and P share the same characteristic line, Eqs. (C.59) and (C.61) imply that

$$\zeta = -a_\zeta \Delta t, \quad \eta = -a_\eta \Delta t, \quad \text{and} \quad t = (n - 1/2)\Delta t, \quad (\text{C.62})$$

for point P .

The numerical domain of dependence of point O referred to in Sec. 5, a hexagon lying on the plane $t = (n - 1/2)\Delta t$, is depicted in Fig. 13(c). The coordinates (ζ, η) of the vertices A, B, C, D, E , and F are also given in the same figure. The six edges of the hexagon and their equations on the ζ - η plane are

$$\begin{aligned} \overline{AB} : & \quad \Delta\eta \cdot \zeta + \Delta\zeta \cdot \eta = \Delta\zeta\Delta\eta, \\ \overline{DE} : & \quad \Delta\eta \cdot \zeta + \Delta\zeta \cdot \eta = -\Delta\zeta\Delta\eta, \\ \overline{BC} : & \quad \eta = \Delta\eta, \\ \overline{EF} : & \quad \eta = -\Delta\eta, \\ \overline{CD} : & \quad \zeta = -\Delta\zeta, \\ \overline{FA} : & \quad \zeta = \Delta\zeta. \end{aligned} \quad (\text{C.63})$$

As a result, a point (ζ, η) is in the interior of the hexagon $ABCDEF$ if and only if

$$|\Delta\eta \cdot \zeta + \Delta\zeta \cdot \eta| < \Delta\zeta\Delta\eta, \quad |\eta| < \Delta\eta, \quad \text{and} \quad |\zeta| < \Delta\zeta. \quad (\text{C.64})$$

Equations (C.62) and (C.64) coupled with Eqs. (2.29) and (2.31) imply that point P is in the interior of the hexagon $ABCDEF$ if and only if Eq. (2.110) is satisfied. QED.

Next we turn to the a - μ scheme. Recall that the equations used to construct the backward marching version of the a scheme, i.e., Eqs. (C.5)–(C.7) and (C.11)–(C.13), are obtained from Eqs. (2.60)–(2.65) by making substitutions in mesh indices and exchanging expressions on the left and the right sides. In a similar manner, the backward marching version of the a - μ scheme can be constructed using Eqs. (2.53)–(2.58) as the starting point. Let $\hat{\Delta}^{(1)}$ and $\hat{\Delta}^{(2)}$ be the determinants of the matrices formed by $\sigma_{k\ell}^{(1)-}$ and $\sigma_{k\ell}^{(2)-}$, $k, \ell = 1, 2, 3$, respectively. Without going into the details, it can be shown that (i)

$$\hat{\Delta}^{(1)} = 3 \left[3(1 + \nu_\zeta)(1 + \nu_\eta)(1 - \nu_\zeta - \nu_\eta) - 2(1 + \nu_\zeta)(1 - \nu_\zeta - \nu_\eta)\xi_\zeta \right. \\ \left. - 2(1 + \nu_\eta)(1 - \nu_\zeta - \nu_\eta)\xi_\eta - 2(1 + \nu_\zeta)(1 + \nu_\eta)\xi_\tau + \left(\frac{9\mu\Delta t}{2wh} \right)^2 \right], \quad (C.65)$$

and

$$\hat{\Delta}^{(2)} = 3 \left[3(1 - \nu_\zeta)(1 - \nu_\eta)(1 + \nu_\zeta + \nu_\eta) - 2(1 - \nu_\zeta)(1 + \nu_\zeta + \nu_\eta)\xi_\zeta \right. \\ \left. - 2(1 - \nu_\eta)(1 + \nu_\zeta + \nu_\eta)\xi_\eta - 2(1 - \nu_\zeta)(1 - \nu_\eta)\xi_\tau + \left(\frac{9\mu\Delta t}{2wh} \right)^2 \right]; \quad (C.66)$$

and (ii) the backward marching version of the a - μ scheme exists if

$$\hat{\Delta}^{(1)} \neq 0, \quad \text{and} \quad \hat{\Delta}^{(2)} \neq 0. \quad (C.67)$$

Recall that the forward marching version exists if

$$\Delta^{(1)} \neq 0, \quad \text{and} \quad \Delta^{(2)} \neq 0. \quad (C.68)$$

We assume Eqs. (C.67) and (C.68). Then the matrices $\hat{Q}_t^{(k)}$, $k = 1, 2$, and $\ell = 1, 2, 3$, can be constructed such that the backward marching version of the a - μ scheme can also be represented by Eqs. (C.24) and (C.25). By using an earlier argument involving Eqs. (C.48)–(C.51), Eqs. (C.45) and (C.46) can also be established. Equations (C.54) and (C.55) follows immediately. However, it should be noted that Eq. (C.47) is *not* applicable for the a - μ scheme except for the case $\mu = 0$. Thus Eq. (5.7) generally is not valid for the a - μ scheme.

Appendix D

The definition of the local CFL number ν_e used in Sec. 6 is given here.

In Fig. 21, point P_0 is a mesh point $(j, k, n) \in \Omega$. Without any loss of generality, we assume that it is also the origin of the x - y plane. As explained in Sec. 5 and Appendix C (see Figs. 13(a)–(c)), the numerical domain of dependence of P_0 on the plane with $t = (n-1)\Delta t$ (i.e., the $(n-1)$ th time level) is the hexagon $ABCDEF$ depicted in Fig. 21. Because $b = 0$, the coordinates (x, y) of the vertices $A, B, C, D, E,$ and F are those given in Fig. 21.

The intersection of (i) the Mach cone [26, p.425] with point P_0 being its vertex, and (ii) the plane with $t = (n-1)\Delta t$, is the circle depicted in Fig. 21. Here a circle, as in the case of the hexagon mentioned above, implies its boundary and interior. For the Euler equations Eq. (4.10), and in the limit of $\Delta t \rightarrow 0$, this circle is the domain of dependence of point P_0 on the plane with $t = (n-1)\Delta t$. Let $u, v,$ and $c,$ be the x -velocity, the y -velocity, and the sonic speed at the point P_0 , respectively. Then (i) $c\Delta t$ is the radius of the circle, and (ii) $x = -u\Delta t$ and $y = -v\Delta t$ are the coordinates of the center of the circle (point P_1). The number ν_e will be defined such that $\nu_e < 1$ if and only if the domain of dependence of the Euler equations (i.e., the circle) is within the interior of the numerical domain of dependence (i.e., the hexagon $ABCDEF$).

In Fig. 21, we assume that $u \leq 0$ and $v \leq 0$. Thus $x \geq 0$ and $y \geq 0$ for point P_1 . Also we have

$$\theta \stackrel{\text{def}}{=} \arcsin \left(w / \sqrt{h^2 + w^2} \right), \quad (0 < \theta < \pi/2) \quad (D.1)$$

and

$$\theta' \stackrel{\text{def}}{=} \begin{cases} \arctan |v/u|, & \text{if } u \neq 0; \\ \pi/2, & \text{if } u = 0 \text{ and } v \neq 0; \\ 0, & \text{if } u = v = 0. \end{cases} \quad (D.2)$$

Here we assume that $0 \leq \arctan |v/u| < \pi/2$. Moreover, the lengths of the line segments $\overline{P_0P_2}, \overline{P_0P_3}, \overline{P_0P_4},$ and $\overline{P_0P_5}$ are

$$|\overline{P_0P_2}| = (c + |u|)\Delta t, \quad (D.3)$$

$$|\overline{P_0P_3}| = w, \quad (D.4)$$

$$|\overline{P_0P_4}| = \left(c + \sqrt{u^2 + v^2} \cos(\theta - \theta') \right) \Delta t, \quad (D.5)$$

and

$$|\overline{P_0P_5}| = 2h \sin \theta, \quad (D.6)$$

respectively. As a result of Eqs. (D.3)–(D.6), we have

$$\nu_e' \stackrel{\text{def}}{=} \frac{|\overline{P_0P_2}|}{|\overline{P_0P_3}|} = \frac{(c + |u|)\Delta t}{w}, \quad (D.7)$$

and

$$\nu_e'' \stackrel{\text{def}}{=} \frac{|P_0 P_4|}{|P_0 P_5|} = \frac{[c + \sqrt{u^2 + v^2} \cos(\theta - \theta')] \Delta t}{2h \sin \theta}. \quad (D.8)$$

By their definitions, (i) $\nu_e' < 1$ if and only if the entire circle is within the domain to the left of the straight line \overrightarrow{AB} ; and (ii) $\nu_e'' < 1$ if and only if the entire circle is within the domain below the straight line \overrightarrow{BC} . Because $x \geq 0$ and $y \geq 0$ for point P_0 , the center of the circle, one concludes that the entire circle is within the interior of the hexagon $ABCDEF$ if and only if $\nu_e < 1$ where

$$\nu_e \stackrel{\text{def}}{=} \max\{\nu_e', \nu_e''\}. \quad (D.9)$$

By using an argument similar to that presented above, it can be shown that, regardless of the signs of u and v , the entire circle is within the interior of the hexagon $ABCDEF$ if and only if $\nu_e < 1$ where ν_e is defined using Eqs. (D.1)–(D.9).

References

- [1] Chang, S.C. and To, W.M., "A New Numerical Framework for Solving Conservation Laws—The Method of Space-Time Conservation Element and Solution Element," NASA TM 104495, August, 1991.
- [2] Chang, S.C., "On An Origin of Numerical Diffusion: Violation of Invariance under Space-Time Inversion," *Proceedings of 23rd Conference on Modeling and Simulation*, April 30–May 1, 1992, Pittsburgh, PA, USA, William G. Vogt and Marlin H. Mickle eds., Part 5, pp. 2727-2738. Also published as NASA TM 105776.
- [3] Chang, S.C. and To, W.M., "A Brief Description of a New Numerical Framework for Solving Conservation Laws—The Method of Space-Time Conservation Element and Solution Element," *Proceedings of the Thirteenth International Conference on Numerical Methods in Fluid Dynamics*, Rome, Italy, 1992, M. Napolitano and F. Sabetta, eds., Lecture Notes in Physics 414, Springer-Verlag, pp. 396-400. Also published as NASA TM 105757.
- [4] Scott, J.R. and Chang, S.C., "A New Flux Conserving Newton's Method Scheme for the Two-Dimensional, Steady Navier-Stokes Equations," NASA TM 106160, June, 1993.
- [5] Chang, S.C., "New Developments in the Method of Space-Time Conservation Element and Solution Element—Applications to the Euler and Navier-Stokes Equations," NASA TM 106226, August, 1993.
- [6] Chang, S.C., "The Method of Space-Time Conservation Element and Solution Element —A New Approach for Solving the Navier-Stokes and Euler Equations," submitted for publication in *J. Comput. Phys.*.
- [7] Wang, X.Y., Chow, C.Y. and Chang, S.C., "Application of the Space-Time Conservation Element and Solution Element Method to Shock-Tube problem." To be published as a NASA Technical Memorandum.
- [8] Wang, X.Y., Chow, C.Y. and Chang, S.C., "Application of the Space-Time Conservation Element and Solution Element Method to Two-Dimensional Advection-Diffusion Problems," in preparation.
- [9] Anderson, D.A., Tannehill, J.C. and Pletcher, R.H., *Computational Fluid Mechanics and Heat Transfer* (Hemisphere, 1984).
- [10] Baker, A.J., *Finite Element Computational Fluid Mechanics* (Hemisphere, 1983).
- [11] Canuto, C., Hussaini, M.Y., Quarteroni, A. and Zang, T.A., *Spectral Methods in Fluid Dynamics* (Springer-Verlag New York Inc., 1988).
- [12] Vinokur, M., "An Analysis of Finite-Difference and Finite-Volume Formulation of Conservation Laws," *J. Comput. Phys.*, 81, 1989, pp. 1-52.
- [13] LeVeque, R.J., *Numerical Methods for Conservation Laws* (Birkhäuser Verlag, 1990).
- [14] Roe, P.L., "Approximate Riemann Solvers, Parameter Vectors and Difference Schemes," *J. Comput. Phys.*, 43, 1981, pp. 357-372.

- [15] van Leer, B., "Flux Vector Splitting for the Euler Equations," *Lecture Notes in Physics* 170, 1982, pp. 501-512.
- [16] Osher, S. and Chakravarthy, S., "Upwind Schemes and Boundary Conditions with Applications to Euler Equations in General Coordinates," *J. Comput. Phys.*, 50, 1983, pp. 447-481.
- [17] van Leer, B., "Toward the Ultimate Conservative Difference Scheme. IV. A New Approach to Numerical Convection," *J. Comput. Phys.*, 23, 1977, pp. 276-299.
- [18] Smith, M.J. and Stoker, R.W., "Extension of CFD Techniques to Computational Aeroacoustics (CAA): Comparative Evaluation," AIAA Paper 93-0150, Reno, Nevada, January 1993.
- [19] Roe, P.L., "A Survey of Upwind Differencing Techniques," *Proceedings of the Eleventh International Conference on Numerical Methods in Fluid Dynamics*, 1988, *Lecture Notes in Physics* 323, Springer-Verlage, 1989, pp. 69-78.
- [20] Warming, R.F., Beam, R.M. and Hyett B.J., "Diagonalization and Simultaneous Symmetrization of the Gas-Dynamics Matrices," *Math. of Comput.*, 29, 1975, pp. 1037-1045.
- [21] Rusanov, V.V., "The Characteristics of General Equations of Gas Dynamics," *Zhurnal vychislitel'noi matematiki matematicheskoi fiziki*, 3, 1963, pp. 508-527.
- [22] Leonard, B.P., "Universal Limiter for Transient Interpolation Modeling of the Advective Transport Equations: The ULTIMATE Conservative Difference Scheme," NASA TM 100916, September, 1988.
- [23] Courant, R. and Hilbert, D., *Methods of Mathematical Physics*, Vol. II (Interscience, 1962).
- [24] Yee, H.C., Warming, R.F. and Harten, A., "Implicit Total Variation Diminishing (TVD) Schemes for Steady-State Calculations," AIAA paper 83-1902.
- [25] Horn, R.A. and Johnson, C.R., *Matrix Analysis*, (Cambridge University Press, 1985).
- [26] Zucrow, M.J. and Hoffman, J.D., *Gas Dynamics*, Vol. II (John Wiley and Sons, 1977).

Table 1.—Definitions of test problems numbers 1 to 6 and the corresponding values of T , v_{ems} , v_{em} , and n_c

	ϵ	α	R	S	Δt	n_t	T	v_{ems}	v_{em}	n_c
1	0.5	2	20	60	0.01	600	6	0.585	0.6204	152.32
2	.5	2	20	60	.015	400	6	.8775	.9305	101.55
3	.5	2	40	120	.0075	800	6	.8775	.9302	203.09
4	.2	2	20	60	.01	600	6	.585	.6303	152.32
5	.8	2	20	60	.01	600	6	.585	.6212	152.32
6	.5	1	20	60	.01	600	6	.585	.6206	152.32

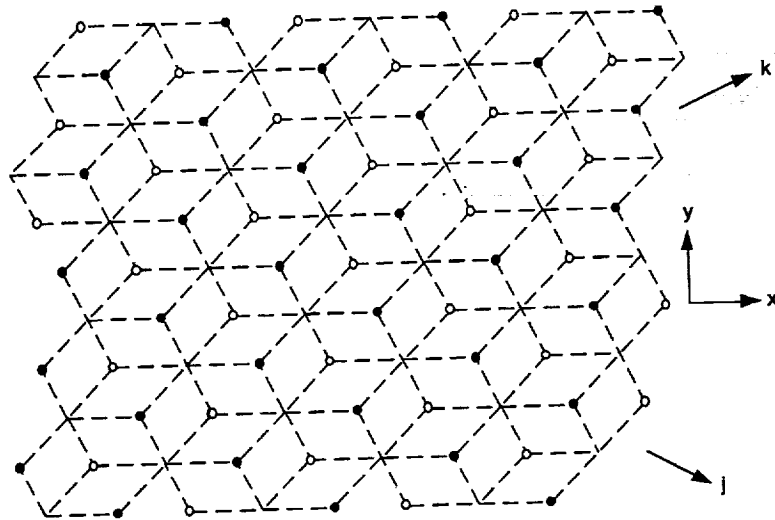


Figure 1.—The relative spatial positions of the mesh points $\in \Omega_1$ and the mesh points $\in \Omega_2$ (dash lines are spatial boundaries of the conservation elements depicted in figs 5(a) and 5(b)).

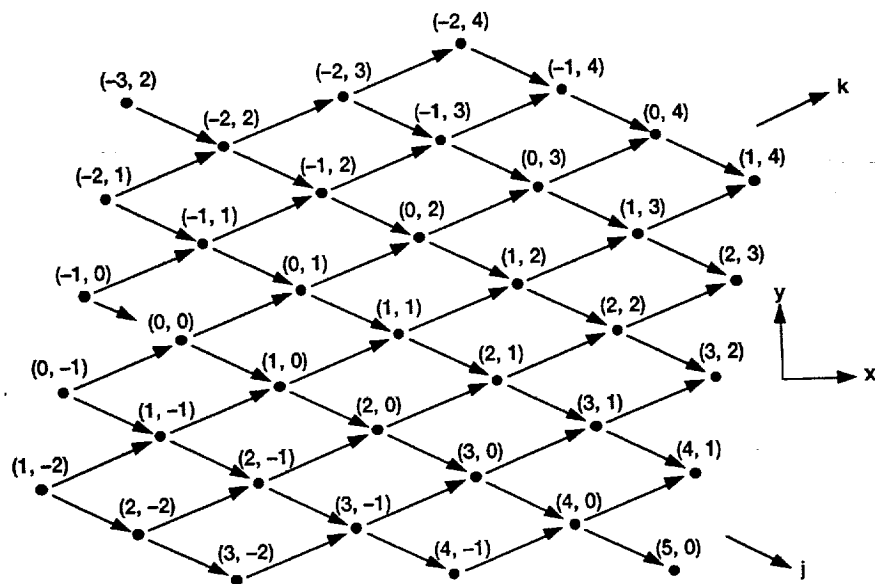


Figure 2.—The spatial mesh indices (j, k) of the mesh points $\in \Omega_1$ ($n = \pm 1/2, \pm 3/2, \pm 5/2, \dots$).

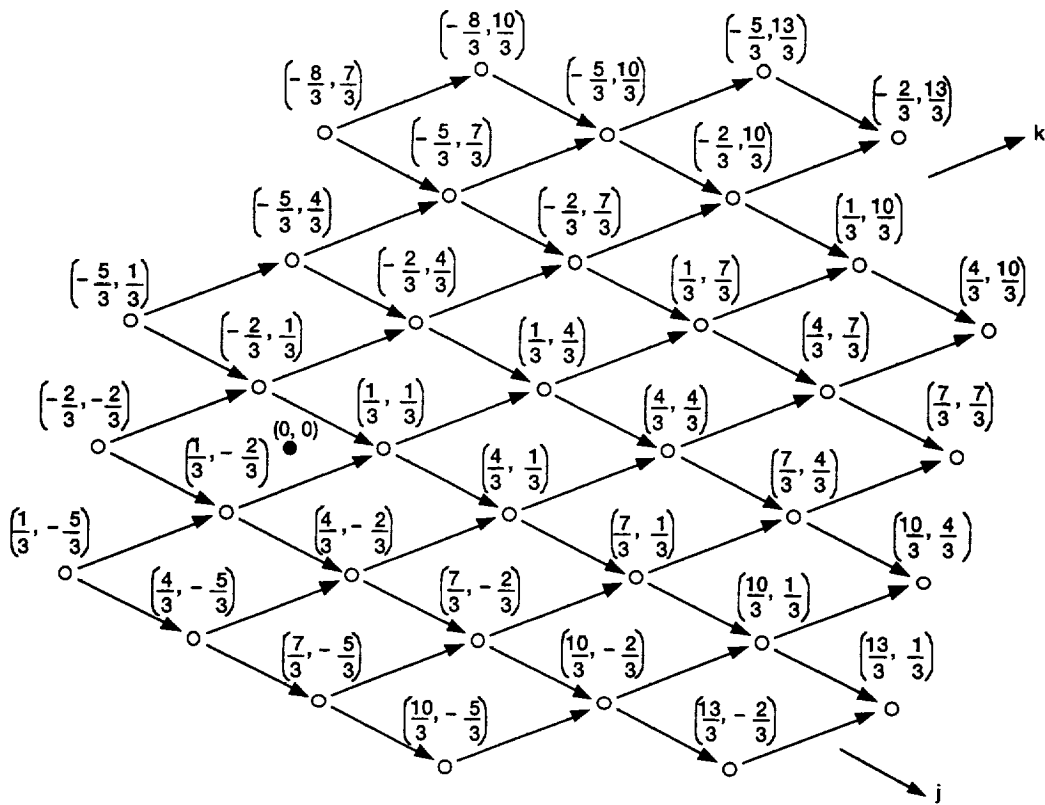


Figure 3.—The spatial mesh indices (j, k) of the mesh points $\in \Omega_2$ ($n = 0, \pm 1, \pm 2, \dots$).

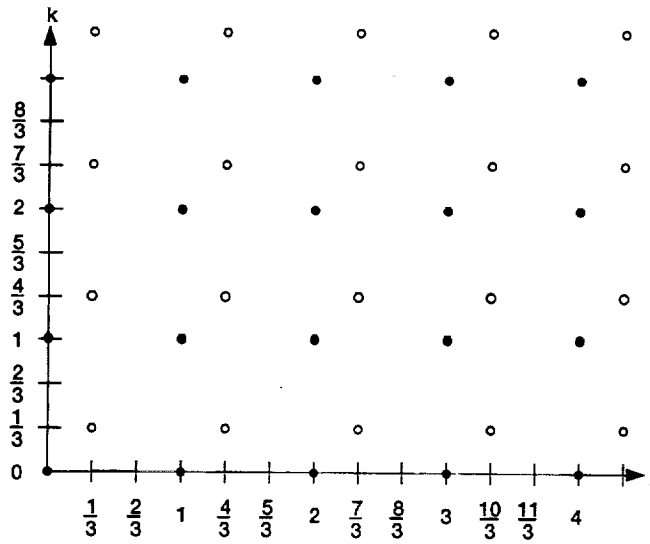


Figure 4.—The spatial mesh positions of the mesh points marked by ● and those marked by ○.

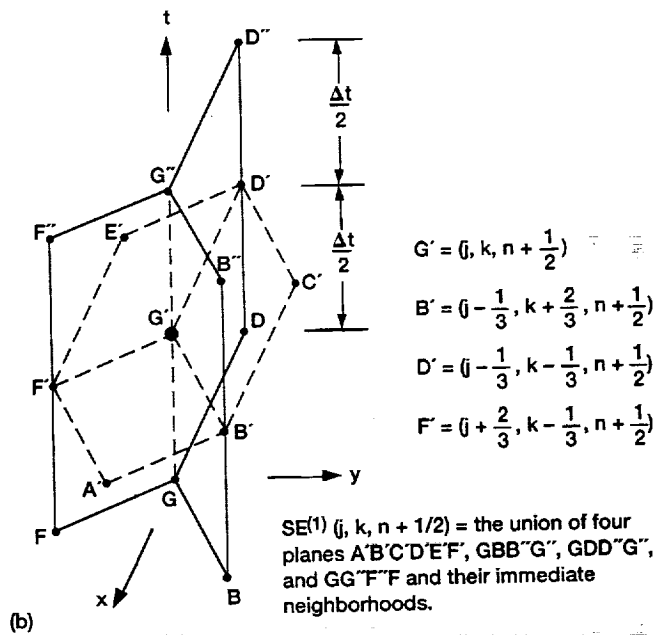
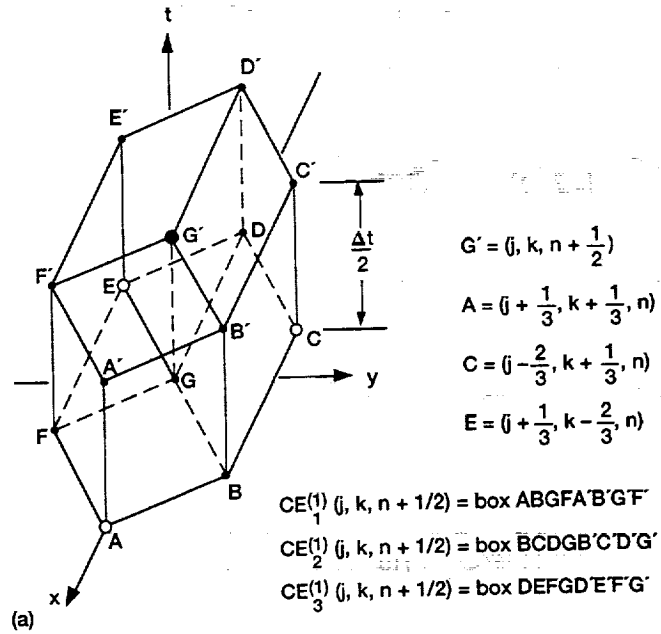


Figure 5.—(a) Conservation elements $CE_\ell^{(1)}(j, k, n + 1/2)$, $\ell = 1, 2, 3$, and $j, k, n = 0, \pm 1, \pm 2, \dots$. (b) Solution elements $SE^{(1)}(j, k, n + 1/2)$, $j, k, n = 0, \pm 1, \pm 2, \dots$.

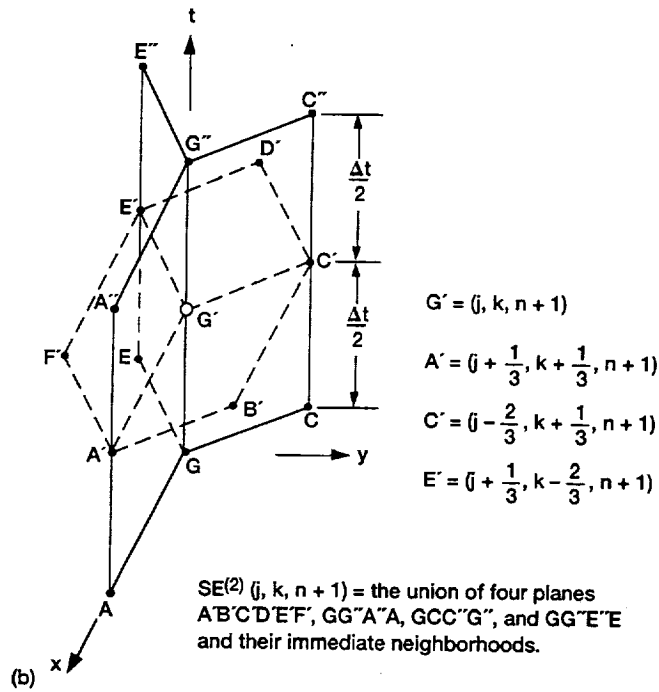
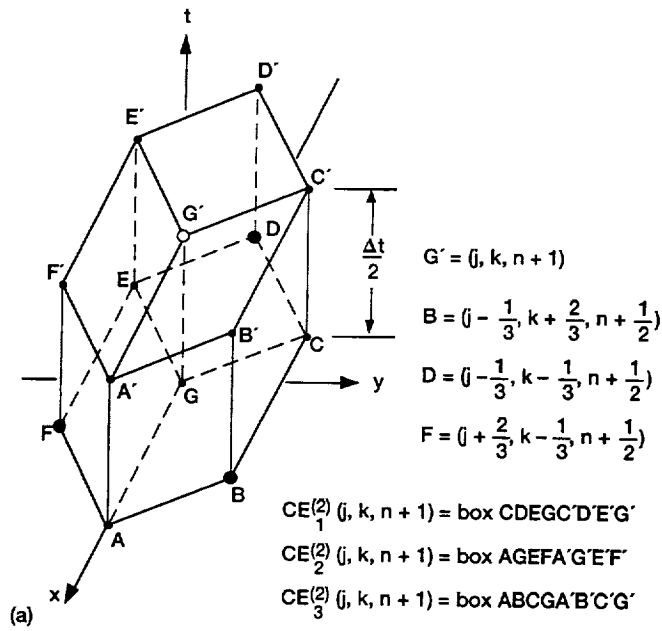


Figure 6.—(a) Conservation elements $CE_\ell^{(2)}(j, k, n + 1)$, $\ell = 1, 2, 3$, $j, k = 1/3, 1/3 \pm 1, 1/3 \pm 2, \dots$, and $n = 0, \pm 1, \pm 2, \dots$. (b) Solution elements $SE^{(2)}(j, k, n + 1)$, $j, k = 1/3, 1/3 \pm 1, 1/3 \pm 2, \dots$, and $n = 0, \pm 1, \pm 2, \dots$.

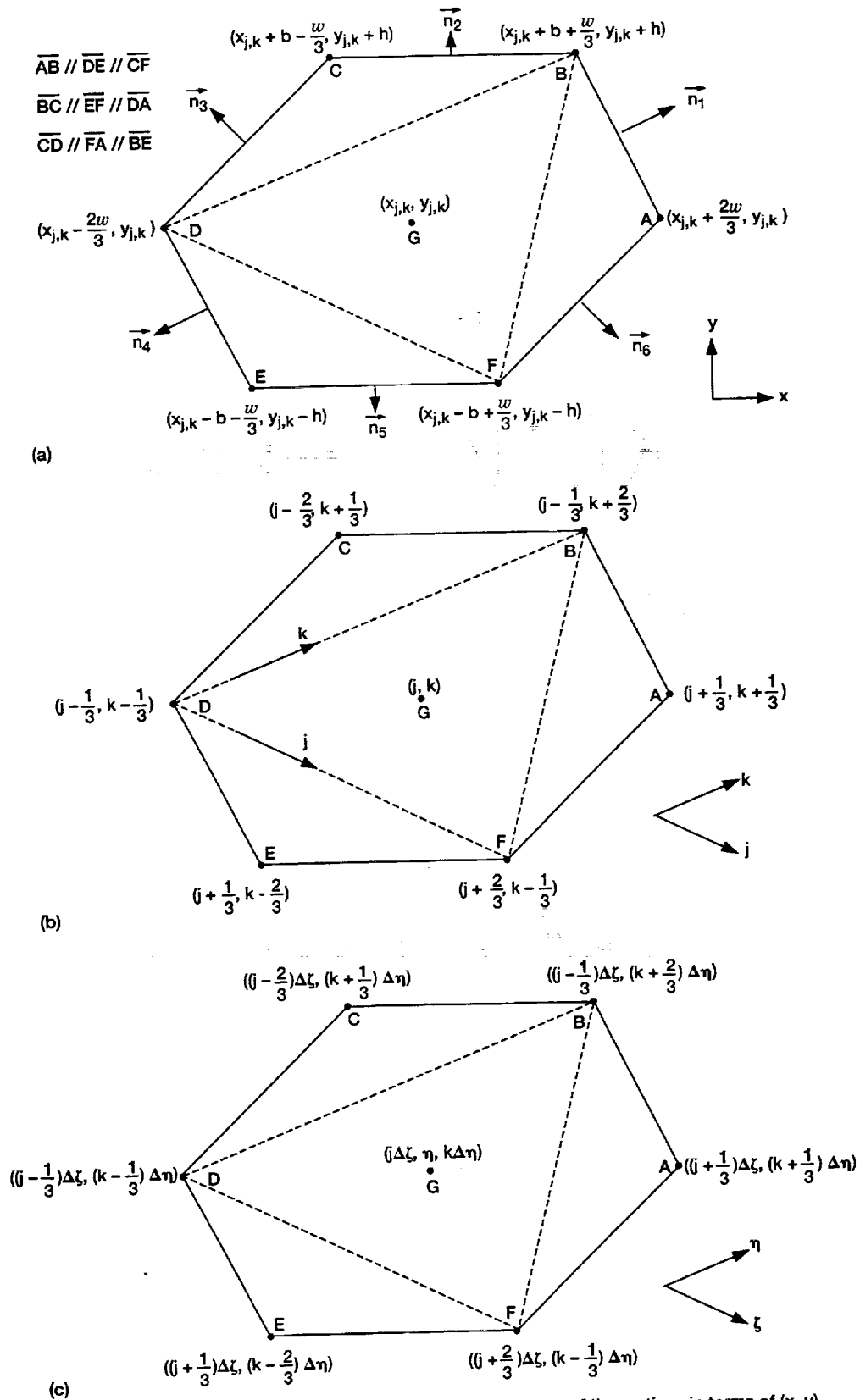


Figure 7.—Geometry of the hexagon ABCDEF. (a) Relative positions of the vertices in terms of (x, y) . (b) Relative positions of the vertices in terms of (j, k) . (c) Relative positions of the vertices in terms of (ζ, η) .

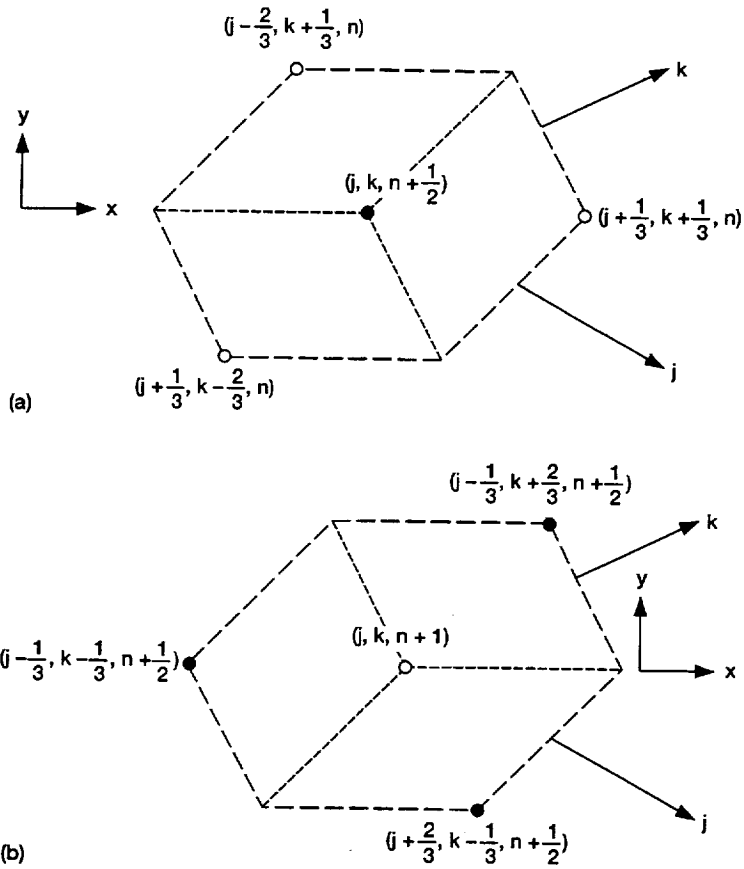


Figure 8.—(a) The mesh points $(j, k, n + 1/2)$, $(j + 1/3, k + 1/3, n)$, $(j - 2/3, k + 1/3, n)$ and $(j + 1/3, k - 2/3, n)$ with $(j, k, n + 1/2) \in \Omega_1$. (b) The mesh points $(j, k, n + 1)$, $(j - 1/3, k - 1/3, n + 1/2)$, $(j + 2/3, k - 1/3, n + 1/2)$, and $(j - 1/3, k + 2/3, n + 1/2)$ with $(j, k, n + 1) \in \Omega_2$.

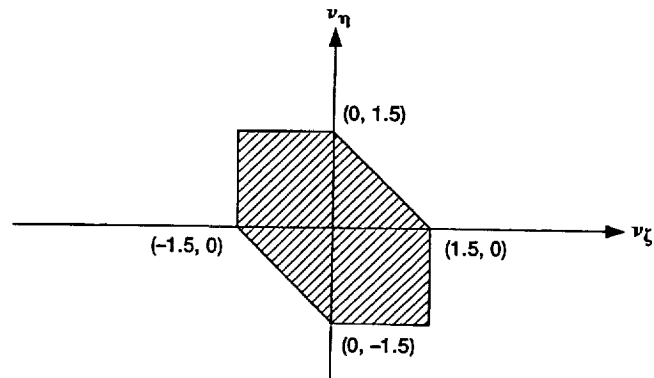
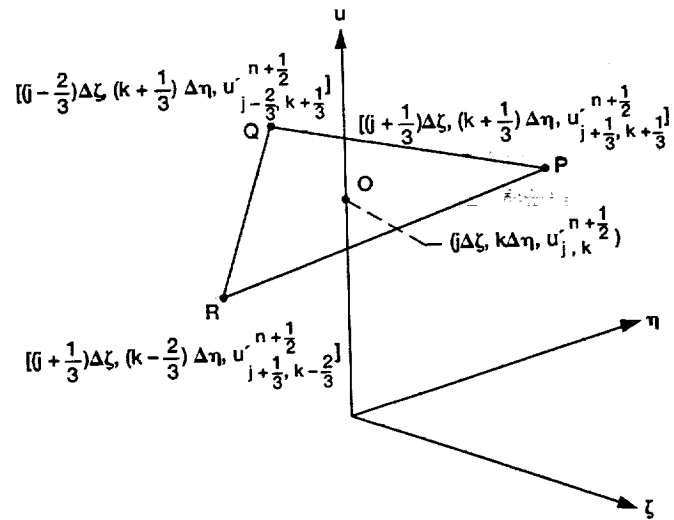
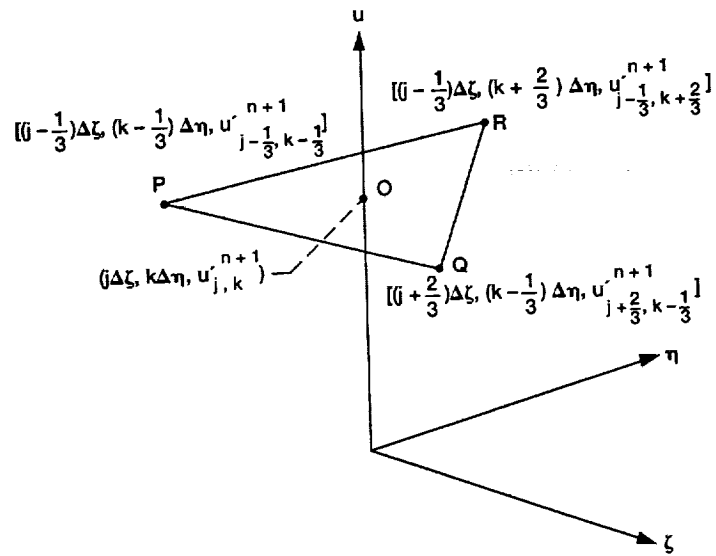


Figure 9.—The stability domain of the a scheme.



(a)



(b)

Figure 10.—The ζ - η - U space. (a) $(j, k, n + 1/2) \in \Omega_1$. (b) $(j, k, n + 1) \in \Omega_2$.

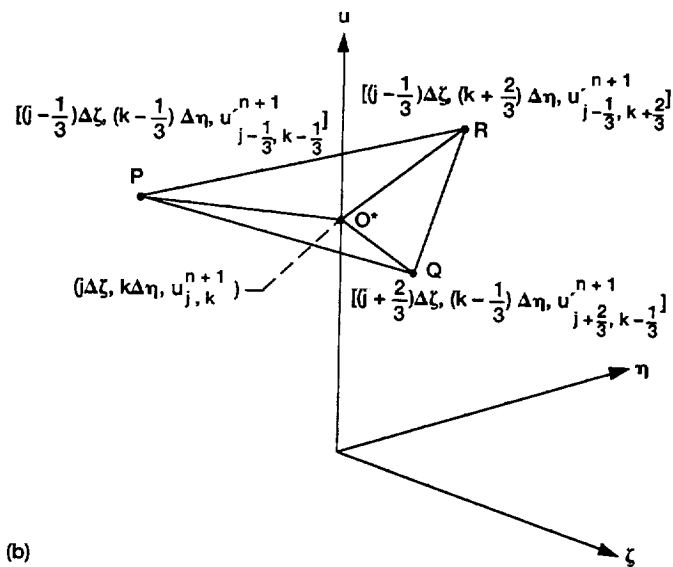
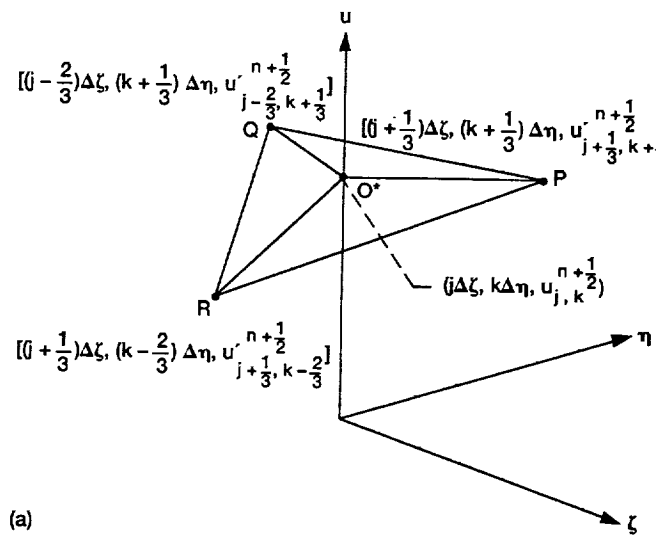


Figure 11.—The weighted-average a-ε scheme. (a) $(j, k, n + 1/2) \in \Omega_1$.
 (b) $(j, k, n + 1) \in \Omega_2$.

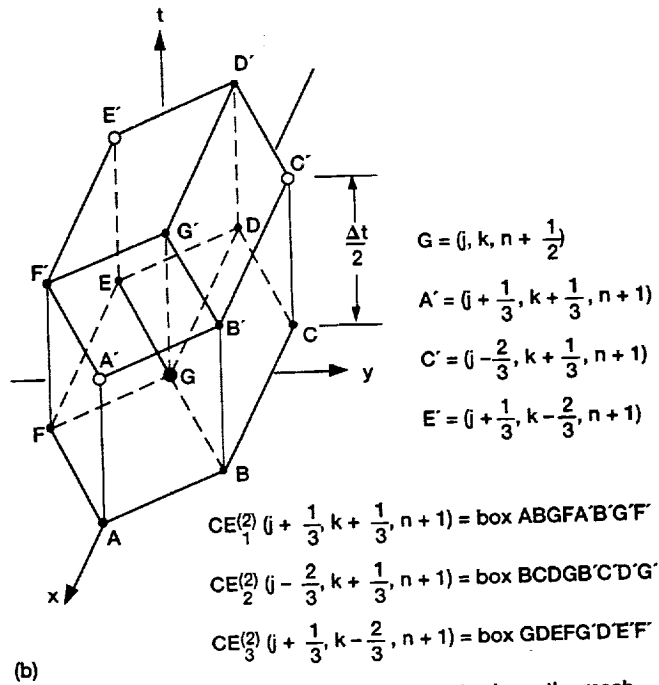
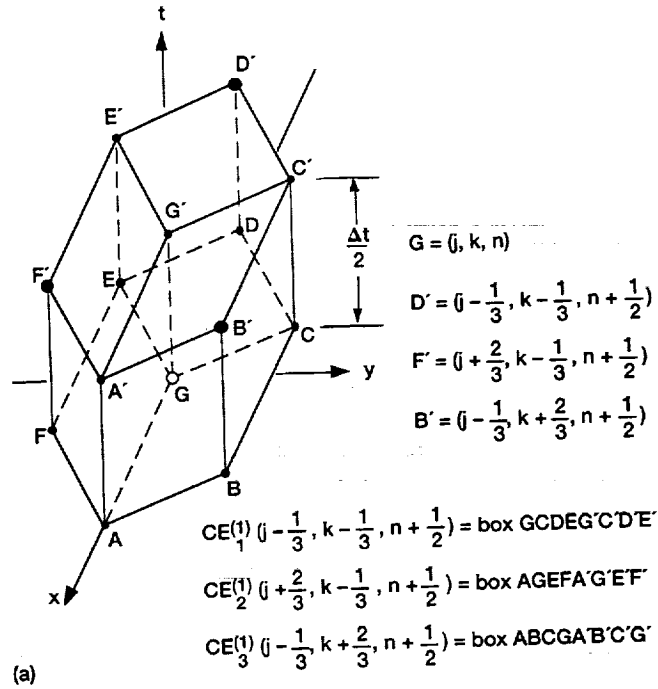


Figure 12.—(a) Three CE's located immediately above the mesh point $G \in \Omega_2$ ($j, k = 1/3, 1/3 \pm 1, 1/3 \pm 2, \dots$, and $n = 0, \pm 1, \pm 2, \dots$).
 (b) Three CE's located immediately above the mesh point $G \in \Omega_1$ ($j, k, n = 0, \pm 1, \pm 2, \dots$).

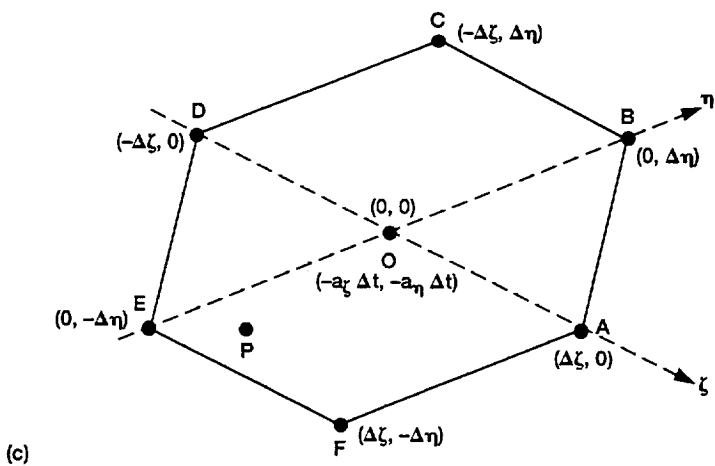
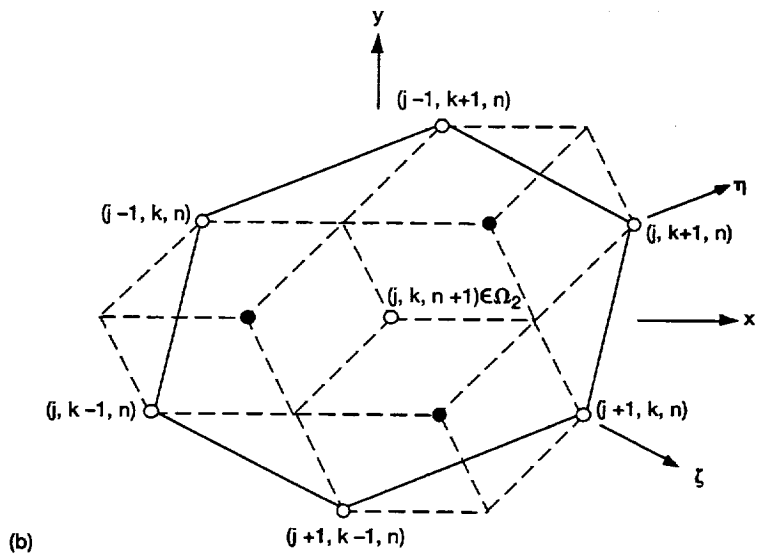
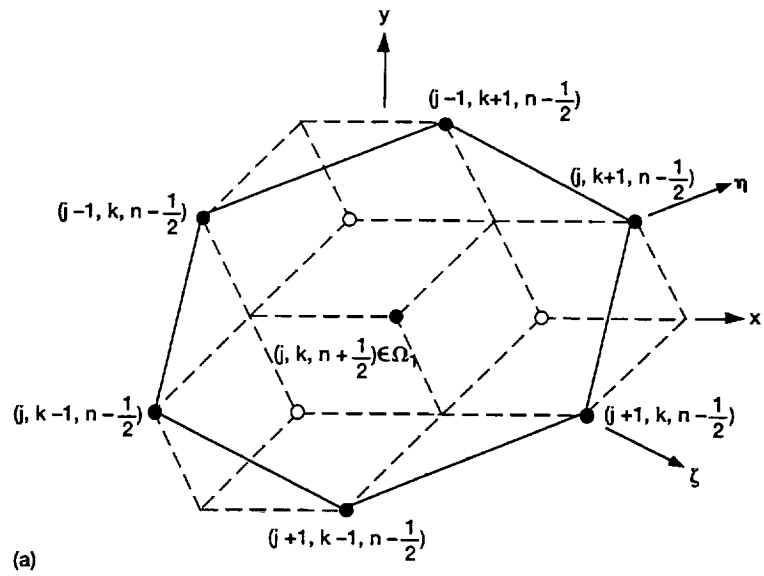


Figure 13.—Numerical domain of dependence.

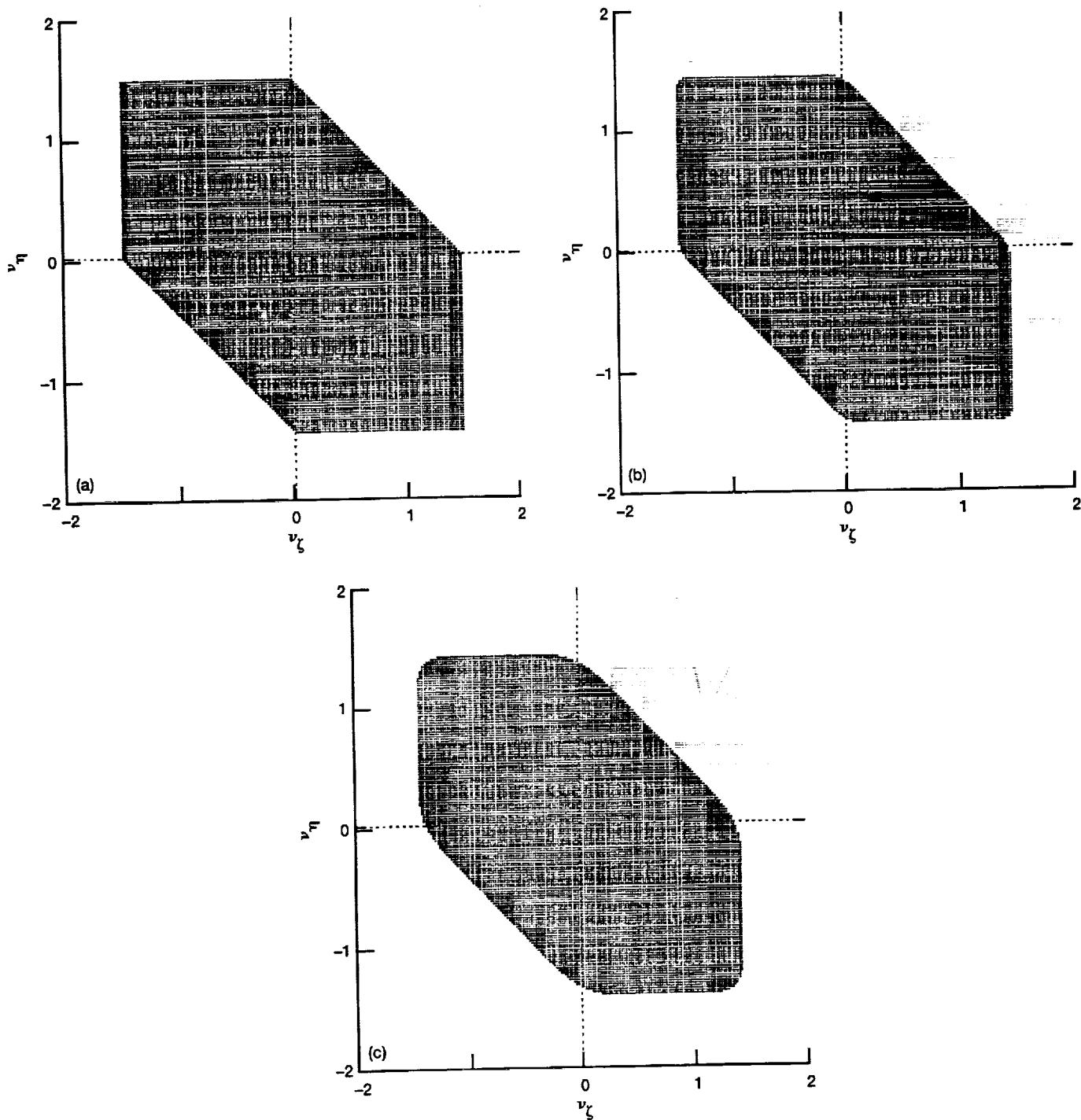


Figure 14.—(a) The stability domain of a- ϵ scheme for $\epsilon = 0.1$. (b) The stability domain of a- ϵ scheme for $\epsilon = 0.5$. (c) The stability domain of a- ϵ scheme for $\epsilon = 0.8$.

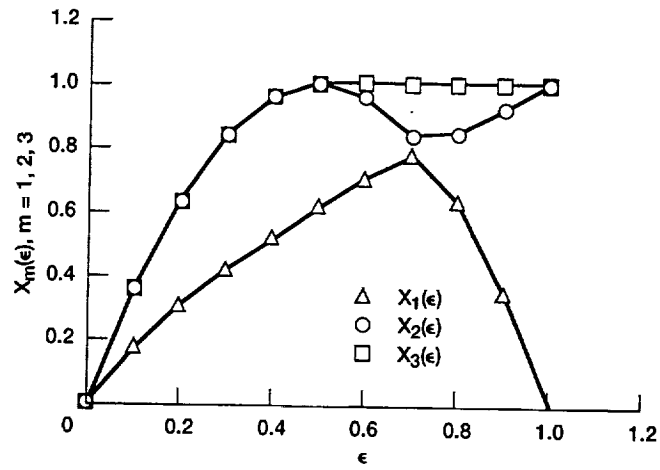


Figure 15.—The numerical diffusion versus ϵ .

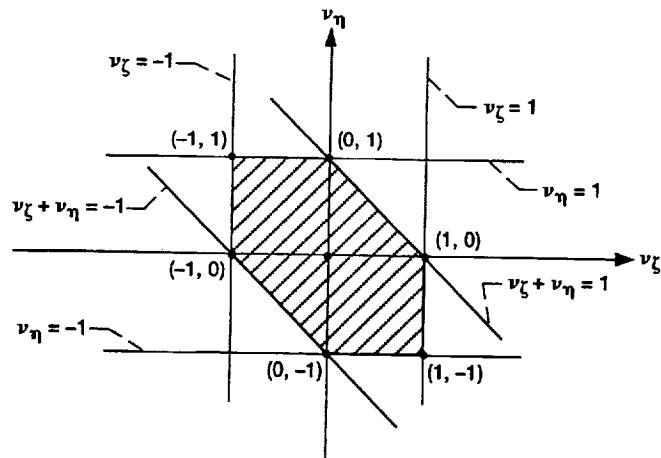


Figure 16.—The straight lines on which $\Delta^{(1)} = 0$ or $\Delta^{(2)} = 0$ when $\mu = 0$.

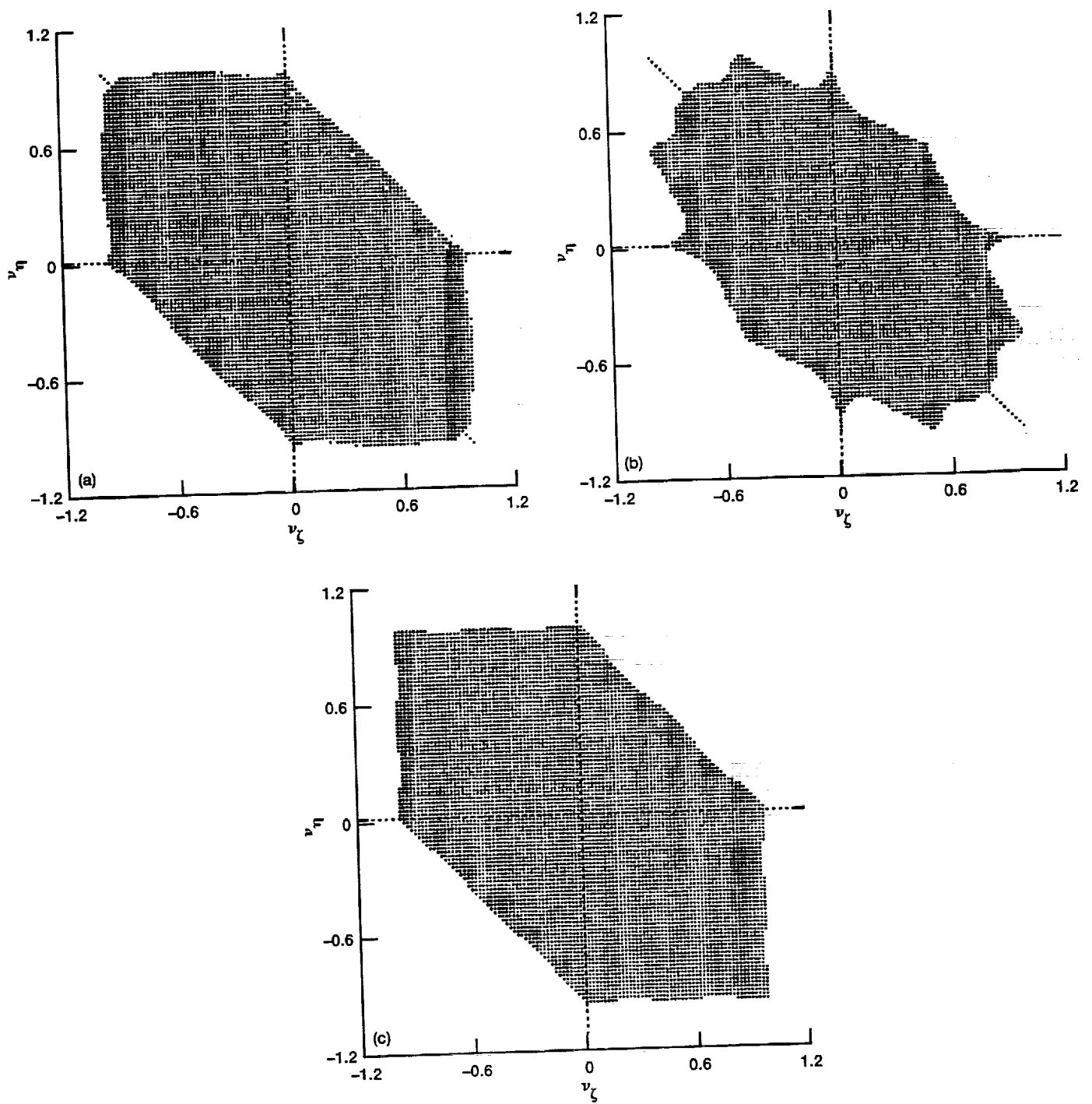


Figure 17.—(a) The stability domain of a- μ scheme for $\xi = 10^{-5}$. (b) The stability domain of a- μ scheme for $\xi = 10^{-3}$. (c) The stability domain of a- μ scheme for $\xi = 10^{-1}$.

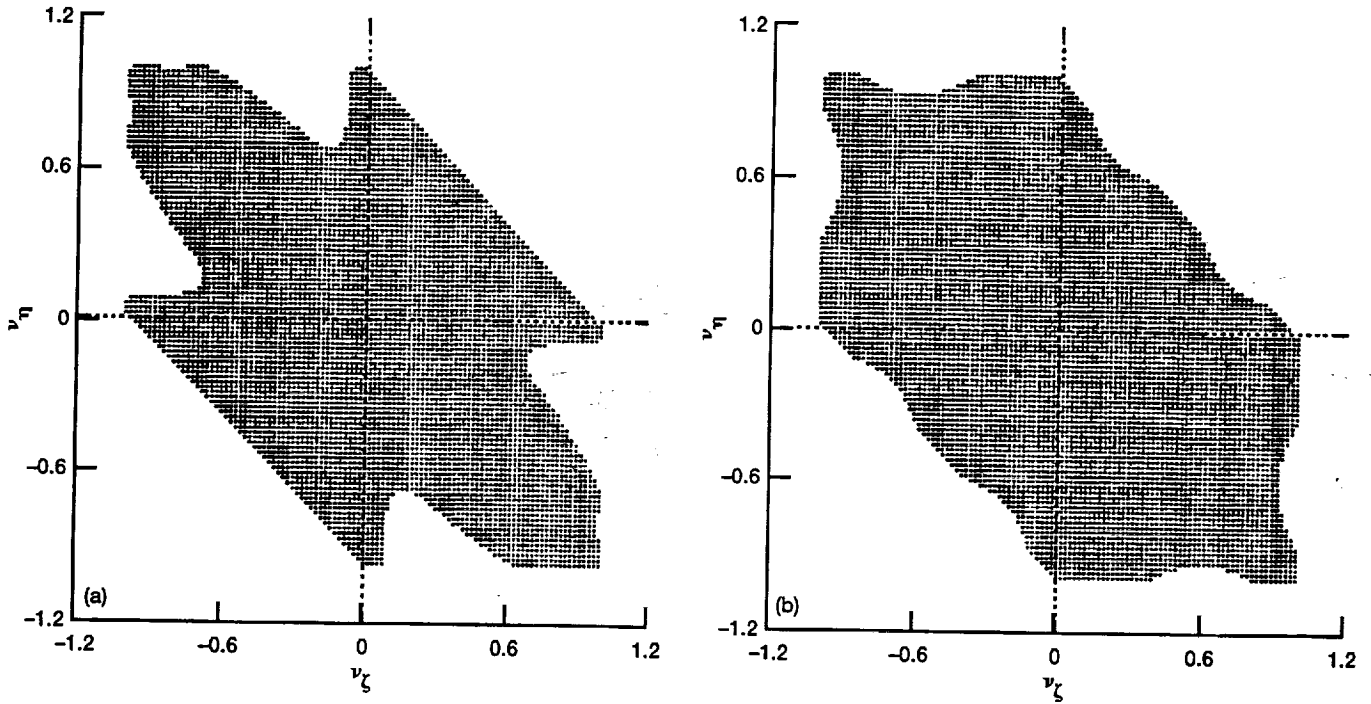


Figure 18.—(a) The stability domain of a- μ scheme for $\xi = 0.1$, $\alpha = 45^\circ$. (b) The stability domain of a- μ scheme for $\xi = 0.1$, $\alpha = 75^\circ$.

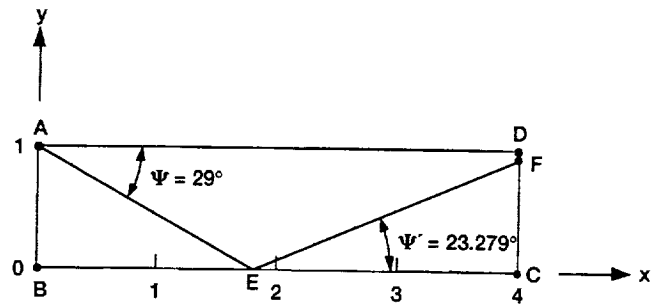


Figure 19.—The computation domain and the shock locations of a steady-state shock reflection problem.

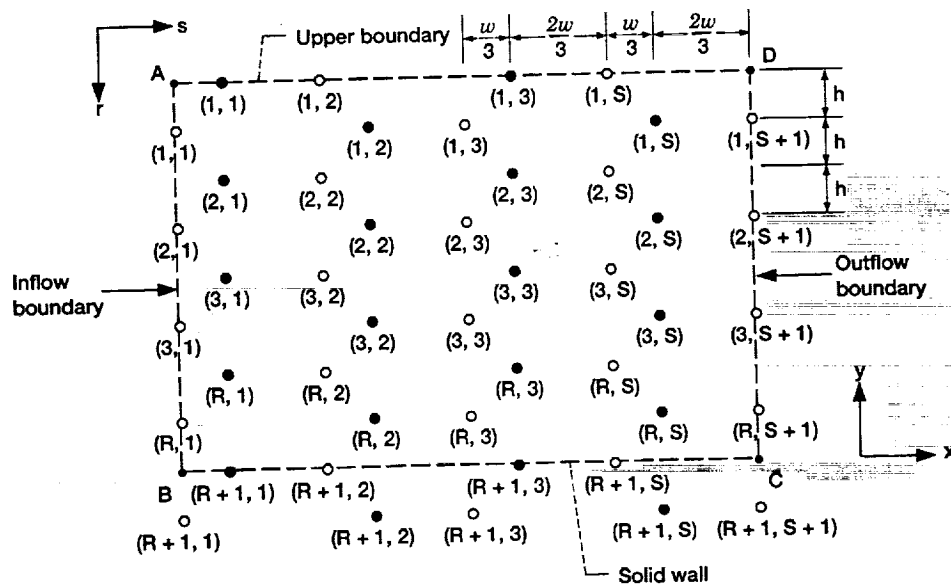


Figure 20.—The spatial locations and the new mesh indices (r, s) of mesh points ($R = S = 4$).

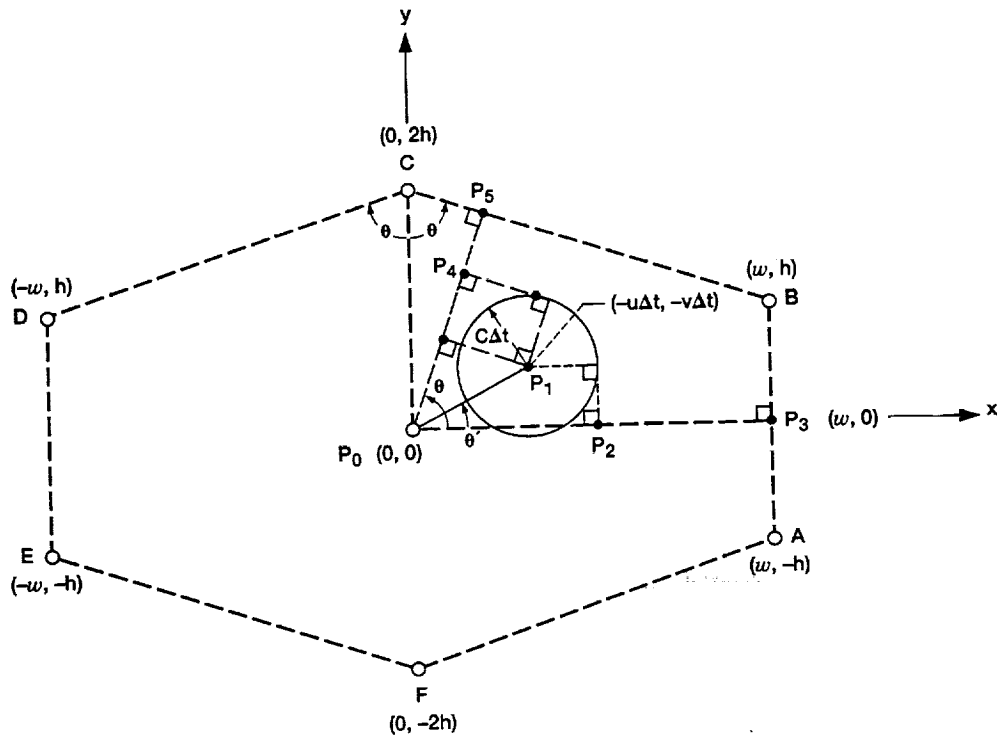


Figure 21.—Definition of the CFL number.

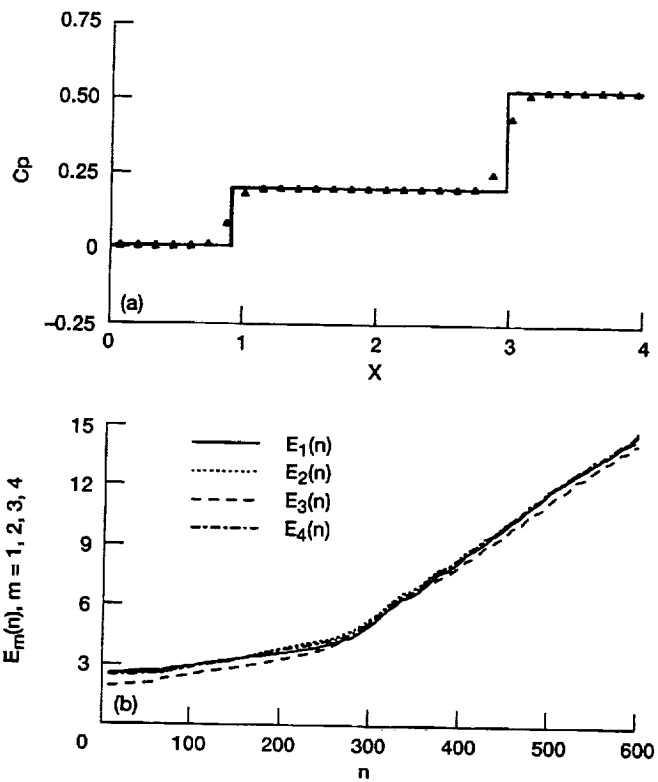


Figure 22.—Numerical results and convergence histories for problem #1. (a) Pressure coefficients at the mid-section of the computation domain ($y = 0.5$ in Fig. 19). (b) Convergence histories for u_m , $m = 1, 2, 3, 4$.

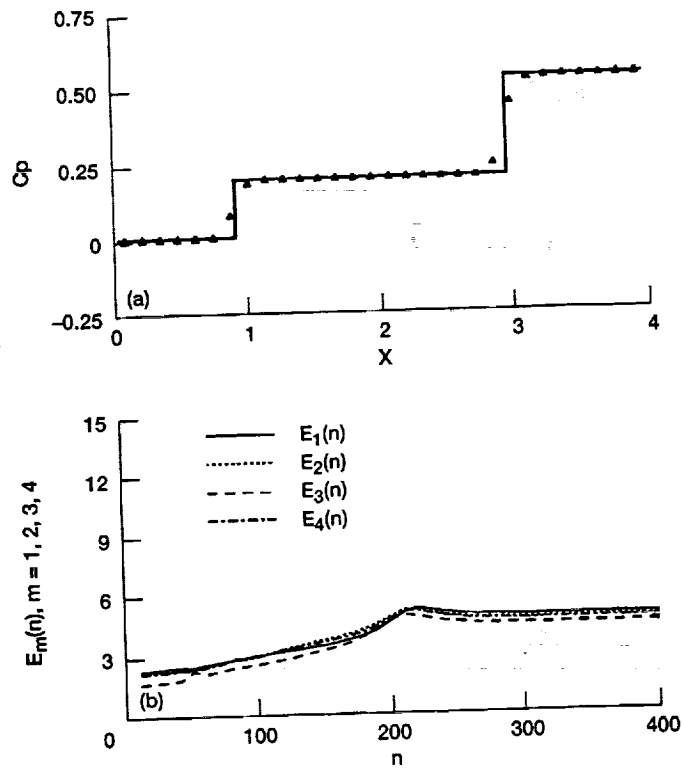


Figure 23.—Numerical results and convergence histories for problem #2. (a) Pressure coefficients at the mid-section of the computation domain ($y = 0.5$ in Fig. 19). (b) Convergence histories for u_m , $m = 1, 2, 3, 4$.

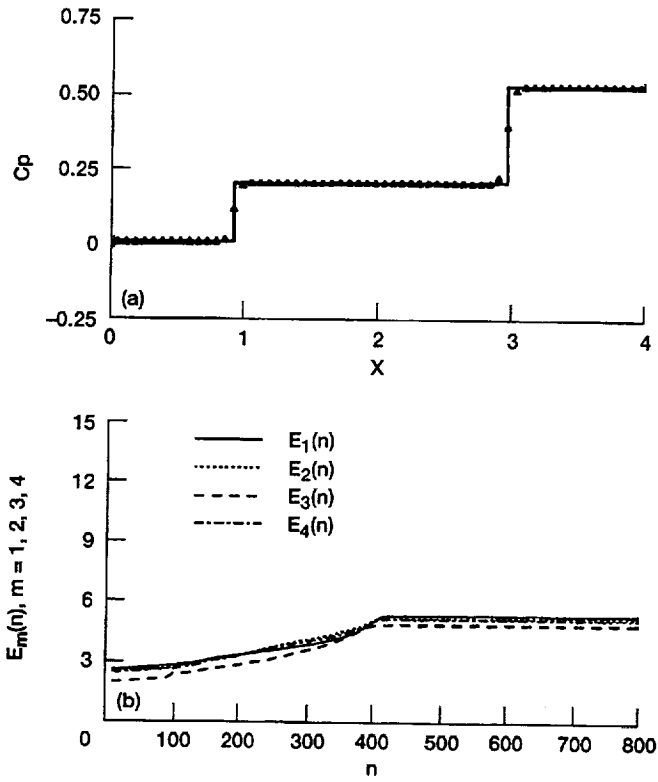


Figure 24.—Numerical results and convergence histories for problem #3. (a) Pressure coefficients at the mid-section of the computation domain ($y = 0.5$ in Fig. 19). (b) Convergence histories for u_m , $m = 1, 2, 3, 4$.

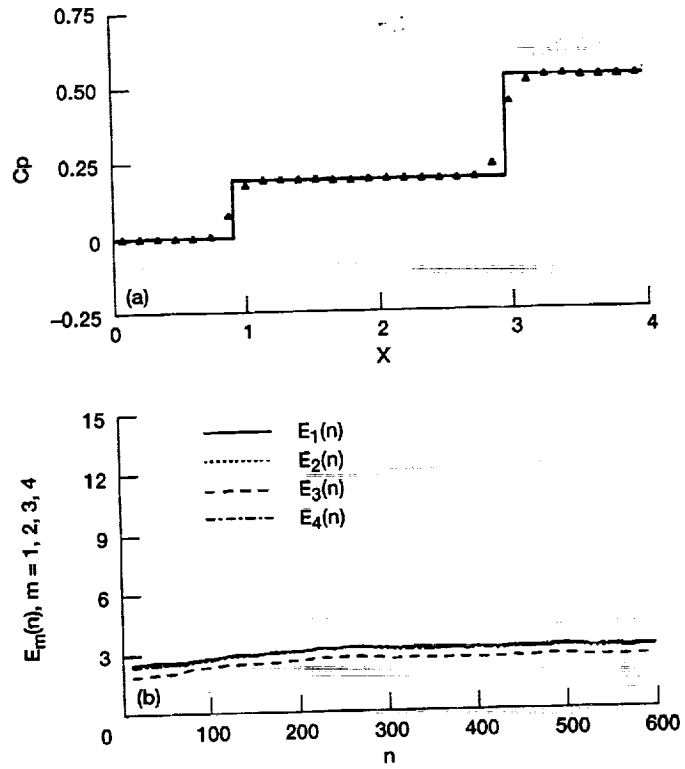


Figure 25.—Numerical results and convergence histories for problem #4. (a) Pressure coefficients at the mid-section of the computation domain ($y = 0.5$ in Fig. 19). (b) Convergence histories for u_m , $m = 1, 2, 3, 4$.

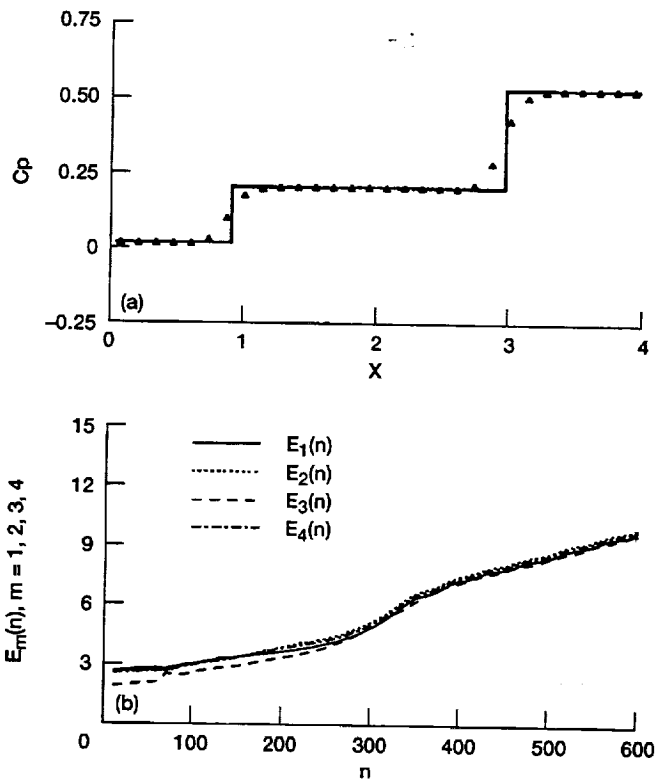


Figure 26.—Numerical results and convergence histories for problem #5. (a) Pressure coefficients at the mid-section of the computation domain ($y = 0.5$ in Fig. 19). (b) Convergence histories for u_m , $m = 1, 2, 3, 4$.

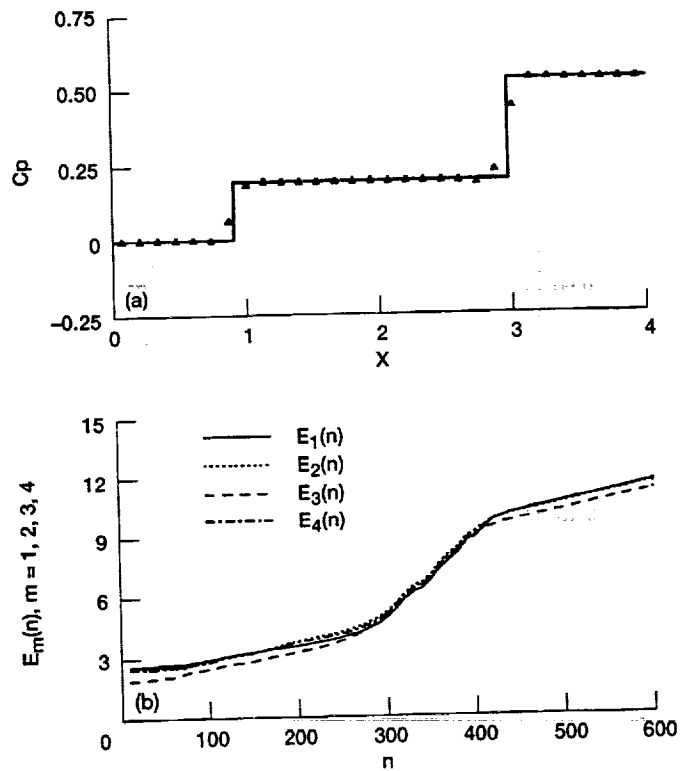


Figure 27.—Numerical results and convergence histories for problem #6. (a) Pressure coefficients at the mid-section of the computation domain ($y = 0.5$ in Fig. 19). (b) Convergence histories for u_m , $m = 1, 2, 3, 4$.

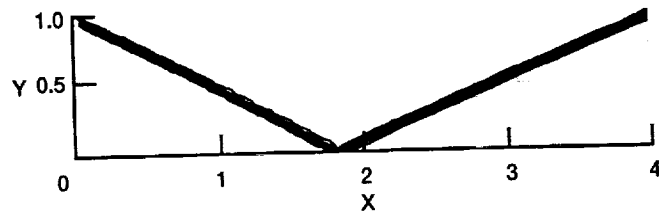


Figure 28.—Pressure contours for problem #3.

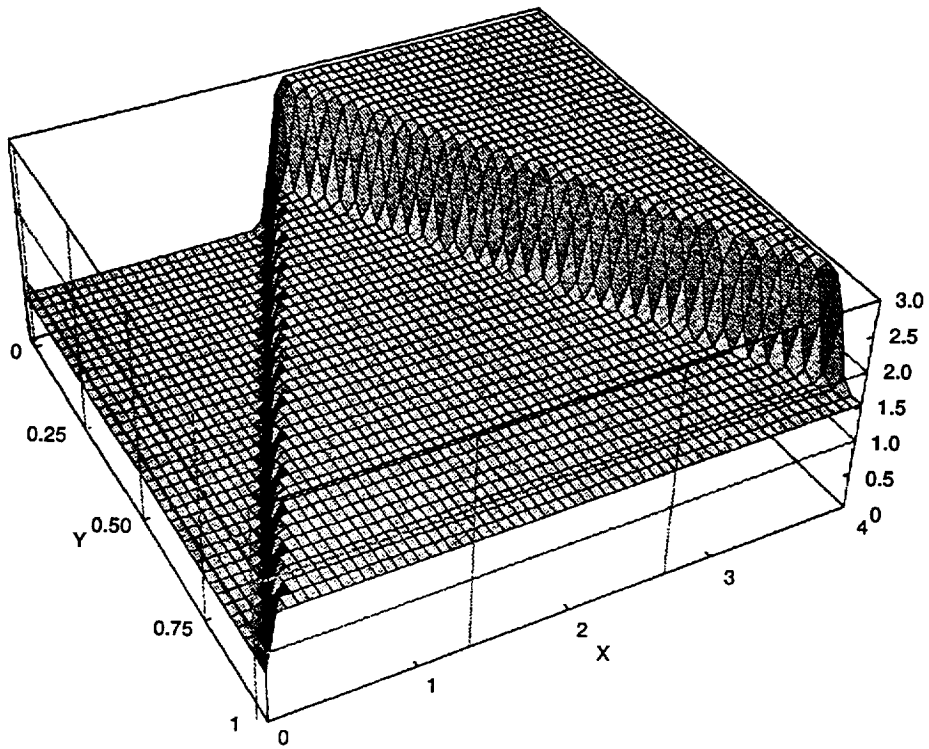


Figure 29.—Pressure distribution for problem #3.

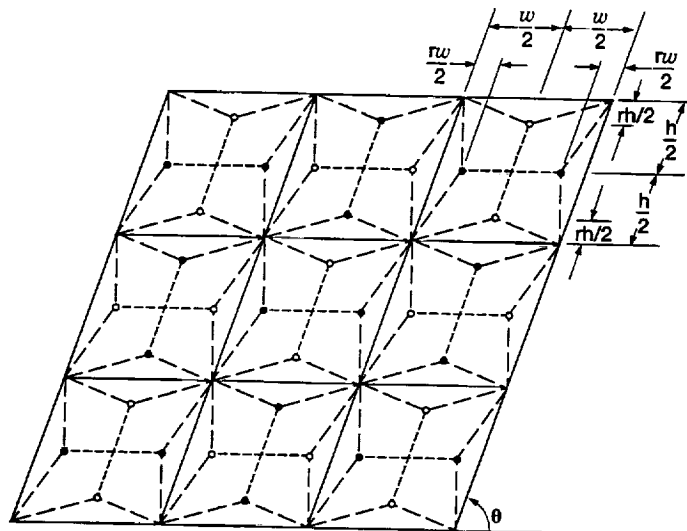


Figure 30.—The spatial projection of an alternative space-time mesh (dash lines are spatial projections of the interfaces which divide CE's).

REPORT DOCUMENTATION PAGE

Form Approved
OMB No. 0704-0188

Public reporting burden for this collection of information is estimated to average 1 hour per response, including the time for reviewing instructions, searching existing data sources, gathering and maintaining the data needed, and completing and reviewing the collection of information. Send comments regarding this burden estimate or any other aspect of this collection of information, including suggestions for reducing this burden, to Washington Headquarters Services, Directorate for Information Operations and Reports, 1215 Jefferson Davis Highway, Suite 1204, Arlington, VA 22202-4302, and to the Office of Management and Budget, Paperwork Reduction Project (0704-0188), Washington, DC 20503.

1. AGENCY USE ONLY (Leave blank)		2. REPORT DATE December 1994	3. REPORT TYPE AND DATES COVERED Technical Memorandum	
4. TITLE AND SUBTITLE New Developments in the Method of Space-Time Conservation Element and Solution Element-Applications to Two-Dimensional Time-Marching Problems			5. FUNDING NUMBERS WU-505-62-52	
6. AUTHOR(S) Sin-Chung Chang, Xiao-Yen Wang, and Chuen-Yen Chow			8. PERFORMING ORGANIZATION REPORT NUMBER E-9180	
7. PERFORMING ORGANIZATION NAME(S) AND ADDRESS(ES) National Aeronautics and Space Administration Lewis Research Center Cleveland, Ohio 44135-3191			10. SPONSORING/MONITORING AGENCY REPORT NUMBER NASA TM-106758	
9. SPONSORING/MONITORING AGENCY NAME(S) AND ADDRESS(ES) National Aeronautics and Space Administration Washington, D.C. 20546-0001			11. SUPPLEMENTARY NOTES Sin-Chung Chang, NASA Lewis Research Center; Xiao-Yen Wang and Chuen-Yen Chow, University of Colorado, Department of Aerospace Engineering Science, Boulder, Colorado 80309-0429 (work funded under NASA Grant NAG3-1566). Responsible person, Sin-Chung Chang, organization code 2660, (216) 433-5874.	
12a. DISTRIBUTION/AVAILABILITY STATEMENT Unclassified - Unlimited Subject Categories 64 and 34			12b. DISTRIBUTION CODE	
13. ABSTRACT (Maximum 200 words) A new numerical discretization method for solving conservation laws is being developed. This new approach differs substantially in both concept and methodology from the well-established methods-i.e., finite difference, finite volume, finite element, and spectral methods. It is motivated by several important physical/numerical considerations and designed to avoid several key limitations of the above traditional methods. As a result of the above considerations, a set of key principles for the design of numerical schemes was put forth in a previous report. These principles were used to construct several numerical schemes that model a 1-D time-dependent convection-diffusion equation. These schemes were then extended to solve the time-dependent Euler and Navier-Stokes equations of a perfect gas. It was shown that the above schemes compared favorably with the traditional schemes in <i>simplicity, generality, and accuracy</i> . In this report, the 2-D versions of the above schemes, except the Navier-Stokes solver, are constructed using the same set of design principles. Their constructions are simplified greatly by the use of a nontraditional space-time mesh. Its use results in the simplest stencil possible, i.e., a tetrahedron in a 3-D space-time with a vertex at the upper time level and other three at the lower time level. Because of the similarity in their design, each of the present 2-D solvers virtually shares with its 1-D counterpart the same fundamental characteristics. Moreover, it will be shown that the present Euler solver is capable of generating highly accurate solutions for a famous 2-D shock reflection problem. Specifically, both the incident and the reflected shocks can be resolved by a single data point without the presence of numerical oscillations near the discontinuity.				
14. SUBJECT TERMS Space-time; Conservation element; Solution element; Two-dimensional; Time-marching			15. NUMBER OF PAGES 123	
			16. PRICE CODE A06	
17. SECURITY CLASSIFICATION OF REPORT Unclassified	18. SECURITY CLASSIFICATION OF THIS PAGE Unclassified	19. SECURITY CLASSIFICATION OF ABSTRACT Unclassified	20. LIMITATION OF ABSTRACT	

**National Aeronautics and
Space Administration**

Lewis Research Center
21000 Brookpark Rd.
Cleveland, OH 44135-3191

Official Business
Penalty for Private Use \$300

POSTMASTER: If Undeliverable — Do Not Return

